Norwegian University of Life Sciences
Faculty of Biosciences
Department of plant sciences

Philosophiae Doctor (PhD)
Thesis 2020:21

Genetic studies of the wheat-*Parastagonospora nodorum* pathosystem

Genetiske studier av vert-patogen samspill for hveteaksprikk

Min Lin

Genetic studies of the wheat-*Parastagonospora nodorum* pathosystem

Genetiske studier av vert-patogen samspill for hveteaksprikk

Philosophiae Doctor (PhD) Thesis

Min Lin

Norwegian University of Life Sciences
Faculty of Biosciences
Department of plant sciences

Ås (2020)

Thesis number 2020:21
ISSN: 1894-6402
ISBN: 978-82-575-1684-0

Table of Contents

Acknowledgement i
Summary iii
Sammendrag v
List of papers vii
1. Introduction 1
1.1 Wheat 1
1.2 Pathogen 2
1.2.1 Symptoms 2
1.2.2 Infection cycle and epidemics 3
1.2.3 Population genetics studies of *P. nodorum* 5
1.2.4 Agricultural importance and disease management 5
1.3 Inverse gene for gene interaction in the wheat-*P. nodorum* pathosystem 7
1.3.1 Well characterized NE-*Snn* interactions 8
1.3.2 Relationship between NE-*Snn* interactions and field SNB severity 10
1.3.3 Relationship between SNB adult plant leaf blotch and glume blotch resistance 11
1.3.4 Current status of SNB knowledge in Norwegian wheat 12
1.4 Linkage QTL mapping and genome wide association scans (GWAS) 12
1.4.1 Molecular markers in wheat 12
1.4.2 Bi-parental genetic mapping populations 13
1.4.3 Genome wide association scans (GWAS) 14
1.4.4 Multi-parental populations: multi-parent advanced generation intercross (MAGIC) and nested association mapping (NAM) 14
2. The thesis 16
2.1 Background and main objectives 16
2.2 Materials and Methods 19
2.2.1 Plant material 19
2.2.2 Fungal materials and population structure analysis 19
2.2.3 Seedling infiltration and inoculation 20
2.2.4 Field assessment 20
2.3 Main results and discussion 21

2.3.1 How can genetic knowledge of the pathogen population be used to improve disease management? 21
2.3.2 NE-*Snn* interactions at the seedling stage 25
2.3.3 Can sensitivity to NEs explain differences in host SNB resistance in the field? 28
2.3.4 Field inoculation methods 29
2.3.5 QTL detected for SNB leaf blotch and glume blotch 30
2.3.6 Candidate QTL for marker assisted selection (MAS) 31
2.3.7 Influences of plant height and days to heading on SNB disease severity in the field . 32
2.4 Future perspectives 34
2.4.1 Fine mapping the QTL *QSnb.niab-2A.3* 34
2.4.2 Applying CRISPR/Cas9 technology to improve SNB resistance 34
2.4.3 Genomic selection (GS) 35
2.5 Conclusions 36
References 37

Acknowledgement

This PhD work was undertaken within the framework of the 2nd call ERA-NET for Coordinating Plant Sciences, within the 'EfectaWheat' project, with funding national from The Research Council of Norway, grant NFR251894. The project work was carried out from 2015 to 2019 at the Department of Plant Sciences (IPV) at the Norwegian University of Life Sciences (NMBU) in collaboration with the Norwegian Institute of Bioeconomy Research (NIBIO), Bavarian State Research Center for Agriculture (LfL), National Institute of Agricultural Botany (NIAB), Aarhus University and Curtin University.

I would like to express my deepest gratitude to my main supervisor Dr. Morten Lillemo for giving me the opportunity to work on this PhD project, always being available and kind. Thank you so much for all your support during my whole PhD period. I would not have been able to conduct this PhD without your guidance. Also, I appreciate this opportunity you gave me which allowed me to live and work in Norway and thank you for letting me travel to different countries for courses and conferences. I benefit a lot from it. I also want to thank my co-supervisor Dr. Andrea Ficke at NIBIO and Dr. James Cockram at NIAB. Andrea-thank you for both your scientific input and creating the friendly work environment in NIBIO, especially for encouraging and helping me to cope with frustrations when my experiments failed again and again. James-thank you for your quick, relevant and insightful responses. In addition, Thank you for the fundamental inputs on improving my thesis and manuscripts.

Additionally, I thank all other co-authors for kindly sharing your expertise. All your assistance is deeply appreciated. Gratefully thank to Dr. Patrick C. Brunner of Institute of Integrative Biology, Zurich (IBZ) for kindly providing the SSR primer sequences and extensive advice on the analysis for the pathogen population genetics study. Unfortunately, he passed away in September 2019, otherwise he would have been a co-author of the first article. It was a great loss to us all and he will be missed in many levels. I would like to thank Prof. Bruce A. McDonald, ETH Zurich for continuing the collaboration with us after Patrick passed away and provided isolate and valuable advice on improving the manuscript. Analysis suggestions from Kar-Chun Tan (Curtin University) is also acknowledged. I also thank members of EfectaWheat Consortium for sharing leaf samples and isolate samples as well as, Dr. Tim Friesen (USDA-ARS, Fargo), Prof. Richard Oliver (Curtin University) and Dr. Pawan K. Singh (CIMMYT) for providing the isolates from USA, Australia and Mexico, respectively. I thank Dr. Keith Gardner (NIAB) and Dr. Beatrice Corsi for organizing the training workshop in NIAB, Cambridge and their genetics advice. I also thank Prof. Richard Oliver (CCDM) and Dr. Huyen Phan (CCDM) for supplying the ToxA and Tox3 effectors.

I would also like to thank the technical support from our technicians. At IPV, my deepest gratitude goes to Anne Guri, Cecilie, Yalew, Marit, Ida and Gry. At NIBIO, I especially want to thank Jafar and Chloe for their helpfulness and advice. This work would not have been possible without your help.

I am very lucky that I am a member of the Genetics and Plant Breeding section at IPV. I am thankful to all the members of our section for creating a culture so work feels like family. I deeply appreciate the friendly work environment. Above all, I want to thank my previous colleagues Anja,

Ronja, Tanya, Tove and Susanne. Thank you for sharing your expertise as well as your life experience. I have been extra lucky to have shared first part of my PhD with Anja and Ronja. Especially Anja who worked on the similar topic as mine. I learned so much from her and it would not have been possible to do all the experiments and analysis without her advice and guidance. Special thanks to Ursula, being my climbing and kayaking partner, who made my life in Norway more joyable. Camilla, Martin, Marian, Stefano, Mallik, Franz, Sahameh and Tomasz, for creating the friendly section environment for PhD students and young researchers. Thank you so much for spending time charting with me and easing my frustrations in the last few months of my PhD.

And finally, I owe my thanks to my beloved parents and friends. Because of them, I was able to cope with stress and enjoy the fun part of my PhD life.

Ås, January 2020

Min

Summary

Septoria nodorum blotch (SNB) caused by the necrotrophic fungus *Parastagonospora nodorum* is the major wheat leaf blotch disease in Norway. It reduces both yield and grain quality by causing symptoms on wheat leaves and glumes, and can cause yield losses up to 30% under warm and humid conditions. To date, complete resistance to SNB is not available. As the resistance to both SNB leaf blotch and glume blotch are quantitatively inherited but controlled by different genetic mechanisms, breeding for SNB resistance is quite challenging. In the past decades, research progress has been made on understanding the interactions at the seedling stage between wheat sensitivity loci (*Snn*) and the corresponding necrotrophic effectors produced by *P. nodorum*. However, even though some NE-*Snn* interactions have been found to contribute to adult plant leaf blotch susceptibilities, correlations between SNB seedling resistance and adult plant resistance are generally low. In order to investigate the *P. nodorum*-wheat pathosystem and ultilize the knowledge to improve SNB resistance, knowledge of both the local *P. nodorum* pathogen population and host resistance is required.

Stage 1: Norwegian *P. nodorum* genetic diversity: In the first stage of this PhD project, I investigated the genetic diversity of the Norwegian *P. nodorum* population and compared the allele frequencies of the three well-known *P. nodorum* NE genes (*SnToxA*, *SnTox1* and *SnTox3*) with other European populations. We found that the Norwegian *P. nodorum* population underwent random mating and had high level of genetic variation while no evidence was observed for population subdivisions. In addition, all three NE genes were common in the Norwegian *P. nodorum* population. However, significantly higher *SnToxA* allele frequency was found compared to other European *P. nodorum* populations and we hypothesized that this was due to the local adaptation to the high frequency of the corresponding sensitivity gene *Tsn1* in Norwegian spring wheat cultivars. This work suggests that the *P. nodorum* population in Norway has high evolutionary potential and can therefore rapidly adapt to local host cultivars.

Stage 2: Genetic mapping of *P. nodorum* resistance/susceptibility using a UK-adapted MAGIC population: genetic studies were conducted to detect SNB resistance associated quantitative trait loci (QTL) at both the seedling stage and the adult plant stage for leaf blotch and for glume blotch. In agreement with previous studies, we found that seedling leaf resistance poorly correlated with adult plant resistance, which may be due to different NEs being expressed by isolates used in

greenhouse testing in comparison to isolates in the natural population. One robust field QTL on chromosome 2A, termed *QSnb.niab-2A.3*, was detected for glume blotch resistance in one year and for leaf blotch resistance across years, locations and inoculation methods using the UK adapted multiparent advanced generation intercross (MAGIC) population ('NIAB Elite MAGIC'). However, haplotype analysis revealed that the QTL detected for leaf blotch and glume blotch could be caused by closely located but different genes or gene clusters. In addition, *QSnb.niab-2A.3* was also identified by culture filtrate infiltration of one *P. nodorum* isolate which lacked *SnToxA, SnTox1* and *SnTox3*, but possessed uncharacterised effector(s) in its culture filtrate. These results indicate that *QSnb.niab-2A.3* might associate to a novel SNB NE-*Snn* interaction.

Stage 3: Genetic mapping of *P. nodorum* resistance/susceptibility using a German-adapted MAGIC population. The QTL *QSnb.niab-2A.3* was validated for adult plant leaf blotch using another winter wheat MAGIC population adapted to German agronomic conditions ('BMWpop'), suggesting the potential value of applying marker assisted selection (MAS) for this QTL to improve SNB resistance in European winter wheat germplasm. In addition, one robust QTL on chromosome 5A was identified across years private to 'BMWpop'. Additive effects were detected when stacking beneficial alleles from both QTL on 2A and 5A. It is beneficial to survey larger numbers of varieties for sources of resistance/susceptibility, and MAGIC populations represent an efficient way of doing this.

Stage 4: SNB association mapping: to complement the QTL mapping undertaken in MAGIC, genome wide association scans (GWAS) for SNB resistance was also conducted using association mapping panels consisting of Nordic winter (102) and spring wheat (296) accessions genotyped with 35 K Axiom array. GWAS confirmed that some of the previously reported NE sensitivity loci (*Tsn1*, *Snn1*, *Snn2* and *Snn3*) contributed to SNB leaf blotch susceptibility at the adult plant stage. In addition, haplotype analysis found a QTL on chromosome 2A, different to *QSnb.niab-2A.3* identified in the UK MAGIC population, showing consistent effect on SNB resistance across seven of the nine years under study. However, the resistant haplotype was rare in both Norwegian winter wheat and spring wheat lines and was only found in lines with German or CIMMYT origin. Integrating this resistant allele in Norwegian wheat germplasm would help to improve the SNB resistance in Norway.

Sammendrag

Hveteaksprikk (SNB) forårsaket av den nekrotrofe soppen *Parastagonospora nodorum* er den viktigste bladflekksjukdommen på hvete i Norge. Den forårsaker symptomer både på bladene og i aksene, og kan gi avlingstap på opptil 30% under varme og fuktige forhold. Fullstendig resistens mot hveteaksprikk er ikke tilgjengelig. Siden resistens mot symptomer på blad og aks blir kvantitativt nedarvet men kontrollert av forskjellige genetiske mekanismer, er det utfordrende å foredle resistens mot hveteaksprikk. I løpet av de siste tiårene har det blitt gjort store framskritt i forståelsen av samspillet mellom nekrotrofe effektorer (NEs) fra *P. nodorum* og korresponderende sensitivitets-gener (*Snn*) i hvete på småplantestadiet. Selv om disse interaksjonene viser noe effekt under feltforhold, er korrelasjonene mellom småplanteresistens og feltresistens generelt lav. Økt kunnskap om den norske *P. nodorum*-populasjonen og hvilke resistensgener som finnes i dagens sortsmateriale vil være til stor hjelp for framtidig resistensforedling og videre studier av patogen-vertsplante-samspill for denne sykdommen.

Del 1: Genetiske studier av den norske *P. nodorum*-populasjonen. I den første delen av doktorgradsarbeidet studerte jeg den genetiske variasjonen i den norske *P. nodorum*-populasjonen og sammenlignet allelfrekvensene til de tre kjente *P. nodorum* NE-genene (*SnToxA*, *SnTox1* og *SnTox3*) med andre europeiske populasjoner. Jeg fant at den norske *P. nodorum*-populasjonen gjennomgikk seksuell rekombinasjon og hadde høy genetisk variasjon, mens det ikke ble observert tegn til populasjonsstruktur. I tillegg var alle tre NE-gener vanlige i den norske *P. nodorum*-populasjonen. Imidlertid ble det funnet signifikant høyere frekvens av *SnToxA* i den norske *P. nodorum*-populasjonen, og vi antar at det skyldes lokal adaptasjon til den høye frekvensen av det korresponderende sensitivitetsgenet *Tsn1* i de norske vårhvetesortene. Dette arbeidet antyder at *P. nodorum*- populasjonen i Norge har et høyt evolusjonspotensial og raskt kan tilpasse seg lokale sorter.

Del 2: Kartlegging av resistens i en britisk MAGIC populasjon. I denne delen ble det utført studier for å kartlegge kvantitative gener (QTL) for resistens mot hveteaksprikk både på småplantestadiet og voksenplantestadiet. I samsvar med tidligere studier fant vi at småplanteresistens og feltresistens var dårlig korrelert, som antagelig skyldtes at forskjellige NE ble produsert av isolater som ble brukt i veksthus sammenlignet med den naturlige populasjonen i felt. Ett robust QTL for feltresistens, *QSnb.niab-2A.3* på kromosom 2A ble avdekket i den britiske MAGIC-populasjonen

'NIAB Elite MAGIC' for resistens mot symptomer i aksene i ett år og resistens mot symptomer på bladene over år, steder og inokuleringsmetoder. Imidlertid avslørte haplotypeanalyser av dette QTL-et at resistensen mot symptomer på bladene og i aksene styres av koblede, men forskjellige gener. I tillegg ble *QSnb.niab-2A.3* også identifisert ved å infiltrere kulturfiltrat av et isolat som produserer ukjente effektor. Det indikerer at den underliggende mekanismen til *QSnb.niab-2A.3* kan være en ny NE-*Snn*-interaksjon.

Del 3: Kartlegging av resistens i en tysk MAGIC populasjon. I denne studien ble *QSnb.niab-2A.3* validert under feltforhold i en annen MAGIC populasjon basert på tyske høsthvetesorter, 'BMWpop'. Dette QTL-et har derfor potensiale til å forbedre hveteaksprikkresistensen i europeisk høsthvete ved bruk av markørassistert seleksjon (MAS). I tillegg ble det avdekket et QTL på kromosom 5A som var robust over år, og spesifikt for 'BMWpop'. Det ble videre vist additive effekter av å kombinere resistensallellene fra QTL-ene på 2A og 5A. Det er nyttig å inkludere genetiske variasjon fra flere sorter når man skal kartlegge resistens og MAGIC populasjoner representerer en effektiv måte å gjøre det på.

Del 4: Assosiasjonskartlegging av hveteaksprikkresistens. Assosiasjonskartlegging ble gjennomført ved bruk av to paneler bestående av nordiske høsthvete (102)- og vårhvetelinjer (296) genotypet med 35K Axiom array. Dette arbeidet bekreftet at noen av de tidligere rapporterte sensitivitetsgenene (*Tsn1, Snn1, Snn2, Snn3*) bidro til mottagelighet for hveteaksprikk under feltforhold. I tillegg fant vi et QTL på kromosom 2A, forskjellig fra *QSnb.niab-2A.3*, som hadde konsistent effekt på hveteaksprikk i sju av de ni årene som ble studert. Den resistente haplotypen var imidlertid sjelden i både norsk høsthvete og vårhvete, og ble bare funnet i linjer med tysk eller CIMMYT-opprinnelse. Å integrere dette resistensallelet i norsk hvete vil være et nyttig bidrag til resistensforedlingen.

List of papers

I. Genetic population structure of Norwegian *Parastagonospora nodorum* population
Min Lin, Andrea Ficke, James Cockram, Morten Lillemo
Submitted manuscript

II. Genetic mapping using a wheat multi-founder population reveals a locus on chromosome 2A controlling resistance to both leaf and glume blotch caused by the necrotrophic fungal pathogen *Parastagonospora nodorum*
Min Lin, Beatrice Corsi, Andrea Ficke, Kar-Chun Tan, James Cockram, Morten Lillemo
Accepted in Theoretical and Applied Genetics

III. Identification and cross-validation of *Parastagonospora nodorum* blotch sensitivity genetic loci using a multi-founder winter wheat population
Min Lin, Melanie Stadlmeier, Volker Mohler, Kar-Chun Tan, Andrea Ficke, James Cockram, Morten Lillemo
Manuscript

IV. Genome-wide association mapping of Septoria nodorum blotch resistance in both a Nordic winter and spring wheat collection
Min Lin, Andrea Ficke, Jon Arne Dieseth, Morten Lillemo
Manuscript

1. Introduction

1.1 Wheat

Wheat (*Triticum spp.*) domestication was thought to have been initiated ca. 10,000 years ago in the Fertile Crescent (Salamini et al. (2002). The global production of wheat in 2017 was around 772 million tonnes (FAO 2017), with allohexaploid bread wheat (*Triticum aestivum* L., AABBDD) dominating wheat production as the most widely grown cereal species. As one of the most important staple food sources, wheat production is a key component of global food security. However, cultivation of this important crop is limited by many stresses, including biotic pressures such as fungal diseases.

Norway is located in western Scandinavia (57-71° N) with a total land area about 324,000 km^2, of which only 3% is arable land (Statistics Norway 2020). The main wheat growing areas are in south-eastern Norway where the climate is more continental with less rainfall compared to the west coast. The average wheat yields in Norway are around 5 tons per hectare, but can be variable due to changes in prevailing growing conditions (Lillemo and Dieseth 2011). In Norway, growing winter wheat usually results in higher yield, however, owing to the difficulties of sowing in rainy autumns, cultivated winter wheat area varies every year in comparison with the relatively more stable cultivated area of spring wheat (45-65,000 ha) (Statistics Norway 2020). As well as high yield and baking quality, wheat breeders in Norway also focus on producing early-maturing varieties with resistances to diseases, lodging and pre-harvest sprouting (Lillemo and Dieseth 2011). Major diseases that challenge the Norwegian wheat production are powdery mildew (PM), Septoria nodorum blotch (SNB), Fusarium head blight (FHB) (Lillemo and Dieseth 2011), as well as yellow rust which has reoccurred in recent years (Abrahamsen et al 2017).

There is strong evidence that hexaploid bread wheat was derived from multiple rounds of naturally occurring hybridization events during its evolutionary history, resulting in the three related subgenomes (A, B and D) that compose the bread wheat genome (Marcussen et al. 2014). Due to its large genome size (approx. 16 Gb), genetic studies of wheat were among the most complicated of all cultivated plants (International Wheat Genome Sequencing 2014). In addition, the large proportion of repetitive DNA (more than 85%) in the genome has made the map-based cloning of

individual genes difficult (International Wheat Genome Sequencing et al. 2018). For example, many hundreds of wheat quantitative trait loci (QTL) have been published so far but few have been characterized at the sequence level (Bernardo 2016; International Wheat Genome Sequencing et al. 2018). Less than 15 wheat disease resistance genes had been cloned before the first wheat sequence draft released in 2014 (Keller et al. 2018). Recently, with the improvement in sequencing technology, an annotated reference genome assembly for bread wheat has become available (cv. Chinese Spring, IWGSC RefSeq v1.0), which has greatly facilitated wheat genetics research (International Wheat Genome Sequencing et al. 2018). Based on the common annotated reference genome, the relative positions of QTL characterized by different genetic maps and molecular markers have now become more straightforward to compare. Moreover, the annotated gene models within QTL intervals provide potential candidates for further application of genome editing technologies, such as CRISPR/Cas9 (Wolter et al 2019) and functional validation of candidate genes (Adamski et al 2019), which reduce both the time and cost of traditional map-based cloning.

1.2 Pathogen

Parastagonospora nodorum (syn. *Phaeosphaeria nodorum* (E. Müll.), syn. *Leptosphaeria nodorum* (E. Müll.), syn. *Stagonospora nodorum* (Berk.), syn. *Septoria nodorum* (Berk.)) is a typical necrotrophic fungal pathogen belonging to the Ascomycota as a member of the Dothideomycetes class (Quaedvlieg et al. 2013). *P. nodorum* is known mostly as a wheat pathogen, but was also reported to infect barley (*Hordeum vulgare*) occasionally and with less damage, reviewed by Cunfer (2000), as well as wild grasses (Williams and Jones, 1973). The disease caused by *P. nodorum* is most commonly called Septoria nodorum blotch (SNB), but also known as Stagonospora nodorum blotch. When *P. nodorum* infects glumes, the resulting disease is called wheat glume blotch (Oliver et al. 2016).

1.2.1 Symptoms

Symptoms of *P. nodorum* infection on wheat leaves start as oval brown necrotic lesions surrounded by chlorosis and develop into irregular dark brown lesions later on (Fig. 1a). In the field, the symptoms can easily be confused with those caused by two other important wheat leaf blotch fungal diseases: septoria leaf blotch (STB) (caused by *Zymoseptoria tritici*) and tan spot (TS) (caused by *Pyrenophora tritici-repentis*) (Ficke et al. 2018a). Co-infection of these three diseases is common in Norwegian field conditions. However, as both STB and TS are well-known as leaf

diseases which seldom cause symptoms on wheat heads, glume infection is an important indicator of SNB infection. Fig. 1b. shows the SNB symptoms on wheat heads, which start from brown to dark brown spots on the glumes.

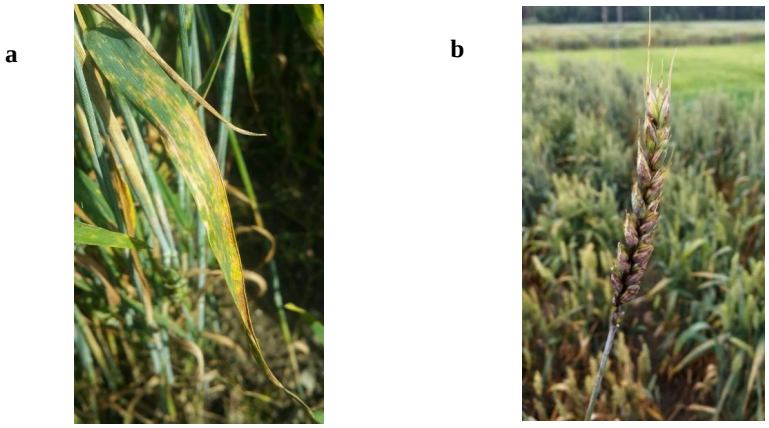

Fig. 1. Symptoms of Septoria nodorum blotch in wheat. (a) Symptoms on leaves (b) Symptoms on head.

1.2.2 Infection cycle and epidemics

P. nodorum is a heterothallic fungus which requires two mating type idiomorphs in the population for sexual reproduction (Bennett et al. 2003). Wind-spread ascospores released from wheat debris are considered as the major primary source of inoculum early in the season (Bathgate and Loughman 2001). As shown in Fig. 2, *P. nodorum* is also seed-transmitted (Sommerhalder et al. 2006). Infected seeds can also be a source of primary inoculum when seed treatments are poorly applied. Once the pathogen has established the initial infection on a plant, large amounts of pycnidiospores can be spread through rain splash to neighboring plants. The pathogen is polycyclic and can complete multiple cycles in one growing season, producing a considerable amount of pycnidiospores as secondary inoculum (Eyal et al. 1987; Sommerhalder et al. 2011).

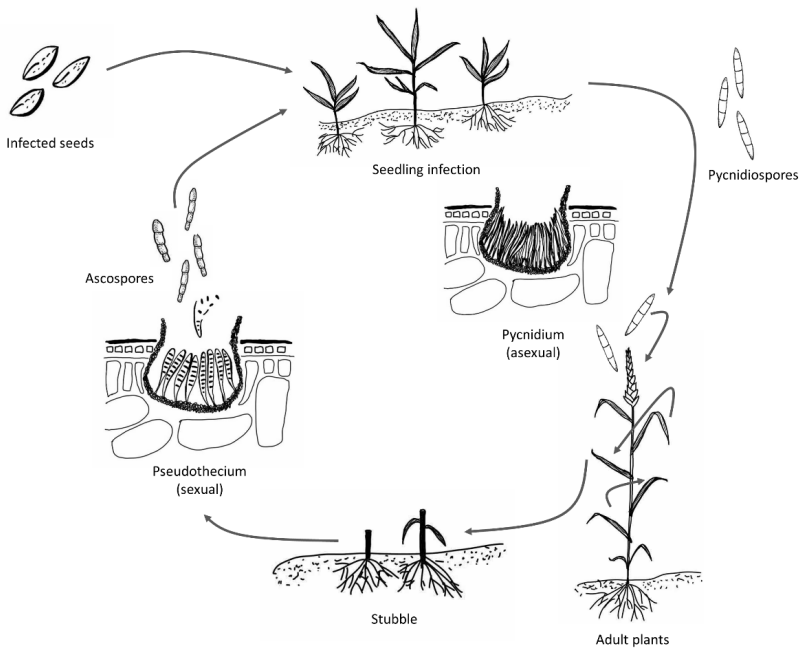

Fig. 2 Infection cycle of *P. nodorum*. Drawing by Ling Su, adapted from Sommerhalder et al. (2011).

Epidemics of *P. nodorum* used to be common in all wheat growing areas with suitable climatic condition for disease development on all six wheat growing continents (Ficke et al. 2018a; Leath et al. 1993). The pathogen shares the same center of origin as its wheat host in the Fertile Crescent and probably spread during wheat germplasm exchange (McDonald et al. 2012). As mentioned previously, *P. nodorum* and *Z. tritici* often cause coinfection on the host in the same field, because their asexual spores are both spread by rain splash and prefer to grow in similar warm and humid conditions (Bearchell et al. 2005). Before the 1980s, *P. nodorum* was the dominating pathogen in the leaf blotch complex in Europe (Bearchell et al. 2005). However, nowadays in the European Union (EU) the dominance of *P. nodorum* has been replaced by *Z. tritici*, and large proportions of fungicide applications are now due to STB management (Bearchell et al. 2005; Shaw et al. 2008; Torriani et al. 2015). The decrease in sulfur pollution has been correlated with the reduction of *P. nodorum* epidemics in the UK (Shaw et al. 2008). However, the same sulfur theory could not

explain the dominance of *P. nodorum* in western Australia (Oliver et al. 2012), or Norway, which is one of the remaining *P. nodorum* hotspots in Europe.

1.2.3 Population genetics studies of *P. nodorum*

As *P. nodorum* undergoes frequent sexual reproduction, high frequency of recombination results in high genetic diversity in the pathogen population (McDonald and Linde 2002). *P. nodorum* population structure studies have been carried out based on different molecular markers or sequence variations of selected genes (McDonald et al. 2012; Murphy et al. 2000; Stukenbrock et al. 2006). McDonald et al. (1994) investigated the genetic variability of two *P. nodorum* populations in the US with eight restriction fragment length polymorphism (RFLP) markers and high level of genetic diversity was found even among isolates collected from the same lesion. A similar population genetic study was carried out to investigate genetic variation between and within *P. nodorum* populations collected from Europe and the US (Keller et al. 1997). Results indicated evidence of high gene flow but little evidence of genetic differentiations between populations (Keller et al. 1997). A western Australian *P. nodorum* population genetic study was undertaken using the same RFLP markers described above, and no evidence of population subdivision was observed due to high genetic variability within the population (Murphy et al. 2000). Stukenbrock et al. (2006) used 12 simple sequence repeat (SSR) markers to characterize the population structure of an international *P. nodorum* collection, which consisted of nine populations from five continents. As expected, high levels of genetic diversity was observed within each population (Stukenbrock et al. 2006). However, moderate population differentiation was found from this study (Stukenbrock et al. 2006). McDonald et al. (2013) compared the genetic diversity of three *P. nodorum* necrotrophic effector (NE) genes (*SnToxA*, *SnTox1* and *SnTox3*), in which they found significant differences in allele frequencies of the three genes among populations. However, *P. nodorum* populations with high *SnTox* gene sequence diversities were not correlated with high diversity at neutral loci, as the *SnTox* genes were under selection by local host cultivars (McDonald et al. 2013).

1.2.4 Agricultural importance and disease management

In modern agro-ecosystems, where high density of crops are grown, favorable environments are provided for multi-infections where different strains of the same pathogen could infect the same host, especially for pathogens with large population sizes combined with high genotypic diversity

(McDonald and Stukenbrock 2016; van Baalen and Sabelis 1995). It also promotes the development of virulence due to competition between strains from the same pathogen species and/or among pathogen species under co-infection conditions (McDonald and Stukenbrock 2016; van Baalen and Sabelis 1995). As described in **1.2.2**, SNB is the major leaf blotch disease in Norway, which reduces both wheat yield and grain quality. Under favorable climate conditions, *P. nodorum* can reduce yield up to 30% (Bhathal et al. 2003). The primary inoculum of SNB is mostly ascospores originating from wheat debris (Bathgate and Loughman 2001). Reduced tillage is advocated to reduce soil erosion; however, this practice leads to higher amounts of infected wheat straw on the soil surface, which can serve as primary inoculum (Ficke et al. 2018a). In addition, the pycnidiospores are spread by rain-splash. The high density of plants within the wheat fields makes it easier for pycnidiospores to spread to neighboring plants.

Disease management of SNB includes cultivar resistance, fungicide treatment and stubble management. Resistance to SNB is a quantitative trait and many resistance QTL have been reported by different studies, reviewed by Ruud and Lillemo (2018). However, currently no cultivar has been found to show complete resistance against SNB (Aguilar et al. 2005). In addition, resistances to SNB leaf blotch and glume blotch might be controlled by different genetic mechanisms (Aguilar et al. 2005; Wicki et al. 1999), which adds to the difficulties of SNB resistance breeding. Most known SNB resistance mechanisms are due to lack of susceptibility genes (*Snn*) in wheat genotypes to corresponding *P. nodorum* NEs (Ruud and Lillemo 2018). So far, two wheat genes (*Tsn1* and *Snn1*) associated with leaf blotch susceptibility have been cloned (Faris et al. 2010; Shi et al. 2016), while no SNB resistance gene has been cloned. Recently, Zhang et al. (2019b) reported the genetic introgression of novel resistance genes to both tan spot and SNB from the diploid wheat species *Aegilops speltoides* to bread wheat by chromosome engineering, which provided new resistance resources and opportunities to investigate SNB resistance mechanisms other than the NE-*Snn* interactions.

Both seed treatment and fungicide application in the field are widely used chemical control methods for SNB management (Solomon et al. 2006). However, Blixt et al. (2009) reported that the majority of tested Swedish *P. nodorum* isolates showed reduced sensitivity to strobilurins, which was caused by amino acid substitutions in the *cytochrome b* gene. Pereira et al. (2017) reported variations in sensitivities to sterol demethylation inhibitors (DMIs) within a global *P.*

nodorum collection, and the reduced sensitivity was due to non-synonymous mutations in the *CYP51* gene. Neither study included *P. nodorum* isolates collected in recent years (2011 - present) for fungicide resistance testing. Therefore, higher frequency of fungicide insensitive isolates would be expected in the natural *P. nodorum* population due to the high selection pressure. However, field resistance to azoles or DMI have not been reported so far.

As mentioned previously, reduced tillage increases the amount of crop residues that can serve as inoculum for residue-borne leaf blotch diseases (Ficke et al. 2018a; Shaner 1995). And as expected, significant correlations have been observed between the amount of residues and SNB disease severity in the field (Mehra et al. 2015). Residue management (e.g. burial of residues and crop rotation) can effectively decrease the amount of primary inoculum and reduce disease severity when healthy seeds are used (Mehra et al., 2015)

1.3 Inverse gene for gene interaction in the wheat-*P. nodorum* pathosystem

The gene-for-gene model was firstly characterized to describe the interaction between *Linum usitatissimum* and the flax rust fungal pathogen *Melampsora lini* (Flor 1956; Flor 1971), which was later applied to interactions between other biotrophic pathogens and their host plants. As biotrophic pathogens require living host tissues, when the host plant contains the resistance (R) gene able to recognize the product of a pathogen`s avirulence (Avr) gene, a hypersensitive reaction (HR) will be induced resulting in plant cell death (PCD), thus limiting the infection of the biotrophic pathogens (Fig. 3a). On the contrary, necrotrophic pathogens, such as *P. nodorum*, utilize nutrients from dead or dying host tissues and interact with host plants via an inverse gene-for gene model (Friesen et al. 2007). Via the production of necrotrophic effectors (NEs) which interact with host susceptibility genes (*Snn*), necrotrophic pathogens can trigger PCD to accelerate their infection (Fig. 3b).

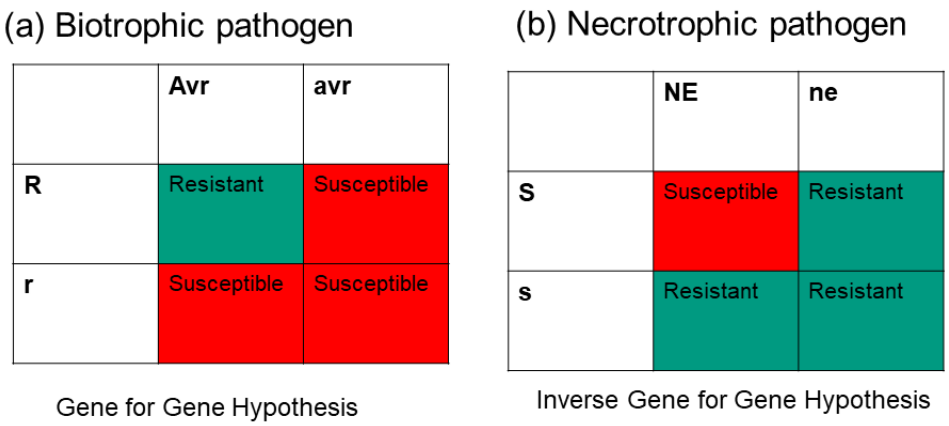

Fig. 3: Different plant-pathogen interaction mechanisms. (a): Gene-for gene model, adapted from Flor (1971). (b): Inverse gene-for-gene model, adapted from Friesen et al. (2007). R: resistant gene, r: absence of resistant gene; Avr: Avirulence gene, avr: absence of avirulence gene; NE: necrotrophic effector, ne: absence of necrotrophic effector; S: susceptibility gene, s: absence of susceptibility gene.

1.3.1 Well characterized NE-*Snn* interactions

Up to now, nine NE-*Snn* interactions have been described, however, only three *P. nodorum* NE coding genes and two host NE sensitivity genes have been cloned (reviewed by Peters Haugrud et al. (2019); Ruud and Lillemo (2018)). Therefore, more studies have been done regarding the interactions between the three known NE genes (*SnToxA*, *SnTox1* and *SnTox3*) and their corresponding host sensitivity loci. In this section, ToxA-*Tsn1*, Tox1-*Snn1* and Tox3-*Snn3* will be described in detail while other NE-*Snn* interactions will be only briefly reviewed.

(1) ToxA-*Tsn1*

ToxA was characterized as a 13 kDa polypeptide host selective toxin, also called necrotic effector (NE) produced by the wheat tan spot pathogen *Pyrenophora tritici-repentis*, and which interacts with the sensitivity gene *Tsn1* on the long arm of wheat chromosome 5B (Faris et al. 1996; Tomas et al. 1990). Later, Liu et al. (2006) reported that *P. nodorum* also contains the *ToxA* gene, the product of which targets the same wheat *Tsn1* locus as tan spot. Through gene diversity analysis, it has been shown that the ToxA coding gene *SnToxA* in *P. tritici-repentis* likely originated from

P. nodorum through a recent horizontal gene transfer event (Friesen et al. 2006). The cloned ToxA sensitivity gene *Tsn1* has a typical R gene structure containing nucleotide binding site (NBS) and a leucine-rich repeat (LRR) domain, as well as a serine/threonine protein kinase (S/TPK) domain (Faris et al. 2010). However, the Tsn1 protein locates to the chloroplast and does not directly interact with ToxA, suggesting that *Tsn1* may mediate the signaling pathway of effector-triggered immunity (ETI) but is not the ToxA receptor (Faris et al. 2010). Recently, it was shown that another wheat and barley pathogen *Bipolaris sorokiniana*, the cause of spot blotch, also possess a *ToxA* gene that likely originated from *P. nodorum*, pointing to a selective advantage of carrying the virulence factor ToxA (Friesen et al. 2018; McDonald et al. 2018).

(2) Tox1-*Snn1*

Tox1-*Snn1* was the first reported NE-*Snn* interaction in the wheat-*P. nodorum* pathosystem, where Tox1 was characterized as a NE produced in *P. nodorum* culture filtrates interacting with the wheat sensitivity locus *Snn1* on chromosome 1B (Liu et al. 2004a). However, the cloning of *SnTox1* was not achieved until eight years after the discovery of the Tox1-*Snn1* interaction (Liu et al. 2012). *SnTox1* encodes a cysteine rich protein with 117 amino acid which is light dependent and critical for fungal penetration (Liu et al. 2012). Further research on Tox1 showed that it serves as a dual function protein, which can bind the host chitinases to protect fungal infection as well as behaving like a virulent NE (Liu et al. 2016). In the same year, Shi et al. (2016) cloned the Tox1 wheat susceptibility gene *Snn1*, which encodes a wall-associated kinase (WAK). WAK proteins are known to be members of pattern recognition receptors (PRRs) which directly interact with pathogen-associated molecular patterns (PAMPs), such as oligogalacturonides (OGs), which trigger PCD and are involved in plant defense mechanisms against biotrophic pathogens (Brutus et al. 2010). In contrast to ToxA-*Tsn1* which interacts in the ETI pathway, the cloning of *Snn1* revealed that *P. nodorum* could also hijack the PAMP-triggered immunity (PTI) pathway against biotrophic pathogens and lead to disease (Shi et al. 2016).

(3) Tox3-*Snn3*

Tox3 was characterized after the discovery of ToxA, Tox1 and Tox2 by Friesen et al. (2008) as a novel *P. nodorum* NE, interacting with the wheat sensitivity locus designated as *Snn3* on the short arm of chromosome 5B. The Tox3 protein is around 29 kDa in size and the coding gene was cloned by Liu et al. (2009) and showed little homology to the two previously cloned *P. nodorum* NE genes

SnToxA and *SnTox1*. In addition, sensitivity to Tox3 was also shown in a diploid wheat relative species *Aegilops tauschii* and the sensitivity locus was mapped to the short arm of chromosome 5D which probably is a homoeologous locus derived from a common ancestor (Zhang et al. 2011). Accordingly, the *Snn3* loci present in bread wheat and *Ae. tauschii* are now denoted *Snn3-B1* and *Snn3-D1*, respectively.

(4) Other characterized but not cloned NE-*Snn* interactions

Tox2 was the third *P. nodorum* NE to be characterized. It interacts with the wheat *Snn2* locus located on the short arm of chromosome 2D (Friesen et al. 2007). The estimated size of Tox2 is between 7-10 kDa (Friesen et al. 2007). Tox4-*Snn4* was characterized as a light dependent interaction, where Tox4 was estimated to be a protein 10 to 30 kDa in size interacting with the sensitivity locus *Snn4* on the short arm of wheat chromosome 1A (Abeysekara et al. 2012; Abeysekara et al. 2009). Tox5-*Snn5* is another light-dependent interaction characterized using a tetraploid wheat mapping population, where Tox5 was also shown to have a size range between 10-30 kDa and the *Snn5* locus was mapped to the long arm of chromosome 4B (Friesen et al. 2012). Gao et al. (2015) reported the eighth NE-*Snn* interaction Tox6-*Snn6*. As well as previously described NE-*Snn* interactions, Tox6-*Snn6* is light dependent (Gao et al. 2015). Tox6 is a small secreted protein with estimated size between 6.5-12.3 kDa and the *Snn6* locus was mapped to the long arm of chromosome 6A (Gao et al. 2015). To date, Tox7-*Snn7* is the latest characterized NE-*Snn* interaction. Tox7 is a small secreted protein less than 30 kDa in size and interacting with the wheat *Snn7* locus on the long arm of chromosome 2D (Shi et al. 2015). Interestingly, except Tox3-*Snn3* and Tox7-*Snn7*, all other NE-*Snn* interactions are strictly light dependent, suggesting that Tox3-*Snn3* and Tox7-*Snn7* may exploit different pathways compared to other known NE-*Snn* interactions (Shi et al. 2015).

1.3.2 Relationship between NE-*Snn* interactions and field SNB severity

Previous studies showed that SNB seedling resistance and adult plant resistance were not highly correlated (Francki 2013; Ruud and Lillemo 2018; Shankar et al. 2008; Uphaus et al. 2007), which could be due to the use of different isolates in the greenhouse experiments than in the field testing (Ruud and Lillemo 2018; Ruud et al. 2017). Therefore, when the same isolate is used for both seedling testing and adult plant testing in the field, the correlations between seedling and adult plant leaf resistance can be relatively high (Jönsson 1985). However, in general, the correlations

between SNB resistance at these two different growing stages are low. Since the natural *P. nodorum* population is usually quite genetically diverse, it is difficult to identify representative isolates for greenhouse assays. In addition, even though Shankar et al. (2008) used the same isolate mixture for inoculation in the greenhouse and in the field in the year 2003, they found the Pearson`s correlation coefficient between seedling and flag leaf disease scores were low (0.31), or even not significant between seedling and glume blotch severity (0.09). However, results of field testing might still be influenced by the natural *P. nodorum* population even though specific isolate or isolates mixture are used as inoculum.

Although all NE-*Snn* interactions were firstly characterized in greenhouse conditions by seedling inoculations and infiltrations, there is evidence that some NE-*Snn* interactions also contribute to field SNB susceptibilities (reviewed by Ruud and Lillemo 2018). Friesen et al. (2009) used an isolate producing both ToxA and Tox2 for spray inoculation in the field on a mapping population segregating for *Tsn1*, *Snn2* and *Snn3-B1*. They found the *Tsn1* and *Snn2* loci to explain 18% and 15% of phenotypic variation, respectively. Another study applied artificial inoculation of an isolate producing all three known NEs, showing that the *Snn1* locus explained 19% of the phenotypic variation for disease severity on adult plants (Phan et al. 2016). Furthermore, a field study conducted with natural *P. nodorum* inoculum showed that *Snn3-B1* was the major determinant of SNB susceptibility in the SHA3/CBRD×Naxos population, explaining up to 24% of the phenotypic variation (Ruud et al. 2017). Whether there are additional NE-*Snn* interactions playing roles in adult plant susceptibilities is still unexplored.

1.3.3 Relationship between SNB adult plant leaf blotch and glume blotch resistance

As described in **1.2.1**, *P. nodorum* causes symptoms on both wheat leaves and glumes. Both traits have been reported to be quantitatively inherited (Wicki et al. 1999). However, previous studies reported that SNB resistance to leaf blotch and glume blotch were mainly controlled by different genetic mechanisms, since few QTL in common were detected (except for those QTL caused by other confounding morphological traits such as plant height, heading date, etc.) (Aguilar et al. 2005; Francki et al. 2018; Schnurbusch et al. 2003; Shankar et al. 2008). To our knowledge, no glume blotch resistance QTL has been characterized at the sequence level nor being applied in marker assisted breeding (MAS).

1.3.4 Current status of SNB knowledge in Norwegian wheat

As described in **1.2.2**, SNB is the dominating wheat leaf blotch disease in Norway. In order to improve SNB resistance in Norwegian germplasm, genetic studies on SNB field resistance started in 2010 in Norway and SNB resistant QTL were detected on wheat chromosomes 1B, 3A, 3B, 5B, 7A and 7B in the SHA3/CBRD × Naxos population (Lu and Lillemo 2014). Ruud et al. (2017) used the same population for both greenhouse and field testing and confirmed that the QTL on the short arm of chromosome 5B detected in the previous study (Lu and Lillemo 2014) was the Tox3 sensitivity locus *Snn3-B1*, which showed a major effect on wheat susceptibility at both seedling and adult plant stages. In addition, by screening the sensitivities to three known NEs, Ruud et al. (2018) found that large proportions of Norwegian spring wheat lines possess the NEs sensitivity genes *Tsn1* and *Snn3-B1*. Interestingly, *SnToxA* and *SnTox3* frequencies in their Norwegian *P. nodorum* isolate collections were also quite high, with *SnToxA* and *SnTox3* frequencies of 69% and 76%, respectively (Ruud et al. 2018). A recent study by Ruud et al. (2019) found many stable adult plant resistant QTL by GWAS using a collection of 121 Nordic spring wheat cultivars and breeding lines. Among those, one QTL on chromosome 2D was robust in most of the tested years and significant correlations were found between field disease severity and sensitivity to ToxA (Ruud et al. 2019). However, although ToxA sensitivity is common in Norwegian spring wheat cultivars and showed positive correlation with SNB severity in the field (Ruud et al. 2018), the *Tsn1* locus was not significantly detected by this association study (Ruud et al. 2019).

1.4 Linkage QTL mapping and genome wide association scans (GWAS)

1.4.1 Molecular markers in wheat

Due to the complexity and size of the wheat genome, molecular markers are widely used for genotyping wheat materials and identifying QTL associated with different traits (Langridge et al. 2001). The first generation of molecular markers were Southern hybridization-based (Southern 1975) restriction fragment length polymorphisms (RFLP), where polymorphisms can be visualized on film after cleavage of the DNA fragment by specific endonucleases and radio labelling, reviewed by Kiszonas and Morris (2018). Later, polymerase chain reaction (PCR) based marker systems became available for wheat genotyping, including random amplification of polymorphic DNA (RAPD), amplified fragment length polymorphisms (AFLP) and simple sequence repeat (SSR, also known as microsatellites) (Kiszonas and Morris 2018; Langridge et al. 2001). Diversity

Arrays Technology (DArT) was first developed for rice genotyping which could simultaneously genotype several thousands of loci using a single microarray (Jaccoud et al. 2001), and subsequently applied to hexaploid wheat in 2006 (Akbari et al. 2006). Due to the high-throughput capability and low cost per sample, nowadays, the most commonly used molecular markers for wheat genotyping are array based single nucleotide polymorphisms (SNPs) (Allen et al. 2017). Several SNP chips have been developed specially for characterizing genotypic variations in wheat, for instance Illumina 90K SNP chip (Wang et al. 2014a) and "the wheat breeder`s array"-Axiom 35K SNP chip (Allen et al. 2017). In addition, SNPs can be used for developing Kompetitive Allele Specific PCR (KASP) markers (Semagn et al. 2014) to genotype a limited number of significant SNPs from QTL analysis and for application in marker assisted selection (MAS). With the development of next generation sequencing technologies and the resulting reduction in cost per sample, the genotyping-by-sequencing (GBS) approach is also available for wheat genetic studies and provides high SNP coverage (Alipour et al. 2019; Hu et al. 2019).

1.4.2 Bi-parental genetic mapping populations

In crops, bi-parental populations are typically created by crossing two parents with contrasting variation at the target trait(s). Through either several rounds of selfing to generate the recombinant inbred lines (RILs) or through chemical treatment to generate doubled haploid (DH) lines, all progenies in the population are homozygous (Cavanagh et al. 2008). Such bi-parental populations have a major advantage that high genetic map resolutions are usually not required in order to detect QTL (Cavanagh et al. 2008; Gupta et al. 2014). All previously described NE-*Snn* interactions were mapped by bi-parental populations, and therefore benefited from the high power of bi-parental populations to detect major QTL (Gupta et al. 2014; Ruud and Lillemo 2018). However, the main disadvantage of using bi-parental population is that the recombination rate is relatively low which makes them cumbersome for either fine mapping or gene cloning (Bernardo 2016; Cavanagh et al. 2008; Huang et al. 2012). In addition, owing to the interaction between QTL and genetic background, it is harder to validate a QTL from one mapping population on another mapping population with different genetic background (Bernardo 2016). Moreover, as the QTL may not segregate in current breeding programs or elite breeding materials, relatively few QTL detected in genetic research have been utilized in practice for crop breeding (Bernardo 2016).

1.4.3 Genome wide association scans (GWAS)

Association mapping (AM) panels used for genome wide association scans (GWAS) are usually collections of germplasm with diverse genetic backgrounds (Bernardo 2016). As an alternative approach to genetic mapping using bi-parental populations, GWAS has two main advantages. First, the AM panel saves the cost and time to construct mapping populations (Bernardo 2016; Gupta et al. 2014). Second, the genetic diversity and map resolution are higher in an AM panel compared to bi-parental populations, since multiple historical recombination and multiple alleles per locus are available in diverse germplasm collections (Bernardo 2016; Gupta et al. 2014). However, genetic subpopulation structure in AM panels may result in false positive associations (Breseghello and Sorrells 2006; Gupta et al. 2014). In addition, GWAS analysis has its limitation for detecting QTL associated with rare alleles or rare variants, therefore it can only be used for detecting QTL controlled by alleles with relatively high allele frequency in the panel (Bernardo 2016; Breseghello and Sorrells 2006; Gupta et al. 2014).

1.4.4 Multi-parental populations: multi-parent advanced generation intercross (MAGIC) and nested association mapping (NAM)

Multiparent advanced generation intercross (MAGIC) population design involves intercrossing of multiple parental lines (2^n), followed by several rounds of selfing to achieve a RIL population (Cavanagh et al. 2008). Nested association mapping (NAM) population design involves many crosses between one common founder parent and several other parents, resulting in a collection of many bi-parental populations which share a common founder parent. Both MAGIC and NAM populations allow for increased allelic diversity and genetic recombination relative to comparatively sized bi-parental populations, while reducing the risk of false positive associations caused by the population structure commonly present in AM panels (Bajgain et al. 2016; Cavanagh et al. 2008; Kover et al. 2009; Mackay et al. 2014; Yu et al. 2008). In addition, interval mapping and association analysis methodologies can be applied to both MAGIC and NAM populations for coarse mapping as well as fine mapping (Cavanagh et al. 2008; Gupta et al. 2014). However, the focus of these two multi-parental population designs are slightly different. As elite cultivars were used as founders, MAGIC was intended to map QTL in breeding relevant germplasm, especially for QTL which are suitable for MAS. In contrast, NAM focuses more on positional cloning of QTL, especially where the underlying beneficial alleles originate from more diverse germplasm (Ladejobi et al. 2016; Paux et al. 2012). Simulation studies by Ladejobi et al. (2016) showed that

both eight-parent and sixteen-parent MAGIC represented a higher potential of haplotype diversity compared to NAM, suggesting MAGIC was superior to NAM for loose linkage. To date, many wheat MAGIC and NAM populations have been developed, representing useful resources to assist wheat genetics research (Huang et al. 2012; Jordan et al. 2018; Mackay et al. 2014; Stadlmeier et al. 2018; Zhang et al. 2019a).

2. The thesis

2.1 Background and main objectives

Cultivar resistance is usually considered as both an effective and environmentally friendly control method in crop disease management. However, the durability of cultivar resistance is always being challenged due to the long timeframe required for resistance breeding and the fast evolution of virulent pathogens. The pathogen population can adapt to new sources of host resistance quickly once a new cultivar is released to the market. Therefore, knowledge of the pathogen population is vital to optimize resistance breeding strategies and to help exploit the limited resistance resources in an effective way. In addition, apart from improving the usage of cultivar resistance, knowledge of the local pathogen population would also be beneficial to improve other disease management approaches such as chemical application and agronomic control methods. For example, a pathogen population, which undergoes regular sexual reproduction has a high mutation rate, high gene flow and a large population size, is considered to have high evolutionary potential. Typically, the risk of breaking qualitative cultivar resistance is high for such populations. Additionally, fungicide resistance alleles may also spread quickly in such a population when it is under high selection pressure. Moreover, as such populations evolves rapidly, they will also adapt to changing environments quickly. Therefore, such characteristics of the pathogen population should be understood to adjust the disease management. For instance, stacking different qualitative resistance genes or using quantitative resistance to breed resistant cultivars should be used, in order to make it more difficult for a highly adaptive pathogen population to overcome host resistance.

In order to gain knowledge of the local Norwegian *P. nodorum* pathogen population, we genotyped a collection of 165 Norwegian *P. nodorum* isolates and 9 foreign isolates using 20 SSR markers, three known *SnTox* genes (*SnToxA*, *SnTox1* and *SnTox3*) and two mating type idiomorphs. We used different methods to analyze whether the pathogen population could be subdivided by location, time, or the cultivars the isolates were collected from. We observed co-infection of *P. nodorum* and *Z. tritici* on Norwegian winter wheat but less on Norwegian spring wheat. Therefore, we hypothesized to find differences between pathogen populations on different wheat types due to different competition pressure. Moreover, we analyzed the allele frequencies of *SnTox* genes and investigated whether local adaptation was evident due to these virulence factors.

Cultivar resistance to SNB is still insufficient and currently no cultivar shows complete resistance to SNB. One of the main objectives of this study was to identify loci associated with SNB resistance in breeder-relevant germplasm in order to improve SNB resistance breeding. On the other hand, NE-*Snn* interactions in the wheat-*P. nodorum* pathosystem have been studied for a decade, with a limited number of such interactions shown to play an important role in SNB susceptibility. Up to now, nine NE-*Snn* interactions have been characterized. However, as the *P. nodorum* population is typically characterized by high genetic diversity, we hypothesized that additional NE-*Snn* interactions might be present, but have not been discovered. One objective of this study was therefore to discover potential novel NE-*Snn* interactions. In addition, although only a limited number of NE-*Snn* interactions show effects in the field, whether field resistance/susceptibility can be more fully explained by additional NE-*Snn* interactions remains unexplored. In this study, we investigated SNB resistance on seedlings by culture filtrate (CF)/NE infiltration and by inoculation, as well as on adult plants by field testing. By comparing QTL identified from seedling and field testing, we investigated the relationship between NE-*Snn* interactions in both controlled environments at the seedling stage and under field conditions at the adult plant stage. Moreover, *P. nodorum* infection can cause symptoms on both wheat leaves and glumes. However, previous research showed that the resistance to leaf blotch and glume blotch were controlled by different mechanisms. Here, we assessed SNB leaf blotch and glume blotch on the same mapping population in the same field trials to investigate the relationship between the two. Additionally, we screened SNB disease severity of a second MAGIC population (BMWpop) adapted to a different agricultural environment than the NIAB Elite MAGIC population. Lastly, in order to further explore robust SNB QTL for adult plant resistance, we conducted a field GWAS study using two Norwegian association mapping panels: one winter wheat panel and one spring wheat panel.

The main objectives were to:

- Investigate the genetic structure of the Norwegian *P. nodorum* pathogen population
- Evaluate NE-*Snn* interaction related QTL at both seedling and adult plant stages using one MAGIC population
- Screening SNB disease severity of a MAGIC population of Germain origin and compare QTL detected from both MAGIC populations

- Discover robust SNB resistance QTL in the field using two association mapping panels

2.2 Materials and Methods

Materials and methods are described in detail in each manuscript. This section will provide an overview of the plant and fungal materials, as well as the seedling and field disease testing assessment and data analysis methodologies.

2.2.1 Plant material

The studies in the thesis were conducted using a winter wheat MAGIC population from the UK (**paper II: NIAB Elite MAGIC**), a winter wheat MAGIC population from Germany (**paper III: BMWpop**), one Norwegian winter wheat association mapping panel and one Norwegian spring wheat association mapping panel (**paper IV: MASBASIS**). The NIAB Elite MAGIC population consists of more than 1,000 RILs and was genotyped using an Illumina iSelect 90K SNP array (Mackay et al. 2014; Wang et al. 2014a). In **paper II**, a subset of around 500 RILs were tested in Norway for four years and in the UK for two years for SNB resistance. The BMWpop consists of 394 $F_{6:8}$ RILs and was genotyped using the 15K+5K Infinium iSelect array (Stadlmeier et al. 2018). In **paper III,** the BMWpop was field tested in Norway from 2016 to 2018 for SNB resistance. MASBASIS winter wheat consists of 103 lines while MASBASIS spring wheat consists of 296 lines, and these two populations were genotyped using the 35K Axiom array (Allen et al. 2017). In **paper IV**, the MASBASIS winter wheat panel was tested for SNB resistance in field trials from 2016 to 2019, while the MASBASIS spring wheat panel was tested from 2016 to 2018.

2.2.2 Fungal materials and population structure analysis

Single spore isolates were isolated from wheat leaves collected from Norwegian wheat fields between 2015 to 2017. DNA was extracted from fungal mycelium and used for genotyping with three known NE encoding genes (Gao et al. 2015), two mating type idiomorphs (Bennett et al. 2003) and 20 SSR markers (Stukenbrock et al. 2005). Three main methods were used for testing for population structure in the Norwegian *P. nodorum* pathogen population. The first is population structure analysis using STRUCTURE v. 2.3.4 (Falush et al. 2003; Pritchard et al. 2000); the second is principal component analysis (PCA) implemented in the R package ade4 and adegenet (Dray and Dufour 2007; Jombart 2008), and the third is the `snapclust` function implemented in adegenet/R (Beugin et al. 2018; Jombart 2008).

2.2.3 Seedling infiltration and inoculation

Prior to infiltration and inoculation, three to four seeds of each genotype were sown in plastic cones. Seedlings were grown in a greenhouse at a temperature of 20/16 ℃ (day/night), 65 % humidity and 16 hours light cycle for 14 days.

For infiltration, culture filtrates (CF) were produced as described by Friesen and Faris (2012). ToxA and Tox3 were produced as described by Tan et al. (2012) and Tan et al. (2014), respectively. Approximately 50 µL of CF/NE was infiltrated to the second leaf of each seedling using a needless 1-mL syringe. Reactions to CF or NE infiltration were scored using either a 0-3 scale (Friesen and Faris 2012) (paper II: 203667 CF and ToxA; paper III: 203649 CF and Tox3) or a 0-4 scale (Tan et al. 2012) (paper II: 202579 CF and 203649 CF), where 0 always represents insensitive while 3 in the 0-3 scale and 4 in the 0-4 scale represents the highest sensitivity.

For inoculation, the spore suspension was adjusted to 1×10^6 spores/mL and sprayed to 14-day-old seedlings until runoff. After inoculation, plants were placed in a mist chamber with 100% relative humidity (RH) for 24 h and returned to greenhouse. Visual assessment was done 7 days post-inoculation using a 0-5 scale where 0 represents complete resistant while 5 represents highly susceptible (Liu et al. 2004b).

2.2.4 Field assessment

All populations mentioned in 2.2.2 were used for conducting SNB field trials in hillplots with mist irrigation and natural infected straw as inoculum, at the Vollebekk field station in Ås, southeast of Oslo, Norway for three to four years. Leaf blotch severity in Norway was scored as percentage infected leaf area per plot for four times in 2014, three times in 2016, 2017 and 2019, and twice in 2018 (due to hot and dry weather). The first leaf blotch assessment was conducted when the most susceptible line reached 70% disease severity and the following assessments were carried out two to three times with approximately one-week time intervals. Glume blotch assessment was conducted directly after the last leaf blotch assessment based on percentages of the infected glume area in the hillplot canopy.

2.3 Main results and discussion

2.3.1 How can genetic knowledge of the pathogen population be used to improve disease management?

In **paper I**, wheat leaf samples were collected from three major Norwegian wheat growing areas including five counties, from year 2015 to 2017. Single spore isolates were isolated from the leaf samples and recorded with information from the source cultivar. McDonald and Linde (2002) hypothesized that pathogen populations with combined sexual and asexual reproduction, high gene flow, high mutation rate and large population size have relatively high evolutionary potential. The *P. nodorum* population in Norway was found to perfectly fit this model. Both mating types (MAT1-1 and MAT1-2) were present in all tested locations and the ratio between the two mating types did not significantly ($p < 0.05$) deviate from 1:1 in any location, although the nationwide mating type ratio showed a slight deviation from 1:1 ($p<0.05$). Overall, the Norwegian *P. nodorum* population exhibited the signature of sexual reproduction. In addition, results from index of association (I_A) and standard index of association (r_d) also revealed that the *P. nodorum* population in Norway undergoes random mating. The potential of gene flow is high, since the ascospores from sexual reproduction are wind-dispersed and can travel long distance. Moreover, gene flow might also be caused by seed-transmission (Sommerhalder et al. 2006). It is typical in Norway that seeds are produced on contracted farms and distributed to the whole country by seed companies. This system provides a potential route of dispersal for seed-transmitted pathogens like *P. nodorum*, especially as seed treatment will not be applied when SNB infection levels are below 5% (Ficke et al. 2018b). Results from PCA, STRUCTURE and `snapclust` analyses revealed that there was no genetic population structure in the Norwegian *P. nodorum* isolate collection. The analysis of molecular variance (AMOVA) confirmed that the genetic variations were larger within location, year, cultivar or wheat type rather than between these classifications, and no population subdivisions could be observed by location, year, cultivar or wheat types. Interestingly, we even didn`t find high genetic differentiation between the Norwegian *P. nodorum* population and the nine foreign isolates included in the PCA analysis. This finding was supported by the observation that genetic distances estimated between Norwegian individual isolates were as large as, or sometimes even larger than those identified between Norwegian isolates and foreign isolates. Consistent with previous *P. nodorum* population genetic studies (Keller et al. 1997; McDonald et al. 2012; Murphy et al. 2000; Stukenbrock et al. 2006), high genetic variability was found in the

Norwegian *P. nodorum* population. Even though we found two isolates with the same SSR multilocus genotype in our collection, no clonal isolates were found in a single sampling location. This finding is also an indicator of large effective population size. As the mutation rate for a pathogen is usually fixed and generally low (McDonald and Linde 2002), large population size also means that a large number of mutants exist in the population.

Pathogens with high evolutionary potential usually have specific characteristics, such as a high potential of adaptation, high risk of breaking down qualitative host resistance, substantial advantage in competition with other pathogens, and a high risk of developing fungicide resistance (McDonald and Linde 2002). The management control for *P. nodorum* should take all these characteristics into account. The results of **paper I** showed that Norwegian *P. nodorum* isolates have significantly higher frequency of the virulence gene *SnToxA* (67.9 %) compared to a previously reported European population study (12%) (McDonald et al. 2013). We hypothesized that this large difference in *SnToxA* allele frequency was due to the local adaptation to the high frequency of the ToxA sensitivity allele *Tsn1* in Norwegian spring wheat cultivars; in Norway more spring wheat is grown than winter wheat, and lines sensitive to ToxA have been previously reported to be common in Norwegian spring wheat cultivars (Ruud et al. 2018). All of our 165 *P. nodorum* isolates were collected from 13 cultivars which covered 95% of the wheat market share from 2015 to 2017 (Table 1 and Table 2). Among these cultivars, only four are sensitive to ToxA and three of those are spring wheat cultivars. The only ToxA sensitive winter wheat cultivar is the relatively old cultivar Magnifik which had only 6 to 7% of the market share, while Mirakel, Krabat, Rabagast and Demonstrant are relatively new spring wheat cultivars which were recently introduced to the market (Table 2). Except Rabagast, the remaining three cultivars are all sensitive to ToxA (Ruud et al. 2018), implying the high frequency of ToxA sensitive alleles at *Tsn1* in current Norwegian spring wheat cultivars. The main results from **paper IV** also supported this, showing that *Tsn1* was significantly detected for one year and the across year mean in the field using the full set of the Norwegian spring wheat association panel. As mentioned in **1.3.1**, ToxA is a virulence factor of three wheat pathogens including *P. nodorum*. Though spot blotch is problematic only in climates with high temperatures, removing the *Tsn1* susceptibility gene from current wheat cultivars or the introduction of additional ToxA insensitive cultivars into the Norwegian market may reduce both SNB and tan spot infection simultaneously.

Table 1 Market share (%) of spring wheat cultivars in Norway from 2006-2017 (Åssveen et al. 2018).

Year	Mirakel	Zebra	Bjarne	Krabat	Rabagast	Demonstrant
2006	0	33.8	64.4	0	0	0
2007	0	45.4	52.2	0	0	0
2008	0	41.2	57.2	0	0	0
2009	0	40.7	57.4	0	0	0.2
2010	0	40.3	45.5	0.1	0	2.2
2011	0	33.6	39.2	0.8	0	20.7
2012	0	29.7	27.6	9.5	0	27.5
2013	0.1	43.6	22.0	10.7	0	23.3
2014	0.5	44.2	26.1	12.6	0	15.8
2015	7.3	42.9	28.7	8.5	0.3	11.9
2016	25.3	40.6	21.6	8.1	2.7	0.5
2017	44.9	26.3	18.5	7.3	2.8	0

Table 2 Market share (%) of winter wheat cultivars in Norway from 2006-2017 (Åssveen et al. 2018).

Year	Ellvis	Kuban	Olivin	Magnifik	Jantarka	KWS Ozon	Skagen
2006	0	0	15.5	48.6	0	0	0
2007	0	0	16.0	59.4	0	0	0
2008	0	0	16.0	61.5	0	0	0
2009	0	0	22.4	49.5	0	0	0
2010	2.5	0.4	27.9	44.4	0	0	0.1
2011	12.3	3.8	16.4	26.4	0	0	0.7
2012	25.7	3.4	15.9	18.6	0	0	0.7
2013	20.4	16.2	12.7	17.3	0	0	2.8
2014	36.0	9.4	18.2	13.1	0	0	3.4
2015	42.9	21.6	16.2	6.8	0	0	2.6
2016	61.1	19.6	7.0	6.2	2.2	0	0.2
2017	54.7	22.2	11.4	6.0	2.4	0.2	0.2

However, eliminating a single susceptibility gene will not manage the disease completely. As discussed earlier, qualitative resistance is easy to break by a pathogen with high evolutionary potential. *P. nodorum* isolates likely carry more than one NE gene, and could regulate the expression level of effector genes based on the host sensitivity (Peters Haugrud et al. 2019). For example, in **paper IV**, *Tsn1* was not significantly associated with SNB in the winter wheat panel, as most winter wheat lines did not carry this susceptibility gene. However, two other NE sensitivity loci *Snn1* and *Snn3*, which were not significant in the Norwegian spring wheat association panel, were significantly associated with SNB resistance/susceptibility in the winter wheat panel. One could also hypothesize that high genetic diversity and frequent sexual recombination also leads to more complicated effector profiles in the natural *P. nodorum* population. Therefore, stacking more resistance QTL is needed to decrease the SNB disease severity (**paper IV**).

As mentioned in **1.2.2**, *Z. tritici* is the dominant pathogen in the leaf blotch disease complex in many other European countries, while *P. nodorum* is still the major pathogen among the three leaf blotch pathogens in Norway (Ficke et al. 2018b). One possible explanation could be that, since more spring wheat is grown in Norway, the limited growing season of spring wheat is too short for the longer latent period in *Z. tritici* development, which limits the expansion of its population size. In the meantime, *P. nodorum* could successfully maintain large natural populations on spring wheat due to its shorter latent period (Cunfer, 1999) and rapid adaptation, which makes it more competitive in comparison to *Z. tritici* on the same host.

Resistances to different groups of fungicides have been reported in *P. nodorum* populations by different studies, as described in **1.2.4**. As Norwegian *P. nodorum* has a large effective population size and has been treated with fungicides for decades, we would expect a large amount of fungicide resistant mutations to exist in the population. When being consistently exposed to the same fungicide, the mutant allele may spread quickly in the population due to rapid sexual recombination and massive production of asexual pycnidiospores. Therefore, the large population size, frequent sexual reproduction and high genetic variability in Norwegian *P. nodorum* indicated a potentially high risk of fungicide resistance.

Thus, integrated pest management (IPM) is recommended to control SNB. Firstly, wheat debris should be removed before the next growing season in order to reduce the primary inoculum source, and consequently the pathogen population size. Alternatively, a two-year crop rotation appears to

effectively reduce the risk of leaf blotch epidemics even under conducive environmental conditions (Pedersen and Hughes, 1992). Secondly, cultivars insensitive to known effectors and possessing other resistance mechanisms should be preferred for better resistance. Thirdly, use of healthy or fungicide treated seeds should be recommended to decrease the spread of disease. Lastly, combining or rotating fungicides with different modes of action may effectively decrease the selection pressure of resistant mutants and reduce the resistant allele frequency in the pathogen population.

2.3.2 NE-*Snn* interactions at the seedling stage

Most NE-*Snn* interactions were first characterized in controlled environments using seedling inoculations and infiltrations, reviewed by Ruud and Lillemo (2018). Interactions between NEs and host *Snn* loci is the molecular basis of SNB susceptibility, where some of the interactions show additive effects (Friesen and Faris 2010; Friesen et al. 2007). However, in some cases, epistatic effects were also detected between NE-*Snn* interactions (Peters Haugrud et al. 2019; Phan et al. 2016). In this thesis, NE-*Snn* interactions in seedlings are discussed by comparing QTL mapping results in the following circumstances: (1) same host population infiltrated with culture filtrates (CF) from different isolates, (2) CF infiltration and inoculation by the same isolate on the same host population, and (3) same isolate CF infiltrated on different host populations.

(1) **Same host population infiltrated with CF of different isolates**

In **paper II**, we used a few selected isolates to investigate the NE-*Snn* interactions at the seedling stage. Three isolates (Isolate 203649, 203667, 202579) were used for CF infiltration experiments on the NIAB Elite MAGIC population, which segregates for all three susceptibility loci (*Tsn1*, *Snn1*, *Snn3-B1*). 'Strong QTL' were defined as QTL above the permutated threshold, while 'weak QTL' were defined as below the permutated threshold but having -log10(p) value above 3 or explaining more than 5% of phenotypic variations. The Norwegian isolate 203649 does not encode any of the three known effectors (*SnToxA*, *SnTox1* and *SnTox3*), the Norwegian isolate 203667 encodes both *SnToxA* and *SnTox3*, while isolate 202579 from CIMMYT (CIMFU 463) carries all three known NE genes.

We know from previous studies that *SnToxA* is likely not expressed or only expressed in low levels *in vitro* (Rybak et al. 2017; Tan et al. 2015). As expected, CF infiltration of isolate 203667 identified only the significant QTL *QSnb.niab-5B.1*, co-locating with *Snn3-B1* ($-\log_{10}(p) = 8.9$).

Since isolate 202579 possess all three known effectors, QTL associated to both Tox1 and Tox3 sensitivities were expected to be detected. However, the only 'strong QTL' for CF infiltration of isolate 202579 was the QTL *QSnb.niab-5B.1* which co-located with *Snn3-B1* and the *SnTox1-Snn1* interaction was not detected at all. Similar to CF infiltration of isolate 202579, Phan et al. (2016) infiltrated CF of isolate SN15 (which possesses all three known effector genes) on a mapping population segregating for *Snn1* and *Snn3-B1*. Interestingly, the Tox3-*Snn3-B1* interaction was not detected until *SnTox1* was knocked out from isolate SN15, indicating that the expression of *SnTox1* suppressed the expression of *SnTox3* (Phan et al. 2016). We didn`t observe the suppression of *SnTox3-Snn3* interaction by *SnTox1-Snn1* in our study, rather the opposite that *SnTox1-Snn1* was suppressed in CF infiltration experiments by *SnTox3-Snn3*.

As none of those three well-characterized effectors was produced by isolate 203649, average host reactions to CF infiltration of 203649 were significantly lower than CF infiltration of isolate 202579 which possesses all three NEs. High correlation of NIAB Elite MAGIC RIL disease scores were found for CF infiltration of isolates 202579 and 203667. But low correlations of CF infiltration disease scores between either isolate 202579 or 203667 and 203649 were observed. This was probably due to the *SnTox3-Snn3* interaction showing the major effect in CF infiltration by both 202579 or 203667, while Tox3 was not produced by isolate 203649. Four 'weak QTL' were detected via CF infiltration of 203649 but no 'strong QTL' were identified. All 'weak QTL' identified here were novel SNB QTL not reported in previous publications.

(2) Same isolates infiltrated and inoculated on the same host population

In **paper II**, both isolate 202579 and isolate 203649 were used for inoculation on the NIAB Elite MAGIC population. For isolate 203649, no common QTL were detected by CF infiltration and inoculation experiments. In contrast to CF infiltration, inoculation with isolate 203649 identified two 'strong QTL', on chromosomes 2D and 7D respectively. The QTL *QSnb.niab-7D.1* was a novel SNB QTL. QTL *QSnb.niab-2D.2* might co-locate with the Tox7 sensitivity locus *Snn7* (Shi et al. 2015).

However, only one 'strong QTL' was significantly detected by inoculation with isolate 202579, namely the ToxA sensitivity locus, *Tsn1*. Interestingly, the same *Snn3-B1* QTL *QSnb.niab-5B.1*, identified in CF infiltration with isolate 202579, was also detected but as a 'weak QTL' for inoculation. The *SnTox1-Snn1* interaction was not detected by inoculation with isolate 202579.

However, *QSnb.niab-2D.2* was identified as a 'weak QTL' by inoculation with isolate 202579. Faris et al. (2011) showed that the expression level of *SnToxA* was isolate dependent, and this principle might apply to other NEs as well. Therefore, expression levels of *SnTox1* could also be isolate dependent. That could be why the epistatic effect of *SnTox1* on *SnTox3* was not observed in isolate 202579. Recently, Peters Haugrud et al. (2019) conducted a study supporting this hypothesis, in which they compared results of inoculation experiments using different *P. nodorum* isolates possessing all three known *SnTox* genes, and used the same bi-parental mapping population which segregated for all three corresponding sensitivity loci. The ToxA-*Tsn1* and Tox3-*Snn3-B1* interactions contributed to disease severity in experiments using all isolates, while the effect caused by the Tox1-*Snn1* interaction varied among isolates and was likely due to variations in *SnTox1* expression levels (Peters Haugrud et al. 2019). In addition, evidence was found that the effects of NE-*Snn* interactions varied from additive to epistatic and were mostly regulated by adjusting the expression level of NEs (Peters Haugrud et al. 2019).

(3) CF infiltration of same isolate on different host populations

In **paper II** and **paper III,** the same isolate 203649 was used for culture filtrate (CF) infiltration. However, different QTL were detected by using different mapping populations. In **paper II**, four QTL were identified by CF infiltration with isolate 203649, on chromosomes 2A, 3B, 7B and 7D, and were all defined as 'weak QTL'. The 2A QTL might be the robust SNB field resistance QTL *QSnb.niab-2A.3* (**paper II**). If CF infiltration could be used to screen germplasm developed for fine-mapping of this locus, a lot of time could be saved for fine mapping this QTL instead of conducting highly time and resource consuming field testing. In **paper III**, a QTL on chromosome 2A was identified in the field using the BMWpop MAGIC population which co-located with *QSnb.niab-2A.3*. Therefore, CF infiltration of the same isolate was tested on BMWpop MAGIC population in the greenhouse. However, infiltration identified three QTL on chromosome 5A, 5B and 7B, where only the 7B QTL could be a common QTL identified by CF infiltration of 203649 on NIAB Elite MAGIC as the confidence intervals of *QInf.nmbu-7B.1* and *QSnb.niab-7B.2* overlapped on the wheat physical map. Moreover, in comparison to the NIAB Elite MAGIC population, where all QTL for CF infiltration of isolate 203649 were identified as 'weak QTL', *QInf.nmbu-7B.1* was identified as a major QTL in BMWpop, explaining 17.1% of the phenotypic variation. One possible explanation for this could be that differences in host genetic background

interfered with the detection of some NE-*Snn* interactions, despite using the CF infiltration of the same isolate.

2.3.3 Can sensitivity to NEs explain differences in host SNB resistance in the field?

Since the discovery of the first NE-*Snn* interaction in the wheat-*P. nodorum* pathogen system by Liu et al. (2004a), many studies have focused on these interactions and more NEs have been characterized (described in **1.2.6**). However, debates as to how much of the host resistance/susceptibility can be explained by NE-*Snn* interactions are still ongoing (Francki 2013; Ruud and Lillemo 2018). We also found interesting results from our own study. In **Paper IV,** we identified SNB field QTL to co-locate with numerous NE sensitivity-loci, such as *Tsn1*, *Snn1*, *Snn2* and *Snn3-B1* using the association mapping panel MASBASIS, even though some of them were not consistently detected across multiple years. However, our results highlighted the potential usefulness of screening NE sensitivities in breeding lines to reduce field SNB susceptibility. In **paper II** which explored the use of a UK-adapted MAGIC population**,** except for QTL *QSnb.niab-2A.3* and *QSnb.niab-3A*, which were detected by both crude CF infiltration and in the field using NIAB Elite MAGIC, no other QTL were detected as significant in both greenhouse (i.e. culture filtrate, NE infiltration and seedling *P. nodorum* resistance) and field conditions. Furthermore, the disease severities of seedling testing and field testing were not highly correlated. One possible explanation could be that the isolates selected in our greenhouse testing were not representative for the Norwegian *P. nodorum* population. As discussed in **2.3.1** and **2.3.2**, different isolates would produce different NEs and regulate NE expressions according to the host genetic background. Probably some uncharacterized NEs played an important role in the field but were not expressed or possessed by the selected isolates in our greenhouse study. Since naturally infected straw was used as inoculum for field experiments in Norway, multiple infections by different isolates were expected in the field. From **paper I**, we knew that all three well characterized NE genes (*SnToxA*, *SnTox1* and *SnTox3*) were common in the Norwegian *P. nodorum* population. NIAB Elite MAGIC segregates for all related sensitivity loci *Tsn1*, *Snn1*, and *Snn3-B1*, but these QTL were not detected in the field in any of the tested years in both Norway and the UK, while only the *Snn2* locus was identified in one year from the UK trial as a 'weak QTL' (**paper II**). Similar results were shown in **paper III**, where BMWpop segregated for both *Snn1* and *Snn3-B1*, however, neither of these QTL were identified in the field using the BMWpop. Therefore, collectively our observations supported the hypothesis proposed by Peters Haugrud et al. (2019) that *P. nodorum* isolates might

not express all of the NE genes they harbor. Instead, depending on the host genetic background, the pathogen exploits a 'cost-effective' way to choose which NE to express when the host possesses many sensitivity loci (Peters Haugrud et al. 2019). Epistasis effects caused by host *Snn* genes may result in this phenomenon as well, however, more gene expression analyses on host *Snn* genes are required to disentangle this issue. Until now, only four NE-*Snn* interactions were reported to show effect on field SNB severities: ToxA-*Tsn1*, Tox1-*Snn1*, Tox2-*Snn2* and Tox3-*Snn3-B1* (Friesen et al. 2009; Phan et al. 2016; Ruud and Lillemo 2018; Ruud et al. 2017). As resistance/susceptibility to SNB is a quantitative trait, some plant defense mechanisms other than NE-*Snn* interactions are likely to be involved in the *P. nodorum*- wheat interaction in the field. For example, some resistant wheat cultivars minimize fungal penetration by producing lignified papillae (Bird and Ride 1981). Other general resistance mechanisms are still unexplored.

2.3.4 Field inoculation methods

From a SNB resistance breeding point of view, our results illustrated the importance of field testing using natural pathogen populations as inoculum instead of arbitrarily selecting isolates for resistance screening. Spraying spore suspensions for SNB field inoculation is a standard method used by many studies (Fried and Meister 1987; Laubscher et al. 1966; Uphaus et al. 2007; Wicki et al. 1999), and it has its own specific advantages. For instance, the same isolates could be used in both greenhouse and field studies. Therefore, higher correlations between field and controlled environments would be expected compared to using natural inoculum. In addition, as inoculum were spread directly to either wheat leaves or heads, this method could reduce the influence of confounding traits such as plant height and days to heading, which was observed in the UK trial in **paper II.** However, as discussed in **2.3.1**, the high genetic diversity of the *P. nodorum* natural population made it difficult to select representative isolates. Such diversity is expected when the natural population has been long established and commonly undergoes sexual reproduction, and the resulting large effective population size increased the difficulty of choosing representative isolates for screening. Moreover, large proportions of field resistance could not be explained by known NE-*Snn* interactions alone. Therefore, NE screening under controlled greenhouse conditions and field testing with natural *P. nodorum* populations should be combined in order to breed for better resistance.

2.3.5 QTL detected for SNB leaf blotch and glume blotch

Although leaf blotch and glume blotch are symptoms caused by the same pathogen on the same host, previous studies showed that the genetic mechanisms controlling resistance to SNB leaf blotch and glume blotch are different (Aguilar et al. 2005; Fried 1987; Wicki et al. 1999). Aguilar et al. (2005) carried out the first study to investigate leaf blotch and glume blotch resistance by assessing the disease on the same mapping population in the same field. They identified one common QTL for both leaf blotch and glume blotch on chromosome 2B, however, that QTL was associated to confounding morphological traits such as heading date and ear length (Aguilar et al. 2005). Therefore, they concluded that the resistance of leaf blotch and glume blotch were controlled by genetically independet mechanisms.

In **paper II**, QTL identified for SNB leaf blotch and glume blotch were compared by scoring the disease severity on the NIAB Elite MAGIC population. By extracting residuals of disease scores from a liner regression using plant height and days to heading as covariates, we tried to reduce the influences caused by these confounding traits in order to detect true SNB resistance QTL. When assessing the disease severities of the MAGIC founders, rankings of disease severities were different for leaf blotch and glume blotch. Notably, the most susceptible founder Xi19 for leaf blotch showed moderate resistance to glume blotch, suggesting that the resistance mechanisms to leaf blotch and glume blotch might be different. Six QTL were identified for leaf blotch, while three QTL were identified for glume blotch and most of the QTL were different. Interestingly, we identified an overlapping QTL on chromosome 2A for both leaf blotch and glume blotch. Therefore, we considered that they represented a common QTL associated with both leaf blotch and glume blotch. Results of haplotype analysis showed that haplotype effects were significant for leaf blotch in many years and one year for glume blotch. However, the susceptible haplotype for leaf blotch showed the opposite haplotype effect for glume blotch, implying that leaf blotch and glume blotch resistance might indeed be controlled by different mechanisms and that the QTL identified might represent two closely located but independent genes or gene clusters, which is in agreement with the results from other studies (Aguilar et al. 2005; Francki 2013; Shankar et al. 2008).

Nevertheless, when comparing published QTL with QTL identified in our study, we found co-location of the glume blotch QTL with a NE sensitivity locus. *QSnb.niab-6A.2* detected for glume

blotch in 2016 might co-locate with the Tox6 sensitivity locus *Snn6* (Gao et al. 2015) indicating that NE-*Snn* interactions might potentially also play a role in glume blotch susceptibility. NE-*Snn* interactions were deeply investigated for leaf blotch at the seedling stage with only a few cases where seedling resistance QTL showed an effect on adult plant leaf resistance. However, whether NE-*Snn* interactions play a role in glume blotch resistance is still unknown. More research on glume blotch is needed to clarify the genetic mechanism of glume blotch resistance and whether NE-*Snn* interactions are involved in glume susceptibility.

2.3.6 Candidate QTL for marker assisted selection (MAS)

The main objective of our study was to find robust QTL in the field which could be utilized in improving SNB resistance breeding. MAS is a fast and cost-effective method for selecting breeding materials for quantitative traits. However, QTL validation should be applied before usage of MAS in order to exclude inconsistent QTL and select for diagnostic markers.

In **paper II,** we identified a robust QTL *QSnb.niab-2A.3* which was significant for leaf blotch across multiple years, locations and inoculation methods. As discussed above, the pathogen population would vary every year according to location and climate. *QSnb.niab-2A.3* was significant across years and locations, and was also identified via CF infiltration, illustrating that the corresponding NE might be produced widely by different *P. nodorum* populations. In addition, we validated this QTL in **paper III** on an independent multi-founder population with different genetic background. The QTL was significantly detected in two years out of a three-year study, the haplotype effect of the QTL was significantly associated with field SNB susceptibility across all years tested, indicating the robustness of the QTL (**paper III**) and the potential value of applying it in MAS.

In **paper IV**, another robust QTL on chromosome 2A was associated with SNB resistance using the Norwegian winter wheat association mapping panel. The QTL was significantly detected in one environment and across most years. Haplotype analysis of this QTL with historical data showed that the haplotype effect was significant in seven out of nine tested years. The resistant allele on chromosome 2A was carried by many lines with German origin while most Norwegian and Swedish lines carried the susceptible allele. In addition, we found that the resistant haplotype was rare in the Norwegian spring wheat panel and all lines with resistant haplotype in this panel

came from CIMMYT. Integrating this resistant allele into local germplasm may improve the SNB resistance in Norwegian wheat.

In addition, we confirmed in this thesis that some published NE-*Snn* interactions contributed to field resistance. A QTL co-locating with the Tox2 sensitivity locus *Snn2* (Friesen et al. 2007) was significantly associated with field resistance in one trial in the UK using the NIAB Elite MAGIC population (**paper II),** one trial in Norway using the BMWpop population (**paper III**) and one trial and the across year mean in Norway using the Norwegian spring wheat association mapping panel (**paper IV**). Detection of the *Snn2* locus using different mapping populations and in different locations illustrated the prevalence of the *Snn2* susceptibility allele in European wheat materials. Even though the *Snn2* gene has not been cloned, closely linked markers are available for MAS (Zhang et al. 2009). In addition, and as discussed in **2.3.1**, *Tsn1* is another important NE sensitivity locus that contributes to field susceptibility in the Norwegian spring wheat panel (**paper IV**). As both the *Tsn1* and *SnToxA* genes have been cloned, screening of breeding materials via either *Tsn1* genotyping or ToxA infiltration is feasible. This approach is used in practice in Australia, where reduction in growing area of ToxA sensitive cultivars from 2009 to 2013 was estimated to have saved 50 million $ in yield losses (Vleeshouwers and Oliver, 2014).

2.3.7 Influences of plant height and days to heading on SNB disease severity in the field

Under natural conditions, SNB develops from the lower leaves to the upper leaves. Thus, tall and late lines may avoid heavy infection due to morphological and phenological avoidance. Therefore, as previously discussed, confounding traits such as plant height and days to heading would interfere with the detection of the true SNB QTL. Correcting the effects caused by such traits were achieved in this study by extracting the residuals of disease scores from a linear regression using plant height and days to heading as covariates. Additionally, we compared QTL detected by the corrected disease data and uncorrected disease data in **paper II** to further investigate the influences caused by these traits. To our surprise, one 'weak QTL' *QDh.niab-6A* on chromosome 6A detected for 'days to heading' in Norway in 2014 might co-locate with corrected leaf blotch QTL *QSnb.niab-6A.1* detected in Norway in 2016. With this exception, no other common QTL for either plant height or days to heading were identified for leaf blotch. However, we note that three novel 'weak QTL' which were not identified with corrected disease data were detected when analyzing the uncorrected leaf blotch data. Nevertheless, all 'strong QTL' identified by uncorrected leaf

blotch data were detected by corrected data, indicating that the methodology used was robust. In addition, in comparison to the corrected leaf blotch data, less QTL were identified by the uncorrected dataset and common significant QTL detected by both corrected and uncorrected dataset became less significant using uncorrected data, highlighting the influence of the confounding traits on the reliable detection of true SNB QTL. In addition, QTL analysis of uncorrected glume blotch data showed that only two 'strong QTL' were detected and both were common with plant height QTL on chromosomes 4B and 4D. 'Weak QTL' detected by uncorrected glume blotch data were all detected using corrected glume blotch data. And similar to the analysis of leaf blotch, those true SNB QTL detected using uncorrected glume blotch phenotypes were less significant than using the corrected glume blotch phenotypes.

2.4 Future perspectives

2.4.1 Fine mapping the QTL *QSnb.niab-2A.3*

In this thesis, *QSnb.niab-2A.3* was detected in field trials across multiple years and locations and validated using an independent multi-founder mapping population with different genetic background. In addition, as the same QTL was detected by CF infiltration, using a biochemical approach to purify the effector would accelerate the fine-mapping process by allowing rapid screening plant materials in the greenhouse instead of conducting more lengthy field assessments which can only be conducted once a year. As stated in **paper II**, we suggest that after Mendelizing target QTL in a near isogenic line (NIL) pair, it may be possible to fine-map the QTL by intercrossing the NIL pair and using seedling stage sensitivity to identify/confirm genetic recombinants.

2.4.2 Applying CRISPR/Cas9 technology to improve SNB resistance

Classic plant breeding is mainly based on crossing and selection, which requires genetic recombination and allelic variability. However, sometimes allelic diversity is limited in domesticated crops or it is only specific traits, such as disease resistance, that is the intended breeding target. In order to introduce beneficial traits from wild relatives to domesticated crops, it often takes 10 to 15 years to break the linkage drag with undesired traits (Steuernagel et al. 2016). While mutation breeding is a fast way to create genetic variation, mutations caused by either physical or chemical mutagens are usually unpredictable. Genome editing can precisely edit the plant genome and create predictable mutations in elite cultivars, which saves the time for backcrossing and overcoming linkage drag. Simultaneously it also accelerates the selection process by decreasing the effect of random mutations (Li et al. 2012). The CRISPR (clustered, regularly interspaced, short palindromic repeats) -Cas9 system is a recent genome editing method (Zhang et al. 2014), and has been applied to multiple crops. CRISPR/Cas9 can also target multiple homoeologues simultaneously in polyploid crops such as hexaploid bread wheat and tetraploid potato (Andersson et al. 2017; Feng et al. 2016; Liang et al. 2017; Wang et al. 2014b; Zong et al. 2017). In addition, CRISPR/Cas9 has been successfully used for editing susceptibility genes to key pathogens, with the knock-out mutants all showing enhanced resistance (Berg et al. 2017; Peng et al. 2017; Wang et al. 2014b). As discussed in **2.2.6**, two NE sensitivity loci *Tsn1* and *Snn1* have been characterized at the gene level, and no yield penalty associated with NE insensitivity

has been found so far (Oliver et al. 2014). Eliminating such NE sensitivity alleles by CRISPR/Cas9 from elite cultivars would reduce susceptibility to SNB, and at the same time keep all other desired traits. However, applying this technology requires sequence knowledge of the candidate gene (and is also currently subject to national laws relating to genetically modified organisms). At the moment, the other seven known *Snn* loci remain un-cloned, therefore eliminating these loci currently still relies on MAS or NE screening assays.

2.4.3 Genomic selection (GS)

Genomic prediction/selection uses large amounts of genetic markers covering all chromosomes and prior phenotypic and genotypic data of a training population to estimate the breeding value or predict the phenotypic performance of genotypes with unknown phenotypes (Meuwissen et al. 2001). Unlike conventional MAS which selects breeding germplasm using a relatively small number of genetic markers linked to previously detected major QTL/genes, GS includes genetic information of the whole genome which might give a more accurate prediction of individual breeding value (Bernardo and Yu 2007). As reviewed by Bernardo (2016), with the increase in marker density, size of the training population and heritability of the trait, the accuracy of genomic prediction will also increase. In addition, compared to treating all markers with equal random effects as is normally used in GS, fixing marker effect of major genes will also improve the prediction accuracy (Bernardo 2014). Genomic selection may well represent an efficient solution towards SNB resistance breeding as the SNB resistance is a complicated quantitative trait and only few diagnostic markers are available for MAS. Indeed, in our GWAS study only a small part (≤ 17%) of the genetic variation for the trait was explained by the QTL detected (**paper IV**). Besides, many markers were detected, which would make MAS unfeasible. Genomic selection using genome-wide markers will likely capture much more of the genetic variances. Juliana et al. (2017) conducted the first genomic prediction study on wheat leaf blotch resistances including SNB. However, the study was based on seedling SNB resistance which might not highly correlate with field resistance, as discussed previously in this thesis. Odilbekov et al. (2019) conducted a genomic prediction study on another wheat leaf blotch disease, septoria tritici blotch, using a Nordic winter wheat panel, and found that by setting significant markers from GWAS as fixed effect, the prediction accuracy improved from 0.47 to 0.62. With the prior knowledge of the significant markers obtained from our GWAS study, genomic prediction based on field SNB resistance will probably be more relevant for breeders to use in practice.

2.5 Conclusions

- The Norwegian *P. nodorum* population has high evolutionary potential, high genetic diversity and no detectable population subdivision.
- Due to its ability of rapid local adaptation and risk of fungicide resistance development, integrated pest management should be used in order to control SNB in Norway.
- ToxA is the major virulence factor in the Norwegian *P. nodorum* population, probably due to the local adaptation to Norwegian spring wheat cultivars. Eliminating the ToxA sensitivity allele *Tsn1* in Norwegian spring wheat cultivars may reduce future SNB infection.
- Correlations between SNB seedling resistance and adult plant resistance are generally low and not all seedling-stage NE-*Snn* interactions detected in the greenhouse are of field relevance.
- In order to improve SNB resistance, field testing should be carried out using natural *P. nodorum* populations as inoculum and cannot be completely replaced by greenhouse assays.
- Resistance to SNB leaf blotch and glume blotch are controlled by different mechanisms.
- SNB resistance is quantitative and most of the SNB resistance associated QTL each explain a low proportion of the phenotypic variations (<10%) under field conditions. However, stacking of resistant alleles in MAGIC RILs and the GWAS panels showed significant effect on reducing disease severity.
- Three robust QTL were detected: two by QTL mapping in MAGIC (on the long arm of chromosome 2A and on 5A) and GWAS (on the short arm of 2A). All haplotype effects were confirmed by haplotype analysis and the corresponding markers can be used in MAS.

References

Abeysekara NS, Faris JD, Chao S, McClean PE, Friesen TL (2012) Whole-genome QTL analysis of Stagonospora nodorum blotch resistance and validation of the SnTox4-*Snn4* interaction in hexaploid wheat Phytopathology 102:94-104 doi:10.1094/PHYTO-02-11-0040

Abeysekara NS, Friesen TL, Keller B, Faris JD (2009) Identification and characterization of a novel host-toxin interaction in the wheat-Stagonospora nodorum pathosystem Theor Appl Genet 120:117-126 doi:10.1007/s00122-009-1163-6

Abrahamsen U, Ficke A, Brodal G, Lillemo M, Dieseth JA, Kim MO (2017) Yellow rust in wheat. Jord og plantekultur 2017 (in Norwegian). NIBIO Bok 3:109-118

Adamski NM, Borrill P, Brinton J, Harrington S, Marchal C, Bentley AR, Bovill WD, Cattivelli L, Cockram J, Contreras-Moreira B, Ford B, Ghosh S, Harwood W, Hassani-Pak K, Hayta S, Hickey LT, Kanyuka K, King J, Maccaferri M, Naamati G, Pozniak CJ, Ramirez-Gonzalez RH, Sansaloni C, Trevaskis B, Wingen LU, Wulff BB, Uauy C. 2019. A roadmap for gene functional characterisation in wheat. PeerJ Preprints 7:e26877v2 https://doi.org/10.7287/peerj.preprints.26877v2

Aguilar V et al. (2005) Inheritance of field resistance to Stagonospora nodorum leaf and glume blotch and correlations with other morphological traits in hexaploid wheat (*Triticum aestivum* L.) Theor Appl Genet 111:325-336 doi:10.1007/s00122-005-2025-5

Akbari M et al. (2006) Diversity arrays technology (DArT) for high-throughput profiling of the hexaploid wheat genome Theor Appl Genet 113:1409-1420 doi:10.1007/s00122-006-0365-4

Alipour H, Bai GH, Zhang GR, Bihamta MR, Mohammadi V, Peyghambari SA (2019) Imputation accuracy of wheat genotyping-by-sequencing (GBS) data using barley and wheat genome references Plos One 14 doi:10.1371/journal.pone.0208614

Allen AM et al. (2017) Characterization of a Wheat Breeders' Array suitable for high-throughput SNP genotyping of global accessions of hexaploid bread wheat (*Triticum aestivum*) Plant Biotechnol J 15:390-401 doi:10.1111/pbi.12635

Andersson M, Turesson H, Nicolia A, Falt AS, Samuelsson M, Hofvander P (2017) Efficient targeted multiallelic mutagenesis in tetraploid potato (*Solanum tuberosum*) by transient CRISPR-Cas9 expression in protoplasts Plant Cell Rep 36:117-128 doi:10.1007/s00299-016-2062-3

Åssveen M, Tangsveen J, Weiseth L (2018) Sorter og sortsprøving 2017. In: Jord- og Plantekultur 2018/NIBIO BOK. Norwegian Institute of Bioeconomy research, pp 28-80

Bajgain P, Rouse MN, Tsilo TJ, Macharia GK, Bhavani S, Jin Y, Anderson JA (2016) Nested Association Mapping of Stem Rust Resistance in Wheat Using Genotyping by Sequencing Plos One 11:e0155760 doi:10.1371/journal.pone.0155760

Bathgate JA, Loughman R (2001) Ascospores are a source of inoculum of *Phaeosphaeria nodorum*, *P. avenaria* f. sp. *avenaria* and *Mycosphaerella graminicola* in Western Australia Australas Plant Path 30:317-322 doi:Doi 10.1071/Ap01043

Bearchell SJ, Fraaije BA, Shaw MW, Fitt BD (2005) Wheat archive links long-term fungal pathogen population dynamics to air pollution Proc Natl Acad Sci U S A 102:5438-5442 doi:10.1073/pnas.0501596102

Bennett RS, Yun SH, Lee TY, Turgeon BG, Arseniuk E, Cunfer BM, Bergstrom GC (2003) Identity and conservation of mating type genes in geographically diverse isolates of

Phaeosphaeria nodorum Fungal Genet Biol 40:25-37 doi:10.1016/s1087-1845(03)00062-8
Berg JA, Appiano M, Bijsterbosch G, Visser RGF, Schouten HJ, Bai Y (2017) Functional characterization of cucumber (*Cucumis sativus* L.) Clade V MLO genes BMC Plant Biol 17:80 doi:10.1186/s12870-017-1029-z
Bernardo R (2014) Genomewide selection when major genes are known Crop Sci 54:68-75 doi:10.2135/cropsci2013.05.0315
Bernardo R (2016) Bandwagons I, too, have known Theoretical and Applied Genetics 129:2323-2332 doi:10.1007/s00122-016-2772-5
Bernardo R, Yu JM (2007) Prospects for genomewide selection for quantitative traits in maize Crop Sci 47:1082-1090 doi:10.2135/cropsci2006.11.0690
Beugin MP, Gayet T, Pontier D, Devillard S, Jombart T (2018) A fast likelihood solution to the genetic clustering problem Methods Ecol Evol 9:1006-1016 doi:10.1111/2041-210X.12968
Bhathal JS, Loughman R, Speijers J (2003) Yield reduction in wheat in relation to leaf disease from yellow (tan) spot and septoria nodorum blotch Eur J Plant Pathol 109:435-443 doi:10.1023/A:1024277420773
Bird PM, Ride JP (1981) The Resistance of Wheat to Septoria-Nodorum - Fungal Development in Relation to Host Lignification Physiol Plant Pathol 19:289-299 doi:10.1016/S0048-4059(81)80063-X
Blixt E, Djurle A, Yuen J, Olson A (2009) Fungicide sensitivity in Swedish isolates of *Phaeosphaeria nodorum* Plant Pathol 58:655-664 doi:10.1111/j.1365-3059.2009.02041.x
Breseghello F, Sorrells ME (2006) Association analysis as a strategy for improvement of quantitative traits in plants Crop Sci 46:1323-1330 doi:10.2135/cropsci2005.09-0305
Brutus A, Sicilia F, Macone A, Cervone F, De Lorenzo G (2010) A domain swap approach reveals a role of the plant wall-associated kinase 1 (WAK1) as a receptor of oligogalacturonides P Natl Acad Sci USA 107:9452-9457 doi:10.1073/pnas.1000675107
Cavanagh C, Morell M, Mackay I, Powell W (2008) From mutations to MAGIC: resources for gene discovery, validation and delivery in crop plants Curr Opin Plant Biol 11:215-221 doi:10.1016/j.pbi.2008.01.002
Cunfer, B.M. (1999). "Stagonospora and Septoria Pathogens of Cereals: The Infection Process," in *Septoria and Stagonospora Diseases of Cereals: A Compilation of Global Research*, eds. M. van Ginkel, A. McNab & J. Krupinsky. (Mexico: CIMMYT), 41-45.
Cunfer BM (2000) Stagonospora and Septoria diseases of barley, oat and rye Can J Plant Pathol 22:332-348 doi:10.1080/07060660009500452
Dray S, Dufour AB (2007) The ade4 package: Implementing the duality diagram for ecologists Journal of Statistical Software 22:1-20 doi:10.18637/jss.v022.i04
Eyal Z, Scharen AL, Prescott JM, Ginkel MV (1987) The septoria diseases of wheat : concepts and methods of disease management. CIMMYT, Mexico
Falush D, Stephens M, Pritchard JK (2003) Inference of population structure using multilocus genotype data: Linked loci and correlated allele frequencies Genetics 164:1567-1587
FAO (2017) Production/Yield quantities of Wheat in World. http://www.fao.org/faostat.
Faris JD, Anderson JA, Francl LJ, Jordahl JG (1996) Chromosomal location of a gene conditioning insensitivity in wheat to a necrosis-inducing culture filtrate from *Pyrenophora tritici-repentis* Phytopathology 86:459-463 doi:10.1094/Phyto-86-459

Faris JD et al. (2010) A unique wheat disease resistance-like gene governs effector-triggered susceptibility to necrotrophic pathogens Proc Natl Acad Sci U S A 107:13544-13549 doi:10.1073/pnas.1004090107

Faris JD, Zhang Z, Rasmussen JB, Friesen TL (2011) Variable expression of the *Stagonospora nodorum* effector SnToxA among isolates is correlated with levels of disease in wheat Mol Plant Microbe Interact 24:1419-1426 doi:10.1094/MPMI-04-11-0094

Feng C, Yuan J, Wang R, Liu Y, Birchler JA, Han F (2016) Efficient Targeted Genome Modification in Maize Using CRISPR/Cas9 System J Genet Genomics 43:37-43 doi:10.1016/j.jgg.2015.10.002

Ficke A, Cowger C, Bergstrom G, Brodal G (2018a) Understanding Yield Loss and Pathogen Biology to Improve Disease Management: Septoria Nodorum Blotch - A Case Study in Wheat Plant Dis 102:696-707 doi:10.1094/PDIS-09-17-1375-FE

Ficke A, Dieseth JA, Kim MO, Lillemo M (2018b) Bladsjukdommer i norsk hvete. Forekomst, betydning of tiltak. In: Jord- og Plantekultur 2018/NIBIO BOK. Norwegian Institute of Bioeconomy Research, pp 108-112

Flor H (1956) The complementary genic systems in flax and flax rust. In: Advances in genetics, vol 8. Elsevier, pp 29-54. doi:10.1016/S0065-2660(08)60498-8

Flor HH (1971) Current Status of the Gene-For-Gene Concept Annual Review of Phytopathology 9:275-296 doi:10.1146/annurev.py.09.090171.001423

Francki MG (2013) Improving Stagonospora nodorum Resistance in Wheat: A Review Crop Sci 53:355-365 doi:10.2135/cropsci2012.06.0347

Francki MG, Walker E, Li DA, Forrest K (2018) High-density SNP mapping reveals closely linked QTL for resistance to Stagonospora nodorum blotch (SNB) in flag leaf and glume of hexaploid wheat Genome 61:145-149 doi:10.1139/gen-2017-0203

Fried PM, Meister E (1987) Inheritance of Leaf and Head Resistance of Winter Wheat toSeptoria nodorumin a Diallel Cross Phytopathology 77:1371-1375 doi:10.1094/Phyto-77-1371

Friesen TL, Chu C, Xu SS, Faris JD (2012) SnTox5-*Snn5*: a novel *Stagonospora nodorum* effector-wheat gene interaction and its relationship with the SnToxA-Tsn1 and SnTox3-Snn3-B1 interactions Mol Plant Pathol 13:1101-1109 doi:10.1111/j.1364-3703.2012.00819.x

Friesen TL, Chu CG, Liu ZH, Xu SS, Halley S, Faris JD (2009) Host-selective toxins produced by *Stagonospora nodorum* confer disease susceptibility in adult wheat plants under field conditions Theor Appl Genet 118:1489-1497 doi:10.1007/s00122-009-0997-2

Friesen TL, Faris JD (2010) Characterization of the wheat-*Stagonospora nodorum* disease system: what is the molecular basis of this quantitative necrotrophic disease interaction?† Can J Plant Pathol 32:20-28 doi:10.1080/07060661003620896

Friesen TL, Faris JD (2012) Characterization of Plant-Fungal Interactions Involving Necrotrophic Effector-Producing Plant Pathogens. In: Bolton MD, Thomma BPHJ (eds) Plant Fungal Pathogens: Methods and Protocols. Humana Press, Totowa, NJ, pp 191-207

Friesen TL, Holmes DJ, Bowden RL, Faris JD (2018) ToxA Is Present in the U.S. B*ipolaris sorokiniana* Population and Is a Significant Virulence Factor on Wheat Harboring *Tsn1* Plant Dis 102:2446-2452 doi:10.1094/PDIS-03-18-0521-RE

Friesen TL, Meinhardt SW, Faris JD (2007) The *Stagonospora nodorum*-wheat pathosystem involves multiple proteinaceous host-selective toxins and corresponding host sensitivity genes that interact in an inverse gene-for-gene manner Plant J 51:681-692 doi:10.1111/j.1365-313X.2007.03166.x

Friesen TL et al. (2006) Emergence of a new disease as a result of interspecific virulence gene transfer Nature genetics 38:953
Friesen TL, Zhang Z, Solomon PS, Oliver RP, Faris JD (2008) Characterization of the interaction of a novel *Stagonospora nodorum* host-selective toxin with a wheat susceptibility gene Plant Physiol 146:682-693 doi:10.1104/pp.107.108761
Gao Y et al. (2015) Identification and Characterization of the SnTox6-*Snn6* Interaction in the Parastagonospora nodorum-Wheat Pathosystem Mol Plant Microbe Interact 28:615-625 doi:10.1094/MPMI-12-14-0396-R
Gupta PK, Kulwal PL, Jaiswal V (2014) Association mapping in crop plants: opportunities and challenges Adv Genet 85:109-147 doi:10.1016/B978-0-12-800271-1.00002-0
Hu W, He X, Dreisigacker S, Sansaloni CP, Juliana P, Singh PK (2019) A wheat chromosome 5AL region confers seedling resistance to both tan spot and Septoria nodorum blotch in two mapping populations The Crop Journal (in press) doi:10.1016/j.cj.2019.05.004
Huang BE, George AW, Forrest KL, Kilian A, Hayden MJ, Morell MK, Cavanagh CR (2012) A multiparent advanced generation inter-cross population for genetic analysis in wheat Plant Biotechnol J 10:826-839 doi:10.1111/j.1467-7652.2012.00702.x
International Wheat Genome Sequencing C (2014) A chromosome-based draft sequence of the hexaploid bread wheat (Triticum aestivum) genome Science 345:1251788 doi:10.1126/science.1251788
International Wheat Genome Sequencing C et al. (2018) Shifting the limits in wheat research and breeding using a fully annotated reference genome Science 361:eaar7191 doi:10.1126/science.aar7191
Jaccoud D, Peng K, Feinstein D, Kilian A (2001) Diversity arrays: a solid state technology for sequence information independent genotyping Nucleic Acids Res 29:E25 doi:10.1093/nar/29.4.e25
Jombart T (2008) adegenet: a R package for the multivariate analysis of genetic markers Bioinformatics 24:1403-1405 doi:10.1093/bioinformatics/btn129
Jönsson J (1985) Evaluation of leaf resistance to Septoria nodorum in winter wheat at seedling and adult plant stage Agri Hortique Genetica:52-68
Jordan KW et al. (2018) The genetic architecture of genome-wide recombination rate variation in allopolyploid wheat revealed by nested association mapping Plant J 95:1039-1054 doi:10.1111/tpj.14009
Juliana P et al. (2017) Comparison of Models and Whole-Genome Profiling Approaches for Genomic-Enabled Prediction of Septoria Tritici Blotch, Stagonospora Nodorum Blotch, and Tan Spot Resistance in Wheat Plant Genome 10:1-16 doi:10.3835/plantgenome2016.08.0082
Keller B, Wicker T, Krattinger SG (2018) Advances in Wheat and Pathogen Genomics: Implications for Disease Control Annu Rev Phytopathol 56:67-87 doi:10.1146/annurev-phyto-080516-035419
Keller SM, McDermott JM, Pettway RE, Wolfe MS, McDonald BA (1997) Gene Flow and Sexual Reproduction in the Wheat Glume Blotch Pathogen Phaeosphaeria nodorum (Anamorph Stagonospora nodorum) Phytopathology 87:353-358 doi:10.1094/PHYTO.1997.87.3.353
Kiszonas AM, Morris CF (2018) Wheat breeding for quality: A historical review Cereal Chem 95:17-34 doi:10.1094/Cchem-05-17-0103-Fi

Kover PX et al. (2009) A Multiparent Advanced Generation Inter-Cross to fine-map quantitative traits in Arabidopsis thaliana PLoS Genet 5:e1000551 doi:10.1371/journal.pgen.1000551
Ladejobi O et al. (2016) Maximizing the potential of multi-parental crop populations Appl Transl Genom 11:9-17 doi:10.1016/j.atg.2016.10.002
Langridge P, Lagudah ES, Holton TA, Appels R, Sharp PJ, Chalmers KJ (2001) Trends in genetic and genome analyses in wheat: a review Aust J Agr Res 52:1043-1077 doi:Doi 10.1071/Ar01082
Laubscher FX, Wechmar B, Schalkwyk D (1966) Heritable Resistance of Wheat Varieties to Glume Blotch (Septoria nodorum Berk.) Journal of Phytopathology 56:260-264 doi:10.1111/j.1439-0434.1966.tb02262.x
Leath S, Scharen AL, Dietzholmes ME, Lund RE (1993) Factors Associated with Global Occurrences of Septoria-Nodorum Blotch and Septoria-Tritici Blotch of Wheat Plant Dis 77:1266-1270 doi:10.1094/Pd-77-1266
Li T, Liu B, Spalding MH, Weeks DP, Yang B (2012) High-efficiency TALEN-based gene editing produces disease-resistant rice Nat Biotechnol 30:390-392 doi:10.1038/nbt.2199
Liang Z et al. (2017) Efficient DNA-free genome editing of bread wheat using CRISPR/Cas9 ribonucleoprotein complexes Nat Commun 8:14261 doi:10.1038/ncomms14261
Lillemo M, Dieseth JA (2011) Wheat breeding in Norway. In: Angus W, Bonjean A, Ginkel MV (eds) The World Wheat Book: A History of Wheat Breeding, vol 2. Lavoisier Publishing, France, pp 45-66
Liu Z et al. (2009) SnTox3 acts in effector triggered susceptibility to induce disease on wheat carrying the Snn3 gene PLoS Pathog 5:e1000581 doi:10.1371/journal.ppat.1000581
Liu Z, Friesen TL, Ling H, Meinhardt SW, Oliver RP, Rasmussen JB, Faris JD (2006) The Tsn1–ToxA interaction in the wheat–Stagonospora nodorum pathosystem parallels that of the wheat–tan spot system Genome 49:1265-1273 doi:10.1139/g06-088
Liu Z et al. (2012) The cysteine rich necrotrophic effector SnTox1 produced by Stagonospora nodorum triggers susceptibility of wheat lines harboring Snn1 PLoS Pathog 8:e1002467 doi:10.1371/journal.ppat.1002467
Liu ZH, Faris JD, Meinhardt SW, Ali S, Rasmussen JB, Friesen TL (2004a) Genetic and Physical Mapping of a Gene Conditioning Sensitivity in Wheat to a Partially Purified Host-Selective Toxin Produced by Stagonospora nodorum Phytopathology 94:1056-1060 doi:10.1094/PHYTO.2004.94.10.1056
Liu ZH, Friesen TL, Rasmussen JB, Ali S, Meinhardt SW, Faris JD (2004b) Quantitative Trait Loci Analysis and Mapping of Seedling Resistance to Stagonospora nodorum Leaf Blotch in Wheat Phytopathology 94:1061-1067 doi:10.1094/PHYTO.2004.94.10.1061
Liu ZH et al. (2016) SnTox1, a Parastagonospora nodorum necrotrophic effector, is a dual-function protein that facilitates infection while protecting from wheat-produced chitinases New Phytol 211:1052-1064 doi:10.1111/nph.13959
Lu Q, Lillemo M (2014) Molecular mapping of adult plant resistance to Parastagonospora nodorum leaf blotch in bread wheat lines 'Shanghai-3/Catbird' and 'Naxos' Theor Appl Genet 127:2635-2644 doi:10.1007/s00122-014-2404-x
Mackay IJ et al. (2014) An eight-parent multiparent advanced generation inter-cross population for winter-sown wheat: creation, properties, and validation G3 (Bethesda) 4:1603-1610 doi:10.1534/g3.114.012963
Marcussen T et al. (2014) Ancient hybridizations among the ancestral genomes of bread wheat Science 345:1250092 doi:10.1126/science.1250092

McDonald BA, Linde C (2002) Pathogen population genetics, evolutionary potential, and durable resistance Annu Rev Phytopathol 40:349-379 doi:10.1146/annurev.phyto.40.120501.101443
McDonald BA, Miles J, Nelson LR, Pettway RE (1994) Genetic-Variability in Nuclear-DNA in-Field Populations of Stagonospora-Nodorum Phytopathology 84:250-255 doi:10.1094/Phyto-84-250
McDonald BA, Stukenbrock EH (2016) Rapid emergence of pathogens in agro-ecosystems: global threats to agricultural sustainability and food security Philos Trans R Soc Lond B Biol Sci 371:20160026 doi:10.1098/rstb.2016.0026
McDonald MC, Ahren D, Simpfendorfer S, Milgate A, Solomon PS (2018) The discovery of the virulence gene ToxA in the wheat and barley pathogen Bipolaris sorokiniana Mol Plant Pathol 19:432-439 doi:10.1111/mpp.12535
McDonald MC, Oliver RP, Friesen TL, Brunner PC, McDonald BA (2013) Global diversity and distribution of three necrotrophic effectors in Phaeosphaeria nodorum and related species New Phytol 199:241-251 doi:10.1111/nph.12257
McDonald MC, Razavi M, Friesen TL, Brunner PC, McDonald BA (2012) Phylogenetic and population genetic analyses of Phaeosphaeria nodorum and its close relatives indicate cryptic species and an origin in the Fertile Crescent Fungal Genet Biol 49:882-895 doi:10.1016/j.fgb.2012.08.001
Mehra LK, Cowger C, Weisz R, Ojiambo PS (2015) Quantifying the Effects of Wheat Residue on Severity of Stagonospora nodorum Blotch and Yield in Winter Wheat Phytopathology 105:1417-1426 doi:10.1094/PHYTO-03-15-0080-R
Meuwissen THE, Hayes BJ, Goddard ME (2001) Prediction of total genetic value using genome-wide dense marker maps Genetics 157:1819-1829
Murphy NE, Loughman R, Appels R, Lagudah ES, Jones MGK (2000) Genetic variability in a collection of Stagonospora nodorum isolates from Western Australia Aust J Agr Res 51:679-684 doi:10.1071/Ar99107
Odilbekov F, Armonienė R, Koc A, Svensson J, Chawade A (2019) GWAS-Assisted Genomic Prediction to Predict Resistance to Septoria Tritici Blotch in Nordic Winter Wheat at Seedling Stage Frontiers in Genetics 10 doi:10.3389/fgene.2019.01224
Oliver R et al. (2014) Absence of detectable yield penalty associated with insensitivity to Pleosporales necrotrophic effectors in wheat grown in the West Australian wheat belt Plant Pathol 63:1027-1032 doi:10.1111/ppa.12191
Oliver R.P., Tan K.-C. and Moffat C.S. (2016) Necrotrophic Pathogens of Wheat. In: Wrigley, C., Corke, H., and Seetharaman, K., Faubion, J., (eds.) Encyclopedia of Food Grains, 2nd Edition, pp. 273-278. Oxford: Academic Press.
Oliver RP, Friesen TL, Faris JD, Solomon PS (2012) Stagonospora nodorum: from pathology to genomics and host resistance Annu Rev Phytopathol 50:23-43 doi:10.1146/annurev-phyto-081211-173019
Paux E, Sourdille P, Mackay I, Feuillet C (2012) Sequence-based marker development in wheat: advances and applications to breeding Biotechnol Adv 30:1071-1088 doi:10.1016/j.biotechadv.2011.09.015
Pedersen EA, Hughes GR (1992) The Effect of Crop-Rotation on Development of the Septoria Disease Complex on Spring Wheat in Saskatchewan Canadian Journal of Plant Pathology-Revue Canadienne De Phytopathologie 14:152-158 doi:10.1080/07060669209500892

Peng AH et al. (2017) Engineering canker-resistant plants through CRISPR/Cas9-targeted editing of the susceptibility gene CsLOB1 promoter in citrus Plant Biotechnology Journal 15:1509-1519 doi:10.1111/pbi.12733
Pereira DA, McDonald BA, Brunner PC (2017) Mutations in the CYP51 gene reduce DMI sensitivity in Parastagonospora nodorum populations in Europe and China Pest Manag Sci 73:1503-1510 doi:10.1002/ps.4486
Peters Haugrud AR, Zhang Z, Richards JK, Friesen TL, Faris JD (2019) Genetics of Variable Disease Expression Conferred by Inverse Gene-For-Gene Interactions in the Wheat-Parastagonospora nodorum Pathosystem Plant Physiol 180:420-434 doi:10.1104/pp.19.00149
Phan HT, Rybak K, Furuki E, Breen S, Solomon PS, Oliver RP, Tan KC (2016) Differential effector gene expression underpins epistasis in a plant fungal disease Plant J 87:343-354 doi:10.1111/tpj.13203
Pritchard JK, Stephens M, Donnelly P (2000) Inference of population structure using multilocus genotype data Genetics 155:945-959
Quaedvlieg W et al. (2013) Sizing up Septoria Stud Mycol 75:307-390 doi:10.3114/sim0017
Ruud AK et al. (2019) Genome-Wide Association Mapping of Resistance to Septoria Nodorum Leaf Blotch in a Nordic Spring Wheat Collection The Plant Genome 12:1-15 doi:10.3835/plantgenome2018.12.0105
Ruud AK, Dieseth JA, Lillemo M (2018) Effects of Three Parastagonospora nodorum Necrotrophic Effectors on Spring Wheat under Norwegian Field Conditions Crop Sci 58:159-168 doi:10.2135/cropsci2017.05.0281
Ruud AK, Lillemo M (2018) Diseases affecting wheat: Septoria nodorum blotch. In: Integrated disease management of wheat and barley. Burleigh Dodds Series in Agricultural Science. Burleigh Dodds Science Publishing Limited, Cambridge, UK, pp 109-144. doi:10.19103/as.2018.0039.06
Ruud AK, Windju S, Belova T, Friesen TL, Lillemo M (2017) Mapping of SnTox3-Snn3 as a major determinant of field susceptibility to Septoria nodorum leaf blotch in the SHA3/CBRD x Naxos population Theor Appl Genet 130:1361-1374 doi:10.1007/s00122-017-2893-5
Salamini F, Ozkan H, Brandolini A, Schafer-Pregl R, Martin W (2002) Genetics and geography of wild cereal domestication in the near east Nat Rev Genet 3:429-441 doi:10.1038/nrg817
Schnurbusch T, Paillard S, Fossati D, Messmer M, Schachermayr G, Winzeler M, Keller B (2003) Detection of QTLs for Stagonospora glume blotch resistance in Swiss winter wheat Theor Appl Genet 107:1226-1234 doi:10.1007/s00122-003-1372-3
Semagn K, Babu R, Hearne S, Olsen M (2014) Single nucleotide polymorphism genotyping using Kompetitive Allele Specific PCR (KASP): overview of the technology and its application in crop improvement Molecular Breeding 33:1-14 doi:10.1007/s11032-013-9917-x
Shaner G (1995) Epidemiology of Leaf Blotch of Soft Red Winter Wheat Caused bySeptoria triticiandStagonospora nodorum Plant Dis 79:928-938 doi:10.1094/pd-79-0928
Shankar M, Walker E, Golzar H, Loughman R, Wilson RE, Francki MG (2008) Quantitative trait loci for seedling and adult plant resistance to Stagonospora nodorum in wheat Phytopathology 98:886-893 doi:10.1094/PHYTO-98-8-0886

Shaw MW, Bearchell SJ, Fitt BDL, Fraaije BA (2008) Long-term relationships between environment and abundance in wheat of Phaeosphaeria nodorum and Mycosphaerella graminicola New Phytol 177:229-238 doi:10.1111/j.1469-8137.2007.02236.x
Shi G et al. (2016) The hijacking of a receptor kinase-driven pathway by a wheat fungal pathogen leads to disease Sci Adv 2:e1600822 doi:10.1126/sciadv.1600822
Shi GJ, Friesen TL, Saini J, Xu SS, Rasmussen JB, Faris JD (2015) The Wheat Snn7 Gene Confers Susceptibility on Recognition of the Parastagonospora nodorum Necrotrophic Effector SnTox7 Plant Genome 8:1-10 doi:10.3835/plantgenome2015.02.0007
Solomon PS, Lowe RG, Tan KC, Waters OD, Oliver RP (2006) Stagonospora nodorum: cause of stagonospora nodorum blotch of wheat Mol Plant Pathol 7:147-156 doi:10.1111/j.1364-3703.2006.00326.x
Sommerhalder RJ, McDonald BA, Mascher F, Zhan J (2011) Effect of hosts on competition among clones and evidence of differential selection between pathogenic and saprophytic phases in experimental populations of the wheat pathogen Phaeosphaeria nodorum BMC Evol Biol 11:188 doi:10.1186/1471-2148-11-188
Sommerhalder RJ, McDonald BA, Zhan J (2006) The Frequencies and Spatial Distribution of Mating Types in Stagonospora nodorum Are Consistent with Recurring Sexual Reproduction Phytopathology 96:234-239 doi:10.1094/PHYTO-96-0234
Southern EM (1975) Detection of Specific Sequences among DNA Fragments Separated by Gel-Electrophoresis J Mol Biol 98:503-508 doi:10.1016/S0022-2836(75)80083-0
Stadlmeier M, Hartl L, Mohler V (2018) Usefulness of a Multiparent Advanced Generation Intercross Population With a Greatly Reduced Mating Design for Genetic Studies in Winter Wheat Front Plant Sci 9:1825 doi:10.3389/fpls.2018.01825
Statistics Norway 2020. https://www.ssb.no/
Steuernagel B et al. (2016) Rapid cloning of disease-resistance genes in plants using mutagenesis and sequence capture Nat Biotechnol 34:652-655 doi:10.1038/nbt.3543
Stukenbrock EH, Banke S, McDonald BA (2006) Global migration patterns in the fungal wheat pathogen Phaeosphaeria nodorum Mol Ecol 15:2895-2904 doi:10.1111/j.1365-294X.2006.02986.x
Stukenbrock EH, Banke S, Zala M, McDonald BA, Oliver RP (2005) Isolation and characterization of EST-derived microsatellite loci from the fungal wheat pathogen Phaeosphaeria nodorum Mol Ecol Notes 5:931-933 doi:10.1111/j.1471-8286.2005.01120.x
Tan KC et al. (2012) Quantitative variation in effector activity of ToxA isoforms from Stagonospora nodorum and Pyrenophora tritici-repentis Mol Plant Microbe Interact 25:515-522 doi:10.1094/MPMI-10-11-0273
Tan KC, Waters ODC, Rybak K, Antoni E, Furuki E, Oliver RP (2014) Sensitivity to three Parastagonospora nodorum necrotrophic effectors in current Australian wheat cultivars and the presence of further fungal effectors Crop Pasture Sci 65:150-158 doi:10.1071/Cp13443
Tomas A, Feng GH, Reeck GR, Bockus WW, Leach JE (1990) Purification of a Cultivar-Specific Toxin from Pyrenophora-Tritici-Repentis, Causal Agent of Tan Spot of Wheat Mol Plant Microbe In 3:221-224 doi:10.1094/Mpmi-3-221
Torriani SF, Melichar JP, Mills C, Pain N, Sierotzki H, Courbot M (2015) Zymoseptoria tritici: A major threat to wheat production, integrated approaches to control Fungal Genet Biol 79:8-12 doi:10.1016/j.fgb.2015.04.010

Uphaus J, Walker E, Shankar M, Golzar H, Loughman R, Francki M, Ohm H (2007) Quantitative trait loci identified for resistance to Stagonospora glume blotch in wheat in the USA and Australia Crop Sci 47:1813-1822 doi:10.2135/cropsci2006.11.0732

van Baalen M, Sabelis MW (1995) The Dynamics of Multiple Infection and the Evolution of Virulence The American Naturalist 146:881-910 doi:10.1086/285830

Wang S et al. (2014a) Characterization of polyploid wheat genomic diversity using a high-density 90,000 single nucleotide polymorphism array Plant Biotechnol J 12:787-796 doi:10.1111/pbi.12183

Wang Y, Cheng X, Shan Q, Zhang Y, Liu J, Gao C, Qiu JL (2014b) Simultaneous editing of three homoeoalleles in hexaploid bread wheat confers heritable resistance to powdery mildew Nat Biotechnol 32:947-951 doi:10.1038/nbt.2969

Wolter F, Schindele P, Puchta H (2019) Plant breeding at the speed of light: the power of CRISPR/Cas to generate directed genetic diversity at multiple sites. BMC Plant Biology 19: 176
https://doi.org/10.1186/s12870-019-1775-1

Wicki W, Winzeler M, Schmid JE, Stamp P, Messmer M (1999) Inheritance of resistance to leaf and glume blotch caused by Septoria nodorum Berk. in winter wheat Theoretical and Applied Genetics 99:1265-1272 doi:10.1007/s001220051332

Williams, J.R. and Jones, D.G. 1973. Infection of grasses by Septoria nodorum and S. tritici. Trans. Br. Micol. Soc. 60:355-358

Yu J, Holland JB, McMullen MD, Buckler ES (2008) Genetic design and statistical power of nested association mapping in maize Genetics 178:539-551 doi:10.1534/genetics.107.074245

Zhang F, Wen Y, Guo X (2014) CRISPR/Cas9 for genome editing: progress, implications and challenges Hum Mol Genet 23:R40-46 doi:10.1093/hmg/ddu125

Zhang J et al. (2019a) A strategy for identifying markers linked with stem rust resistance in wheat harbouring an alien chromosome introgression from a non-sequenced genome Theor Appl Genet 132:125-135 doi:10.1007/s00122-018-3201-8

Zhang W, Zhu X, Zhang M, Shi G, Liu Z, Cai X (2019b) Chromosome engineering-mediated introgression and molecular mapping of novel Aegilops speltoides-derived resistance genes for tan spot and Septoria nodorum blotch diseases in wheat Theor Appl Genet 132:2605-2614 doi:10.1007/s00122-019-03374-5

Zhang Z, Friesen TL, Xu SS, Shi G, Liu Z, Rasmussen JB, Faris JD (2011) Two putatively homoeologous wheat genes mediate recognition of SnTox3 to confer effector-triggered susceptibility to Stagonospora nodorum Plant J 65:27-38 doi:10.1111/j.1365-313X.2010.04407.x

Zhang ZC, Friesen TL, Simons KJ, Xu SS, Faris JD (2009) Development, identification, and validation of markers for marker-assisted selection against the Stagonospora nodorum toxin sensitivity genes Tsn1 and Snn2 in wheat Molecular Breeding 23:35-49 doi:10.1007/s11032-008-9211-5

Zong Y et al. (2017) Precise base editing in rice, wheat and maize with a Cas9-cytidine deaminase fusion Nat Biotechnol 35:438-440 doi:10.1038/nbt.3811

Genetic population structure of the Norwegian *Parastagonospora nodorum* population

Min Lin [1], Andrea Ficke [2], James Cockram[3], Morten Lillemo [1, *]

[1] Department of Plant Sciences, Faculty of Biosciences, Norwegian University of Life Sciences (NMBU), Ås, Norway

[2] Division of Biotechnology and Plant Health, Norwegian Institute of Bioeconomy Research (NIBIO), Ås, Norway

[3]John Bingham Laboratory, NIAB, Huntingdon Road, Cambridge, CB3 0LE, United Kingdom

*** Correspondence:**

Morten Lillemo

morten.lillemo@nmbu.no

Abstract

The necrotrophic fungal pathogen *Parastagonospora nodorum* causes Septoria nodorum blotch (SNB), which is one of the dominating leaf blotch diseases of wheat in Norway. A total of 165 *P. nodorum* isolates were collected from three wheat growing regions in Norway from 2015 to 2017. These isolates, as well as nine isolates from other countries, were analyzed for genetic variation using 20 simple sequence repeat (SSR) markers. Genetic analysis of the isolate collection indicated that the *P. nodorum* pathogen population infecting Norwegian spring and winter wheat underwent regular sexual reproduction and exhibited a high level of genetic diversity, with no genetic subdivisions between sampled locations, years or host cultivars. A high frequency of the presence of necrotrophic effector (NE) gene *SnToxA* was found in Norwegian *P. nodorum* isolates compared to other parts of Europe, and we hypothesize that the *SnToxA* gene is the major virulence factor among the three known *P. nodorum* NE genes (*SnToxA*, *SnTox1* and *SnTox3*) in the Norwegian pathogen population. While the importance of SNB as declined in much of Europe, Norway has remained as a *P. nodorum* hotspot, likely due at least in part to local adaptation of the pathogen population to ToxA sensitive Norwegian spring wheat cultivars.

1 Introduction

Parastagonospora nodorum (syn. *Phaeosphaeria nodorum; Septoria nodorum, Stagonospora nodorum or Leptosphaeria nodorum*) is one the most devastating necrotrophic fungal pathogens of wheat (*Triticum aestivum*), causing septoria nodorum blotch (SNB) on wheat leaves and glume blotch on glumes (Wicki et al., 1999). The yield loss caused by SNB can reach 50% when susceptible cultivars are grown under weather conditions conducive for *P. nodorum* (Eyal, 1981). Currently, no commercially available cultivar has shown complete resistance to SNB, so tillage, crop rotation and chemical control are still the most effective disease management practices used.

Epidemics of *P. nodorum* have been reported in all six continents where wheat is grown (Leath et al., 1993; Ficke et al., 2018a). SNB causes necrotic lesions in wheat leaves, with similar symptoms observed for other leaf blotch diseases of wheat, such as Septoria tritici blotch (STB, caused by *Zymoseptoria tritici*) and tan spot (caused by *Pyrenophora tritici-repentis*). Growth of these three pathogens is favored by warm and humid weather conditions, with dispersal of asexual spores mediated by rain splash and/or wind (Morrall and Howard, 1975; Bearchell et al., 2005), and often cause co-infections on wheat in Europe (Jalli et al., 2011; Ficke et al., 2018b). Although systematic *P. nodorum* incidence data from all European countries over the last 20 years is not available, fewer *P. nodorum* epidemics have been observed compared to *Z. tritici* in western Europe since the 1980s (Wiik, 2009). In the United Kingdom (UK) for example, data from 1844 to 2003 indicates that *P. nodorum* was the predominating pathogen on wheat until 1980s, after which its dominance was replaced by *Z. tritici* (Bearchell et al., 2005; Shaw et al., 2008). This change in pathogen dominance was correlated with the reduction of sulfur pollution, although other explanations were proposed earlier such as differences in cultivar resistance and respond to fungicide application (Shaw et al., 2008). However, reduction of sulfur in the atmosphere does not explain why *P. nodorum* still dominates in western Australia (Oliver et al., 2012) and Norway. Indeed in Norway *P. nodorum* is still the dominating leaf blotch pathogen of wheat, and sulfur pollution has not been reported to be higher than in any other of the European countries in which *Z. tritici* has come to dominate the leaf blotch complex in wheat.

As a model organism for necrotrophic fungal pathogens, *P. nodorum* is known to produce necrotrophic effectors (NEs), which interact with wheat effector sensitivity loci, causing programmed cell death in order to accelerate infections (Friesen et al., 2007; Oliver et al., 2012). So far, eight *P. nodorum* NEs have been characterized, (reviewed by Ruud and Lillemo, 2018), and three NE coding genes have been cloned: *SnToxA*, *SnTox1* and *SnTox3* (Liu et al., 2006; Liu et al., 2009; Liu et al., 2012). ToxA encoded by the *P. nodorum* gene *SnToxA*, was first characterized as the virulence factor of *P. tritici-repentis* (Tomas et al., 1990). Subsequently, it was shown that the *SnToxA* gene likely originated from *P. nodorum* and was passed on to *P. tritici-repentis* during a recent horizontal gene transfer (Friesen et al., 2006). Horizontal gene transfer of *P. nodorum SnToxA* into another wheat pathogen *Bipolaris sorokiniana*, has recently been reported in natural populations in Australia (McDonald et al., 2018) and the USA (Friesen et al., 2018). Reducing the growing area of ToxA sensitive cultivars or eliminating the wheat ToxA susceptibility locus *Tsn1* from breeding programs might reduce yield loss due to leaf blotch diseases substantially, since *SnToxA* is a virulence factor of three different wheat pathogens.

Population genetics studies of *P. nodorum* have previously been carried out at national to global scales using either restriction fragment length polymorphism (RFLP) probes or simple sequence repeat (SSR) markers, and high genetic variability within *P. nodorum* populations were observed (Keller et al., 1997; Murphy et al., 2000; Stukenbrock et al., 2006; Blixt et al., 2008). The reason why Norway is still one of the few countries in Europe where SNB remains the dominating leaf blotch disease of wheat remains unknown. One explanation could include the highly specialized host pathogen relationship based on necrotrophic effectors and their corresponding susceptibility genes in the wheat varieties grown in Norway. However, the genetic structure of the *P. nodorum* pathogen population in Norway and genotypic analysis of their NE genes has not been characterized to date, as Norwegian isolates were not included in the previously published global *P. nodorum* genetic studies (Stukenbrock et al., 2006; McDonald et al., 2013).

The purpose of the current study was to establish a Norwegian *P. nodorum* isolate collection, and to study their genetic structure and NE gene allele frequencies and to compare these genetic datasets with isolates from other countries. Specifically, we (1) established a collection of 165 Norwegian *P. nodorum* isolates, (2) genotyped the collection using 20 SSRs, (3) calculated both regional and nation-wide *P. nodorum SnTox* gene (*SnToxA*, *SnTox1* and *SnTox3*) frequencies (4)

compared the *P. nodorum* isolates collected from winter wheat and spring wheat, (5)investigated the relationship between *SnTox* gene frequencies and the cultivars where isolates were collected from, (6) assessed the multi-effector genotype distribution and the correlation with the corresponding cultivar NE sensitivities.

2 Material and methods

2.1 Sampling

P. nodorum isolates were collected from 23 fields in five wheat growing counties in Norway (Akershus, Østfold, Vestfold, Hedmark and Trøndelag). As Akershus, Østfold and Vestfold counties are geographically close to each other and have similar climate, these three regions were grouped as a single large region in this study (Figure 1). Field sampling was undertaken in 2015, 2016 and 2017. Roughly 30 wheat leaves were collected per cultivar per wheat field, which was naturally infected by *P. nodorum*. Leaf samples were collected from a total of 13 cultivars, dried and kept in room temperature. Only one single spore isolate was collected per leaf. In 2015, samples were collected only from winter wheat, while in 2016 and 2017 samples were collected from both winter and spring wheat cultivars. Except Jantarka, all cultivars have been tested for sensitivity to three known *P. nodorum* effectors (ToxA, Tox1 and Tox3) (Ruud et al., 2018). Two isolates (Isolate ID: 201865, 201982) were collected from wheat leaf samples sent by EffectaWheat project collaborators in 2017 from Denmark and Germany, respectively. One isolate (ID: 202580) was received from our EffectaWheat project collaborator in the UK. An additional set of six isolates from Switzerland (Sn99CH1A7a), USA (Sn6 and Sn79-1087), Mexico (CIMFU460-SN1, and CIMFU463-SN4), and Australia (SN15) were also included in this study.

2.2 Fungal material for DNA extraction

Isolates were grown on petri dishes containing Potato Dextrose Agar (PDA) for 14 days at 20 °C in darkness to promote mycelium growth. DNA was extracted using the DNEasy plant DNA Extraction Kit (Qiagen) from fungal biomass which was scraped from the surface of each petri dish.

2.3 Determination of mating type and *SnTox* gene profiles

To identify the mating type idiomorphs of each isolate, the mating type primers described by Bennett et al. (2003) were utilized for multiplex polymerase chain reaction (PCR), as described by Sommerhalder et al. (2006). For mating type MAT1-1, a 360 bp fragment was amplified while for MAT1-2, a 510 bp fragment was amplified. The MAT1-1 to MAT1-2 idiomorphs` ratio was tested to determine whether the deviation was significantly different from the 1:1 ratio by Chi-square test. Genotyping of *Actin* and *SnTox* genes (*SnToxA, SnTox1* and *SnTox3*) was performed by PCR as described by Gao et al. (2015). The Chi-squared test for given probabilities was carried out to compare *SnTox* gene allele frequency with the global *P. nodorum* collection published by McDonald et al.(2013). Pearson's Chi-squared tests were used to compare *SnTox* gene allele frequencies between locations, cultivars, wheat types and another Norwegian *P. nodorum* isolate collection from spring wheat (Ruud et al., 2018).

2.4 SSR analysis

Three expressed sequence tag (EST) derived SSR loci SNOD1, SNOD3, SNOD5, one minisatellite locus SNOD8 (Stukenbrock et al., 2005) and 16 newly developed SSR loci (Table S1) were used for genotyping. The new SSR markers were designed by Dr. Patrick C. Brunner at ETH Zurich based on the reference genome SN15 and alignments with genome sequences of 164 global strains of *P. nodorum* (Pereira et al. 2019). PCR was carried out with M13 tailed (Schuelke, 2000), fluorescent labeled primers (Table S1), PCR products separated by capillary electrophoresis using an ABI3730 Gene Analyzer (Applied Biosciences) and a GeneScan™ 500 LIZ™ dye Size Standard from Applied Biosystems (Life technologies), and the resulting data analyzed using Software: GeneMapper v.5 (Applied Biosystems).

2.5 Population genetic analyses

The genotype accumulation curve was calculated by R Studio Version 1.1.442 (RStudio Team 2015) using the function genotype_curve implemented in the R package `poppr` (Kamvar et al., 2014) in order to determine the number of loci required to discriminate individuals in a population. A UPGMA (unweighted pair group method with arithmetic mean) tree was created with non-parametric bootstrapping (n =100) using the function bruvo.boot/poppr, with genetic distance between individuals estimated by Bruvo`s distance (Bruvo et al., 2004) and a distance matrix generated by the UPGMA hierarchical clustering method. Genotype diversity information,

including allele frequency, Simpson`s index (λ) (Simpson, 1949), unbiased gene diversity H_{exp} (Nei, 1973), and evenness of each SSR locus, were calculated using the poppr package (Kamvar et al., 2014). In addition, the index of association (I_A) (Brown et al., 1980), the standard index of association (r_d), and corresponding p values for I_A and r_d were calculated using 1000 permutations by `poppr` package (Kamvar et al., 2014) to test the null hypothesis of linkage equilibrium of SSR loci due to random mating. The analysis of molecular variance (AMOVA) was also carried out by function implemented in the `poppr` package.

Population structure analysis of the Norwegian *P. nodorum* isolates was done using three different approaches. (1) Using STRUCTURE v. 2.3.4 (Pritchard et al., 2000; Falush et al., 2003). The number of genetic populations were tested from K = 1 to K = 5, and each K was iterated 10 times. The following parameters were used for structure analysis: admixed model using sampling location as prior, initial burn-in period of 30,000 with 10^6 additional cycles. The best value for K was estimated based on the deltaK approach (Evanno et al., 2005) implemented in Structure Harvester (Earl and vonHoldt, 2011). (2) Estimating SSR variation between isolates using principal component analysis (PCA) implemented in the R packages ade4 and adegenet (Dray and Dufour, 2007; Jombart, 2008). (3) Estimate optimal number of K using `snapclust` function implemented in adegenet/R (Jombart, 2008; Beugin et al., 2018), which combined both geometric and fast likelihood optimization.

3 Results

3.1 Sampling

A total of 165 *P. nodorum* isolates were collected in Norway over three years, from 2015 to 2017. Sample site information is listed in Table S2, including geographical origin, year of collection and from which wheat cultivar leaf material was collected. In summary, 48 isolates were collected in 2015, 74 isolates in 2016 and 43 isolates in 2017. Among those, 31% of the whole collection were isolated from spring wheat cultivars while the remaining 69% were isolated from winter wheat cultivars. From a geographical perspective, 92 isolates were collected from the main wheat growing region including Akershus, Østfold and Vestfold (southeast of Norway), 53 isolates were from Hedmark (inland Norway) and 20 isolates were from Trøndelag (central Norway) (Figure 1).

3.2 Genetic diversity of Norwegian *P. nodorum* isolates

All 20 SSR loci were amplified successfully across all 174 *P. nodorum* isolates, with less than 5% missing data for each locus. Based on these SSR profiles, the genotype-accumulation curve showed that the whole *P. nodorum* collection (including the nine international isolates) had 173 multilocus genotypes (MLG) (Figure S1). The minimum number of loci required to distinguish all individuals in this collection was 7 (Figure S1). Clone-corrections based on SSR profiles indicated that no clonal isolates were detected in any single region, however, isolate 202552 collected from Hedmark (2016) and isolate 202522 collected from Trøndelag (2016) showed the same SSR profile (Table 1). Therefore, only one isolate with this MLG was kept for the following clone-corrected analyse. The genetic diversity H_{exp} of the 16 new SSR markers ranged from 0.47 to 0.93 which was comparable with the range (0.35-0.80) of the four EST-SSR loci (SNOD1, SNOD 3, SNOD5 and SNOD8) which have been used in previously published *P. nodorum* population studies (Stukenbrock et al., 2006) (Table S3). An average of 12.65 alleles were observed for all 20 SSR loci and two loci (SNO301 and SNO1301) had notably high genetic diversity ($H_{exp} > 0.90$ and $\lambda > 0.90$) (Table S3). The average Nei`s genetic diversity for all markers was 0.69 (Table S3).

3.3 Test for random mating

PCR amplification for mating type idiomorphs were successful for all 174 tested isolates. Mating type ratios for isolates from each of the three tested regions did not significantly deviate from the expected 1:1 ratio (Table 1). However, the mating type distribution for the whole Norwegian isolate collection was skewed with ratio MAT1-1: MAT 1-2 (96: 69) ($p < 0.05$). The test of index of association (I_A) and standard index of association (r_d) estimated the linkage equilibrium in the Norwegian *P. nodorum* population. From Table 1, no significant deviation was observed from the null-hypothesis of no associations between loci, indicating that the Norwegian *P. nodorum* population undergoes regular cycles of sexual reproduction.

3.4 SnTox gene profile and allele frequency

PCR screening for presence/absence of the three known NE genes *SnToxA*, *SnTox1* and *SnTox3* revealed that the Norwegian *P. nodorum* population had relatively high *SnToxA* frequency

(67.9 %) compared to the other two NE genes *SnTox1* (46.1 %) and *SnTox3* (47.9%) (Table 2). As shown in Figure 2, genotype A+1+3- with presence of *SnToxA* and *SnTox1* but absence of *SnTox3* (N = 34) was the dominating multi-effector genotype and was identified in *P. nodorum* isolated from all 13 cultivars sampled in this study. The second most abundant genotype was A+1-3- (N = 31), and large proportions of this multi-effector genotype were isolated from the winter wheat cultivar Magnifik (Figure 2). Ten isolates in our collection did not possess any of the three known *SnTox* genes and were isolated from five different cultivars (Figure 2).

A subset of 160 isolates (excluding isolates collected from the wheat variety Jantarka) were tested for the association between *SnTox* gene frequencies and the sampling cultivars (Table S4). Chi-square test showed that *SnToxA*, *SnTox1* or *SnTox3* frequencies in *P. nodorum* isolates were independent from the wheat cultivars from which isolates were collected (Table S5). Additionally, Chi-square tests were carried out to test the association between *SnToxA*, *SnTox1* or *SnTox3* frequencies with mating type, sampling location, wheat types and cultivar NE sensitivities. Except for *SnTox3*, which was associated with mating types, no significant association was observed in the Chi-square tests of the remaining *SnTox* genes (Table S5).

3.5 Population structure of Norwegian *P. nodorum* isolates

Based on the SRUCTURE analysis results, the DeltaK method indicated two genetic subpopulations (clusters) in the Norwegian *P. nodorum* collection (K = 2) (Figure S2A). However, no geographical division of subpopulations was observed between the three regions investigated, with roughly equal proportions of isolates from each location assigned to the two K groups (Figure S2C). PCA analysis for the Norwegian isolate collection and the whole collection including foreign isolates were done separately. Figure S2B showed the PCA scatter plot of Norwegian *P. nodorum* isolates which were color coded by the two STRUCTURE genetic subpopulations, with no obvious separation of K within the PCA space observed. In addition, for the Norwegian isolates, no clear evidence of population subdivision by either location or year of collection wasfound (Figure 3A). Both PC1 and PC2 only explained 4.2% of the variance, which is probably due to the high genetic diversity in the Norwegian *P. nodorum* collection. In addition, PCA analysis of the whole collection including foreign isolates indicated that the two Mexican isolates clustered together and were separated from the other foreign (non-Norwegian) isolates along PC2 (Figure

3B). The Norwegian *P. nodorum* isolates showed quite high diversity and could not be differentiated from foreign isolates (Fig 3B). Population differentiation by mating type or by multi-effector genotypes in the Norwegian isolates was also tested by PCA (Fig S3(A) and S3(B)), but no clear pattern of clusters could be detected.

Similar to the PCA results, the snapclust method based on analysis of Akaike information content also estimated that the most likely number of genetic subpopulations in the Norwegian *P. nodorum* collection was 1 (Figure S4), as the lowest Akaike information criterion (AIC) value was 1 and the value increased when increasing the number of clusters estimated. The result didn`t change when adding all foreign isolates for the same snapclust analysis, indicating that there were no significant differences between Norwegian *P. nodorum* isolates and the foreign isolates included in our collection.

According to the UPGMA tree, only isolate Sn79-1087 from the USA formed a distinct branch. All other foreign isolates were connected to Norwegian isolates by medium to long branches (Figure 4). Two Mexican isolates were clustered closely together in the UPGMA tree, which corresponded to the results from PCA (Figure 3). Most *P. nodorum* isolates were connected by long branches (Figure 4), revealing the existence of high genetic diversity in the Norwegian *P. nodorum* population. Analysis of AMOVA also revealed that high genetic variance existed within predicted populations rather than between populations (Table S6), which was expected as the predicted subpopulations were not significantly differentiated.

4 Discussion

Table 1 (MAT ratio) showed that mating type ratio of the whole country deviated significantly ($p < 0.05$) from the 1:1 ratio. However, the ratio deviation for each location was not significantly different from 1:1, even though more MAT1-1 types were observed than MAT1-2 types in all locations (Table 1). It possible this might be caused by type I error and false rejection of the null hypothesis, since the p value was just 0.04. However, there are other possibilities which could explain this result. For example, according to Sommerhalder et al. (2006), when seedborne inoculum played the major role for *P. nodorum* primary inoculation, it might lead to a skewed ratio of mating types with rare sexual reproduction. In addition, asexual inoculum coming from wheat

debris might also serve as primary inoculum due to the reduced tillage practices (Mehra et al., 2015). The ratio of mating types deviated significantly from the 1:1 ratio when considering the nationwide Norwegian *P. nodorum* population (Table 1). However, the Norwegian *P. nodorum* population showed high genetic diversity, low clonal fraction, and the mating type ratios were not significantly different from 1:1 in any tested location. Moreover, index of association (I_A) and standard index of association (r_d) results confirmed that the Norwegian *P. nodorum* population underwent regular sexual reproduction (Table 1). Ascospores have also been found regularly in southeast Norway by trapping them with Burkhard spore traps (Ficke et al., 2016). We hypothesize that the major *P. nodorum* primary inoculum in Norway are ascospores, however, combined with considerable amount of seedborne and/or residue-borne inoculum. The regular sexual recombination contributes to the high genetic diversity. Therefore, no clear subdivision of the pathogen population was observed by either PCA or snapclust method. In addition, the deltaK approach used to estimate the best value of K from STRUCTURE analysis, can only be applied when the clusters in one population are equal to or more than 2. Therefore, the K = 2 estimated by this method might be an artefact, since there was no clear separation of isolates grouped to cluster 1 and cluster 2 (Figure S2B). In addition, statistical analysis of molecular variance (AMOVA) also supported our conclusion that no genetic subdivision of the Norwegian isolate collection is present (Table S6).

STB disease is the major problem on winter wheat in Europe, as *Z. tritici* ascospores surviving on stubble between crops (Fones and Gurr, 2015). Large volumes of *Z. tritici* ascospores are produced around crop harvesting time in the summer and autumn sown winter wheat provides a bridge for *Z. tritici* winter survival (Eriksen and Munk, 2003). Countries neighboring Norway such as Denmark and Sweden grow winter wheat in quite large scales compared to spring wheat (Statistics Sweden, 2018; Statistics Denmark, 2019). However, in Norway typically, more spring wheat is planted than winter wheat due to difficulties for sowing in rainy autumn (Statistics Norway, 2018). We hypothesize that STB is not the major leaf blotch pathogen in Norwegian spring wheat due to the lack of sufficient developing time for the long latent period which *Z. tritici* needs in comparison to *P. nodorum* (Cunfer, 1999). This could also explain the relatively higher occurrence of *Z. tritici* on winter wheat than spring wheat in Norway. Moreover, *P. nodorum* would compete with *Z. tritici* on winter wheat, but will encounter less competition on spring wheat

in Norway. Because of this we first expected the pathogen populations infecting Norwegian spring wheat might be different from the populations on winter wheat. However, the PCA scatter plot (Figure S3D) showed that this was not the case, as no clear differentiation of pathogen populations was observed by wheat type, suggesting that there is effectively only one large and diverse *P. nodorum* population infecting both winter wheat and spring wheat in Norway. A recent study by Richards et al. (2019) found two different *P. nodorum* populations in the US corresponding to spring wheat and winter wheat growing regions respectively, which was likely due to distinct selection pressure caused by the cultivars grown in each region. However, both spring wheat and winter wheat are grown in all wheat growing regions in Norway (and even in the same field but in different years). Therefore, the selection pressure on *P. nodorum* in Norway is likely multidirectional and non-constant, which might also contribute to the high genetic diversity in the pathogen population. High genetic variability within *P. nodorum* populations has also been reported by other population genetic studies in Australia, Sweden, and even the global collection (Murphy et al., 2000; Stukenbrock et al., 2006; Blixt et al., 2008), indicating this is a common feature in *P. nodorum*.

Ruud et al. (2018) studied the *SnTox* gene frequencies of 62 Norwegian *P. nodorum* isolates, collected from spring wheat during 2012 to 2014, and the allele frequencies for *SnToxA*, *SnTox1* and *SnTox3* were 0.69, 0.53 and 0.76, respectively. Table 3 shows the *SnTox* gene allele frequencies in our collection compared with the *P. nodorum* collection by Ruud et al. (2018), where significantly lower *SnTox3* frequencies were observed in our collection ($p < 0.001$). Significant differences were also detected when comparing *SnTox3* allele frequency in Ruud et al. (2018) with subsets of isolates collected from either spring wheat or winter wheat in our study. One possible explanation could be the relatively small sample size of Ruud et al. (2018)`s collection. Therefore, those isolates might not be as representative of the highly diverse *P. nodorum* pathogen population in Norway. In addition, the *SnTox* gene allele frequencies in a population may also change due to adaptation to the host NE sensitivities. The *SnToxA* frequency in our Norwegian *P. nodorum* isolate collection (67.9%) was significantly higher than the European level (12%), while the *SnTox1* (46.1%) and *SnTox3* (47.9 %) frequencies were significantly lower than the European levels (McDonald et al., 2013) (Table 2). Similar high *SnToxA* frequency was also observed in the *P. nodorum* isolate collection by Ruud et al. (2018).

Furthermore, Ruud et al. (2018) found that large proportions (46.5%) of Norwegian spring wheat cultivars and breeding lines carry the ToxA sensitivity locus, *Tsn1*. This is in contrast to a previous study of north-west European wheat varieties, which found high ToxA sensitivity to be present in just ~10% of varieties (Downie et al., 2018). We sampled isolates from 13 commercial wheat cultivars grown in Norway, which collectively covered more than 95% of the seed sales in the growing seasons (2015-2017) (Åssveen et al., 2018). Of these 13 cultivars, 30% were sensitive to ToxA, much higher than the proportion sensitive to either Tox1 (7.6 %) or Tox3 (15.3 %) (Table S4). In addition, we found that three of the four ToxA sensitive cultivars were spring wheat. Ruud et al. (2018) found, field SNB disease level in Norway was significantly correlated with ToxA sensitivity. While *SnTox1* has previously been found to be the most prevalent effector gene in the wider European *P. nodorum* population (89%) (McDonald et al., 2013), in Norway we found significantly lower *SnTox1* allele frequencies (46.1%). This is possibly due to the low selection pressure in Norway, as few cultivars grown in Norway are Tox1 sensitive (Ruud et al., 2018). Varieties sensitive to ToxA but insensitive to Tox3 have been shown to have the highest SNB disease severity in Norway (Ruud et al., 2018). Our *SnTox* gene profile results showed that the most abundant multi-effector genotype in our Norwegian isolate collection was A+1+3-, and the second largest genotype was A+1-3- (Figure 2). This A+(1+/-)3- genotype accounted for nearly 40% of the total Norwegian *P. nodorum* collection, which suggests that the NE profile of the pathogen population is under selection by corresponding NE sensitivities of the host.

The *SnToxA* frequency in *P. nodorum* isolates collected from ToxA sensitive cultivars was expected to be higher compared to the ToxA insensitive cultivars, as Richards et al. (2019) found low *SnToxA* frequency in the *P. nodorum* population where *Tsn1* is rare in the region, indicating there might be a fitness cost to carrying the *SnToxA* gene. However in our study, no significant difference was detected in *SnToxA* frequencies between isolates collected from ToxA sensitive and insensitive cultivars and the population was not clustered by cultivar sensitivity to ToxA (Fig S3C). We hypothesize that because of the inconsistent and multilateral selection pressure in Norway, carrying *SnToxA* still gives higher levels of competitive ability regardless of the fitness cost. In addition, a recent study from Peters Haugrud et al. (2019) revealed that *P. nodorum* isolates might not express all the necrotrophic effector genes they possess simultaneously. Depending on the host NE sensitivities, *P. nodorum* isolates would `adjust` expression profile of the effectors to the host

sensitivity (Peters Haugrud et al., 2019). This may therefore modulate any cost carrying a specific effector gene.

In summary, *P. nodorum* is considered as a pathogen with relatively high evolutionary potential and high expected risk (McDonald and Linde, 2002), which would facilitate rapid adaption to and breaking of host qualitative genetic resistance. Because of its ability of rapid local adaptation, high frequency of the *Tsn1* allele existing in Norwegian spring wheat cultivars helped to maintain the large *P. nodorum* population in Norway. Moreover, different selection pressures caused by cultivars with different NE sensitivities in spring and winter wheat may contribute to the high genetic diversity of the Norwegian *P. nodorum* population. Our results also suggest that eliminating *Tsn1* allele in Norwegian spring wheat cultivars might be a possible way to reduce SNB severity, as this approach was successfully applied in Australia (Vleeshouwers and Oliver, 2014). However, more research on this sophisticated *P. nodorum* -wheat pathosystem is still needed, as the diversified *P. nodorum* population in Norway harbors many other NE genes (Lin et al., 2020), which may enable rapid adaptation to new susceptibility loci once the *Tsn1* allele is removed from wheat cultivars.

5 Conflict of Interest

The authors declare that the research was conducted in the absence of any commercial or financial relationships that could be construed as a potential conflict of interest.

6 Author Contributions

MIL, AF and MOL collected leaf samples. MIL conducted the experiments and analyzed the data. MOL and JC gained project funding. MOL, AF and JC supervised the research. MIL drafted the manuscript. All authors revised and approved the manuscript.

7 Funding

Research was undertaken within the framework of the 2nd call ERA-NET for Coordinating Plant Sciences, within the ‘EfectaWheat’ project, with funding national from The Research Council of Norway, grant NFR251894

8 Acknowledgments

We gratefully thank Dr. Patrick C. Brunner and Prof. Bruce A. McDonald of Institute of Integrative Biology, Zurich (IBZ), ETH Zurich for providing SSR primer sequences and extensive advice on the analysis. Analysis suggestions from Kar-Chun Tan (Curtin University) is also acknowledged. We thank Anne Guri Marøy (NMBU) for genotyping the isolates with SSR markers, Jafar Razzaghian (NIBIO) for sharing the knowledge on single spore isolation. We thank the EfectaWheat Consortium for sharing leaf and isolate samples as well as Prof. Bruce A. McDonald (ETH Zurich), Dr. Tim Friesen (USDA-ARS, Fargo), Prof. Richard Oliver (Curtin University) and Dr. Pawan K. Singh (CIMMYT) for providing the isolates from Switzerland, USA, Australia and Mexico, respectively.

9 References

Åssveen, M., Tangsveen, J., and Weiseth, L. (2018). "Sorter og sortsprøving 2017," in *Jord- og Plantekultur 2018/NIBIO BOK*. Norwegian Institute of Bioeconomy research), 28-80.

Bearchell, S.J., Fraaije, B.A., Shaw, M.W., and Fitt, B.D. (2005). Wheat archive links long-term fungal pathogen population dynamics to air pollution. *Proc Natl Acad Sci U S A* 102(15)**,** 5438-5442. doi: 10.1073/pnas.0501596102.

Bennett, R.S., Yun, S.H., Lee, T.Y., Turgeon, B.G., Arseniuk, E., Cunfer, B.M., et al. (2003). Identity and conservation of mating type genes in geographically diverse isolates of Phaeosphaeria nodorum. *Fungal Genet Biol* 40(1)**,** 25-37. doi: 10.1016/s1087-1845(03)00062-8.

Beugin, M.P., Gayet, T., Pontier, D., Devillard, S., and Jombart, T. (2018). A fast likelihood solution to the genetic clustering problem. *Methods Ecol Evol* 9(4)**,** 1006-1016. doi: 10.1111/2041-210X.12968.

Blixt, E., Olson, A., Hogberg, N., Djurle, A., and Yuen, J. (2008). Mating type distribution and genetic structure are consistent with sexual recombination in the Swedish population of Phaeosphaeria nodorum. *Plant Pathology* 57(4)**,** 634-641. doi: 10.1111/j.1365-3059.2008.01826.x.

Brown, A.H., Feldman, M.W., and Nevo, E. (1980). Multilocus Structure of Natural Populations of HORDEUM SPONTANEUM. *Genetics* 96(2)**,** 523-536. doi: http://www.genetics.org/content/96/2/523.

Bruvo, R., Michiels, N.K., D'Souza, T.G., and Schulenburg, H. (2004). A simple method for the calculation of microsatellite genotype distances irrespective of ploidy level. *Mol Ecol* 13(7)**,** 2101-2106. doi: 10.1111/j.1365-294X.2004.02209.x.

Cunfer, B.M. (1999). "Stagonospora and Septoria Pathogens of Cereals: The Infection Process," in *Septoria and Stagonospora Diseases of Cereals: A Compilation of Global Research*, eds. M. van Ginkel, A. McNab & J. Krupinsky. (Mexico: CIMMYT), 41-45.

Downie, R.C., Bouvet, L., Furuki, E., Gosman, N., Gardner, K.A., Mackay, I.J., et al. (2018). Assessing European Wheat Sensitivities to Parastagonospora nodorum Necrotrophic Effectors and Fine-Mapping the Snn3-B1 Locus Conferring Sensitivity to the Effector SnTox3. *Front Plant Sci* 9**,** 881. doi: 10.3389/fpls.2018.00881.

Dray, S., and Dufour, A.B. (2007). The ade4 package: Implementing the duality diagram for ecologists. *Journal of Statistical Software* 22(4)**,** 1-20. doi: 10.18637/jss.v022.i04.

Earl, D.A., and vonHoldt, B.M. (2011). STRUCTURE HARVESTER: a website and program for visualizing STRUCTURE output and implementing the Evanno method. *Conservation Genetics Resources* 4(2)**,** 359-361. doi: 10.1007/s12686-011-9548-7.

Eriksen, L., and Munk, L. (2003). The occurrence of Mycosphaerella graminicola and its anamorph Septoria tritici in winter wheat during the growing season. *European Journal of Plant Pathology* 109(3)**,** 253-259. doi: 10.1023/A:1022851502770.

Evanno, G., Regnaut, S., and Goudet, J. (2005). Detecting the number of clusters of individuals using the software STRUCTURE: a simulation study. *Mol Ecol* 14(8)**,** 2611-2620. doi: 10.1111/j.1365-294X.2005.02553.x.

Eyal, Z. (1981). Integrated Control of Septoria Diseases of Wheat. *Plant Disease* 65(9)**,** 763-768. doi: 10.1094/Pd-65-763.

Falush, D., Stephens, M., and Pritchard, J.K. (2003). Inference of population structure using multilocus genotype data: Linked loci and correlated allele frequencies. *Genetics* 164(4)**,** 1567-1587.

Ficke, A., Asalf, B. and Ruud, A., 2016, December. Ascospore biology of Parastagonospora nodorum under Norwegian field conditions. In PHYTOPATHOLOGY (Vol. 106, No. 12, pp. 30-31).

Ficke, A., Cowger, C., Bergstrom, G., and Brodal, G. (2018a). Understanding Yield Loss and Pathogen Biology to Improve Disease Management: Septoria Nodorum Blotch - A Case Study in Wheat. *Plant Dis* 102(4)**,** 696-707. doi: 10.1094/PDIS-09-17-1375-FE.

Ficke, A., Dieseth, J.A., Kim, M.O., and Lillemo, M. (2018b). "Bladsjukdommer i norsk hvete. Forekomst, betydning of tiltak," in *Jord- og Plantekultur 2018/NIBIO BOK*. Norwegian Institute of Bioeconomy Research), 108-112.

Fones, H., and Gurr, S. (2015). The impact of Septoria tritici Blotch disease on wheat: An EU perspective. *Fungal Genet Biol* 79**,** 3-7. doi: 10.1016/j.fgb.2015.04.004.

Friesen, T.L., Holmes, D.J., Bowden, R.L., and Faris, J.D. (2018). ToxA Is Present in the U.S. Bipolaris sorokiniana Population and Is a Significant Virulence Factor on Wheat Harboring Tsn1. *Plant Dis* 102(12)**,** 2446-2452. doi: 10.1094/PDIS-03-18-0521-RE.

Friesen, T.L., Meinhardt, S.W., and Faris, J.D. (2007). The Stagonospora nodorum-wheat pathosystem involves multiple proteinaceous host-selective toxins and corresponding host

sensitivity genes that interact in an inverse gene-for-gene manner. *Plant J* 51(4)**,** 681-692. doi: 10.1111/j.1365-313X.2007.03166.x.

Friesen, T.L., Stukenbrock, E.H., Liu, Z., Meinhardt, S., Ling, H., Faris, J.D., et al. (2006). Emergence of a new disease as a result of interspecific virulence gene transfer. *Nature genetics* 38(8)**,** 953. doi: 10.1038/ng1839

Gao, Y., Faris, J.D., Liu, Z., Kim, Y.M., Syme, R.A., Oliver, R.P., et al. (2015). Identification and Characterization of the SnTox6-Snn6 Interaction in the Parastagonospora nodorum-Wheat Pathosystem. *Mol Plant Microbe Interact* 28(5)**,** 615-625. doi: 10.1094/MPMI-12-14-0396-R.

Jalli, M., Laitinen, P., and Latvala, S. (2011). The emergence of cereal fungal diseases and the incidence of leaf spot diseases in Finland. *Agricultural and Food Science* 20(1)**,** 62-73. doi: 10.2137/145960611795163015.

Jombart, T. (2008). adegenet: a R package for the multivariate analysis of genetic markers. *Bioinformatics* 24(11)**,** 1403-1405. doi: 10.1093/bioinformatics/btn129.

Kamvar, Z.N., Tabima, J.F., and Grunwald, N.J. (2014). Poppr: an R package for genetic analysis of populations with clonal, partially clonal, and/or sexual reproduction. *PeerJ* 2**,** e281. doi: 10.7717/peerj.281.

Keller, S.M., McDermott, J.M., Pettway, R.E., Wolfe, M.S., and McDonald, B.A. (1997). Gene Flow and Sexual Reproduction in the Wheat Glume Blotch Pathogen Phaeosphaeria nodorum (Anamorph Stagonospora nodorum). *Phytopathology* 87(3)**,** 353-358. doi: 10.1094/PHYTO.1997.87.3.353.

Leath, S., Scharen, A.L., Dietzholmes, M.E., and Lund, R.E. (1993). Factors Associated with Global Occurrences of Septoria-Nodorum Blotch and Septoria-Tritici Blotch of Wheat. *Plant Disease* 77(12)**,** 1266-1270. doi: 10.1094/Pd-77-1266.

Lin, M., Corsi, B., Ficke, A., Tan, K.-C., Cockram, J., and Lilemo, M. Genetic mapping using a wheat multi-founder population reveals a locus on chromosome 2A controlling resistance to both leaf and glume blotch caused by the necrotrophic fungal pathogen Parastagonospora nodorum. *Theoretical and Applied Genetics,* (in press)

Liu, Z., Faris, J.D., Oliver, R.P., Tan, K.C., Solomon, P.S., McDonald, M.C., et al. (2009). SnTox3 acts in effector triggered susceptibility to induce disease on wheat carrying the Snn3 gene. *PLoS Pathog* 5(9)**,** e1000581. doi: 10.1371/journal.ppat.1000581.

Liu, Z., Friesen, T.L., Ling, H., Meinhardt, S.W., Oliver, R.P., Rasmussen, J.B., et al. (2006). The Tsn1–ToxA interaction in the wheat–Stagonospora nodorum pathosystem parallels that of the wheat–tan spot system. *Genome* 49(10)**,** 1265-1273. doi: 10.1139/g06-088.

Liu, Z., Zhang, Z., Faris, J.D., Oliver, R.P., Syme, R., McDonald, M.C., et al. (2012). The cysteine rich necrotrophic effector SnTox1 produced by Stagonospora nodorum triggers susceptibility of wheat lines harboring Snn1. *PLoS Pathog* 8(1)**,** e1002467. doi: 10.1371/journal.ppat.1002467.

McDonald, B.A., and Linde, C. (2002). Pathogen population genetics, evolutionary potential, and durable resistance. *Annu Rev Phytopathol* 40**,** 349-379. doi: 10.1146/annurev.phyto.40.120501.101443.

McDonald, M.C., Ahren, D., Simpfendorfer, S., Milgate, A., and Solomon, P.S. (2018). The discovery of the virulence gene ToxA in the wheat and barley pathogen Bipolaris sorokiniana. *Mol Plant Pathol* 19(2)**,** 432-439. doi: 10.1111/mpp.12535.

McDonald, M.C., Oliver, R.P., Friesen, T.L., Brunner, P.C., and McDonald, B.A. (2013). Global diversity and distribution of three necrotrophic effectors in Phaeosphaeria nodorum and related species. *New Phytol* 199(1)**,** 241-251. doi: 10.1111/nph.12257.

Mehra, L.K., Cowger, C., Weisz, R., and Ojiambo, P.S. (2015). Quantifying the Effects of Wheat Residue on Severity of Stagonospora nodorum Blotch and Yield in Winter Wheat. *Phytopathology* 105(11)**,** 1417-1426. doi: 10.1094/PHYTO-03-15-0080-R.

Morrall, R.A.A., and Howard, R.J. (1975). The epidemiology of leaf spot disease in a native prairie. II. Airborne spore populations of Pyrenophora tritici-repentis. *Canadian Journal of Botany* 53(20)**,** 2345-2353. doi: 10.1139/b75-260.

Murphy, N.E., Loughman, R., Appels, R., Lagudah, E.S., and Jones, M.G.K. (2000). Genetic variability in a collection of Stagonospora nodorum isolates from Western Australia. *Australian Journal of Agricultural Research* 51(6)**,** 679-684. doi: 10.1071/Ar99107.

Nei, M. (1973). Analysis of gene diversity in subdivided populations. *Proc Natl Acad Sci U S A* 70(12)**,** 3321-3323. doi: https://doi.org/10.1073/pnas.70.12.3321.

Oliver, R.P., Friesen, T.L., Faris, J.D., and Solomon, P.S. (2012). Stagonospora nodorum: from pathology to genomics and host resistance. *Annu Rev Phytopathol* 50**,** 23-43. doi: 10.1146/annurev-phyto-081211-173019.

Pereira, D., Brunner, P.C. and McDonald, B.A., 2019. Natural selection drives population divergence for local adaptation in a wheat pathogen. *bioRxiv*, p.805127.

Peters Haugrud, A.R., Zhang, Z., Richards, J.K., Friesen, T.L., and Faris, J.D. (2019). Genetics of Variable Disease Expression Conferred by Inverse Gene-For-Gene Interactions in the Wheat-Parastagonospora nodorum Pathosystem. *Plant Physiol* 180(1)**,** 420-434. doi: 10.1104/pp.19.00149.

Pritchard, J.K., Stephens, M., and Donnelly, P. (2000). Inference of population structure using multilocus genotype data. *Genetics* 155(2)**,** 945-959.

Richards, J.K., Stukenbrock, E.H., Carpenter, J., Liu, Z., Cowger, C., Faris, J.D., et al. (2019). Local adaptation drives the diversification of effectors in the fungal wheat pathogen Parastagonospora nodorum in the United States. *PLoS Genet* 15(10)**,** e1008223. doi: 10.1371/journal.pgen.1008223.

RStudio Team (2015) RStudio: Integrated Development for R. RStudio, Inc., Boston, MA URL http://www.rstudio.com/.

Ruud, A.K., Dieseth, J.A., and Lillemo, M. (2018). Effects of Three Parastagonospora nodorum Necrotrophic Effectors on Spring Wheat under Norwegian Field Conditions. *Crop Science* 58(1)**,** 159-168. doi: 10.2135/cropsci2017.05.0281.

Ruud, A.K., and Lillemo, M. (2018). "Diseases affecting wheat: Septoria nodorum blotch," in *Integrated disease management of wheat and barley*. (Cambridge, UK: Burleigh Dodds Science Publishing Limited), 109-144.

Schuelke, M. (2000). An economic method for the fluorescent labeling of PCR fragments. *Nat Biotechnol* 18(2), 233-234. doi: 10.1038/72708.

Shaw, M.W., Bearchell, S.J., Fitt, B.D.L., and Fraaije, B.A. (2008). Long-term relationships between environment and abundance in wheat of Phaeosphaeria nodorum and Mycosphaerella graminicola. *New Phytologist* 177(1)**,** 229-238. doi: 10.1111/j.1469-8137.2007.02236.x.

Simpson, E.H. (1949). Measurement of Diversity. *Nature* 163(4148)**,** 688-688. doi: 10.1038/163688a0.

Sommerhalder, R.J., McDonald, B.A., and Zhan, J. (2006). The Frequencies and Spatial Distribution of Mating Types in Stagonospora nodorum Are Consistent with Recurring Sexual Reproduction. *Phytopathology* 96(3)**,** 234-239. doi: 10.1094/PHYTO-96-0234.

Statistics Denmark (2019). Statistics Denmark.

Statistics Norway (2018). Statistics Norway.

Statistics Sweden (2018). Statistics Sweden.

Stukenbrock, E.H., Banke, S., and McDonald, B.A. (2006). Global migration patterns in the fungal wheat pathogen Phaeosphaeria nodorum. *Mol Ecol* 15(10)**,** 2895-2904. doi: 10.1111/j.1365-294X.2006.02986.x.

Stukenbrock, E.H., Banke, S., Zala, M., McDonald, B.A., and Oliver, R.P. (2005). Isolation and characterization of EST-derived microsatellite loci from the fungal wheat pathogen Phaeosphaeria nodorum. *Molecular Ecology Notes* 5(4)**,** 931-933. doi: 10.1111/j.1471-8286.2005.01120.x.

Tomas, A., Feng, G.H., Reeck, G.R., Bockus, W.W., and Leach, J.E. (1990). Purification of a Cultivar-Specific Toxin from Pyrenophora-Tritici-Repentis, Causal Agent of Tan Spot of Wheat. *Molecular Plant-Microbe Interactions* 3(4)**,** 221-224. doi: 10.1094/Mpmi-3-221.

Vleeshouwers, V.G., and Oliver, R.P. (2014). Effectors as tools in disease resistance breeding against biotrophic, hemibiotrophic, and necrotrophic plant pathogens. *Mol Plant Microbe Interact* 27(3)**,** 196-206. doi: 10.1094/MPMI-10-13-0313-IA.

Wicki, W., Winzeler, M., Schmid, J.E., Stamp, P., and Messmer, M. (1999). Inheritance of resistance to leaf and glume blotch caused by Septoria nodorum Berk. in winter wheat. *Theoretical and Applied Genetics* 99(7-8)**,** 1265-1272. doi: 10.1007/s001220051332.

Wiik, L. (2009). Yield and disease control in winter wheat in southern Sweden during 1977–2005. *Crop Protection* 28(1), 82-89. doi: 10.1016/j.cropro.2008.09.002

Table 1. The clonal fraction, the linkage equilibrium test results and mating idiomorphs of Norwegian *P. nodorum* isolate collection from different regions.' Main' includes three counties in the major wheat growing region (Akershus, Vestfold and Østfold)

Population	No.of isolates	Clone corrected	Clonal fraction	I_A	p.I_A	r_d	p. r_d	Ratio MAT	χ^2	p. χ2
Hedmark	53	53	0	-0.16	0.98	-0.01	0.98	30:23	0.92	0.33
Main	92	92	0	0.03	0.30	0.002	0.30	55:37	4.26	0.06
Trøndelag	20	20	0	-0.16	1.00	-0.008	1.00	11:9	0.2	0.65
Whole population	165	164	0.01	-0.02	0.85	-0.0001	0.85	96:69	4.42*	0.04

P < 0.05 *, I_A: the index of association (Brown et al., 1980), p.I_A: p values of I_A, r_d: the standard index of association , p. r_d: p values of r_d, χ^2: Chi-square value for deviation from the 1:1 mating idiomorphs ratio, p. χ2: p value for chi-square test

Table 2 Frequencies of the three known effectors in Norway and chi-square test for *SnTox* gene frequencies in Norway compared with the frequencies in Europe

Population	*SnToxA*	*SnTox1*	*SnTox3*
Europe (McDonald et al., 2013)	12%	89%	67%
Hedmark (N=53)	39 (73.6%)***	24 (45.3%)***	25 (47.2%)**
Main (N=92)	60 (65.2%)***	45 (48.9%)***	48 (52.2%)**
Trøndelag (N=20)	13 (65.0%)***	7 (35.0%)***	6 (30.0%)***
All population (N=165)	112 (67.9%)***	76 (46.1%)***	79 (47.9%)***

***p < 0.0001, **p <0.01

Table 3 Frequencies of the three known effectors in Norway and chi-square test for *SnTox* frequency in Norway compared with another Norwegian *P. nodorum* collection. The number of isolates included were labeled in parenthesis.

Number of isolates	*SnToxA*	*SnTox1*	*SnTox3*
Ruud et al. (2018)`s collection (N = 62)	43 (69%)	33 (53%)	47 (76%)
Spring wheat (N = 51)	37 (72.5%)	29 (56.9%)	21 (41.2%) ***
Winter wheat (N = 114)	75 (65.8%)	47 (41.2%)	58 (50.9%) **
Total (N= 165)	112 (67.9%)	76 (46.1%)	79 (47.9%) ***

***p < 0.001, ** p < 0.01

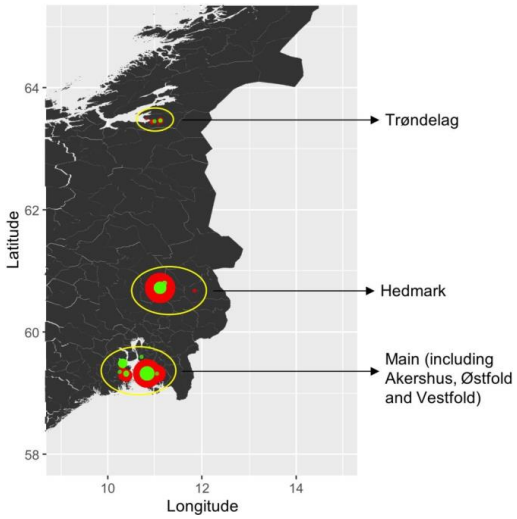

Figure 1 Sampling locations of *P. nodorum* isolates in Norway. The wheat cultivar types from which isolates were collected from are coded by color (red: winter cultivars; green: spring cultivars), and the size of each dot indicates the sample size.

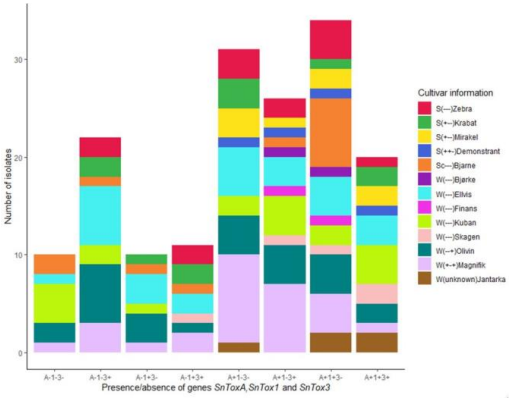

Figure 2 Distribution of multi-effector genotypes in the Norwegian *P. nodorum* isolate collection (N = 165). The wheat cultivar from which the *P. nodoroum* isolates were identified are color coded. S: spring wheat, W: winter wheat. Cultivar sensitivities to the *P. nodorum* effectors ToxA, Tox1 and Tox3 are indicated in parentheses. ("+": sensitive, "-": insensitive).

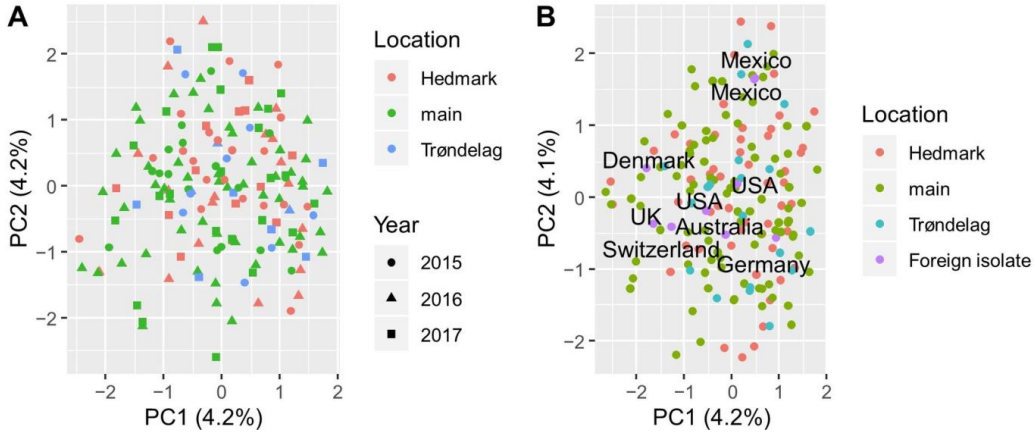

Figure 3 PCA analysis of population structure in *P. nodorum* isolates. (A) PCA scatter plot based on Norwegian isolates, sampling locations are coded by color, the year of collection is coded by shape. (B) PCA scatter plot based on whole isolate collection including nine isolates from outside of Norway, sampling locations in Norway are coded by color, country names of foreign isolates are indicated in the plot.

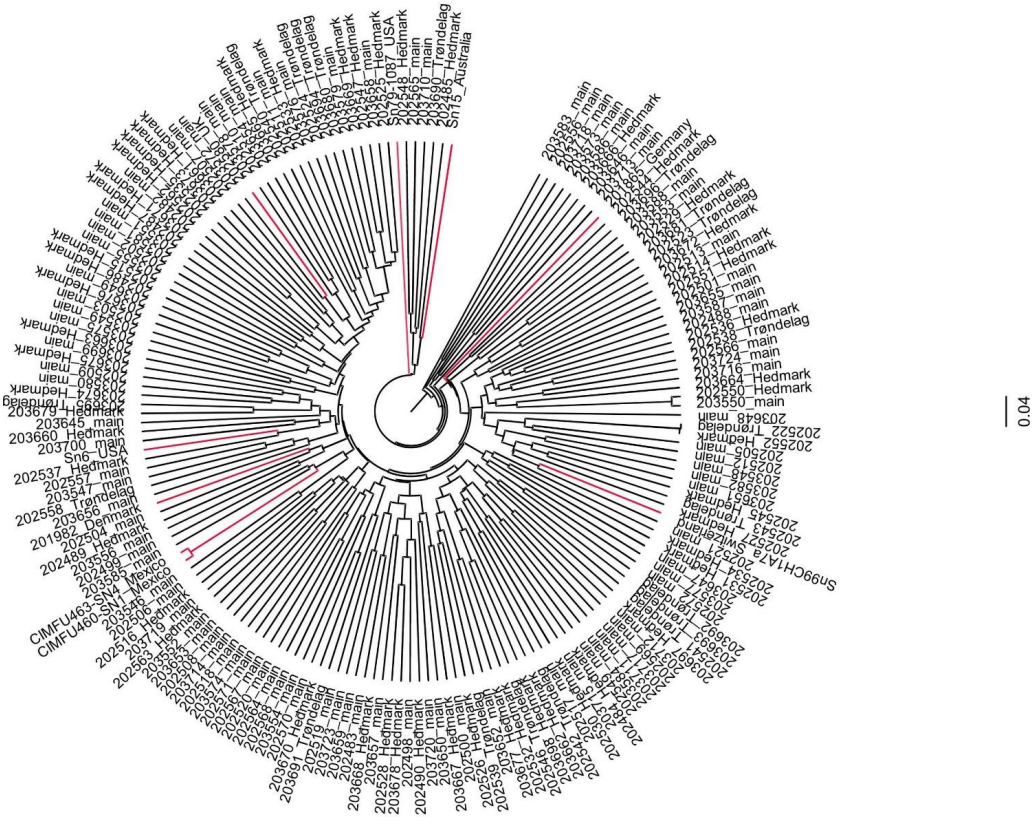

Figure 4 UPGMA tree of 165 Norwegian and 9 foreign *P.nodorum* isolates. Isolates are labeled by the Isolate ID and region of collection. Foreign isolates are marked in red.

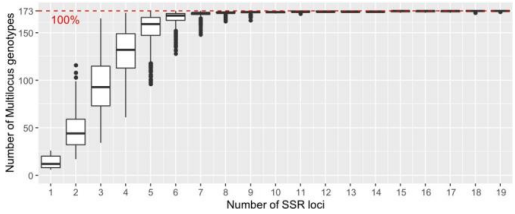

Figure S1 The genotype-accumulation curve for 174 *P. nodorum* isolates genotyped by 20 SSR markers. The horizontal axis indicates the number of SSR loci randomly sampled up to (n-1) loci, and the vertical axis represents the number of multilocus genotypes. The red-dashed line represents the total number of multilocus genotype observed in the collection.

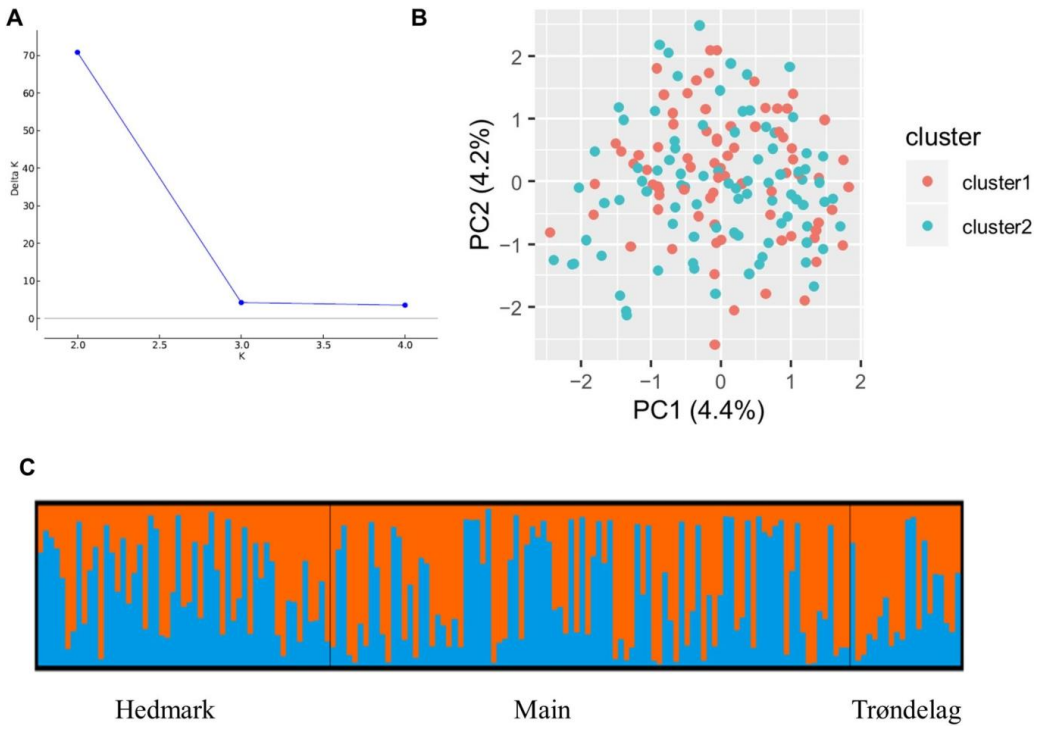

Figure S2 Genetic structure analysis of the Norwegian *P. nodorum* population. (A), DeltaK plot, indicating K=2 or lower as the best fit for the Norwegian *P. nodorum* population. (B), PCA scatter plot of Norwegian *P. nodorum* isolates color coded by the predicted clusters (genetic substructure) from STRUCTURE results. (C), Estimated genetic substructure across all 165 Norwegian isolates using STRUCTURE (K = 2), vertical bars indicate the probability of each isolate being assigned to the two substructure groups.

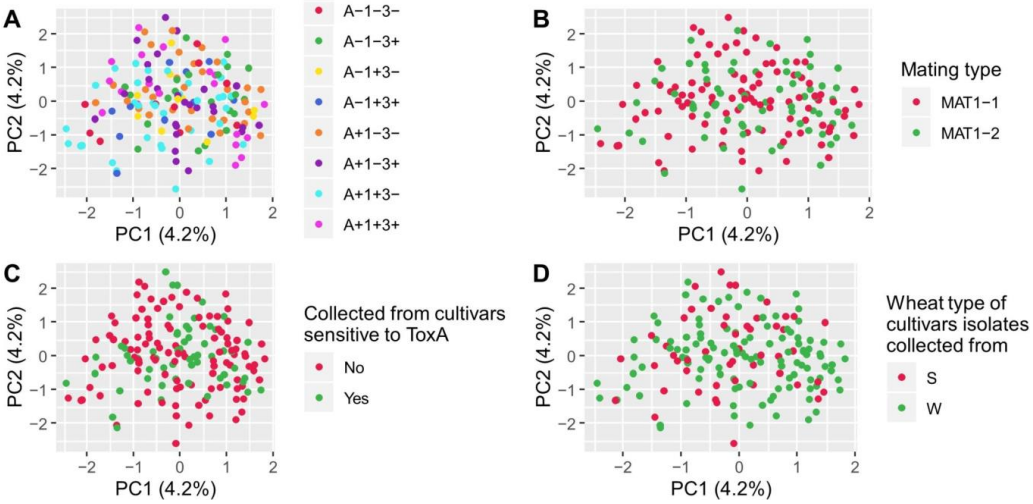

Figure S3 PCA scatter plot of Norwegian *P. nodorum* isolates according to: (A) NE profiles, (B) mating type, (C) host cutivars sensitivity to ToxA, (D) wheat type of host cultivar (S: spring wheat, W: winter wheat)

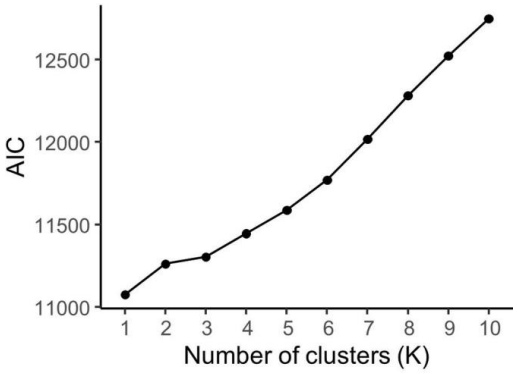

Figure S4 The Akaike information criterion (AIC) value of different number of clusters (K) considered in Norwegain *P. nodorum* isolate collection estimated by `snapclust`.

Supplementary Material

Table S1 Newly developed SSR primer sequences

SSR Name	Repeat motif	Labelling dye	Primer left (5' to 3')	Primer right (5' to 3')	PCR product size range (bp)
SNO101	ACC	PET	TCGGTCAGAAGCATAACGGT	TCGCGATGACTACGGCTC	155-179
SNO301	TC	NED	CAGGGCATCATTTCGTAACGT	GGGAGGTGTGTCTGGTACTT	114-174
SNO402	TTG	FAM	GAGAGCGTTGTTGTTGCCA	GCCAAGGTCAGAACAACGG	113-158
SNO501	GTT	VIC	CTGGGTGTTCTGCTCGTTG	ACTCTACATCACTCATCATGGAC	112-130
SNO702	ACC	PET	CAAACGAGCCTCATACGACC	TATAAGGTGGTTCTCGGCGG	123-144
SNO801	GCA	NED	ACAATCACATGCCATCCCTG	ACTATCTGGTCGAGCGTCTG	108-153
SNO802	TCTAC	NED	TTCTATCAGTCGCGGATCAC	TGGAGATAGCGAGAATGGCA	95-225
SNO901	TGT	FAM	CTGCTTCTCGGTCGCCAT	TCGTCTTCCATCTGTCCACG	188-257
SNO1001	TG	PET	GTAGACCAGCTGCGGAAATG	CAAGCTACTACCCACTTTACAGG	149-229
SNO1002	TGG	VIC	GTGTTGGTATTGTAACGTGTGC	CTACCCCAGCTACACCACG	123-144
SNO1301	TCT	FAM	TGGCGAACAGTAGAGGATCC	TTCGCCAATGATGTCACGTC	185-266

SNO1302	GGCGTA	NED	TCTTGGATGGTGTGAAGCCT	CATCTTTACGGGCGCATTGA	87-159
SNO1801	TCA	FAM	TGCACGCCTCTTCAAATAGC	GCCACCCTATTTCTCTTCTGG	198-351
SNO1802	CA	VIC	GCTGCACTTCATACTCAGATAGC	GAGGGTGTCGATTGAGGTCA	116-202
SNO3001	GAA	NED	GCTTCTCCGACAACACTGC	CGATCTCAGTCGGCAGTACT	90-240
SNO3701	GAA	PET	CAAACACAACACGCGCGG	AGGCAATGTATACCCGCCAT	133-145

Table S2 Field sampling information

Region	Year collected	Number of isolates collected	Wheat cultivar(s)	Wheat type
Trøndelag	2015	9	Magnifik, Olivin	Winter wheat
Trøndelag	2016	4	Magnifik,Bjarne, Zebra	Winter wheat, Spring wheat
Trøndelag	2017	7	Magnifik, Ellvis, Bjarne, Zebra,Mirakel,	Winter wheat, Spring wheat
Hedmark	2015	22	Ellvis, Kuban, Magnifik, Olivin	Winter wheat
Hedmark	2016	18	Ellvis, Kuban, Magnifik, Olivin, Jantarka, Bjarne, Skagen, Demonstrant, Krabat, Zebra	Winter wheat, Spring wheat
Hedmark	2017	13	Ellvis, Kuban, Magnifik, Olivin, Bjarne, Krabat, Mirakel, Zebra	Winter wheat, Spring wheat
Akershus, Østfold, Vestfold	2015	17	Ellvis, Kuban, Magnifik, Olivin	Winter wheat
Akershus, Østfold, Vestfold	2016	52	Bjoerke, Ellvis, Finans, Jantarka, Kuban, Magnifik, Olivin, Skagen, Bjarne, Demonstrant, Krabat, Mirakel, Zebra	Winter wheat, Spring wheat

Akershus, Østfold, Vestfold	2017	23	Ellvis, Kuban, Magnifik, Olivin, Bjarne, Krabat, Mirakel, Zebra	Winter wheat, Spring wheat
Other countries (Denmark, Germany, Switzerland, UK, USA, Mexico, and Australia)		9		

Table S3 Number of SSR alleles detected, Simpson`s index, Nei`s gene diversity H_{exp} and evenness for each SSR marker

SSR	Alleles	λ^a	$H_{exp}{}^b$	Evenness
SNOD1	9	0.37	0.37	0.41
SNOD3	6	0.35	0.35	0.47
SNOD5	12	0.79	0.80	0.69
SNOD8	5	0.40	0.40	0.64
SNO101	7	0.63	0.64	0.69
SNO301	21	0.90	0.90	0.77
SNO402	12	0.80	0.80	0.75
SNO501	7	0.56	0.56	0.68
SNO702	8	0.81	0.81	0.84
SNO801	15	0.88	0.89	0.81
SNO802	11	0.56	0.56	0.51
SNO901	10	0.79	0.80	0.79
SNO1001	15	0.79	0.80	0.62
SNO1002	8	0.63	0.63	0.62
SNO1301	24	0.92	0.93	0.77
SNO1302	10	0.67	0.67	0.67
SNO1801	23	0.87	0.88	0.69
SNO1802	20	0.85	0.86	0.63
SNO3001	25	0.47	0.47	0.29
SNO3701	5	0.71	0.72	0.80
Mean	12.65	0.69	0.69	0.66

a: Simpson`s index (λ) (Simpson, 1949),

b: unbiased gene diversity (H_{exp}) (Nei, 1973)

Table S4 Wheat cultivar type and sensitivity to the three known *P. nodorum* NEs: ToxA, Tox1 and Tox3

Cultivar name	No. of isolates collected from	Wheat type	Cultivar sensitivity to		
			ToxA	Tox1	Tox3
Bjarne	14	S	-	-	-
Demonstrant	4	S	+	+	-
Krabat	11	S	+	-	-
Mirakel	8	S	+	-	-
Zebra	14	S	-	-	-
Bjørke	2	W	-	-	-
Ellvis	27	W	-	-	-
Finans	2	W	-	-	-
Jantarka	5	W	unknown	unknown	unknown
Kuban	19	W	-	-	-
Magnifik	28	W	+	-	+
Olivin	26	W	-	-	+
Skagen	5	W	-	-	-
Total			4 (30.1%)	1 (7.6%)	2 (15.3%)

S: spring wheat, W: winter wheat, +: sensitive, -: insensitive

Table S5 Chi-square test for independence of *SnTox* frequency and cultivars where isolates were collected from. NE = necrotrophic effector

	Cultivar (χ^2)	*P. nodorum* mating type (χ^2)	Sampling location (χ^2)	Wheat type (χ^2)	Cultivars`NE sensitivity (χ^2)
ToxA frequency	16.51	0.01	1.28	0.61	5.37
Tox1 frequency	12.69	1.23	1.91	3.06	4.82
Tox3 frequency	6.38	4.58*	2.71	1.01	0.09

*: $p < 0.05$

Table S6 Analysis of molecular variance (AMOVA). Df: degree of freedom

	Df	Sum of squares	Mean square	Variance	Percentage %	Phi statistics	P value
By locations							
Between regions	2	30.29	15.15	0.03	0.21		
Within regions	161	2223.61	13.81	13.81	99.79		
Total	163	2253.91	13.83	13.84	100.00	0.002	0.65
By cultivars							
Between Cultivars	12	162.69	13.56	-0.02	-0.17		
Within Cultivars	151	2091.22	13.85	13.85	100.17		
Total	163	2253.91	13.83	13.82	100.00	-0.002	0.66
By Years							
Between years	2	25.67	12.84	-0.02	-0.14		
Within years	161	2228.23	13.84	13.84	100.14		
Total	163	2253.91	13.83	13.82	100.00	-0.001	0.73
By Mating type							
Between Mating type	1	13.96	13.96	0.002	0.01		
Within mating type	162	2239.95	13.83	13.83	99.99		

Total	163	2253.91	13.83	13.83	100.00	0.0001	0.44
Between *SnToxA* presence and absence							
Between *SnToxA* presence and absence	1	14.65	14.65	0.01	0.08		
Within *SnToxA* presence or absence group	162	2239.26	13.82	13.82	99.92		
Total	163	2253.91	13.83	13.83	100.00	0.0008	0.33
Between locations and years							
Between locations	2	30.29	15.15	0.07	0.52	0.005	0.06
Between years within location	6	71.51	11.92	-0.12	-0.85	-0.009	0.99
Within year	155	2152.11	13.88	13.88	100.33	-0.003	0.94
Total	163	2253.91	13.83	13.84	100.00		

Genetic mapping using a wheat multi-founder population reveals a locus on chromosome 2A controlling resistance to both leaf and glume blotch caused by the necrotrophic fungal pathogen *Parastagonospora nodorum*

Min Lin1, Beatrice Corsi2, Andrea Ficke3, Kar-Chun Tan4, James Cockram2, Morten Lillemo1

1Department of Plant Sciences, Norwegian University of Life Sciences, Post Box 5003, NO-1432 Ås, Norway

2John Bingham Laboratory, NIAB, Huntingdon Road, Cambridge, CB3 0LE, United Kingdom

3 Norwegian Institute of Bioeconomy Research Høgskoleveien 7, NO-1433 Ås, Norway

4 Centre for Crop and Disease Management, School of Molecular and Life Sciences, Curtin University, Bentley, Western Australia, Australia

Correspondence:
Morten Lillemo
morten.lillemo@nmbu.no

Abstract

The necrotrophic fungal pathogen *Parastagonospora nodorum* is the causal agent of septoria nodorum leaf blotch and glume blotch, which are common wheat (*Triticum aestivum* L.) diseases in humid and temperate areas. Susceptibility to septoria nodorum leaf blotch can partly be explained by sensitivity to corresponding *P. nodorum* necrotrophic effectors (NEs). Susceptibility to glume blotch is also quantitative, however the underlying genetics have not been studied in detail. Here we genetically map resistance/susceptibility loci to leaf and glume blotch using an eight-founder wheat multiparent advanced generation intercross (MAGIC) population. The population was assessed in six field trials across two sites and four years. Seedling infiltration and inoculation assays using three *P. nodorum* isolates were also carried out, in order to compare quantitative trait loci (QTL) identified under controlled conditions with those identified in the field. Three significant field resistance QTL were identified on chromosomes 2A and 6A, while four significant seedling resistance QTL were detected on chromosomes 2D, 5B and 7D. Among these, *QSnb.niab-2A.3* for field resistance to both leaf blotch and glume blotch was detected in Norway and the UK. Colocation with a QTL for seedling reactions against culture filtrate from a Norwegian *P. nodorum* isolate indicated the QTL could be caused by a novel NE sensitivity. The consistency of this QTL for leaf blotch at the seedling and adult plant stages and culture filtrate infiltration was confirmed by haplotype analysis. However, opposite effects for the leaf blotch and glume blotch reactions suggest that different genetic mechanisms may be involved.

Introduction

Septoria nodorum blotch (SNB), caused by the necrotrophic pathogen *Parastagonospora* (synonyms *Septoria, Stagonospora*) *nodorum* (Berk.) is one of the most important fungal diseases of wheat (*Triticum aestivum*, L.), and has been reported in almost all wheat-producing areas worldwide (Ficke et al. 2018; Francki 2013; Friesen et al. 2007; Oliver et al. 2012). It can cause lesions on both wheat leaves and glumes, and can reduce grain yield by 30 % (Bhathal et al. 2003; Wicki et al. 1999). Infected seeds and wheat debris are the primary inoculum sources, with infection favored by warm and humid conditions at later wheat developmental stages, as the asexual pycnidosores are dispersed by rain-splash (Blixt et al. 2008; King et al. 1983; Ruud and Lillemo 2018; Sommerhalder et al. 2011). Currently, control of SNB relies heavily on fungicide application. Due to its mixed reproduction system, the genetic diversity and evolutionary potential of the pathogen population is considerable (McDonald and Linde 2002; Stukenbrock et al. 2006). Therefore, regardless of the environmental side effects caused by fungicide application, the risk of losing the chemical control efficacy is quite high as pathogen populations are being exposed to high selection pressure against limited groups of fungicides (Pereira et al. 2017). Thus, improving wheat genetic resistance to SNB is both a more environmentally friendly and durable method to control SNB. However, SNB resistance is controlled by many genes with additive effects (Friesen and Faris 2010). The durability of cultivar resistance to SNB is also challenged by the variability of the pathogen population within and between locations.

As a necrotrophic pathogen, the host interaction of *P. nodorum* follows an inverse gene for gene model (Friesen et al. 2007) whereby necrotrophic effectors (NEs) produced by the pathogen interact with corresponding host sensitivity loci (*Snn*) and trigger programmed cell death in host tissues. By definition, the necrotrophic pathogen feeds on dying tissues and benefits from the host-NE interactions to expand infection. *P. nodorum* NEs are small secreted proteins, previously called host-selective toxins (HSTs), which act as virulence factors facilitating disease development (Liu et al. 2004a; Liu et al. 2004b). Up to now, eight NEs have been identified which interact with nine wheat sensitivity loci (Ruud and Lillemo 2018; Shi et al. 2015). Among those, only three *P. nodorum* NE genes have been cloned: ToxA, Tox1 and Tox3 (Friesen et al. 2009; Liu et al. 2009; Liu et al. 2012). In addition, two of the host sensitivity genes have been cloned in wheat: *Tsn1* and *Snn1* (Faris et al. 2010; Shi et al. 2016). Interestingly, both genes encode receptor-like proteins, classes of genes which are well known for controlling disease resistance to biotrophic pathogens.

For example, *Tsn1* encodes a protein containing a nucleotide-binding site and leucine-rich repeats (NBS-LRR) (Faris et al. 2010), while *Snn1* encodes a wall-associated kinase (WAK). Based on these results, Shi et al (2016) hypothesized that necrotrophic pathogens hijack the signaling pathways of plant resistance to biotrophs and manipulate it to become a susceptibility pathway for necrotrophs.

In addition, NE/*Snn* interactions have been reported to underlie the molecular basis of the quantitative susceptibility for SNB leaf blotch (Friesen and Faris 2010). NE-*Snn* interactions were first identified under greenhouse conditions using plants at the seedling stage, where Tox1 was characterized as a host selective toxin (HST) which interacted with the *Snn1* locus on the short arm of chromosome 1B (Liu et al. 2004). Since then, additional NE-*Snn* interactions have been found to be relevant to field SNB resistance/susceptibility. For example, Friesen et al. (2009) evaluated the BR34×Grandin wheat mapping population in the field using artificial *P. nodorum* inoculation, finding *Tsn1* and *Snn2* to confer susceptibility under field conditions. Via inoculation with *P. nodorum* isolate SN15, Phan et al. (2016) found the Tox1-*Snn1* interaction as contributing to SNB susceptibility at both the seedling and adult plant stage. Similarly, a recent study by Ruud et al. (2017) confirmed a major effect of *Snn3-B1* in field susceptibility, finding this locus to be significant in two years out of a four-year field study. In contrast to the established relevance of sensitive NE-*Snn* interactions to field resistance, correlations between seedling resistances and adult plant resistances are low (Shankar et al. 2008). This might be because isolates used in such seedling tests produce different NEs in comparison to the NEs which showed effects in the field (Ruud and Lillemo 2018). For instance, Ruud et al. (2017) found that when *P. nodorum* isolate 201618 which lacks the *SnTox3* gene was used for seedling testing, correlation between seedling disease scores and field disease scores was less significant than those for Tox3 producing isolates. Further isolation of NEs, surveys of NE genes and alleles in current *P. nodorum* isolates collected from the field and additional studies of seedling and field QTL resistance in different host genetic backgrounds, are needed to provide a clearer picture of the pathways and genes that control SNB resistance/susceptibility.

While both leaf blotch and glume blotch are caused by the same pathogen on the same host, the inheritance of resistance to glume blotch is reported to be genetically different from leaf blotch (Chu et al. 2010; Wicki et al. 1999; Xu et al. 2004). Eighteen QTL have previously been identified

for glume blotch resistance on chromosome 2A, 2B, 2D, 3B, 4B, 5A, 6B and 7D, reviewed by Ruud and Lillemo (2018). However, most glume blotch studies were undertaken before Friesen et al (2007) hypothesized the inverse gene-for-gene model for leaf blotch, and the resistance/sensitivity mechanism for glume blotch is still unclear (Solomon et al. 2006; Uphaus et al. 2007; Wainshilbaum and Lipps 1991; Wicki et al. 1999). Linkage mapping with bi-parental populations have widely been used for detecting and localizing genes for quantitative traits such as SNB (Friesen et al. 2007; Ruud et al. 2017). As only two alleles segregate at a given QTL in such populations, the power of QTL detection is generally high and therefore high genetic map resolution is usually not required (Cavanagh et al. 2008; Cockram and Mackay 2018; Kover et al. 2009). However, low recombination rates in standard bi-parental populations derived from a single round of intercrossing limit QTL mapping resolution for a given population size, potentially making them less amenable for fine mapping (Bandillo et al. 2013; Cavanagh et al. 2008; Huang et al. 2012). One alternative approach to linkage mapping is using collections of unrelated lines for genome wide association scans (GWAS), which is efficient especially for collections with low linkage disequilibrium (LD) (Gupta et al. 2014; Korte and Farlow 2013; Pascual et al. 2016). The genetic variability for the target trait is usually much higher in an association mapping (AM) panel, as multiple alleles may exist per locus and high genetic recombination rates are captured due to the historic recombination within the genealogy of the panel (Gupta et al. 2014; Mackay et al. 2009). However, GWAS in AM panels also has its own specific limitations. For example, subpopulation structure should be taken into account, otherwise it will result in high risk of false positive associations (Breseghello and Sorrells 2006; Gupta et al. 2014; Sneller et al. 2009). Multiparent advanced generation intercross (MAGIC) population designs include higher allelic diversity and higher genetic recombination rate than equivalently sized bi-parental populations, and avoid the loss of power resulting from correction for subpopulation structure in AM panels (Cavanagh et al. 2008; Mackay et al. 2014). As a result, MAGIC populations can be used for both coarse mapping and fine mapping at relatively high resolution (Cavanagh et al. 2008; Stadlmeier et al. 2019). The recently developed wheat eight founder 'NIAB Elite MAGIC' population (Mackay et al. 2014) is estimated to capture around 80% of the single nucleotide polymorphism (SNP) variation in north-western European wheat germplasm (Gardner et al. 2016), and includes founders of prominence within the European wheat pedigree (Fradgley et al. 2019). In addition, this population has been used to fine map the *Snn1* and *Snn3-B1* effector sensitivity loci (Cockram

et al. 2015; Downie et al. 2018). Therefore, the population is well-suited to survey the occurrence of *P. nodorum* resistance loci within a multi-site, multi-year experimental design.

Here, we used the 'NIAB Elite MAGIC' population to (1) identify QTL associated with leaf blotch sensitivity or resistance by both seedling and field testing (2) investigate the relationship between effector/seedling sensitivity and field SNB resistance, (3) compare QTL identified for leaf blotch from different experimental locations, and (4) compare QTL identified for both leaf blotch and glume blotch to investigate the relationship between the host resistance/sensitivity mechanism against these diseases.

Materials and methods

Plant material

The 'NIAB Elite MAGIC' population has been previously described (Mackay et al. (2014). The founders (Alchemy, Brompton, Claire, Hereward, Rialto, Robigus, Soissons and Xi19) are elite winter wheat cultivars selected to capture key traits, such as high yield and good disease resistance. Briefly, the population was derived by inter-crossing the eight founders over three generations, followed by multiple rounds of selfing to produce homozygous recombinant inbred lines (RILs). The full set of the population consists of more than 1,000 RILs. In this study, a subset of 486 lines were tested in Norway both in the greenhouse for seedling resistance/susceptibility to leaf blotch and in the field for both leaf blotch and glume blotch resistance/susceptibility in adult plants. In the United Kingdom (UK), 498 lines were tested for leaf blotch resistance/susceptibility in the field.

Field trials

In total, six autumn sown field trials were undertaken across two locations (four in Norway and two in the UK). In the 2014 harvest season, leaf blotch field trials were conducted with a subset 187 MAGIC RILs and seven of the founders (Alchemy, Brompton, Claire, Hereward, Robigus, Soissons and Xi19) at the Vollebekk Research Station in Ås, Norway. From 2016 to 2018, a subset of 486 RILs and all eight founders were tested in hillplot (small plots sown 50 cm apart in rows, 40 cm between rows) trials at the Vollebekk research station. Naturally *P. nodorum* infected straw was put out in the field as inoculum early in the season before stem elongation. Plots were arrayed using an incomplete alpha lattice design, with founders and additional controls being repeated ten times. Mist irrigation for 5 min every half hour from 10 am to 8 pm was undertaken to promote

SNB infection. From 2016 to 2018, the selective fungicide Forbel 750 (Bayer Crop Science, a.i.: Phenpropimorph) was applied (750 g/ha Phenpropimorph) every three weeks to control stripe rust and powdery mildew. This fungicide has little to no effect on *P. nodorum* infection.

In the UK, two field trials were conducted (2017 and 2018), at NIAB, Cambridge, UK. The trial consisted of 498 RILs in two reps each, and eight founders in four reps each, plus 29 additional controls in four or five reps each, considered interesting for some characteristics. The trials consisted of 1178 plots, with each plot consisting of two 1 m rows. The agronomy packages used are listed in Supplementary Table S11. Trial design was undertaken in R (R Core Team, 2013) using the package Blocks Design v2.8, and each trial arranged in two randomized, complete replicates, each of 13 blocks. Mist irrigation was applied for 20 minutes twice a day. The same fungicide program described above was applied. Representative UK *P. nodorum* isolates were used to inoculate the UK field trials. A spore suspension (5×10^6 spores/mL) was used to inoculate the trials with sprayers. The inoculation was carried out once a week for two weeks, once the plants reached growth stage 39 (GS39, flag leaf fully visible).

Field phenotypic evaluation

Leaf blotch

Leaf blotch severity in Norway was scored four times in the 2014 trial, three times in each of the 2016 and 2017 season trials, and twice in 2018 (due to hot and dry weather). The first scoring was done when the most susceptible line reached 70% severity (approximately the 'early dough' stage, GS83), and then the second and third scoring were each undertaken approximately one week after the previous scoring. Disease severity was estimated visually as the percentage of leaf area with leaf blotch symptoms in each hillplot canopy. In the UK, a 0-to-9 qualitative lesion-type rating was used to evaluate each variety. A score of 0 = the absence of visible lesions; 2 = 1 lesion per 10 tillers; 3 = 2 small lesions per tiller; 4 = small lesions beginning to form areas of dead tissue across the width of the leaf; 5 = large areas of diseased tissue covering 1/3 of the leaf surface; 6 = infected tissue covering half of the leaf surface; 7 = infected tissue covering most of the leaf, more than the green tissue remaining; 8 = very little green tissue left on the leaf; 9 = large coalescent lesions with no green tissue remaining . The first score was undertaken when the 5% of the total plots showed symptoms of the disease and then, once a week. Disease severity was scored a total of four times in 2017 and five times in 2018

Glume blotch

Glume blotch was scored in the same field trials as leaf blotch in Norway, but only once per season, in 2016 and 2017. The date of scoring was immediately after the final leaf blotch scoring. The glume blotch scoring system was based on the percentage of infected glume area in each hillplot canopy. As naturally infected straw were used as inoculum, it took time for the disease to advance from the lower leaves to the spikes. Glume blotch was not scored in the 2018 season owing to insufficient disease development due to the dry and warm weather and the resulting early maturity.

Other traits

Plant height was measured as the height from ground to either the bottom of the spikes (Norway) or to the top of the spike (UK). Heading date was scored in both countries when the majority of plants within a plot had fully emerged ears.

Seedling inoculation experiments and *P. nodorum* isolates

Three *P. nodorum* isolates were used in the seedling study. Accessions 203667 and 203649 were Norwegian single spore isolates collected from wheat leaf samples. Isolate 203667 was collected from the winter wheat cultivar Olivin at Staur, Hedmark, Norway in 2015. Isolate 203649 was collected from the winter wheat cultivar Kuban at Sarpsborg, Østfold, Norway in 2015. Isolate 202579 is a Mexican isolate collected from Tlanepantla, Estado de Mexico, Mexico in 2007, and is commonly used for SNB inoculation at the International Maize and Wheat Improvement Center (CIMMYT) (CIMMYT accession: CIMFU 463). Isolates were grown on Potato Dextrose Agar (PDA) for two weeks in darkness at temperature around 20 °C in order to obtain enough mycelium for DNA extraction. The DNEasy Plant Kit (Qiagen) was used for DNA extraction following the manufacturer's instructions. Genotyping of the three necrotrophic effector genes *ToxA*, *Tox1* and *Tox3* was undertaken as described by Gao et al. (2015).

P. nodorum isolates were grown for seven days on V8-PDA media in an incubation chamber with 24 h white and near ultraviolet light (NUV) at around 20 °C to enhance sporulation. Pycnidiospores were used to prepare spore suspension, and the final concentration of the spore suspension was adjusted to 1×10^6 spores/mL for inoculation. Tween 20 was added to the spore suspension to reduce surface tension at a concentration of one drop per 50 mL.

Three to four seeds of each of the 472 MAGIC RILs and the 8 founders were sown in plastic cones fitting a 98 cone-rack (Stuewe and sons, Tangent, Orlando, USA) filled with peat soil (Gartnerjord, Tjerbo, Norway). Entries were randomly assigned across 8 blocks (60 entries per block) using an incomplete block design. The SNB susceptible cultivar Brakar was sown as border plants to reduce edge effect. Prior to inoculation, seedlings were grown in a greenhouse at a temperature of 20/16 ℃ (day/night), 65 % humidity and 16 hours light cycle for 14 days. Inoculation was undertaken by spraying the spore suspension onto 14-day-old plants until runoff. Inoculated plants were first placed in a mist chamber with 100 % relative humidity for 24 hours and then returned to the greenhouse. The second leaf of each plant was scored for disease severity using a 0 to 5 scale, where 0 indicated highly resistant and 5 indicated highly susceptible to SNB (Liu et al. 2004b), seven days post inoculation. Each experiment was repeated three times.

ToxA production

Heterologous expression of ToxA was undertaken in *Escherichia coli* BL21E using the pET21a expression vector, as previously described (Tan et al. 2012), udertaken at the Protein Expression Facility (The University of Queensland). ToxA preparations were desalted in 20 mM sodium phosphate pH 7.0m freeze-dried for storage, and re-suspended prior to use in ultra-pure water and stored at 4 °C.

Seedling infiltration using culture filtrates and ToxA

Three to four seeds of each MAGIC line were sown in plastic cones following the protocol listed above for the inoculation experiments. *P. nodorum* isolates were cultivated in liquid Fries 3 medium (Friesen and Faris 2012) for the production of necrotrophic effectors. Three weeks after the stationary phase, culture filtrates were sterilized filtered through membranes filters (white gridded: 0.45 µm, diameter: 47 mm, S-PAK, France) and roughly 50 µL culture filtrates or ToxA preparation were infiltrated into the second leaf of each plant by using a 1-mL syringe with the needle removed. The reactions to isolate 203649 and 202579 were scored 5 days post infiltration using a 0 to 4 scale (Tan et al. 2012), where score 0 indicates no symptoms, 1 indicates slight chlorosis, 2 indicates extensive chlorosis, 3 indicates complete chlorosis without tissue collapse, and 4 indicated complete necrosis. The reaction to isolate 203667 and ToxA were scored using a 0 to 3 scale (Friesen and Faris 2012), where 0 indicates no symptoms, 1 is mottled chlorosis, 2 is

complete chlorosis without tissue collapse, and 3 is complete necrosis. Individual seedlings of each genotype growing in the same cone were used as replicates.

Statistical Analysis

For leaf blotch and glume blotch phenotypic data, the average scores from the three to four timepoints measured for each trait were calculated for each line and then corrected for block effects using SAS v.9.4 (SAS Institute Inc.) to estimate the mean disease severity of each line and variances. For the straw-inoculated field trials in Norway, plant height and days to heading were used as covariates in multi-linear regression to calculate corrected disease severities. This was done using R Studio Version 1.1.442 (RStudio Team 2015) by subtracting the estimated disease severities based on the fitted model from the observed field severities recorded in the field. For leaf blotch data from the spray-inoculated trials in the UK, neither plant height nor heading date were significantly correlated with disease scores. Therefore, the mean disease severities were used without correction of confounding traits. Since few variations were explained by the first scoring in 2018 of the UK trial, average disease scores were calculated by taking the average of the second to fifth scores.

The calculations of the Pearson correlation coefficients were carried out in R Studio using the package Hmisc (Harrell 2019). Paired Wilcoxon sign rank test was carried out using R Studio. Broad sense heritability of line means was calculated as broad sense by first estimating components of variation from REML while taking into account all features of the experimental designs. Heritability was then estimated as $h^2 = \sigma^2G/ (\sigma^2G + \sigma^2e)$ where σ^2G is the genetic variation between line means and σ^2e is the error variance appropriate to those means. Calculations were carried out in GenStat (VSN International, 2011) and the package lme4 (Bates et al. 2015) in R Studio.

QTL mapping

The 643 NIAB Elite MAGIC RILs were previously genotyped at the F_5 generation using the 90K SNP array (Wang et al. 2014) resulting in 20,643 polymorphic SNPs (Mackay et al. 2014; Gardner et al. 2016), and the data used to make a genetic map consisting of 18,601 SNPs (Gardner et al. 2016). Of these, markers assigned to the 7,367 unique map positions were used for QTL mapping. QTL analyses were carried out using haplotype analyses, using the 7,369 SNPs that map to unique positions in the MAGIC genetic map (Gardner et al. 2016). Founder haplotype

probabilities were calculated using the 'mpprob' function in R/mpMap (Huang and George 2011) implemented in R/qtl (Broman et al. 2003) with a threshold of 0.5. QTL analysis using these haplotype probabilities was carried out via two methods: (a) by linear mixed model using all mapped markers (termed here 'identity by descent' mapping, IBD), and (b) by interval mapping using the 'mpIM' mapping function in R/mpMap, with the inclusion of 0 (interval mapping, IM), 5, or 10 covariates (composite interval mapping, CIM). For IBD analysis, correction for multiple testing was accounted for by using a significance threshold of q=0.05 using the package R/qvalue. For interval mapping, two significance thresholds were used: (1) Using the 'sim.sigthr' function from R/mpMap package, 100 simulations of the dataset were conducted based on no QTL hypothesis, followed by calculation of the genome wide p value, and determination of the significance threshold using p = 0.05. QTL above this permutated significance threshold are designated here as 'strong QTL'. (2) An arbitrary threshold of $-\log_{10}(p) = 3$. QTL with $-\log_{10}(p)$ between 3 and the permutated threshold or QTL explaining > 5% of phenotypic variation but $-\log_{10}(p)$ lower than 3 are designated here as 'weak QTL'. A full QTL model was then fitted with all QTL using R/fit.mpQTL. IM was used to call QTL, with additional detection using CIM-cov5, CIM-cov10 and IBD used to further confirm IM QTL calls. Significance values and percentage variation explained for all QTL reported in the manuscript are derived from IM. Flanking markers were defined by CIM-cov10 when QTL were detected by both IM and CIM, otherwise intervals were defined by IM.

DNA sequences flanking selected SNP markers within QTL intervals were obtained from the website https://triticeaetoolbox.org, allowing SNPs to be anchored to the wheat cv. Chinese Spring reference genome assembly (IWGSC RefSeq v1.0; IWGSC 2018) via BLASTn analysis.

Haplotype analysis

Haplotype analysis was performed for the QTL *QSnb.niab-2A.3*. Two peak markers (*BS00062679_51* and *RAC875_c9372_94*) from *QSnb.niab-2A.3* were selected for constructing haplotypes. The mean corrected disease severities for the population were calculated based on haplotypes. Kruskal–Wallis Test was calculated using the R/ pgirmess package (Giraudoux 2018) in R Studio, and the significant interval was obtained by $p < 0.05$.

Results

Phenotypic evaluation of field resistance

The eight MAGIC founders showed different levels of SNB severity in all four years in Norway, except Rialto which was not tested in 2014 (Fig. 1a and 1b). Alchemy and Robigus were relatively resistant to leaf blotch, as low levels of infection were observed in all years, while Soissons and Xi19 were more susceptible compared to the other parents (Fig. 1a). However, the disease severity of the founders in the UK trials did not show the same trend of severity as observed in Norway (Fig. 1c). For glume blotch, Brompton and Rialto were the most susceptible, while Alchemy and Robigus were relatively resistant (Fig. 1b).

Broad variation in leaf blotch severity among the MAGIC RILs indicated that the inheritance of SNB resistance was quantitative (Fig. 2a). For glume blotch, the majority of lines over all tested years varied between 0 and 25% infection (Fig. 2b). The range of leaf blotch disease severity was from 0 to 100 % in all four years in Norway (2014, 2016-2018). Due to dry and hot conditions, only 425 lines yielded reliable data that were included for QTL analysis in 2018, and the overall infection level was lower compared to 2016 and 2017 (Fig. 2a).

Significant negative correlation between leaf blotch severity (LB) and plant height (PH) were observed in all tested years in Norway except 2014 (Table 1). The correlation coefficients in year 2016, 2017 and 2018 were -0.22, -0.22 and -0.21, respectively ($p < 0.0001$). Similarly, the correlation between days to heading (DH) and LB were also significant in each year: -0.30 ($p < 0.0001$) in 2014, -0.30 ($p < 0.0001$) in 2016, -0.22 ($p < 0.0001$) in 2017, while slightly less significant in 2018 ($r = -0.10$, $p < 0.05$). There was also significant negative correlation between glume blotch severity and PH in all years in Norway (Table 1). However, DH was positively correlated with glume blotch: 0.21 ($p < 0.0001$) in 2016 and 0.10 ($p < 0.05$) in 2017. Neither PH nor DH was significantly correlated with leaf blotch in the UK (Table 1).

After correction for the effects of PH and DH in the Norway trials, leaf blotch severities were all significantly correlated between years and locations, except for LB in the UK 2017 and LB in Norway 2014 (Table 2). Similarly, the correlation of corrected glume blotch severity between 2016 and 2017 was also significant ($r = 0.31$, $p < 0.0001$). For the same year same location, correlations between leaf blotch and glume blotch were also significant: $r = 0.22$ ($p < 0.0001$) in 2016 and 0.13 in 2017 ($p < 0.01$) (Table 2). Heritability (h^2) for leaf blotch in Norway was between

48.00 % and 77.45% among years, while in the UK heritability was 13.61% and 57.25% in 2017 and 2018, respectively (see Supplementary Table S1).

Genetic analysis of field experiments

Sixteen QTL ($-\log_{10}(p) > 3$) were identified by IM/CIM using field data for leaf blotch from six trials across two locations and glume blotch for two years at one location (Table 3, Fig. 3). Among them, 10 QTL were detected for leaf blotch in Norway, three QTL were detected for leaf blotch in the UK, and three QTL were detected for glume blotch in Norway. QTL were mapped to chromosomes 2A, 3A, 4A, 5D, 6A and 7D (Table 3). As some QTL were located to overlapping chromosomal regions and were significant in multiple years and/or environments, these were subsequently grouped into ten distinct genetic loci. Of these, three were above the permutated p = 0.05 significance threshold (Table 3): (i) QTL *QSnb.niab-2A.3* on the short arm of chromosome 2A was detected as a 'strong' QTL for leaf blotch in Norway during 2014, 2016 and 2018 and glume blotch in Norway in 2016, explaining 16%, 6.8%, 6.57% and 4.12% of the phenotypic variation, respectively (Table 3, Fig. 4). *QSnb.niab-2A.3* was additionally detected as a 'weak' QTL ($-\log_{10}(p) = 3.17$) in the 2017 UK trial, explaining 3.87% of the phenotypic variation. Anchoring the most significant SNP markers to the wheat genome assembly found *QSnb.niab-2A.3* to be approximately located at 574 – 635 Mb on chromosome 2A. (ii) The 'strong' QTL *QSnb.niab-2A.4* on the long arm of chromosome 2A was identified in Norway 2016, and as a 'weak' QTL in Norway 2017, explaining 3.74% and 4.53% of the phenotypic variation, respectively. The *QSnb.niab-2A.4* peak marker was located at 237.13 cM in 2016 (SNP *wsnp_Ra_c17622_26522072*, $-\log_{10}(p) = 4.41$, 759 Mb) and at 236.12 cM in 2017 (SNP *Excalibur_c4372_363*, $-\log_{10}(p) = 3.97$, 758 Mb) in 2017 (Table 3, Fig. 5). (iii) *QSnb.niab-6A.1*, identified as a 'strong' QTL for leaf blotch resistance in Norway 2016, was located at 129 cM (SNP *TA004558_1018*, 97.81 Mb) and explained 3.85% of the phenotypic variation. Genetic analysis of plant height, flowering time and SNB for Norway trials unadjusted for the effect of plant height and days to heading are presented in Supplementary Tables S6-S9 and discussed in more detail in Supplementary Text 1. In summary, the confounding effects of plant height and days to heading influenced the detection of glume blotch related QTL more than leaf blotch, as all strong QTL detected by unadjusted glume blotch phenotypic data collocated with plant height QTL. Except one 'weak QTL' *QDh.niab-6A* on chromosome 6A detected for days to heading in Norway in 2014 might collocate with adjusted leaf blotch QTL *QSnb.niab-6A.1* detected in

Norway in 2016. No other plant height or days to heading QTL were found to collocate with both adjusted and unadjusted leaf blotch QTL. However, in general for both leaf blotch and glume blotch, less QTL were detected by unadjusted data and QTL detected using adjusted data were found to be less significant when using unadjusted data.

Phenotypic evaluation of seedling inoculation and infiltration

The *ToxA*, *Tox1* and *Tox3* profiles for the three isolates used for seedling experiments were determined using previously published assays (Gao et al. 2015). Norwegian isolate 203649 was found to lack the *ToxA*, *Tox1* and *Tox3* genes, Norwegian 203667 possessed *ToxA* and *Tox3*, while isolate 202579 from CIMMYT (CIMFU 463) possessed all three effector genes.

Infiltration

The reactions of the eight MAGIC founders to *P. nodorum* infiltration (using culture filtrate or the effector ToxA) or inoculation (using spore suspensions) are shown in Fig. 6. Hereward was the most sensitive founder to culture filtrate from isolate 203649 (which does not produce any of the three toxins tested), while Claire, Robigus and Soissons showed a complete insensitive reaction. The remaining founders showed moderate susceptibility. However, very few MAGIC RILs had complete necrosis symptoms and even the most susceptible founder, Hereward, only had a reaction score of 3 (complete chlorosis without tissue collapse) using a 0 to 4 scoring scale. For infiltration with isolate 203667, Hereward, Soissons and Xi19 showed high sensitivity, Claire was moderately sensitive while the remaining founders were insensitive (Fig. 6). Infiltration with ToxA found Soissons and Xi19 to be sensitive (score = 3) while the rest of the founders were all insensitive (score = 0). 37.9% and 36.1% of the MAGIC RILs were insensitive to infiltration using culture filtrate from isolates 203667 and 202529, respectively, while 55.8% were insensitive to infiltration using isolate 203649. 34.1 % of the MAGIC RILs were highly sensitive to infiltration using isolate 203667 culture filtrate (score = 3), 19.2 % were highly sensitive to infiltration using ToxA (score = 3), 10% were highly sensitive to infiltration using isolate 202579 (score = 4), while just one RIL was identified as possessing a sensitivity score of 4 to infiltration using culture filtrate from isolate 203649 (Fig. 7). Heritabilities (h^2) for culture filtrate infiltration with isolate 203667, 203649, 202579 and infiltration with effector ToxA were 0.89, 0.84, 0.84 and 0.88, respectively.

Inoculation

Inoculation of the MAGIC founders using spore suspensions from each of the two isolates investigated (202759 and 203649) found the same trends in sensitivity as observed for culture filtrate infiltration, with Hereward, Soissons and Xi19 found to be the most susceptible, followed by Brompton and Rialto. Claire and Robigus were even less susceptible, while Alchemy was the most resistant founder (Fig. 6). However, 53.5% of the MAGIC RILs showed high susceptibility (sore >4) to isolate 202579, compared to just 11.6% for isolate 203649 (Fig. 7). As the same phenotypic scoring scale was used to record phenotypes from infiltration and inoculation experiments using isolates 202579 and 203649, paired Wilcoxon sign rank test were carried out. Mean scores for inoculation and infiltration using isolate 203649 were all significantly ($p < 0.0001$) lower than inoculation and infiltration results treated with isolate 202579. The distribution of inoculation phenotypic results for isolate 202579 were skewed towards susceptibility, while the results for inoculation with 203649 had most scores between 2-4 (Fig. 7). The phenotypic correlation between inoculation and culture filtrate infiltration experiments using the same isolate was highly significant ($p < 0.0001$) for both isolates 203649 and 202579 (Table 4). Culture filtrate infiltration with isolate 203667 was significantly correlated with glume blotch in 2016 ($r = 0.10$, $p < 0.05$) and highly significantly correlated with both infiltration ($r = 0.70$, $p < 0.0001$) and inoculation ($r = 0.45$, $p < 0.0001$) using isolate 202579 (Table 4). Isolate 203649 infiltration results were significantly correlated with leaf blotch field data in 2016 ($r = 0.16$, $p < 0.01$), 2017 ($r = 0.09$, $p < 0.05$) and 2018 ($r = 0.11$, $p < 0.05$) in Norway, while infiltration with isolate 202579 was significantly correlated with leaf blotch in Norway in 2014 ($r = 0.18$, $p < 0.05$) and 2017 ($r = 0.13$, $p < 0.01$) (Table 4). Furthermore, leaf blotch 2016 ($r = 0.14$, $p < 0.01$), 2017 ($r = 0.13$, $p < 0.01$) and 2018 ($r = 0.13$, $p < 0.05$) in Norway were significantly correlated with the seedling disease phenotypes resulting from inoculation using isolate 203649, while inoculation with isolate 202579 was significantly correlated with leaf blotch in Norway in 2014 ($r = 0.24$, $p < 0.01$), 2016 ($r = 0.20$, $p < 0.0001$) and 2017 ($r = 0.26$, $p < 0.0001$) (Table 4). Heritability (h^2) for inoculation with isolates 203649 and 202579 was 0.31 and 0.49, respectively.

Genetic analysis of seedling experiments

Sixteen QTL on chromosomes 2A, 2D, 3A, 3B, 5B, 7B and 7D were identified via the seedling inoculation and infiltration experiments at a significance threshold of $-\log_{10}(p) > 3$ (Table 3, Fig. 3). Of these, eight QTL were detected for spore suspension inoculations, seven for culture filtrate infiltrations, and one for infiltration with ToxA. Among these, six QTL were significant

using the more stringent significance threshold determined by permutation (listed on a trait by trait basis in Table S2), and termed here 'strong' QTL: (i) *QSnb.niab-2D.2* on chromosome 2D, detected by inoculation using both isolate 203649 and 202579 and explaining 11.42% and 4.86% of the variation, respectively. The peak markers *Excalibur_c42413_442* and *Ra_c19051_1446* at this QTL mapped to 198.36 cM and 192.18 cM on the genetic map, and were located at 636 Mb and 638 Mb on the physical map (IWGSC RefSeq v1.0). (ii) QTL *QSnb.niab-7D.1*, contributing to resistance to inoculation of isolate 203649, explained 7.89% of the variation ($-\log_{10}(p) = 9.90$) and was located at 69.65 cM/174 Mb on chromosome 7D. (iii) *QSnb.niab-5B.2* on the long arm of chromosome 5B was detected via inoculation with isolate 202579 and explained 8.54 % of the variation ($-\log_{10}(p) = 7.93$). This QTL co-located with the *Tsn1* locus identified here via infiltration with ToxA (Table 3). (iv) The previously identified Tox3 effector sensitivity locus *Snn3-B1* on the short arm of chromosome 5B (Downie et al. 2018; Liu et al. 2009; Ruud et al. 2017) located at 6.65 Mb, collocated with QTL *QSnb.niab-5B.1* detected via infiltration with isolates 202579 (8.1 % variation, $-\log_{10}(p) = 5.48$) and 203667 (10.4 % variation, $-\log_{10}(p) = 8.90$) (Table 3).

Haplotype analysis of *QSnb.niab-2A.3*

Markers *BS00062679_51* at 142.7 cM/615 Mb and *RAC875_c9372_94* at 144.8 cM/636 Mb were used to construct haplotypes at the *QSnb.niab-2A.3* locus, resulting in the eight founders being designated as one of three haplotypes. The corrected leaf blotch severity of haplotype 0_2 (inherited from Xi19 and Rialto), was significantly ($p < 0.05$) higher than that of haplotype 2_0 (inherited from Alchemy, Claire and Hereward). This result was consistent for all leaf blotch trials except Norway 2014, likely due to the low number of RILs tested that year (Fig. 8). The remaining haplotype 2_2 (inherited from Soissons, Brompton and Robigus) showed inconsistent resistance or susceptibility to leaf blotch in comparison with the susceptible haplotype 0_2. In contrast to the analysis of leaf blotch, haplotype 0_2 (inherited from Rialto and Xi19) was the most resistant haplotype for glume blotch in 2016 (mean corrected disease severity: -2.44 %) compared to susceptible haplotype 2_2 (mean corrected disease severity: 1.63 %) although the haplotype effect was not significant in 2017 (Fig. 8h). Haplotype analysis was also carried out for phenotypic data derived from the seedling experiments (Fig. 9), with significant differences between resistant haplotype 2_0 and susceptible haplotype 0_2 observed for culture filtrate infiltration and inoculation with isolate 203649.

Discussion

Field inoculation methods

Naturally infected straw was used as inoculum in Norway to simulate natural infection in the field. Disease developed from the bottom to the top of the canopy. As expected, plant height and days to heading were negatively correlated with leaf blotch severity in the Norwegian trials, as reported previously (Lu and Lillemo 2014; Ruud et al. 2017). The UK field trials, were infected by spraying spore suspensions derived from a single local isolate, the most common method of infection (eg Fried 1987; Laubscher 1966; Uphaus et al. 2007; Wicki et al. 1999). The heritabilities of SNB disease severity were higher in Norway than in the UK. This might be due to various factors, including more conductive environmental conditions for pathogen infection, and the mixed local *P. nodorum* population assumed from the straw inoculation method. We used naturally infected straws as inoculum in Norway and we would also expect variations in pathogen populations every year due to variations in climate in recent years. Therefore, relatively low but significant correlations between leaf blotch disease scores from different years as could be expected given the very different agronomic environments and likely differences in *P. nodorum* isolates present between locations. Significantly, despite the contrasting inoculation methods, pathogen isolates, agronomy and geographical/environmental factors associated with these trials, we were able to identify a common QTL between sites located in Norway and the UK (*QSnb.niab-2A.3*). This illustrates that it is possible to identify robust field QTL for leaf blotch resistance/sensitivity that are relevant to multiple agronomic environments.

In Norway, plant height was negatively correlated to glume blotch, agreeing with previously published studies (Shatalina et al. 2014). However, in contrast to our observations for leaf blotch and with previous studies of glume blotch resistance (Aguilar et al. 2005; Wicki et al. 1999), we found days to heading to be positively correlated with glume blotch in our Norwegian trials. This might be explained by the differences between leaf blotch and glume blotch infection time, and/or different inoculation methods being used. In natural conditions, ear infection occurs later in the season compared to leaves. Thus, ears of later lines which possess relatively young tillers are usually exposed to higher infection pressure compared to early lines, as early lines mature before the disease spreads to the ears. This also explains why the mean disease severity was lower for glume blotch compared to leaf blotch: the short time in which glume blotch can develop before maturity limits the disease development. In other glume blotch studies using spray inoculation

(Aguilar et al. 2005; Shatalina et al. 2014; Wicki et al. 1999), wheat ears were exposed to the pathogen directly, and the disease development was therefore less affected by the earliness of the lines. In the UK, plant height and days to heading was not found to show strong correlation with SNB. Lack of correlation with plant height in the 2018 trial may have be due to the use of plant growth regulators, following local agronomic practice. Indeed, the observation that plant height was not a significant confounding factor supports the use of local agronomic practice for the UK 2018 trial, and may have helped to avoid detection of pleiotropic effects of height on the detection of SNB resistance QTL. Plant growth regulators were not deemed necessary under growth conditions in the 2017 UK trial, and no confounding effect of height was observed.

Seedling experiments

Seedling testing was carried out to investigate whether there was any commonality between seedling and adult plant resistance. Higher mean scores for both the inoculation and infiltration results were observed for isolate 202579 compared to isolate 203649, indicating the high aggressiveness of isolate 202579. High numbers of MAGIC RILs were found to have a strong hypersensitive reaction (score 4 and 5) after inoculation using isolate 202579. This phenomenon is likely explained by more of the known NEs being produced by 202579: the isolate possess all three of the well characterized effectors genes (*ToxA, Tox1* and *Tox3*) and the MAGIC population segregates for all three corresponding sensitivity loci (*Tsn1, Snn1* and *Snn3-B1*). In contrast, isolate 203649 does not produce any of these three NEs. If this isolate produces NEs, they are currently unknown, as is the allelic state of any corresponding host sensitivity loci in the MAGIC founders.

Inoculation using both isolate 203649 and 202579 identified one QTL in common, *QSnb.niab-2D.2* on chromosome 2D (Fig. 10). So far, only two sensitivity loci interacting with necrotrophic effectors have been characterized on chromosome 2D. The first is the Tox2 sensitivity locus *Snn2*, located on the short arm of chromosome 2D (Zhang et al. 2009). Comparison of genetic map locations indicates that *Snn2* co-locates with the 'weak' leaf blotch QTL *QSnb.niab-2D.1* identified in the UK 2018 trial (Table S4 and Fig. 10). The second is *Snn7* on the long arm of chromosome 2D, which interacts with the necrotrophic effector Tox7 (Shi et al. 2015). Various field studies have identified QTL for adult plant leaf or glume blotch resistance on wheat chromosome 2D (Aguilar et al. 2005; Francki et al. 2018; Ruud 2019; Shankar et al. 2008; Uphaus

et al. 2007). However, these studies mostly used relatively small mapping populations genotyped with DArT and/or SSR markers, making it harder to accurately compare these QTL locations with those identified using the 90K SNP array in this study. Nevertheless, to help facilitate QTL comparison, we anchored flanking markers for QTL from published sources to the wheat reference genome by BLASTn (Table S4). Peak markers for both isolates tested in our inoculation experiment were located within the region defined by the published *Snn7* flanking markers, between 608 to 647 Mb on chromosome 2D (Fig. 10). Interestingly, the flanking markers of previously published glume blotch resistance QTL (Francki et al. 2018; Uphaus et al. 2007) were also located within this region. Shi et al. (2015) claimed that the glume blotch resistance QTL *QSng.pur-2DL.1*, identified in the P92201D5 × P91193D1 population by Uphaus et al. (2007), was not *Snn7*, because none of the parent lines were sensitive to Tox7. Therefore, our QTL *QSnb.niab-2D.2* could be allelic to either *Snn7* or *QSng.pur-2DL.1*. Sensitive alleles at *Snn7* are relatively rare in wheat, found only in a few genotypes to date (Shi et al. 2015). Whether the NIAB Elite MAGIC founders carry sensitive alleles at *Snn7* is unknown, and further research would be needed to clarify this. Notably, we did not detect *QSnb.niab-2D.2* by culture filtrate infiltration for either of the two isolates studied here. Therefore, the underlying effector, putatively Tox7, was either not produced and/or secreted by either isolate in liquid culture, or its expression level was very low *in vitro*.

Another notable observation from the seedling experiments was that while infiltration with culture filtrate produced by isolate 202579 identified just the Tox3 sensitivity locus *Snn3-B1*, inoculation using the same isolate identified *Snn3-B1* and the ToxA sensitivity locus *Tsn1* (Table 3, Fig. S1 and Fig. S2). *Tsn1* was likely not detected through culture filtrate infiltration as ToxA is reported to not be expressed *in vitro* (Rybak et al. 2017; Tan et al. 2015). Phan et al. (2016) evaluated a population segregating for both *Snn1* and *Snn3-B1* using isolate SN15, which produces ToxA, Tox1 and Tox3. The wheat *Snn3-B1* locus was only detected in genetic analyses after knocking out the SN15 *Tox1* gene, indicating expression of Tox3 was suppressed by Tox1 in SN15. However, in our study, isolate 202579 carries all three known effector genes, *ToxA*, *Tox1* and *Tox3*. ToxA was not expressed *in vitro*, therefore, according to the hypothesis that *Tox3* expression is suppressed by Tox1, it might be expected that a QTL at the *Snn1* locus would be detected using culture filtrate infiltration, rather than *Snn3-B1* as was detected here. This may be because the expression levels of necrotrophic effectors are isolate dependent (Faris et al. 2011). The

mechanism by which the effects of Tox1-*Snn1* interaction is masked by ToxA-*Tsn1* and Tox3-*Snn3-B1* interaction in our inoculation experiment is still unclear, but could be explained by reduced *Tox1* expression level when the pathogen interacted with the host, or epistatic effects caused by host susceptibility genes.

Isolate 203667 possessed both *ToxA* and *Tox3*. Only *Snn3-B1* was detected after culture filtrate infiltration, again supporting reports that ToxA is not expressed *in vitro*. The observation of significant correlations between culture filtrate infiltration using 203667 and infiltration/inoculation using 202579, while low correlations were found between culture filtrate infiltration using 203667 and infiltration/inoculation using 203649 (Table 4), was likely due to the similar effector profiles of isolates 203667 and 202579. Finally, *QSnb.niab-7D.1* is identified here as a novel QTL for SNB seedling resistance, since to our knowledge, no SNB-related QTL close to this location on chromosome 7D have previously been reported.

QTL and haplotype analysis of field experiments

From previous studies, four QTL on chromosome 2A have been identified for SNB leaf blotch resistance/susceptibility (Francki et al. 2018; Phan et al. 2016; Rybak et al. 2017), one for glume blotch (Jighly et al. 2016) and one for Tox3 sensitivity (Downie et al. 2018). After anchoring flanking markers for these QTL to the wheat reference genome (Table S3, Fig. 11), comparison with the chromosome 2A QTL identified in this study indicated that our SNB resistance QTL *QSnb.niab-2A.3* (574 to 639 Mb) may correspond to the seedling sensitivity QTL *Qsnb.cur-2AS.1* identified by Phan et al. (2016). However, since the *Qsnb.cur-2AS.1* interval defined by SSR markers *gwm339* and *gwm312* is very large (from 112 to 709 Mb), the probability that these two QTL are the same is currently difficult to estimate. In addition, previous studies (Aguilar et al. 2005; Fried 1987; Wicki et al. 1999) showed that resistance to SNB leaf blotch and glume blotch were controlled by genetically different mechanisms. Here, we found leaf blotch and glume blotch severity in the MAGIC founders to be quite different (Fig. 1a and 1b), supporting the hypothesis that the genetic control of these *P. nodorum*-mediated diseases might be controlled by different genetic mechanisms. Aguilar et al. (2005) studied resistance to both leaf blotch and glume blotch in the same population by artificial inoculation, finding one QTL in common on chromosome 2B. However, this QTL was also associated with morphological traits such as heading date, flowering date and ear length. In our study, we subtracted variance caused by plant height and heading date

before QTL analysis, which avoided the epistatic effects of these traits. As the QTL intervals on chromosome 2A overlapped for leaf blotch and glume blotch, we firstly considered that they represented a single QTL. However, haplotype analysis indicated that the most susceptible haplotype for leaf blotch did not show the same effect for glume blotch, suggesting the resistant mechanisms controlling those two traits might be different. Nevertheless, *QSnb.niab-2A.3* is a very robust QTL for leaf blotch as haplotype analysis revealed the consistency of this QTL for leaf blotch in all years and all locations, except the Norway 2014 experiment in which a much lower numbers of RILs were trialed. In addition, while *QSnb.niab-2A.3* was not detected in the isolate 203649 culture filtrate infiltration experiment using IM, this locus was identified as a 'weak' QTL via CIM, using 1, 5 and 10 cofactors (Table 3). Furthermore, haplotype analysis showed significant increase in disease severity associated with the haplotype found to increase field SNB susceptibility (Fig. 9a and 9c). Therefore, isolate 203649 may produce an unknown effector which interacts with the susceptible allele underlying the *QSnb.niab-2A.3* haplotype. Significant correlations were observed between the infiltration experiment for isolate 203649 and leaf blotch in Norway for three years (2016 to 2018), while infiltration with isolate 202579 was significantly correlated with two years (2014 and 2017) and infiltration using 203667 was not significantly correlated with any leaf blotch field data. This indicates that even though isolate 203649 is less aggressive than 202579 under greenhouse conditions, the unknown effector(s) produced by this isolate may still play an important role in the field. Nevertheless, low correlations on average were found between seedling inoculation/infiltration and leaf blotch field data, indicating genetic control of SNB resistance is largely controlled by different genes/pathways between these growth stages in MAGIC lines. However, the identification of *QSnb.niab-2A.3* via seedling and field testing indicates that at least some genetic components are in common. One possible reason for an overall lack of strong correlation is that the *P. nodorum* isolates used for seedling screens might not be the most representative isolates of the local *P. nodorum* population in the field. Another possible reason would be that some of the field resistances/susceptibility could not be fully explained by NE-*Snn* interactions, as up to now, only four such interactions have been found contributing to field resistances/susceptibility (Friesen et al. 2009; Phan et al. 2016; Ruud and Lillemo 2018). Other underexplored plant resistant mechanisms may be involved in field SNB resistance.

Anchoring *QSnb.niab-2A.4* peak markers to the 2A physical map (758-759 Mb) found it to overlap with the previously identified minor Tox3 sensitivity QTL, *QTox3.niab-2A.1* (Table S3) (Downie et al. 2018). However, we did not detect the major Tox3 sensitivity locus *Snn3-B1* in the field, while *QSnb.niab-2A.4* was one of the major field QTL identified, detected in two out of the four years investigated. *QSnb.niab-2A.4* was also detected as a 'weak' QTL via inoculation using isolate 203649 (Table 3). The QTL *QSnb.niab-3A*, anchored using peak marker *wsnp_Ex_c6833_11782875* to 10 Mb on chromosome 3A (Table 3, Fig. S4), represents a previously unreported QTL for SNB leaf blotch resistance. Here, the QTL was detected in two field seasons in Norway ($-\log_{10}(p) > 3$), as well as via culture filtrate infiltration using isolate 202579 ($-\log_{10}(p) > 3$) indicating *P. nodorum* effector(s) may play a role in controlling field SNB sensitivity for this QTL. Additional QTL on chromosomes 2A, 2D and 6A were identified as potentially co-locating with previously reported QTL (Table 3); however, they were only 'weakly' significant and identified in just one environment in our study (Table 3). For example, the 'weak' QTL *QSnb.niab-6A.2* identified for glume blotch in 2016 collocated with the previously reported sensitivity locus *Snn6* (Table S5) (Gao et al. 2015). Finally, *QSnb.niab-6A.1* has not previously been reported, and therefore represents a novel QTL for leaf blotch disease resistance under field conditions (Table 3 and S6).

The finding that *QSnb.niab-2A.3* haplotype 0_2 for higher leaf blotch severity was associated with increased sensitivity to culture filtrate from strain 203649 compared to haplotype 2_0, indicates this QTL for field SNB resistance/susceptibility may be controlled by an a previously undescribed NE/*Snn* interaction, making this a target for identification of the underlying gene(s) in both the pathogen and host. Similarly, identification of *QSnb.niab-3A* in the field as well as via culture filtrate infiltration indicate this too may represent a new NE/*Snn* interaction. Development of diagnostic KASP markers (Semagn et al. 2014) for field SNB resistance/culture filtrate insensitivity could allow marker assisted selection for beneficial alleles in order to breed new wheat varieties with increased resistance to SNB leaf blotch. Furthermore, the observation that these field-relevant QTL is also detected via seedling culture filtrate infiltration indicates it could be possible to further refine the downstream genetic analyses of this QTL via seedling screens of progeny derived from crosses between near isogenic line pairs developed for each QTL, greatly simplifying the logistics of screening for genetic recombinants within the QTL interval. Combining such seedling phenotyping with approaches such as 'speed breeding' (Watson et al.

2018) may greatly reduce experimental timelines for future map-based cloning of the gene(s) underlying *QSnb.niab-2A.3* and *QSnb.niab-3A*.

Acknowledgements: We thank Dr. Keith Gardner (NIAB) for genetics advice, Rob Day (NIAB) and Cecilie Yri (NMBU) for help with field phenotyping, Dr. Pawan K. Singh (CIMMYT) for providing the 202579 (CIMFU 463) isolate, and Prof. Richard Oliver (CCDM) and Dr. Huyen Phan (CCDM) for supplying the ToxA effector.

Author contributions: M. Lin carried out glasshouse phenotyping and genetic analyses. M. Lin and BC carried out field work, with help from M. Lillemo. M. Lin and BC carried out genetic analyses. JC. KT and M. Lillemo gained project funding. JC, AF and M. Lillemo supervised the research. KT supplied ToxA effector. M. Lin drafted the manuscript. All authors revised and approved the manuscript.

Funding: Research was undertaken within the framework of the 2nd call ERA-NET for Coordinating Plant Sciences, within the 'EfectaWheat' project, with funding from The Research Council of Norway, grant NFR251894, UK Biotechnology and Biological Sciences Research Council (BBSRC) grant BB/N00518X/1 and Grains Research and Development Corporation grant CUR00023.

Conflict of Interest: The authors declare that they have no conflict of interest.

References:

Aguilar V et al. (2005) Inheritance of field resistance to Stagonospora nodorum leaf and glume blotch and correlations with other morphological traits in hexaploid wheat (Triticum aestivum L.) Theor Appl Genet 111:325-336 doi:10.1007/s00122-005-2025-5

Arseniuk E, Czembor PC, Czaplicki A, Song QJ, Cregan PB, Hoffman DL, Ueng PP (2004) QTL controlling partial resistance to Stagonospora nodorum leaf blotch in winter wheat cultivar Alba. Euphytica 137:225-231 doi: 10.1023/B:EUPH.0000041589.47544.de

Bandillo N et al. (2013) Multi-parent advanced generation inter-cross (MAGIC) populations in rice: progress and potential for genetics research and breeding Rice (N Y) 6:11 doi:10.1186/1939-8433-6-11

Bates D, Machler M, Bolker BM, Walker SC (2015) Fitting Linear Mixed-Effects Models Using lme4 Journal of Statistical Software 67:1-48 doi:10.18637/jss.v067.i01

Bhathal J, Loughman R, Speijers J (2003) Yield reduction in wheat in relation to leaf disease from yellow (tan) spot and septoria nodorum blotch Eur J Plant Pathol 109:435-443 doi 10.1023/A:1024277420773

Blixt E, Olson A, Hogberg N, Djurle A, Yuen J (2008) Mating type distribution and genetic structure are consistent with sexual recombination in the Swedish population of Phaeosphaeria nodorum Plant Pathol 57:634-641 doi:10.1111/j.1365-3059.2008.01826.x

Breseghello F, Sorrells ME (2006) Association analysis as a strategy for improvement of quantitative traits in plants Crop Sci 46:1323-1330 doi:10.2135/cropsci2005.09-0305

Broman KW, Wu H, Sen S, Churchill GA (2003) R/qtl: QTL mapping in experimental crosses Bioinformatics 19:889-890 doi:10.1093/bioinformatics/btg112

Cavanagh C, Morell M, Mackay I, Powell W (2008) From mutations to MAGIC: resources for gene discovery, validation and delivery in crop plants Curr Opin Plant Biol 11:215-221 doi:10.1016/j.pbi.2008.01.002

Chu CG, Faris JD, Xu SS, Friesen TL (2010) Genetic analysis of disease susceptibility contributed by the compatible Tsn1-SnToxA and Snn1-SnTox1 interactions in the wheat-Stagonospora nodorum pathosystem Theor Appl Genet 120:1451-1459 doi:10.1007/s00122-010-1267-z

Cockram J, Mackay I (2018) Genetic Mapping Populations for Conducting High-Resolution Trait Mapping in Plants Adv Biochem Eng Biotechnol 164:109-138 doi:10.1007/10_2017_48

Cockram J et al. (2015) Fine-Mapping the Wheat Snn1 Locus Conferring Sensitivity to the Parastagonospora nodorum Necrotrophic Effector SnTox1 Using an Eight Founder Multiparent Advanced Generation Inter-Cross Population. G3 (Bethesda) 5:2257-2266 doi:10.1534/g3.115.021584

Downie RC et al. (2018) Assessing European Wheat Sensitivities to Parastagonospora nodorum Necrotrophic Effectors and Fine-Mapping the Snn3-B1 Locus Conferring Sensitivity to the Effector SnTox3 Front Plant Sci 9:881 doi:10.3389/fpls.2018.00881

Faris JD et al. (2010) A unique wheat disease resistance-like gene governs effector-triggered susceptibility to necrotrophic pathogens Proc Natl Acad Sci U S A 107:13544-13549 doi:10.1073/pnas.1004090107

Faris JD, Zhang Z, Rasmussen JB, Friesen TL (2011) Variable expression of the Stagonospora nodorum effector SnToxA among isolates is correlated with levels of disease in wheat Mol Plant Microbe Interact 24:1419-1426 doi:10.1094/MPMI-04-11-0094

Ficke A, Cowger C, Bergstrom G, Brodal G (2018) Understanding Yield Loss and Pathogen Biology to Improve Disease Management: Septoria Nodorum Blotch - A Case Study in Wheat. Plant Disease 102:696-707 doi:10.1094/PDIS-09-17-1375-FE

Fradgley N et al. (2019) A large-scale pedigree resource of wheat reveals evidence for adaptation and selection by breeders PLoS Biol 17:e3000071 doi:10.1371/journal.pbio.3000071

Francki MG (2013) Improving Stagonospora nodorum Resistance in Wheat: A Review Crop Sci 53:355-365 doi:10.2135/cropsci2012.06.0347

Francki MG, Walker E, Li DA, Forrest K (2018) High-density SNP mapping reveals closely linked QTL for resistance to Stagonospora nodorum blotch (SNB) in flag leaf and glume of hexaploid wheat Genome 61:145-149 doi:10.1139/gen-2017-0203

Fried PM (1987) Inheritance of Leaf and Head Resistance of Winter Wheat to Septoria nodorum in a Diallel Cross. Phytopathology 77: 1371-1375 doi:10.1094/Phyto-77-1371

Friesen TL, Chu CG, Liu ZH, Xu SS, Halley S, Faris JD (2009) Host-selective toxins produced by Stagonospora nodorum confer disease susceptibility in adult wheat plants under field conditions Theor Appl Genet 118:1489-1497 doi:10.1007/s00122-009-0997-2

Friesen TL, Faris JD (2010) Characterization of the wheat-Stagonospora nodorumdisease system: what is the molecular basis of this quantitative necrotrophic disease interaction?†. Can J Plant Pathol 32:20-28 doi: 10.1080/07060661003620896

Friesen TL, Faris JD (2012) Characterization of Plant-Fungal Interactions Involving Necrotrophic Effector-Producing Plant Pathogens. In: Bolton MD, Thomma BPHJ (eds) Plant Fungal Pathogens: Methods and Protocols. Humana Press, Totowa, NJ, pp 191-207

Friesen TL, Meinhardt SW, Faris JD (2007) The Stagonospora nodorum-wheat pathosystem involves multiple proteinaceous host-selective toxins and corresponding host sensitivity

genes that interact in an inverse gene-for-gene manner Plant J 51:681-692 doi:10.1111/j.1365-313X.2007.03166.x
Gao Y et al. (2015) Identification and Characterization of the SnTox6-Snn6 Interaction in the Parastagonospora nodorum-Wheat Pathosystem Mol Plant Microbe Interact 28:615-625 doi:10.1094/MPMI-12-14-0396-R
Gardner KA, Wittern LM, Mackay IJ (2016) A highly recombined, high-density, eight-founder wheat MAGIC map reveals extensive segregation distortion and genomic locations of introgression segments Plant Biotechnol J 14:1406-1417 doi:10.1111/pbi.12504
Giraudoux P (2018) pgirmess: Spatial Analysis and Data Mining for Field Ecologists. R package version 1.6.9. https://CRAN.R-project.org/package=pgirmess
Gupta PK, Kulwal PL, Jaiswal V (2014) Association mapping in crop plants: opportunities and challenges Adv Genet 85:109-147 doi:10.1016/B978-0-12-800271-1.00002-0
Harrell, F. E. with contributions from Charles Dupont and many others. (2019). Hmisc: Harrell Miscellaneous. R package version 4.2-0. https://CRAN.R-project.org/package=Hmisc
Huang BE, George AW (2011) R/mpMap: a computational platform for the genetic analysis of multiparent recombinant inbred lines Bioinformatics 27:727-729 doi:10.1093/bioinformatics/btq719
Huang BE, George AW, Forrest KL, Kilian A, Hayden MJ, Morell MK, Cavanagh CR (2012) A multiparent advanced generation inter-cross population for genetic analysis in wheat Plant Biotechnol J 10:826-839 doi:10.1111/j.1467-7652.2012.00702.x
International Wheat Genome Sequencing C et al. (2018) Shifting the limits in wheat research and breeding using a fully annotated reference genome Science 361: eaar7191 https://doi.org/10.1126/science.aar7191
Jighly A, Alagu M, Makdis F, Singh M, Singh S, Emebiri LC, Ogbonnaya FC (2016) Genomic regions conferring resistance to multiple fungal pathogens in synthetic hexaploid wheat Molecular Breeding 36 doi:10.1007/s11032-016-0541-4
King JE, Cook RJ, Melville SC (1983) A Review of Septoria Diseases of Wheat and Barley Ann. Appl. Biol.103:345-373 doi:10.1111/j.1744-7348.1983.tb02773.x
Korte A, Farlow A (2013) The advantages and limitations of trait analysis with GWAS: a review Plant Methods 9:29 doi:10.1186/1746-4811-9-29
Kover PX et al. (2009) A Multiparent Advanced Generation Inter-Cross to fine-map quantitative traits in Arabidopsis thaliana PLoS Genet 5:e1000551 doi:10.1371/journal.pgen.1000551
Laubscher FvW, B. von Schalkwyk, D. (1966) Heritable resistance of wheat varieies to glume blotch (septoria nodoum Berk.). Phytopathology Z 56:260-264 doi: 10.1111/j.1439-0434.1966.tb02262.x
Liu Z et al. (2015) Evaluation and Association Mapping of Resistance to Tan Spot and Stagonospora Nodorum Blotch in Adapted Winter Wheat Germplasm Plant Dis 99:1333-1341 doi:10.1094/PDIS-11-14-1131-RE
Liu Z et al. (2009) SnTox3 acts in effector triggered susceptibility to induce disease on wheat carrying the Snn3 gene PLoS Pathog 5:e1000581 doi:10.1371/journal.ppat.1000581
Liu Z et al. (2012) The cysteine rich necrotrophic effector SnTox1 produced by Stagonospora nodorum triggers susceptibility of wheat lines harboring Snn1 PLoS Pathog 8:e1002467 doi:10.1371/journal.ppat.1002467
Liu ZH, Faris JD, Meinhardt SW, Ali S, Rasmussen JB, Friesen TL (2004a) Genetic and Physical Mapping of a Gene Conditioning Sensitivity in Wheat to a Partially Purified

Host-Selective Toxin Produced by Stagonospora nodorum Phytopathology 94:1056-1060 doi:10.1094/PHYTO.2004.94.10.1056
Liu ZH, Friesen TL, Rasmussen JB, Ali S, Meinhardt SW, Faris JD (2004b) Quantitative Trait Loci Analysis and Mapping of Seedling Resistance to Stagonospora nodorum Leaf Blotch in Wheat. Phytopathology 94:1061-1067 doi: 10.1094/PHYTO.2004.94.10.1061
Lu Q, Lillemo M (2014) Molecular mapping of adult plant resistance to Parastagonospora nodorum leaf blotch in bread wheat lines 'Shanghai-3/Catbird' and 'Naxos' Theor Appl Genet 127:2635-2644 doi:10.1007/s00122-014-2404-x
Mackay IJ et al. (2014) An eight-parent multiparent advanced generation inter-cross population for winter-sown wheat: creation, properties, and validation G3 (Bethesda) 4:1603-1610 doi:10.1534/g3.114.012963
Mackay TF, Stone EA, Ayroles JF (2009) The genetics of quantitative traits: challenges and prospects Nat Rev Genet 10:565-577 doi:10.1038/nrg2612
McDonald BA, Linde C (2002) Pathogen population genetics, evolutionary potential, and durable resistance Annu Rev Phytopathol 40:349-379 doi:10.1146/annurev.phyto.40.120501.101443
Oliver RP, Friesen TL, Faris JD, Solomon PS (2012) Stagonospora nodorum: from pathology to genomics and host resistance Annu Rev Phytopathol 50:23-43 doi:10.1146/annurev-phyto-081211-173019
Pascual L et al. (2016) Dissecting quantitative trait variation in the resequencing era: complementarity of bi-parental, multi-parental and association panels Plant Sci 242:120-130 doi:10.1016/j.plantsci.2015.06.017
Pereira DA, McDonald BA, Brunner PC (2017) Mutations in the CYP51 gene reduce DMI sensitivity in Parastagonospora nodorum populations in Europe and China. Pest Management Science 73:1503-1510 doi:10.1002/ps.4486
Phan HT, Rybak K, Furuki E, Breen S, Solomon PS, Oliver RP, Tan KC (2016) Differential effector gene expression underpins epistasis in a plant fungal disease. Plant J 87:343-354 doi:10.1111/tpj.13203
RStudio Team (2015) RStudio: Integrated Development for R. RStudio, Inc., Boston, MA URL http://www.rstudio.com/.
Ruud AK et al. (2019) Genome-Wide Association Mapping of Resistance to Septoria Nodorum Leaf Blotch in a Nordic Spring Wheat Collection. The Plant Genome 12:1-15 doi:10.3835/plantgenome2018.12.0105
Ruud AK, Lillemo M (2018) Diseases affecting wheat: Septoria nodorum blotch. In: Integrated disease management of wheat and barley. Burleigh Dodds Series in Agricultural Science. Burleigh Dodds Science Publishing Limited, Cambridge, UK, pp 109-144. doi:10.19103/as.2018.0039.06
Ruud AK, Windju S, Belova T, Friesen TL, Lillemo M (2017) Mapping of SnTox3-Snn3 as a major determinant of field susceptibility to Septoria nodorum leaf blotch in the SHA3/CBRD x Naxos population Theor Appl Genet 130:1361-1374 doi:10.1007/s00122-017-2893-5
Rybak K, See PT, Phan HT, Syme RA, Moffat CS, Oliver RP, Tan KC (2017) A functionally conserved Zn2 Cys6 binuclear cluster transcription factor class regulates necrotrophic effector gene expression and host-specific virulence of two major Pleosporales fungal pathogens of wheat Mol Plant Pathol 18:420-434 doi:10.1111/mpp.12511

Semagn K, Babu R, Hearne S, Olsen M (2014) Single nucleotide polymorphism genotyping using Kompetitive Allele Specific PCR (KASP): overview of the technology and its application in crop improvement Molecular Breeding 33:1-14 doi:10.1007/s11032-013-9917-x

Shankar M, Walker E, Golzar H, Loughman R, Wilson RE, Francki MG (2008) Quantitative trait loci for seedling and adult plant resistance to Stagonospora nodorum in wheat Phytopathology 98:886-893 doi:10.1094/PHYTO-98-8-0886

Shatalina M et al. (2014) High-resolution analysis of a QTL for resistance to Stagonospora nodorum glume blotch in wheat reveals presence of two distinct resistance loci in the target interval Theor Appl Genet 127:573-586 doi:10.1007/s00122-013-2240-4

Shi G et al. (2016) The hijacking of a receptor kinase-driven pathway by a wheat fungal pathogen leads to disease Sci Adv 2:e1600822 doi:10.1126/sciadv.1600822

Shi GJ, Friesen TL, Saini J, Xu SS, Rasmussen JB, Faris JD (2015) The Wheat Snn7 Gene Confers Susceptibility on Recognition of the Parastagonospora nodorum Necrotrophic Effector SnTox7 Plant Genome 8 doi:10.3835/plantgenome2015.02.0007

Sneller CH, Mather DE, Crepieux S (2009) Analytical Approaches and Population Types for Finding and Utilizing QTL in Complex Plant Populations. Crop Science 49:363-380 doi:10.2135/cropsci2008.07.0420

Solomon PS, Waters OD, Jorgens CI, Lowe RG, Rechberger J, Trengove RD, Oliver RP (2006) Mannitol is required for asexual sporulation in the wheat pathogen Stagonospora nodorum (glume blotch) Biochem J 399:231-239 doi:10.1042/BJ20060891

Sommerhalder RJ, McDonald BA, Mascher F, Zhan J (2011) Effect of hosts on competition among clones and evidence of differential selection between pathogenic and saprophytic phases in experimental populations of the wheat pathogen Phaeosphaeria nodorum BMC Evol Biol 11:188 doi: 10.1186/1471-2148-11-188

Stadlmeier M, Jorgensen LN, Corsi B, Cockram J, Hartl L, Mohler V (2019) Genetic Dissection of Resistance to the Three Fungal Plant Pathogens Blumeria graminis, Zymoseptoria tritici, and Pyrenophora tritici-repentis Using a Multiparental Winter Wheat Population. G3 (Bethesda) 9:1745-1757 doi:10.1534/g3.119.400068

Stukenbrock EH, Banke S, McDonald BA (2006) Global migration patterns in the fungal wheat pathogen Phaeosphaeria nodorum Mol Ecol 15:2895-2904 doi:10.1111/j.1365-294X.2006.02986.x

Tan KC et al. (2012) Quantitative variation in effector activity of ToxA isoforms from Stagonospora nodorum and Pyrenophora tritici-repentis Mol Plant Microbe Interact 25:515-522 doi:10.1094/MPMI-10-11-0273

Tan KC, Phan HT, Rybak K, John E, Chooi YH, Solomon PS, Oliver RP (2015) Functional redundancy of necrotrophic effectors - consequences for exploitation for breeding Front Plant Sci 6:501 doi:10.3389/fpls.2015.00501

Uphaus J, Walker E, Shankar M, Golzar H, Loughman R, Francki M, Ohm H (2007) Quantitative Trait Loci Identified for Resistance to Stagonospora Glume Blotch in Wheat in the USA and Australia. Crop Science 47:1813-1822 doi:10.2135/cropsci2006.11.0732

Wainshilbaum SJ, Lipps PE (1991) Effect of Temperature and Growth Stage of Wheat on Development of Leaf and Glume Blotch Caused by Septoria-Tritici and S-Nodorum Plant Dis 75:993-998 doi:10.1094/Pd-75-0993

Wang S et al. (2014) Characterization of polyploid wheat genomic diversity using a high-density 90,000 single nucleotide polymorphism array Plant Biotechnol J 12:787-796 doi:10.1111/pbi.12183
Watson A et al. (2018) Speed breeding is a powerful tool to accelerate crop research and breeding Nat Plants 4:23-29 doi:10.1038/s41477-017-0083-8
Wicki W, Winzeler M, Schmid JE, Stamp P, Messmer M (1999) Inheritance of resistance to leaf and glume blotch caused by Septoria nodorum Berk. in winter wheat Theor Appl Genet 99:1265-1272 doi:10.1007/s001220051332
Xu SS, Friesen TL, Mujeeb-Kazi A (2004) Seedling resistance to tan spot and Stagonospora nodorum blotch in synthetic hexaploid wheats Crop Sci 44:2238-2245 doi:10.2135/cropsci2004.2238
Zhang ZC, Friesen TL, Simons KJ, Xu SS, Faris JD (2009) Development, identification, and validation of markers for marker-assisted selection against the Stagonospora nodorum toxin sensitivity genes Tsn1 and Snn2 in wheat Molecular Breeding 23:35-49 doi:10.1007/s11032-008-9211-5

Table 1 Pearson correlation coefficients for leaf blotch (LB) and glume blotch (GB) severities, days to heading (DH) and plant height (PH) within years. Trials are coded to indicate year (2016, 2017, 2018), country (N = Norway, U = UK) and disease (LB = leaf blotch, GB = glume blotch).

	2016NLB	2016NGB
16DH	-0.30***	0.21***
16PH	-0.22***	-0.34***

	2017NLB	2017NGB
17DH	-0.22***	0.10*
17PH	-0.22***	-0.40***

	2018NLB
18DH	-0.10*
18PH	-0.21***

***<0.0001, *<0.05

	2017ULB
17DH	-0.04
17PH	-0.03

	2018ULB
18DH	0.05
18PH	-0.04

	2014NLB
14DH	-0.30***
14PH	-0.07

***<0.0001, *<0.05

Table 2 Pearson correlation coefficients for leaf blotch and glume blotch severities between years, after correction for the effects of plant height and days to heading. Trials are coded to indicate year (2016, 2017, 2018), country (N = Norway, U = UK) and disease (LB = leaf blotch, GB = glume blotch).

	2014NLB	2016NLB	2016NGB	2017NLB	2017NGB	2018NLB	2017ULB
2016NLB	0.36***						
2016NGB	0.07	0.22***					
2017NLB	0.27**	0.50***	0.04				
2017NGB	-0.04	0.06	0.31***	0.13**			
2018NLB	0.23**	0.29***	-0.01	0.36***	-0.13*		
2017ULB	0.09	0.24***	0.00	0.21***	0.00	0.22***	
2018ULB	0.18*	0.17**	0.04	0.17**	0.07	0.11*	0.23***

***<0.0001, **<0.01, *<0.05.

Table 3 *P. nodorum* resistance/sensitivity QTL identified in the 'NIAB Elite MAGIC' population from field trials, seedling culture filtrate infiltration, ToxA infiltration and seedling inoculation. Significance values and proportion of the variance explained (R^2) for all QTL reported are derived from IM analysis and the intervals determined via CIM-cov10, unless otherwise indicated. References of studies where QTL were found in similar positions: 1 = (Rybak et al. 2017), 2 = (Phan et al. 2016), 3 = (Liu et al. 2009), 4 = (Downie et al. 2018), 5 = (Faris et al., 2010), 6 = (Liu et al. 2015), 7 = (Gao et al. 2015). QTL with $-\log_{10}(p)$ value > 3 are presented, with QTL above the permutated trait-specific significance threshold highlighted in bold. Reference (Ref.), Chromosome (Chr.), IM (interval mapping), CIM (composite interval mapping), IBD (identity by descent). The –log10(p) value for *Tsn1* is recorded as 'Inf', as the p-value was 0, resulting in an error when converted to the $\log_{10}$ scale. †Detected via CIM-cov1, -cov5 and –cov10.

QTL	Ref.	Trait	Year	Chr	Interval (cM)	Flanking markers	Peak Marker	-$\log_{10}$ (p)	IWGSC RefSeq v1.0 start (bp)	IWGSC RefSeq v1.0 end (bp)	R^2 (%)	Detected by QTL methods
QSnb.niab-2A.1	1	Inoc_203649		2A	0 - 1.01	RAC875_c44680_90 and BS00111318_51	BS00111318_51	3.00	2378473	2378574	5.11	IM,CIM (cov5, cov10),IBD
QSnb.niab-2A.2		LB (Norway)	2017	2A	100.36 -109.94	Kukri_c24852_466 and BS00008805_51	Excalibur_c637_1078	3.19	78844360	111457371	3.88	IM,CIM (cov5, cov10)
QSnb.niab-2A.3		**LB** (Norway)	**2014**	**2A**	**121.07-138.24**	**JD_c2056_506 and Kukri_c7825_288**	**BS00059475_51**	**5.82**	**410872779**	**588258104**	**16.00**	IM,CIM (cov5, cov10),IBD
QSnb.niab-2A.3		**LB** (Norway)	**2018**	**2A**	**135.19 -146.82**	**Excalibur_c1793_97 and BS00022241_51**	**RAC875_c9372_94**	**4.67**	**558953000**	**663329017**	**6.80**	IM,CIM (cov5, cov10),IBD
QSnb.niab-2A.3		**LB** (Norway)	**2016**	**2A**	**130.65-146.82**	**BS00059475_51 and BS00022241_51**	**Ku_c5710_312**	**6.20**	**574172945**	**663329017**	**6.57**	IM,CIM (cov5, cov10),IBD
QSnb.niab-2A.3		**GB** (Norway)	**2016**	**2A**	**141.26 -142.77**	**RAC875_c20247_398 and BS00062679_51**	**BS00062679_51**	**4.21**	**611946675**	**615287757**	**4.12**	IM,CIM (cov5, cov10),IBD
QSnb.niab-2A.3		Infil_203649 (ncov1)†		2A	142.2-150.6	BS00022641_51 and IAAV4015	BS00090569_51	3.49	612422267	677529836	2.98	CIM (cov1, cov5, cov10)
QSnb.niab-2A.3		LB (UK)	2017	2A	144.81-145.31	RAC875_c9372_94 and BS00012320_51	RAC875_c9372_94	3.17	635606922	647927416	3.87	IM,CIM (cov5, cov10)
QSnb.niab-2A.4		**LB (Norway)**	**2016**	**2A**	**229.02 -241.18**	**wsnp_Ra_c6586_11477949 and BS00022252_51**	**wsnp_Ra_c17622_26522072**	**4.41**	**755929525**	**775619939**	**3.74**	IM,CIM (cov5, cov10),IBD

QSnb.niab-2A.4		LB (Norway)	2017	2A	234.62 -237.63	JD_c11825_1135 and Tdurum_contig8350_350	Excalibur_c4372_363	3.97	758396871	780714672	4.53	IM,CIM (cov5, cov10)
QSnb.niab-2A.4		Inoc_203649		2A	252.80-256.82	BS00064836_51 and Kukri_c365_345	BS00101944_51	3.17	761248555	765269621	5.06	IM,IBD
QSnb.niab-2D.1	2	LB (UK)	2018	2D	32.58-50.83	wsnp_JD_rep_c63957_40798083 and BobWhite_c59161_181	BS00029208_51	3.51	14897896	27859806	3.91	IM,CIM (cov5, cov10),IBD
QSnb.niab-2D.2		**Inoc_203649**		**2D**	**188.01 -198.36**	**RFL_Contig1128_620 and Kukri_c36328_419**	**Excalibur_c42413_442**	**4.61**	**635950166**	**637636412**	**11.42**	IM,CIM (cov5, cov10),IBD
QSnb.niab-2D.2		Inoc_202579		2D	188.01-198.86	RFL_Contig1128_620 and BS00010685_51	Ra_c19051_1446	4.33	635950166	638147754	4.86	IM,CIM (cov5, cov10),IBD
QSnb.niab-3A		LB (Norway)	2016	3A	0 - 9.55	RAC875_c46403_277 and Kukri_rep_c69028_347	Tdurum_contig83209_316	3.95	1031134	10300906	4.37	IM,CIM (cov5, cov10),IBD
QSnb.niab-3A		LB (Norway)	2017	3A	7.04 - 16.64	Kukri_rep_c89183_282 and BS00066230_51	wsnp_Ex_c6833_11782875	4.09	8685996	32325166	4.31	IM,CIM (cov5, cov10)
QSnb.niab-3A		Infil_202579		3A	14.63-31.02	TA003589_0518 and RAC875_c20134_535	BS00055211_51	3.49	8865639	14851061	5.09	IM,CIM (cov5, cov10),IBD
QSnb.niab-3B		Infil_203649		3B	147.39 -156.96	BS00076872_51 and Excalibur_c5977_1409	BobWhite_c13099_755	3.47	566843633	578616694	4.69	IM,CIM (cov5, cov10),IBD
QSnb.niab-4A		LB (UK)	2017	4A	110.56-112.09	BS00072025_51 and IAAV6581	Kukri_c96129_147	3.68	598590361	605713556	3.56	IM,CIM (cov5, cov10)
QSnb.niab-5B.1	**3, 4**	**Infil_202579**		**5B**	**0-13.16**	**Tdurum_contig44048_276 and wsnp_Ex_c26252_35497729**	**Tdurum_contig44048_276**	**5.48**	**13428116**	**27830730**	**8.10**	IM,CIM (cov5, cov10),IBD
QSnb.niab-5B.1 *(Snn3)*		**Infil_203667**		**5B**	**0-13.16**	**Tdurum_contig44048_276 and wsnp_Ex_c26252_35497729**	**BS00022336_51**	**8.90**	**13428116**	**27830730**	**10.40**	IM,CIM (cov5, cov10),IBD
QSnb.niab-5B.1 (Snn3)		Inoc_202579		5B	0-6.88	Tdurum_contig44048_276 and Kukri_c60322_490	Excalibur_rep_c104354_205	3.59	13428116	19438610	4.84	IM,CIM (cov10), IBD

QSnb.niab-5B.2 *(Tsn1)*	**4, 5**	**Inoc_202579**		**5B**	**123.06-138.93**	**IACX7649 and wsnp_Ex_c6695_11577150**	**Kukri_c54078_114**	**7.93**	**539294940**	**547404553**	**8.54**	IM,CIM (cov5, cov10),IBD
Tsn1		**Infil_ToxA**		**5B**	**124.06-142.56**	**IACX11840 and Excalibur_c33675_201**	**Kukri_c54078_114**	**Inf**	**539935182**	**550847459**	**73.43**	IM,CIM (cov5, cov10),IBD
QSnb.niab-5D	6	GB (Norway)	2017	5D	49.43-66.08	BobWhite_c7263_337 and BS00063971_51	BS00110475_51	3.57	389934855	431201019	4.44	IM,CIM (cov10),IBD
QSnb.niab-6A.1		**LB (Norway)**	**2016**	**6A**	**123.39-135.99**	**IAAV5188 and RFL_Contig3088_949**	**TA004558_1018**	**4.85**	**74025753**	**249160705**	**3.85**	IM,CIM (cov5, cov10),IBD
QSnb.niab-6A.2	7	GB (Norway)	2016	6A	229.10	BS00096240_51 and GENE_4028_152	GENE_4028_152	3.68	600395629	600406208	3.56	IM,CIM (cov5, cov10),IBD
QSnb.niab-7B.1		Inoc_203649		7B	100.24-110.66	BS00067599_51 and Excalibur_rep_c67475_1420	BS00067599_51	4.31	115244415	498523237	4.06	IM,CIM (cov5, cov10), IBD
QSnb.niab-7B.2		Infil_203649		7B	168.06-184.77	Kukri_c15912_860 and Excalibur_c50612_409	BS00077956_51	2.91	673961429	700551772	5.83	IM,CIM (cov5, cov10), IBD
QSnb.niab-7D.1		**Inoc_203649**		**7D**	**69.65-81.20**	**GENE_4292_204 and BS00049220_51**	**GENE_4292_204**	**9.90**	**174445641**	**458015017**	**7.89**	IM,CIM (cov5, cov10),IBD
QSnb.niab-7D.2		Infil_203649		7D	116.86-118.37	BS00023150_51 and BS00070188_51	BS00070188_51	3.03	554596126	559460390	4.13	IM,IBD
QSnb.niab-7D.3		LB (Norway)	2016	7D	215.78-218.30	RAC875_c10022_23 and JD_c2708_1512	JD_c2708_1512	3.49	629325776	724128709	4.06	IM,CIM (cov5, cov10),IBD

Table 4 Pearson correlation coefficients for corrected leaf blotch and glume blotch severities, greenhouse infiltration and inoculation. N: Norway, U: UK, LB: leaf blotch, GB: glume blotch. Infil = infiltration. Inoc = inoculation.

	2014NLB	2016NLB	2016NGB	2017NLB	2017NGB	2018NLB	2017ULB	2018ULB	Infil 203649	Inoc 203649	Inf 202579	Inoc 202579
Infiltration 203649	0.03	0.16**	0.00	0.09*	-0.08	0.11*	0.06	0.06				
Inoculation 203649	0.01	0.14**	0.03	0.13**	-0.01	0.13*	0.07	-0.06	0.35***			
Infiltration 202579	0.18*	0.08	0.01	0.13**	0.01	0.05	0.03	0.03	0.07	0.08		
Inoculation 202579	0.24**	0.20***	0.09	0.26***	0.08	0.08	0.00	-0.05	0.06	0.40***	0.43***	
Infiltration 203667	0.09	0.07	0.10*	0.09	0.05	-0.02	-0.01	0.01	0.05	0.03	0.70***	0.45***

***<0.0001, **<0.01, *<0.05

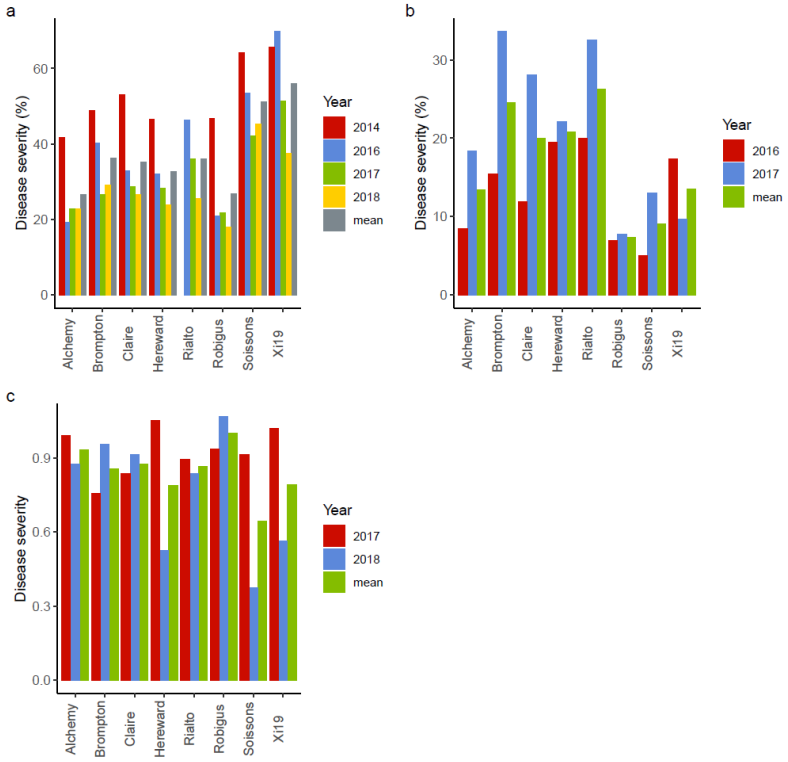

Fig. 1 Disease severity of the MAGIC founders in different years and locations. Mean disease severity of each line are indicated. (a) Leaf blotch severity in Ås, Norway, (b) Glume blotch severity in Ås, Norway, (c) Leaf blotch severity in Cambridge, UK.

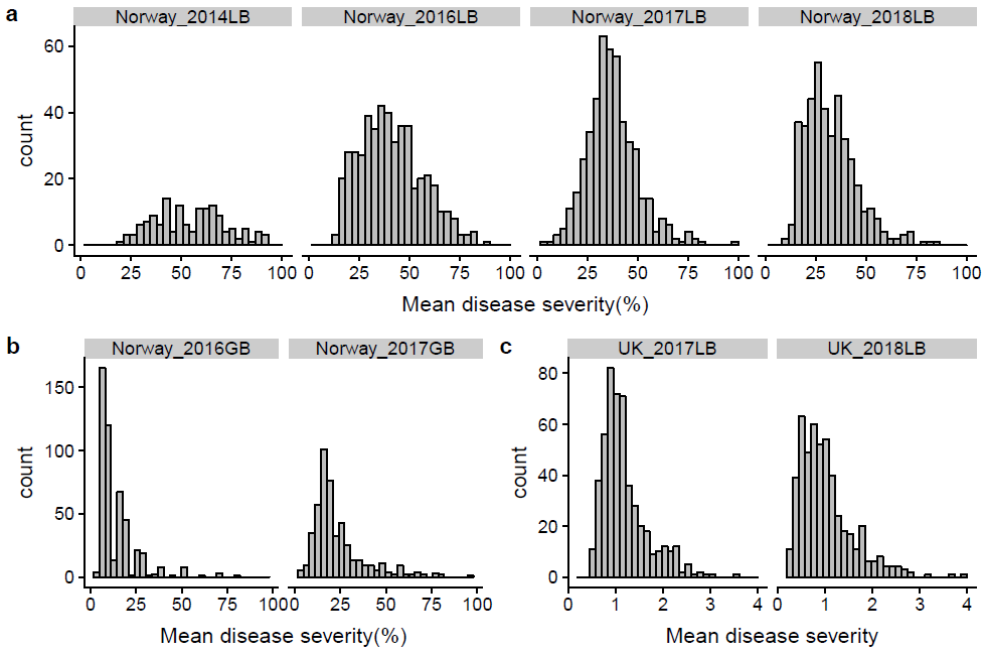

Fig. 2 Disease severity of the MAGIC population in different years and locations. (a) Leaf blotch severity in Ås, Norway, (b) Glume blotch severity in Ås, Norway, (c) Leaf blotch severity in Cambridge, UK, LB = leaf blotch, GB = glume blotch.

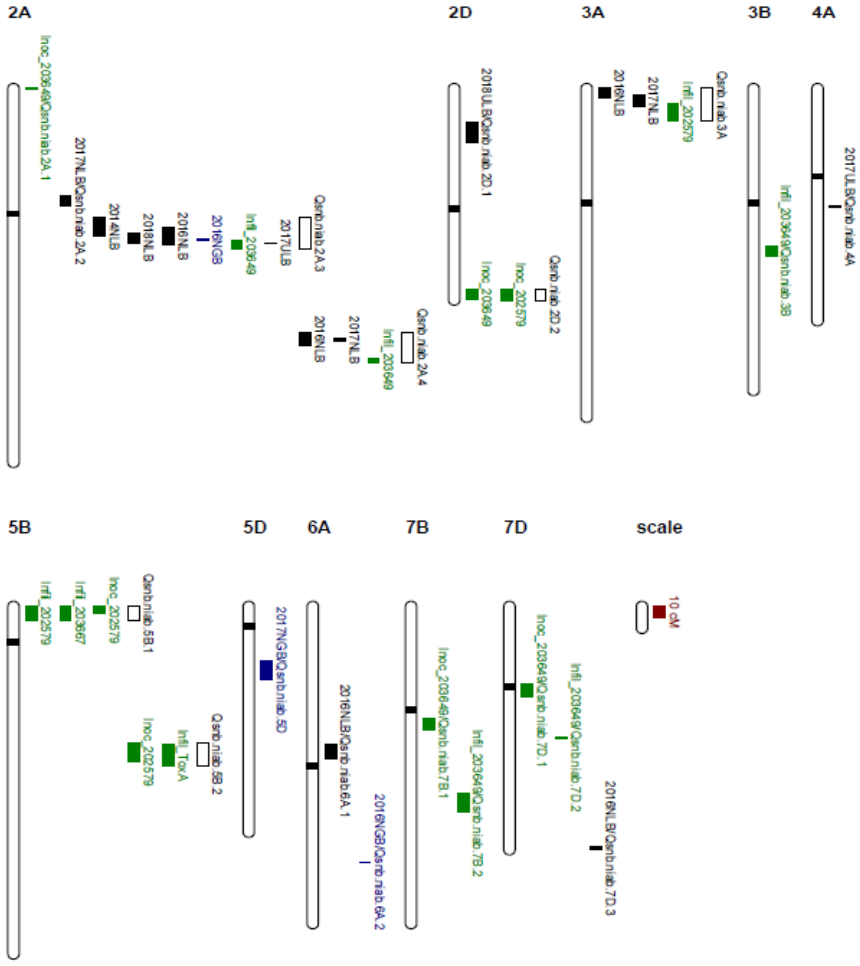

Fig. 3 Genetic map locations of all QTL detected in this study. QTL locations and interval sizes are indicated by bars on the right hand side of each chromosome, and are based on the genetic marker information in Table 3.. Field leaf blotch QTL are indicated in black, field glume blotch QTL in blue (N: Norway, U: UK, LB: leaf blotch, GB: glume blotch), and seedling QTL in green (Inoc: greenhouse inoculation, Infil: greenhouse infiltration). Of these QTL, those detected in more than one environment are indicated using a white bar, along with the designated QTL name assigned in this study.

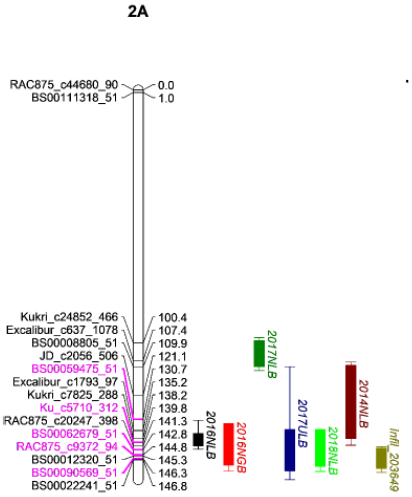

Fig. 4 Genetic map of the *QSnb.niab-2A.3* locus and on the short arm of chromosome 2A in the NIAB Elite MAGIC population. N: Norway, U: UK, LB: leaf blotch, GB: glume blotch, Infil: infiltration, Peak markers are indicated in pink.

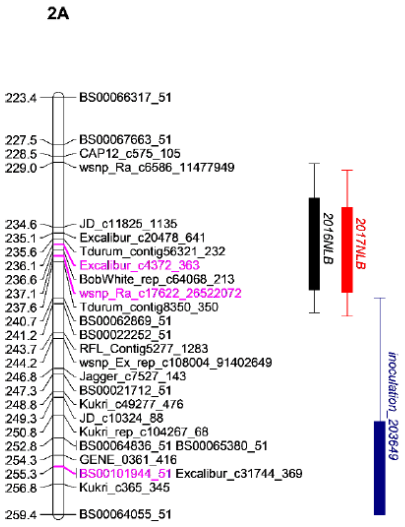

Fig. 5 Genetic map of the *QSnb.niab-2A.4* locus on the long arm of chromosome 2A in the NIAB Elite MAGIC population. N: Norway, LB: leaf blotch. Peak markers are indicated in pink.

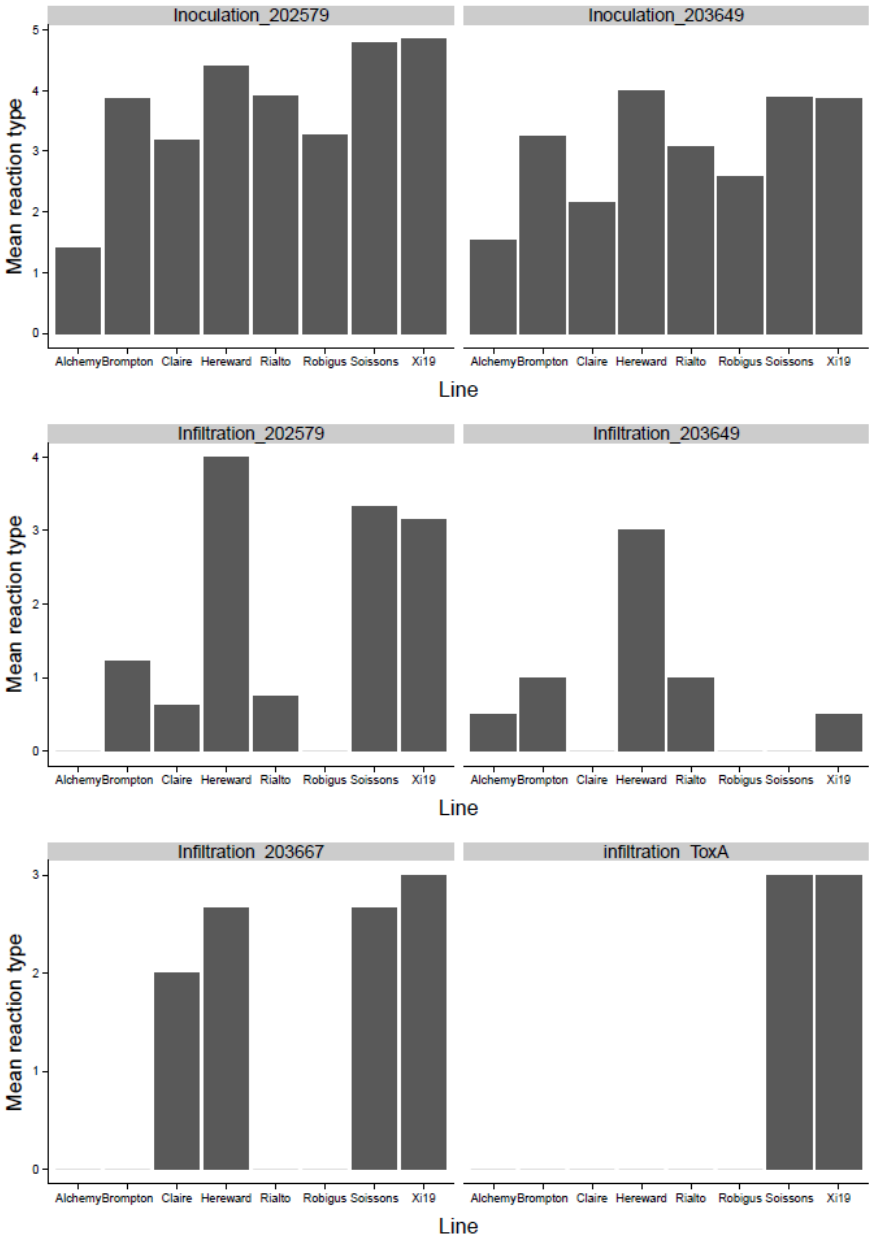

Fig. 6 Reactions of MAGIC founders to infiltration (using isolate culture filtrate and the effector ToxA) and inoculation experiment treatment with two *P. nodorum* isolates. Isolate 203649 was found to lack the *ToxA*, *Tox1* and *Tox3* genes, 203667 possessed *ToxA* and *Tox3*, while isolate 202579 possessed all three effectors.

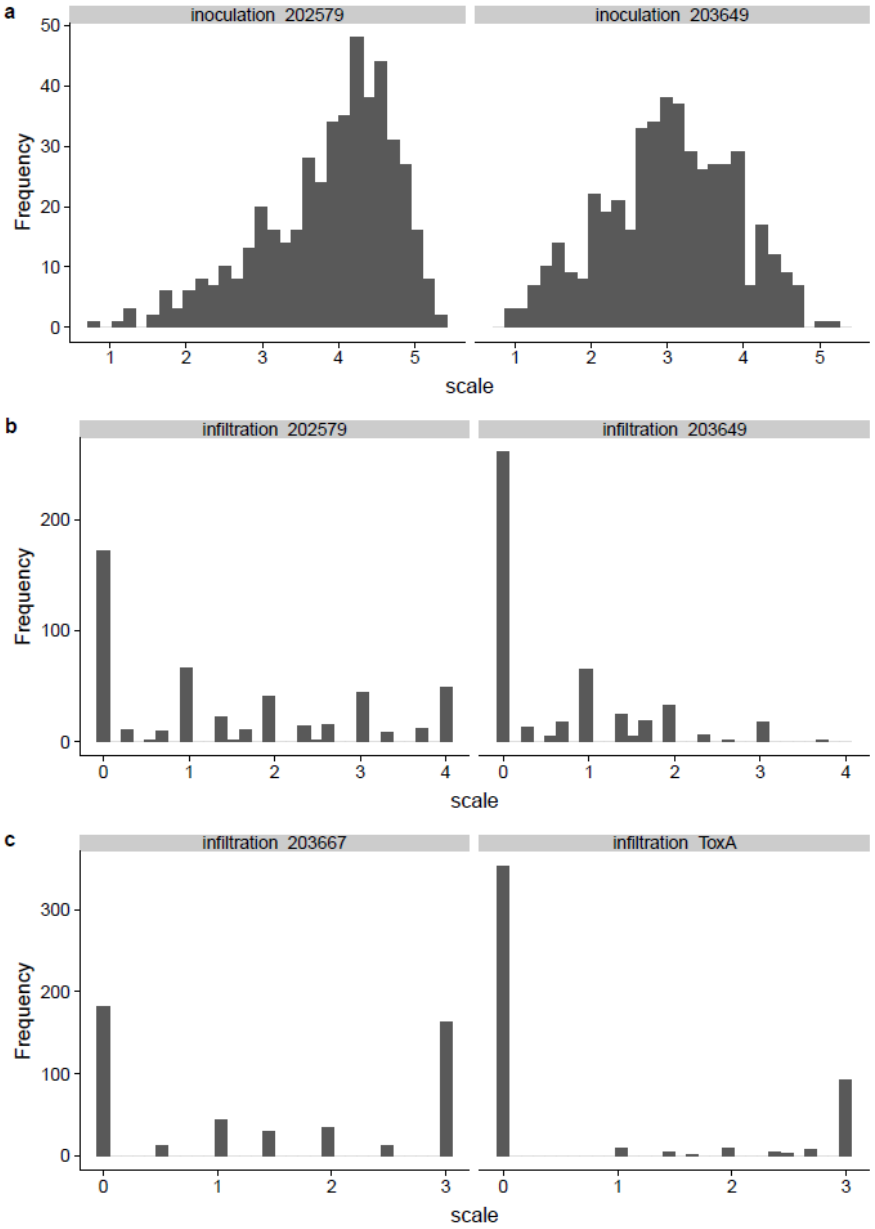

Fig. 7 Seedling disease severity of the MAGIC population. (a) Inoculation with isolate 202579 and 203649, (b) infiltration with isolate 202579 and 203649, (c) infiltration with isolate 203667 culture filtrate and ToxA.

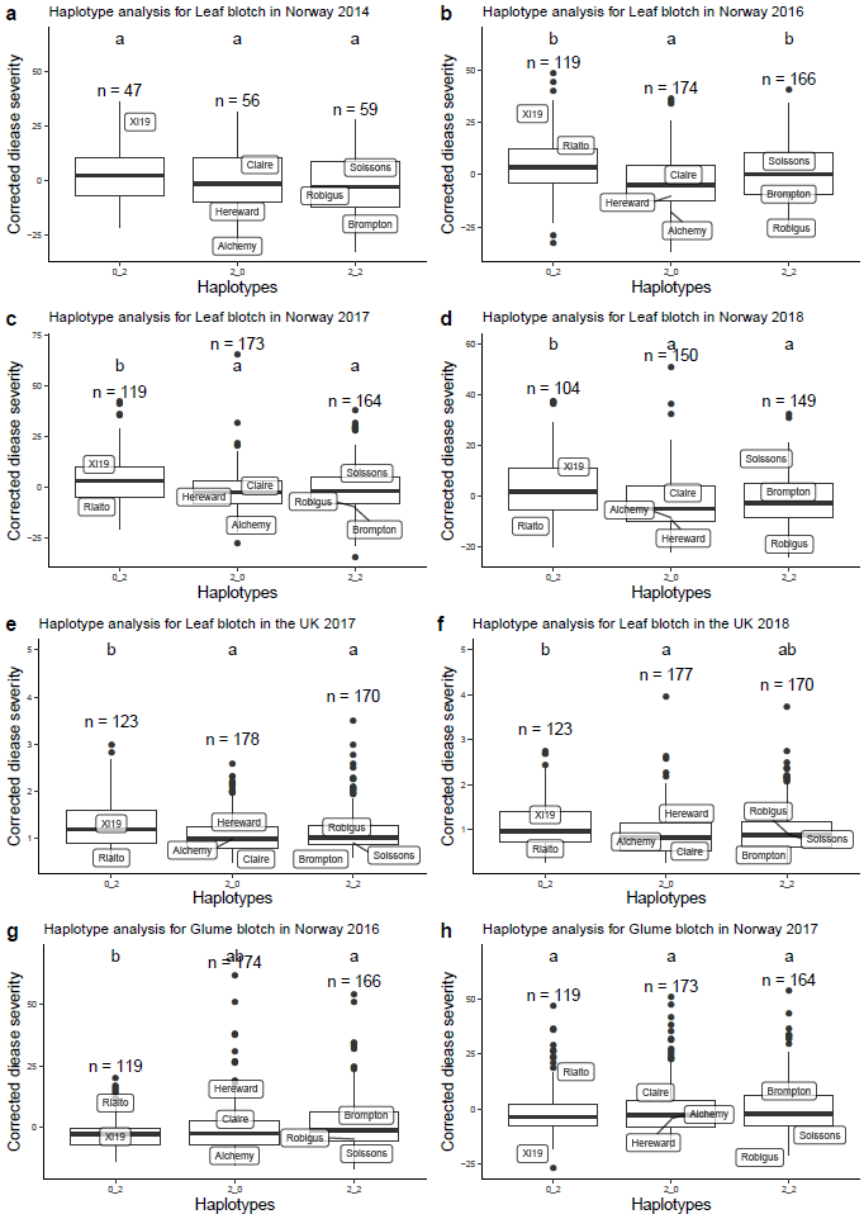

Fig. 8 Haplotype analysis for *QSnb.niab-2A.3* constructed using two markers for leaf blotch in Norway (a-d), for leaf blotch in the UK (e and f) and for glume blotch in Norway (g and h), Same letter on boxplots indicate no significant difference between haplotypes determined by Kruskal–Wallis test ($p < 0.05$).

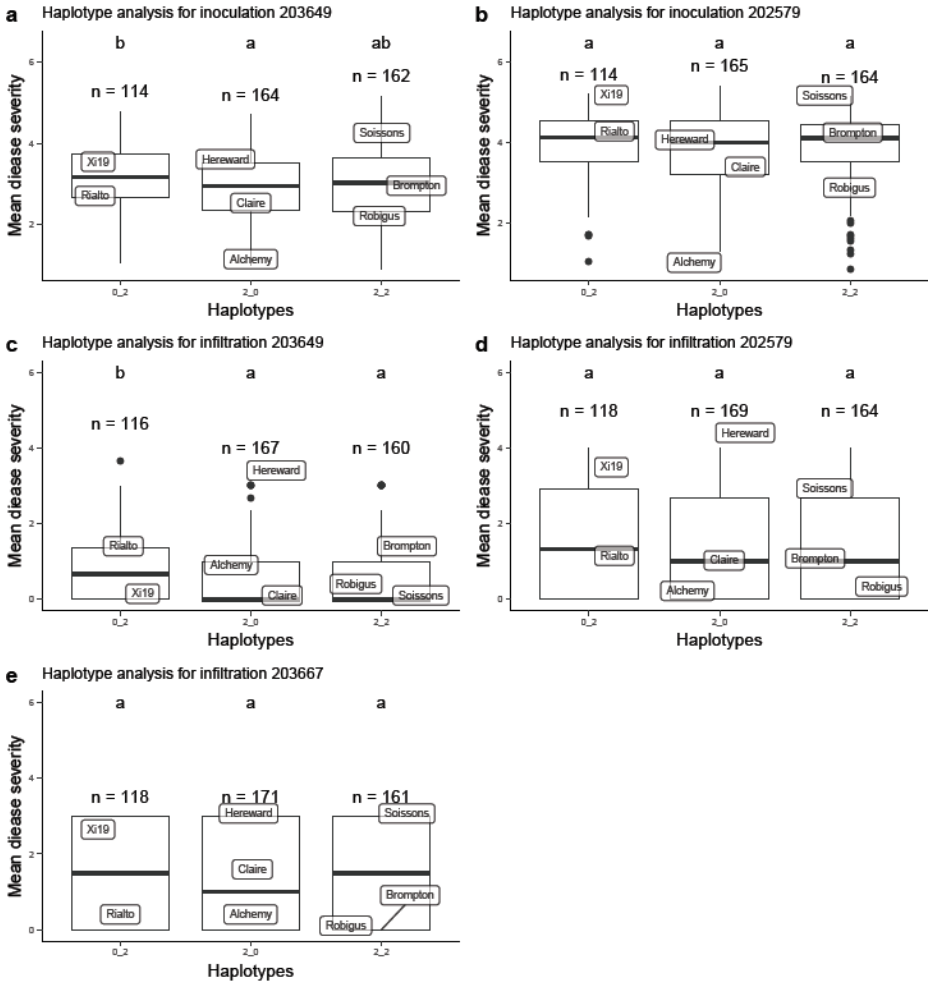

Fig. 9 Haplotype analysis for *QSnb.niab-2A.3* for greenhouse inoculation experiment (a-b), greenhouse infiltration experiment (c-e). Same letter on boxplots indicate no significant difference between haplotypes determined by Kruskal–Wallis test ($p < 0.05$).

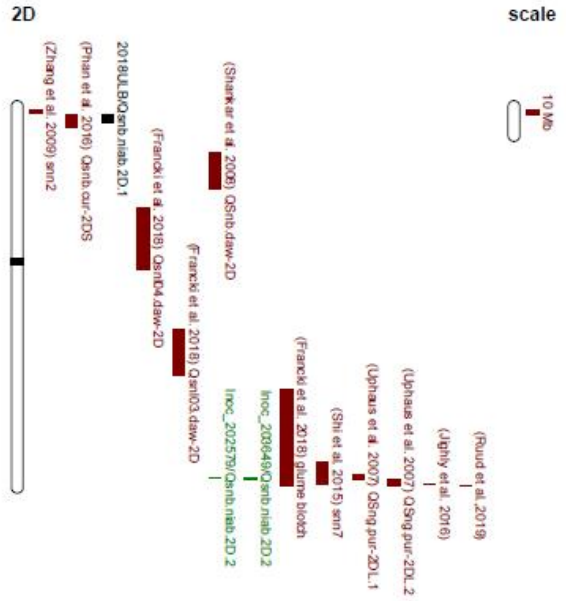

Fig. 10 Physical map locations of QTL on chromosome 2D. QTL locations and interval sizes are indicated by bars on the right hand side of chromosome, and are based on the data in Supplementary Table S4. *QSnb.niab-2D.1* detected for leaf blotch 2018 in the UK and *QSnb.niab-2D.2* detected by greenhouse inoculation in the 'NIAB Elite MAGIC' population. U: UK, LB: leaf blotch. QTL detected by this study: field leaf blotch QTL is indicated in black and seedling QTL in green. Published QTL are indicated in brown.

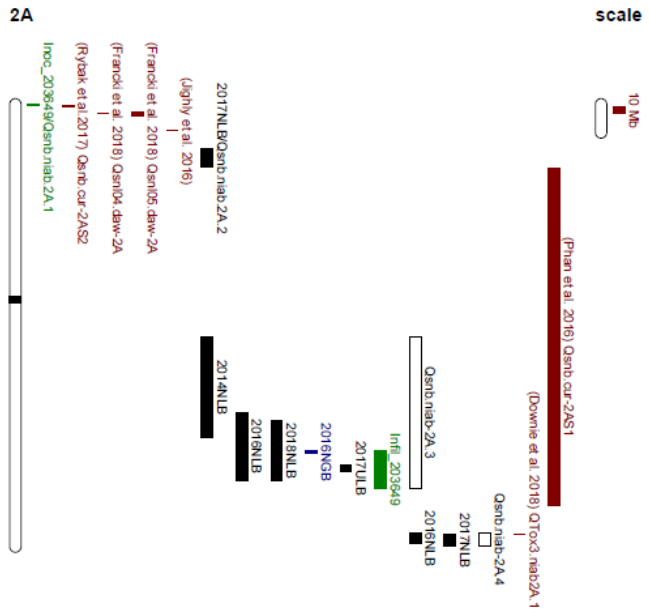

Fig. 11 Physical map locations of QTL on chromosome 2A. QTL locations and interval sizes are indicated by bars on the right hand side of chromosome, and are based on the data in Supplementary Table S3. QTL detected by this study: field leaf blotch QTL are indicated in black, field glume blotch QTL in blue (N: Norway, U: UK, LB: leaf blotch, GB: glume blotch), and seedling QTL in green (Inoc: greenhouse inoculation, Infil: greenhouse infiltration). Of these QTL, those detected in more than one environment are indicated using a white bar, along with the designated QTL name assigned in this study. Published QTL are indicated in brown.

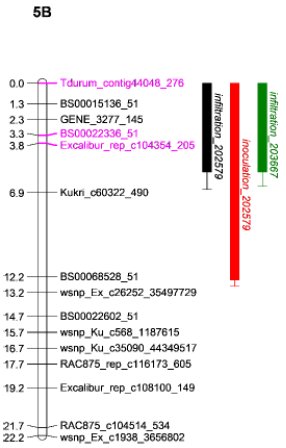

Fig. S1 Genetic map of the *Snn3-B1* locus detected by greenhouse experiment on the short arm of chromosome 5B (*QSnb.niab-5B.1)* in the NIAB Elite MAGIC population. Peak markers are indicated in pink.

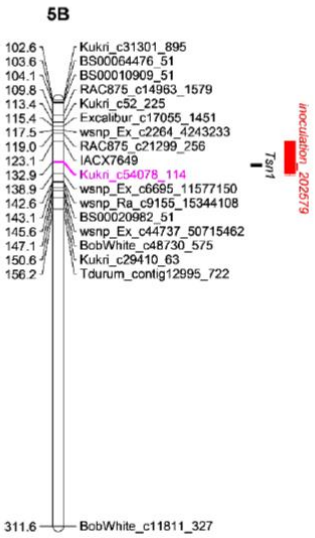

Fig. S2 Genetic map of the *Tsn1* locus detected by seedling inoculation using isolate 202579 on the long arm of chromosome 5B (*QSnb.niab-5B.2*) in the 'NIAB Elite MAGIC' population. Peak markers are indicated in pink.

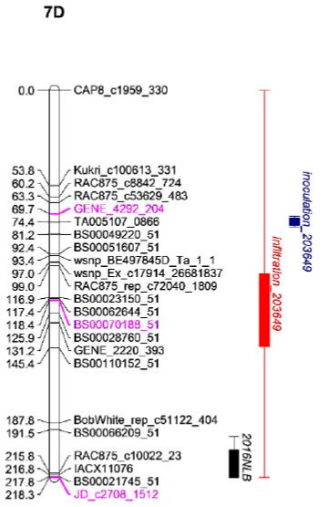

Fig. S3 Genetic map of the *QSnb.niab-7D.1* and *QSnb.niab-7D.2* loci, detected by infiltration of isolate 203649, and *QSnb.niab-7D.3* detected by leaf blotch 2016 in Norway on chromosome 7D in the 'NIAB Elite MAGIC' population. N: Norway, LB: leaf blotch, Peak markers are indicated in pink.

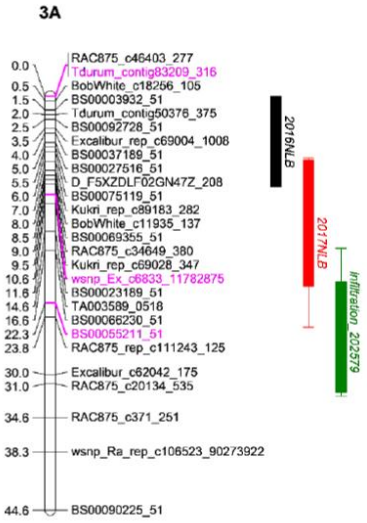

Fig. S4 Genetic map of the *QSnb.niab-3A* locus on the short arm of chromosome 3A in the 'NIAB Elite MAGIC' population. N: Norway, LB: leaf blotch. Peak markers are indicated in pink.

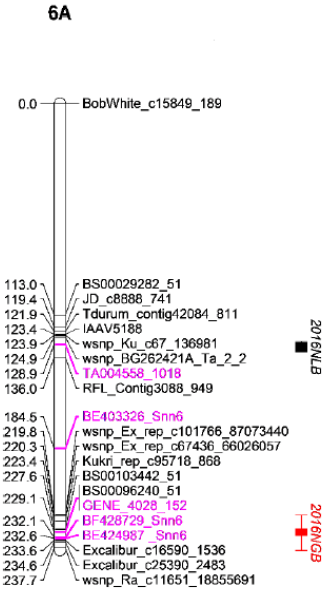

Fig. S5 Genetic map of the *QSnb.niab-6A.1* and *QSnb.niab-6A.2* loci, detected by glume blotch 2016 in Norway on chromosome 6A in the 'NIAB Elite MAGIC' population. N: Norway, LB: leaf blotch, GB: glume blotch. Peak markers and *Snn6* markers (Gao et al. 2015) are indicated in pink.

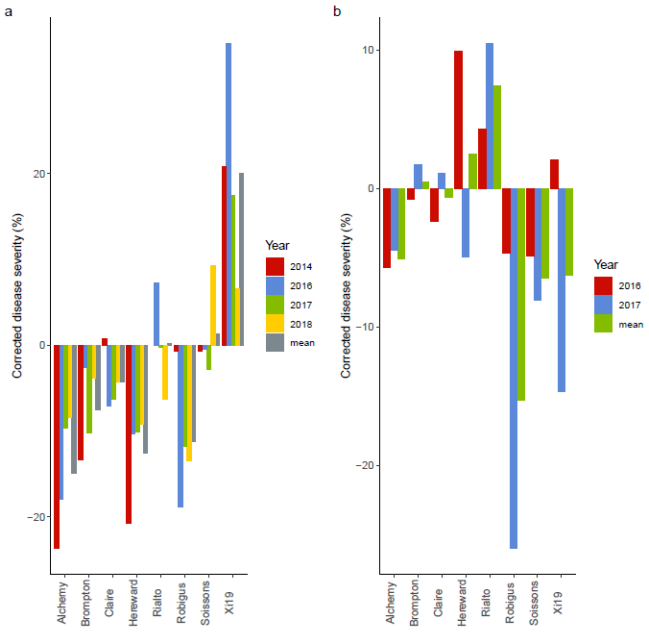

Fig. S6 Corrected disease severity of MAGIC founders in different years and locations. (a) Leaf blotch severity in Ås, Norway, (b) glume blotch severity in Ås, Norway.

Table S1 Heritability (h^2) of leaf blotch severity N: Norway, U: UK, LB: leaf blotch, GB: glume blotch.

Environment	Heritability (%)
2014NLB	73.59
2016NLB	77.45
2017NLB	48.00
2018NLB	57.49
2017ULB	13.61
2018ULB	57.25
2016NGB	59.56
2017NGB	45.64

Table S2 QTL significance thresholds calculated by permutation for each environment.

Environment	Location	Threshold (-log10P)
2014 Leaf blotch	Field, Norway	4.64
2016 Leaf blotch	Field, Norway	4.39
2016 Glume blotch	Field, Norway	4.09
2017 Leaf blotch	Field, Norway	4.28
2017 Glume blotch	Field, Norway	4.42
2018 Leaf blotch	Field, Norway	4.63
2017 Leaf blotch	Field, UK	4.41
2018 Leaf blotch	Field, UK	4.23
Infiltration 202579	Greenhouse	4.22
Inoculation 202579	Greenhouse	4.43
Infiltration 203649	Greenhouse	4.34
Inoculation 203649	Greenhouse	4.41
Infiltration 203667	Greenhouse	4.49

Table S3 Overview of QTL identified by published SNB studies on wheat chromosome 2A., based on the wheat reference genome (RefSeq v1.0). The genomic locations of the peak SNPs have been included and shown in bold. Marker used for constructing haplotype analysis are shown bold and underlined. N: Norway, LB: leaf blotch, left: left flanking marker of the QTL, right: right flanking marker of QTL, peak: peak marker of QTL.

Marker ID	Population	Physical position start (bp)	Physical position end (bp)	Reference	Source/gene function
RAC875_c44680_90	NIAB Elite MAGIC	820543	820443	This study/ *QSnb.niab-2A.1*	203649_inoculation_left
wmc382a	Calingiri × Wyalkatchem	2320465	2320686	(Rybak et al. 2017)/ *Qsnb.cur-2AS2*	Seedling leaf blotch
BS00111318_51	NIAB Elite MAGIC	2378473	2378574	This study/ *QSnb.niab-2A.1*	203649_inoculation_peak
barc124a	Calingiri × Wyalkatchem	3784350	3784367	(Rybak et al. 2017)/ *Qsnb.cur-2AS2*	Seedling leaf blotch
IWB29103	P92201D5 × P91193D1	14815405	14815505	(Francki et al. 2018)/ *Qsnl05.daw-2A*	Adult plant leaf blotch
IWB32474	P92201D5 × P91193D1	15608826	15608891	(Francki et al. 2018)/ *Qsnl04.daw-2A*	Adult plant leaf blotch
IWB9206	P92201D5 × P91193D1	16321845	16321745	(Francki et al. 2018)/ *Qsnl04.daw-2A*	Adult plant leaf blotch
IWB22268	P92201D5 × P91193D1	19649717	19649817	(Francki et al. 2018)/ *Qsnl05.daw-2A*	Adult plant leaf blotch
wPt-1657	GWAS of 320 synthetic hexaloid wheat (SHW) lines	47152165	47152854	(Jighly et al. 2016)	Glume blotch
Kukri_c24852_466	NIAB Elite MAGIC	78844360	78844461	This study/ *QSnb.niab-2A.2*	2017NLB-left
Excalibur_c637_1078	NIAB Elite MAGIC	90029248	90029349	This study/ *QSnb.niab-2A.2*	2017NLB-peak
BS00008805_51	NIAB Elite MAGIC	111457270	111457371	This study/ *QSnb.niab-2A.2*	2017NLB-right
gwm339	Calingiri × Wyalkatchem	112746128	112746147	(Phan et al. 2016)/ *Qsnb.cur.2AS1*	Seedling leaf blotch

JD_c2056_506	NIAB Elite MAGIC	410872779	410872879	This study/ *QSnb.niab-2A.3*	2014NLB-left
BS00055514_51	NIAB Elite MAGIC	543625443	543625544	This study/ *QSnb.niab-2A.3*	2014NLB-peak/2016NLB-left
Excalibur_c1793_97	NIAB Elite MAGIC	558953000	558953100	This study/ *QSnb.niab-2A.3*	2018NLB-left
Kukri_c7825_288	NIAB Elite MAGIC	588258005	588258104	This study/ *QSnb.niab-2A.3*	2014NLB-right
Ku_c5710_312	NIAB Elite MAGIC	605800158	605800259	This study/ *QSnb.niab-2A.3*	2016NLB-peak
RAC875_c20247_398	NIAB Elite MAGIC	611946675	611946776	This study/ *QSnb.niab-2A.3*	2016NGB-left
BS00022641_51		612422267	612422167		203649_infiltration_left
BS00062679_51	NIAB Elite MAGIC	615287656	615287757	This study/ *QSnb.niab-2A.3*	2016NGB-peak/right
RAC875_c9372_94	NIAB Elite MAGIC	635606921	635606992	This study/ *QSnb.niab-2A.3*	2018NLB-peak/2017ULB-peak&left
BS00012320_51	NIAB Elite MAGIC	647927316	647927416	This study/ *QSnb.niab-2A.3*	2017ULB-right
BS00090569_51	NIAB Elite MAGIC	653680962	653680862	This study/ *QSnb.niab-2A.3*	203649_infiltration_peak
BS00022241_51	NIAB Elite MAGIC	663328916	663329017	This study/ *QSnb.niab-2A.3*	2016NLB-right /2018NLB-right
IAAV4015	NIAB Elite MAGIC	677529636	677529836	This study/ *QSnb.niab-2A.3*	203649_infiltration_right
gwm312	Calingiri × Wyalkatchem	709048504	709048682	(Phan et al. 2016)/ *Qsnb.cur.2AS1*	Seedling leaf blotch
wsnp_Ra_c6586_11477949	NIAB Elite MAGIC	755929525	755929615	This study/ *QSnb.niab-2A.4*	2016NLB-left
Excalibur_c4372_363	NIAB Elite MAGIC	758396871	758396972	This study/ *QSnb.niab-2A.4*	2017NLB-peak
JD_c11825_1135	NIAB Elite MAGIC	758397388	758397464	This study/ *QSnb.niab-2A.4*	2017NLB -left
Excalibur_c20478_641	NIAB Elite MAGIC	758554464	758554565	(Downie et al. 2018)/ *QTox3.niab2A.1*	Tox3-infiltration
BS00070979_51	NIAB Elite MAGIC	758692088	758692189	(Downie et al. 2018)/ *QTox3.niab2A.1*	Tox3-infiltration

wsnp_Ra_c17622_26522072	NIAB Elite MAGIC	759489122	759489310	This study/ *QSnb.niab-2A.4*	2016NLB -peak
BS00022252_51	NIAB Elite MAGIC	775619839	775619939	This study/ *QSnb.niab-2A.4*	2016NLB-right
Tdurum_contig8350_350	NIAB Elite MAGIC	780714571	780714672	This study/ *QSnb.niab-2A.4*	2017NLB -right

Table S4 Overview of QTL identified by published SNB studies on wheat chromosome 2D, based on the wheat reference genome (RefSeq v1.0). The genomic locations of the peak SNPs have been included and shown in bold. N: Norway, U: UK, LB: leaf blotch, GB: glume blotch. left: left flanking marker of the QTL, right: right flanking marker of QTL, peak: peak marker of QTL.

Marker ID	Population	Physical position start (bp)	Physical position end (bp)	Reference	Source
Xcfd56	BR34×Grandin	6158983	6158963	(Zhang et al. 2009)	*Snn2*
Xcfd51	BR34×Grandin	12360665	12360684	(Zhang et al. 2009)	*Snn2*
cfd36	Calingiri × Wyalkatchem	14362782	14362981	(Phan et al. 2016)/ *Qsnb.cur-2DS*	
BS00029208_51	NIAB Elite MAGIC	14897896	14897996	This study/ *QSnb.niab-2D.1*	2017ULB-peak
wsnp_JD_rep_c63957_40798083	NIAB Elite MAGIC	20768482	20768682	This study/ *QSnb.niab-2D.1*	2017ULB -left
BobWhite_c59161_181	NIAB Elite MAGIC	27859904	27859806	This study/ *QSnb.niab-2D.1*	2017ULB -right
wPt-669517	Calingiri × Wyalkatchem	37053347	37053740	(Phan et al. 2016)/ *Qsnb.cur-2DS*	
cfd11	WAWHT2074 × 6HRWSN125	79231376	79231506	(Shankar et al. 2008)/ *QSnb.daw-2D*	Adult plant leaf blotch
gwm30	WAWHT2074 × 6HRWSN125	142336641	142336663	(Shankar et al. 2008)/ *QSnb.daw-2D*	Adult plant leaf blotch
IWA8151	WAWHT2074 × 6HRWSN125	173007798	173007990	(Francki et al. 2018)/ *Qsnl04.daw-2D*	Adult plant leaf blotch
IWB38724	WAWHT2074 × 6HRWSN125	279049474	279049410	(Francki et al. 2018)/ *Qsnl04.daw-2D*	Adult plant leaf blotch
Excalibur_c4248_1411	NIAB Elite MAGIC	316144729	316144828	This study/ *QSnb.niab-2D.2*	202579_inoculation-left
IWB46396	WAWHT2074 × 6HRWSN125	382170351	382170451	(Francki et al. 2018)/ *Qsnl03.daw-2D*	Adult plant leaf blotch
IWB38687	WAWHT2074 × 6HRWSN125	461301212	461301312	(Francki et al. 2018)/ *Qsnl03.daw-2D*	Adult plant leaf blotch
IWB31450	P92201D5 × P91193D1	484328365	484328343	(Francki et al. 2018)	Glume blotch

cfd44	Chinese Spring × Timstein	608561046	608633134	(Shi et al. 2015)	*Snn7*
Xgwm526.1	P92201D5 × P91193D1	630399094	630399233	(Uphaus et al. 2007)/ *Qng.pur-2DL.1*	Glume blotch
Excalibur_c42413_442	NIAB Elite MAGIC	635950166	635950267	This study/ *QSnb.niab-2D.2*	203649_inoculation-peak
BS00010685_51	NIAB Elite MAGIC	635950569	635950669	This study/ *QSnb.niab-2D.2*	202579_inoculation-right
Kukri_c36328_419	NIAB Elite MAGIC	635951859	635951940	This study/ *QSnb.niab-2D.2*	203649_inoculation-right
Xcfd50	P92201D5 × P91193D1	637443897	637444139	(Uphaus et al. 2007)/ *QSng.pur-2DL.1/ QSng.pur-2DL.2*	Glume blotch
RFL_Contig1128_620	NIAB Elite MAGIC	638147672	638147754	This study/ *QSnb.niab-2D.2*	203649_inoculation-left
Ra_c19051_1446	NIAB Elite MAGIC	638147672	638147754	This study/ *QSnb.niab-2D.2*	202579_inoculation-peak
wPt-7825	GWAS of 320 synthetic hexaloid wheat (SHW) lines	646772948	646773564	(Jighly et al. 2016)	Glume blotch
gwm311	Chinese Spring × Timstein	647509839	647509858	(Shi et al. 2015)	*Snn7*
wPt-9848	P92201D5 × P91193D1	648059097	648058258	(Uphaus et al. 2007)/*QSng.pur-2DL.2*	Glume blotch
Excalibur_c31806_912	GWAS of 121 spring lines	649815122	649815222	(Ruud et al, 2019 in press)	Adult plant leaf blotch
BS00015680_51	GWAS of 121 spring lines	650322729	650322629	(Ruud et al, 2019 in press)	Adult plant leaf blotch
IAAV1322	GWAS of 121 spring lines	650322873	650322991	(Ruud et al, 2019 in press)	Adult plant leaf blotch
Excalibur_rep_c67599_2154	GWAS of 121 spring lines	650325174	650325274	(Ruud et al, 2019 in press)	Adult plant leaf blotch
IAAV6032	GWAS of 121 spring lines	650325193	650325352	(Ruud et al, 2019 in press)	Adult plant leaf blotch
IWB21124	P92201D5 × P91193D1	650326781	650326881	(Francki et al. 2018)	Glume blotch
Excalibur_rep_c67599_242	GWAS of 121 spring lines	650327186	650327086	(Ruud et al, 2019 in press)	Adult plant leaf blotch

Table S5 Overview of QTL identified by published SNB studies on wheat chromosome 6A, based on the wheat reference genome (RefSeq v1.0). The genomic locations of the peak SNPs have been included and shown in bold. N: Norway, U: UK, LB: leaf blotch, GB: glume blotch. Left: left flanking marker of the QTL, right: right flanking marker of QTL, peak: peak marker of QTL.

Marker ID	Population	Physical position start (bp)	Physical position end (bp)	Reference	Source
IAAV5188	NIAB Elite MAGIC	74025753	74025954	This study/ *QSnb.niab-6A.1*	2016NLB- Left
TA004558_1018	NIAB Elite MAGIC	97809626	97809680	This study/ *QSnb.niab-6A.1*	2016NLB - peak
RFL_Contig3088_949	NIAB Elite MAGIC	249160604	249160705	This study/ *QSnb.niab-6A.1*	2016NLB-right
BE403326	W-7984 × Opata 85	574221943	574221462	(Gao et al. 2015)	*Snn6*
gwm570	Alba × Begra	579125838	579125980	(Arseniuk et al. 2004)	Seedling leaf
mwg934	Alba × Begra	583269284	583269303	(Arseniuk et al. 2004)	Seedling leaf
GENE_4028_152	NIAB Elite MAGIC	600395629	600395722	This study/ *QSnb.niab-6A.2*	2016NGB-Peak
BS00096240_51	NIAB Elite MAGIC	600406107	600406208	This study/ *QSnb.niab-6A.2*	2016NGB - right
BF428729	W-7984 × Opata 85	603135924	603136145	(Gao et al. 2015)	*Snn6*
BE424987	W-7984 × Opata 85	606979803	606979976	(Gao et al. 2015)	*Snn6*

Table S6 Plant height (PH) QTL identified in the 'NIAB Elite MAGIC' population from field trials conducted in Norway in 2014, 2016, 2017 and 2018, and the UK in 2017 and 2018. QTL with $-\log_{10}(p)$ value > 3 are presented, with QTL above the permutated trait-specific significance threshold highlighted in bold. Chromosome (Chr.), proportion of the variance explained by QTL (R^2). The –log10(p) values coded as 'Inf' are due to a p-value of 0, resulting in an error when converted to the $\log_{10}$ scale. † Genetic map: Gardner et al. (2016).

QTL	Location	Trait	Year	Chr	Interval (cM)†	Flanking markers	Peak Marker	$-\log_{10}$ (p)	R^2 (%)	Detected by QTL methods
QPh.niab-2D	**UK**	**PH**	**2017**	**2D**	**52.86-62.71**	**BS00011425_51 and wsnp_CAP12_c1503_764765**	**wsnp_CAP12_c1503_764765**	**7.96**	**7.19**	**IM, CIM (cov5, cov10),IBD**
QPh.niab-4B	**Norway**	**PH**	**2014**	**4B**	**38.66-57.22**	**wsnp_CAP11_c1103_647926 and BS00076259_51**	**BS00023766_51**	**13.74**	**18.36**	**IM, CIM (cov5, cov10),IBD**
QPh.niab-4B	**Norway**	**PH**	**2016**	**4B**	**40.17-57.22**	**BS00022534_51 and BS00076259_51**	**RAC875_c27536_611**	**Inf**	**6.99**	**IM, CIM (cov5, cov10),IBD**
QPh.niab-4B	**Norway**	**PH**	**2017**	**4B**	**47.14-57.22**	**BS00100838_51 and BS00076259_51**	**RAC875_c27536_611**	**Inf**	**7.24**	**IM, CIM (cov5, cov10),IBD**
QPh.niab-4B	**Norway**	**PH**	**2018**	**4B**	**47.14-57.22**	**BS00100838_51 and BS00076259_51**	**BS00021984_51**	**11.50**	**5.54**	**IM, CIM (cov5, cov10),IBD**
QPh.niab-4B	**UK**	**PH**	**2017**	**4B**	**38.66-57.22**	**wsnp_CAP11_c1103_647926 and BS00076259_51**	**RAC875_c27536_611**	**Inf**	**7.18**	**IM, CIM (cov5, cov10),IBD**
QPh.niab-4B	**UK**	**PH**	**2018**	**4B**	**47.14-57.22**	**BS00100838_51 and BS00076259_51**	**RAC875_c27536_611**	**11.73**	**5.86**	**IM, CIM (cov5, cov10),IBD**
QPh.niab-4D	**Norway**	**PH**	**2014**	**4D**	**24.93-42.63**	**Kukri_rep_c68594_530 and Excalibur_c53541_723**	**RHT2**	**Inf**	**32.38**	**IM, CIM (cov5, cov10),IBD**
QPh.niab-4D	**Norway**	**PH**	**2016**	**4D**	**24.93-42.13**	**Kukri_rep_c68594_530 and Excalibur_c23163_98**	**RAC875_c1673_663**	**Inf**	**17.55**	**IM, CIM (cov5, cov10),IBD**
QPh.niab-4D	**Norway**	**PH**	**2017**	**4D**	**24.93-42.13**	**Kukri_rep_c68594_530 and Excalibur_c23163_98**	**RAC875_c1673_663**	**Inf**	**17.82**	**IM, CIM (cov5, cov10),IBD**

QPh.niab-4D	**Norway**	**PH**	**2018**	**4D**	**24.93-42.63**	**Kukri_rep_c68594_530 and Excalibur_c53541_723**	**RHT2**	**Inf**	**13.81**	**IM, CIM (cov5, cov10),IBD**
QPh.niab-4D	**UK**	**PH**	**2017**	**4D**	**29.93-42.13**	**Kukri_rep_c68594_530 and Excalibur_c23163_98**	**RAC875_c1673_663**	**Inf**	**19.48**	**IM, CIM (cov5, cov10),IBD**
QPh.niab-4D	**UK**	**PH**	**2018**	**4D**	**24.93-42.13**	**Kukri_rep_c68594_530 and Excalibur_c23163_98**	**RAC875_c1673_663**	**Inf**	**14.77**	**IM, CIM (cov5, cov10),IBD**
QPh.niab-6A.1	Norway	PH	2016	6A	0-8.63	BobWhite_c15849_189 and RAC875_c6135_95	Excalibur_c18072_214	3.30	4.82	IM, CIM (cov5, cov10),IBD
QPh.niab-6A.2	UK	PH	2017	6A	88.28-103.35	wsnp_Ex_c31149_39976103 and Tdurum_contig50698_601	Kukri_c27958_334	3.09	3.4	IM, CIM (cov5, cov10)

Table S7 Days to heading (DH) QTL identified in the 'NIAB Elite MAGIC' population from field trials conducted in Norway in 2014, 2016, 2017 and 2018, and the UK in 2017 and 2018. QTL with $-\log_{10}(p)$ value > 3 are presented, with QTL above the permutated trait-specific significance threshold highlighted in bold. Chromosome (Chr.), proportion of the variance explained by QTL (R^2). The –log10(p) values coded as 'Inf' are due to a p-value of 0, resulting in an error when converted to the $\log_{10}$ scale. † Genetic map: Gardner et al. (2016).

QTL	Location	Trait	Year	Chr	Interval (cM)†	Flanking markers	Peak Marker	$-\log_{10}$ (p)	R^2 (%)	Detected by QTL methods
QDh.niab-1B	**Norway**	**DH**	**2017**	**1B**	**341.89-351.10**	**RAC875_c28629_101 and Kukri_c44587_130**	**BS00027006_51**	**7.55**	**6.43**	**IM, CIM (cov5, cov10), IBD**
QDh.niab-2A	**Norway**	**DH**	**2014**	**2A**	**140.76-159.02**	**Kukri_c24064_2095 and BS00065865_51**	**IAAV4015**	**4.55**	**13.15**	**IM, CIM (cov5, cov10)**
QDh.niab-2B	UK	DH	2018	2B	160.78-172.37	wsnp_Ex_c3044_5620102 and Ra_c23048_474	Tdurum_contig19413_656	3.50	4.13	**IM, CIM (cov5, cov10), IBD**
QDh.niab-2D	**Norway**	**DH**	**2016**	**2D**	**50.84-62.71**	**BobWhite_c59161_181 and wsnp_CAP12_c1503_764765**	**RAC875_c7319_195**	**5.02**	**6.11**	**IM, CIM (cov5, cov10), IBD**
QDh.niab-2D	**Norway**	**DH**	**2017**	**2D**	**50.84-62.71**	**BobWhite_c59161_181 and wsnp_CAP12_c1503_764765**	**RAC875_c7319_195**	**6.73**	**5.71**	**IM, CIM (cov5, cov10), IBD**
QDh.niab-2D	**UK**	**DH**	**2017**	**2D**	**50.84-62.71**	**BobWhite_c59161_181 and wsnp_CAP12_c1503_764765**	**BS00064538_51**	**Inf**	**37.55**	**IM, CIM (cov5, cov10), IBD**
QDh.niab-2D	**UK**	**DH**	**2018**	**2D**	**60.67-62.71**	**BS00011425_51 and wsnp_CAP12_c1503_764765**	**wsnp_CAP12_c1503_764765**	**6.31**	**6.86**	**IM, CIM (cov5, cov10), IBD**
QDh.niab-3A	**Norway**	**DH**	**2016**	**3A**	**197.83-214.37**	**Ex_c15087_564 and BS00039498_51**	**GENE_1549_110**	**4.33**	**3.56**	**IM, CIM (cov10)**
QDh.niab-4D	**Norway**	**DH**	**2016**	**4D**	**0-26.97**	**BS00054978_51 and RAC875_c6922_291**	**Excalibur_c26088_184**	**5.06**	**4.98**	**IM, CIM (cov5,**

										cov10), IBD
QDh.niab-5A	**Norway**	**DH**	**2016**	**5A**	**167.30-183.69**	**IAAV5294 and BS00067209_51**	**wsnp_Ra_c17216_26044790**	**5.73**	**4.99**	**IM, CIM (cov5, cov10), IBD**
QDh.niab-5D	Norway	DH	2018	5D	124.29-133.32	BS00033770_51 and BS00067651_51	BS00067651_51	3.42	5.02	IM, CIM (cov5, cov10), IBD
QDh.niab-6A	Norway	DH	2014	6A	124.90-142.54	wsnp_BG262421A_Ta_2_2 and Tdurum_contig78006_158	RAC875_c23305_563	3.52	10.5	IM, CIM (cov5, cov10)
QDh.niab-6B	Norway	DH	2016	6B	206.35-217.64	IACX2322 and BS00068245_51	Excalibur_c57840_227	3.64	3.5	IM, CIM (cov5)

Table S8 Uncorrected leaf blotch severity (uLB) QTL identified in the 'NIAB Elite MAGIC' population from field trials conducted in Norway in 2014, 2016, 2017 and 2018, and the UK in 2017 and 2018. QTL with $-\log_{10}(p)$ value > 3 are presented, with QTL above the permutated trait-specific significance threshold highlighted in bold. Chromosome (Chr.), proportion of the variance explained by QTL (R2). † Genetic map: Gardner et al. (2016).

QTL	Location	Trait	Year	Chr	Interval (cM) †	Flanking markers	Peak Marker	$-\log_{10}$ (p)	R^2 (%)	Detected by QTL methods
QSnb.niab-2A.3	**Norway**	**uLB**	**2014**	**2A**	**121.07-140.25**	**JD_c2056_506 and BS00022903_51**	**BS00059475_51**	**5.49**	**16.22**	**IM, CIM (cov5, cov10), IBD**
QSnb.niab-2A.3	**Norway**	**uLB**	**2016**	**2A**	**129.14-146.83**	**BobWhite_c1049_338 and BS00022241_51**	**Ku_c5710_312**	**5.30**	**6.63**	**IM, CIM (cov5, cov10), IBD**
QSnb.niab-2A.3	Norway	uLB	2018	2A	127.63-146.83	RAC875_c15213_1942 and BS00022241_51	RAC875_c9372_94	4.45	6.11	IM, CIM (cov5, cov10), IBD
QSnb.niab-2A.4	Norway	uLB	2017	2A	227.51-241.18	BS00022321_51 and Kukri_c50116_644	Excalibur_c4372_363	3.76	4.93	IM, CIM (cov5, cov10)
QSnb.niab-3A	**Norway**	**uLB**	**2017**	**3A**	**2.01-34.65**	**Tdurum_contig50376_375 and RAC875_c371_251**	**BS00023189_51**	**4.35**	**4.52**	**IM, CIM (cov5, cov10)**
QSnb.niab-4A.2	Norway	uLB	2016	4A	129.70-141.35	BS00099725_51 and RAC875_c35819_165	BS00012482_51	3.38	4.19	IM, CIM (cov5, cov10), IBD
QSnb.niab-5B.3	Norway	uLB	2014	5B	76.62-94.35	RAC875_c24376_704 and wsnp_Ex_rep_c68003_66744451	BS00066138_51	3.06	10.16	IM, CIM (cov5, cov10)
QSnb.niab-7B.3	Norway	uLB	2018	7B	18.74-31.67	Kukri_c67849_109 and BobWhite_c44404_312	BS00081132_51	3.88	5.45	IM, CIM (cov5, cov10), IBD

Table S9 Uncorrected glume blotch severity (uGB) QTL identified in the 'NIAB Elite MAGIC' population from field trials conducted in Norway in 2014, 2016, 2017 and 2018, and the UK in 2017 and 2018. QTL with $-\log_{10}(p)$ value > 3 are presented, with QTL above the permutated trait-specific significance threshold highlighted in bold. Chromosome (Chr.), proportion of the variance explained by QTL (R^2). Genetic map: Gardner et al. (2016).

QTL	Location	Trait	Year	Chr	Interval (cM) †	Flanking markers	Peak Marker	$-\log_{10}$ (p)	R^2 (%)	Detected by QTL methods
QSnb.niab-2A.3	Norway	uGB	2016	2A	133.18-151.97	BS00055512_51 and BS00027830_51	BS00090569_51	3.32	3.68	IM, CIM (cov5, cov10), IBD
QSnb.niab-6A.2	Norway	uGB	2016	6A	229.11-238.67	BS00096240_51 and BS00094893_51	GENE_4028_152	3.23	3.77	IM, CIM (cov5, cov10), IBD
QSnb.niab-4B	**Norway**	**uGB**	**2017**	**4B**	**47.14-57.22**	**BS00100838_51 and BS00076259_51**	**CAP7_c1893_424**	**5.90**	**4.7**	**IM, CIM (cov5, cov10), IBD**
QSnb.niab-4D	**Norway**	**uGB**	**2017**	**4D**	**24.93-34.28**	**Kukri_rep_c68594_530 and RHT2**	**RAC875_c1673_663**	**5.79**	**3.53**	**IM, CIM (cov5, cov10), IBD**
QSnb.niab-5D	Norway	uGB	2017	5D	49.43-66.08	BobWhite_c7263_337 and BS00063971_51	BS00110475_51	3.85	3.72	IM, CIM (cov5, cov10), IBD

Table S10 QTL significance -log10(p) thresholds calculated by permutation for each environment and each trait. PH: plant height, DH: Days to heading, uLB: uncorrected leaf blotch disease data, uGB: uncorrected glume blotch disease data

Environment	Year	PH	DH	uLB	uGB
Field, Norway	2014	4.28	4.24	5.34	
Field, Norway	2016	4.10	4.09	4.04	4.60
Field, Norway	2017	4.13	4.58	4.28	4.30
Field, Norway	2018	4.00	4.38	4.73	
Field, UK	2017	4.43	4.72		
Field, UK	2018	4.16	4.65		

	Type	Product Name	Product Rate	Unit
2017 UK trial				
12/09/2016	Herbicide	Rosate 36	0.25	l/ha
12/09/2016	Adjuvant	Companion Gold	2.7	l/ha
27/10/2016	Herbicide	Trooper	4	l/ha
01/03/2017	Fertiliser	Origin Sulphur N	154	kg/ha
06/04/2017	Fungicide	Bravo	1	l/ha
06/04/2017	Fungicide	Tebucur	0.5	l/ha
13/04/2017	Fertiliser	Prilled 34.5 N	217	kg/ha
28/04/2017	Herbicide	Starane XL	1.4	l/ha
28/04/2017	Herbicide	Ally Max SX	35	g/ha
02/05/2017	Fungicide	Aviator 235 Pro	1	l/ha
02/05/2017	Fungicide	Bravo	1	l/ha
11/05/2017	Fertiliser	Prilled 34.5 N	217	kg/ha
2018 UK trial				
27/10/2017	Molluscicide	Derrex	3.5	kg/ha
14/11/2017	Herbicide	Avadex	15	kg/ha
14/11/2017	Herbicide	Liberator	0.6	l/ha
14/11/2017	Adjuvant	Backrow	0.2	l/ha
16/04/2018	Fertiliser	Sulphur N	154	kg/ha
20/04/2018	Plant growth regulator	Agrovista 3 See 750	1	l/ha
20/04/2018	Fungicide	Bravo 500	1	l/ha
20/04/2018	Fungicide	Tebucur	0.5	l/ha
20/04/2018	Fungicide	Talius	0.15	l/ha
21/04/2018	Fertiliser	Yara prilled 34.5	217	kg/ha
01/05/2018	Fertiliser	Yara prilled 34.5	217	kg/ha
18/05/2018	Fungicide	Cherokee	1	l/ha
18/05/2018	Fungicide	Adexar	1	l/ha
25/05/2018	Herbicide	Starane XL	1.5	l/ha
25/05/2018	Herbicide	Ally Max SX	35	g/ha
31/05/2018	Fungicide	Corbel	1	l/ha
01/06/2018	Insecticide	Markate	0.1	l/ha

Table S11. Details of the agronomic package used in the UK 2017 and 2018 season trials.

Supplementary Text 1

Five QTL were identified for plant height, on chromosome 2D, 4B, 4D and 6A, respectively. Ten QTL were detected for trait days to heading on chromosome 1B, 2A, 2B, 2D, 3A, 4D, 4D, 5A, 5D, 6A and 6B. For leaf blotch uncorrected data, six QTL were detected on 2A, 3A, 4A, 5B and 7B.

We found that 'strong QTL' QSnb.niab-6A.1 detected in Norway in 2016 for the corrected leaf blotch phenotype might collocate with one 'weak QTL' QDh.niab-6A for days to heading detected in Norway in 2014. However, except that, other colocation of QTL with confounding traits were not found for using both corrected leaf blotch and uncorrected leaf blotch phenotypes. 'Strong QTL' *detected with uncorrected disease data all had been detected by previous corrected disease data (QSnb.niab-2A.3 and QSnb.niab-3A). In total, five 'weak QTL' were detected by uncorrected leaf blotch data. QSnb.niab-2A.3 and QSnb.niab-2A.4 had been detected previously using corrected leaf blotch phenotypes, but three other 'weak QTL' were not detected by corrected disease data.*

For glume blotch, five QTL were detected with the uncorrected data, however all Strong QTL collocated with the plant height QTL on chromosome 4B and 4D. The rest three glume blotch QTL were previously identified by corrected disease data, however mostly with less significance using uncorrected disease data.

Identification and cross-validation of *Parastagonospora nodorum* blotch resistance genetic loci using a multi-founder winter wheat population

Min Lin[1], Melanie Stadlmeier[2], Volker Mohler[2], Kar-Chun Tan[3], Andrea Ficke[4], James Cockram[5], Morten Lilemo[1,*]

[1]Department of Plant Sciences, Norwegian University of Life Sciences, Ås, Norway

[2]Bavarian State Research Center for Agriculture, Institute for Crop Science and Plant Breeding, Freising, Germany

[3]Division of biotechnology and plant health, Norwegian Institute of Bioeconomy Research (NIBIO), Ås, Norway

[4]Centre for Crop and Disease Management, School of Molecular and Life Sciences, Curtin University, Bentley, Western Australia, Australia

[5]John Bingham Laboratory, NIAB, Huntingdon Road, Cambridge, CB3 0LE, United Kingdom

*** Correspondence:**
Morten Lillemo
morten.lillemo@nmbu.no

Abstract

Septoria nodorum blotch (SNB) is a disease of wheat (*Triticum aestivum* L.) caused by the necrotrophic fungal pathogen *Parastagonospora nodorum*. Resistance/susceptibility to SNB is a typical quantitative trait, controlled by multiple quantitative trait loci (QTL) of minor effect. In order to maximize the capture of SNB resistance alleles within the framework of a single genetic mapping population, we undertook genetic analysis of SNB resistance using an eight-founder German Multiparent Advanced Generation Inter-Cross (MAGIC) population, termed the 'Bavarian MAGIC winter wheat population' (BMWpop). Field trials and greenhouse testing were conducted over three seasons in Norway, with genetic analysis identifying ten SNB resistance QTL. Of these, two QTL were identified over two seasons: *QSnb.nmbu-2A.1* on chromosome 2A and *QSnb.nmbu-5A.1* on chromosome 5A. Aligning the chromosome 2A BMWpop QTL to the wheat physical map indicated that it co-located with a robust SNB resistance QTL recently identified in an independent eight-founder MAGIC population constructed using varieties released in the United Kingdom (UK). The validation of this SNB resistance QTL in two independent multi-founder mapping populations, regardless of the differences in genetic background and agricultural environment, highlights the value of integrating beneficial alleles at this locus into SNB resistance

breeding programs. The second robust SNB resistance QTL identified in the BMWpop, *QSnb.nmbu-5A*.1, was not identified in the UK MAGIC population. Investigation of the additive effects of the 2A and 5A QTL in the BMWpop indicated that combining resistance alleles at both loci results in additive effects on SNB resistance. Therefore, using marker assisted selection to combine resistance alleles in wheat breeding programmes could provide a promising strategy for developing new varieties with increased genetic resistance to SNB. Indeed, the multi-locus haplotypes for the BMWpop chromosome 2A and 5A SNB resistance QTL determined in this study provide markers for efficient tracking of these beneficial alleles in future wheat genetics and breeding activities.

1 Introduction

Wheat (*Triticum aestivum* L.) is one of the most important staple food sources worldwide, with gross production valued at around 168 billion US dollars (Food and Agriculture Organization of the United Nations, 2016). However, wheat production is threatened by various bacterial, fungal and viral diseases. *Parastagonospora nodorum* is a devastating fungal wheat pathogen with disease epidemics reported in nearly all wheat producing regions with warm and humid growing conditions (Oliver et al., 2012; Francki, 2013; Ficke et al., 2018). By causing damage to both wheat leaves and ears, *P. nodorum* can reduce yield by up to 30% (Bhathal et al., 2003). So far, regardless of resistance breeding efforts, no cultivar has shown complete resistance to *P. nodorum* in the field, and control of SNB still largely depends on fungicide application (Duba et al., 2018; Trainar et al., 2018). However, intensive use of fungicides increases the risk of fungicide resistance, and the resulting reduction in available modes of action challenges the effectiveness of future chemical control (Holloman, 2015). Therefore, research on host genetic resistance is needed in parallel with efforts to find new modes of action for chemical control.

P. nodorum is the model organism for necrotrophic fungal pathogens and much research has been done to characterize the interactions between *P. nodorum* and wheat (Oliver et al., 2012). *P. nodorum* can trigger plant cell death and expand infections by secreting proteinaceous necrotrophic effectors (NEs) that target dominant susceptibility loci in the wheat host (Friesen et al., 2007). Accumulation of multiple susceptibility loci in a wheat cultivar may result in higher disease severity to certain *P. nodorum* isolates, as some wheat susceptibilities to NEs have been

shown to be quantitative and additive (Friesen et al., 2009). To date, eight *P. nodorum* NEs have been characterized, which interact with nine susceptibility loci distributed over seven wheat chromosomes (Ruud and Lillemo, 2018). Among those, three *P. nodorum* NE-coding genes (*SnToxA, SnTox1* and *SnTox3*) (Liu et al., 2006; Liu et al., 2009; Liu et al., 2012) and two wheat susceptibility genes (*Tsn1* and *Snn1*) (Faris et al., 2010; Shi et al., 2016) have been cloned. When used in conjunction with traditional marker assisted selection for SNB resistance QTL, eliminating susceptibility alleles from wheat cultivars could be a potential strategy to enhance SNB resistance breeding. For example, in Australia the ToxA-*Tsn1* interaction was found to be a significant factor in field SNB susceptibility. Subsequent reduction of the ToxA sensitive wheat growing area by 13.5% between 2009 to 2013 was estimated to have saved 50 million $ in crop losses (Vleeshouwers and Oliver, 2014).

Genotype by environment interaction commonly plays an important role in determining SNB resistance/susceptibility field phenotype. In addition, QTL identified using one mapping population may not necessarily be identified in another mapping population, due to differences caused by the genetic background (Langridge et al., 2001). Of the nine known NE susceptibility genetic loci, four have been reported to co-locate with field SNB QTL: *Tsn1*, *Snn1*, *Snn2* and *Snn3-B1* (Friesen et al., 2009; Phan et al., 2016; Ruud et al., 2017; Ruud and Lillemo, 2018). Genetic analysis of target traits using multi-parent advanced generation inter-cross (MAGIC) populations could be considered as more relevant for breeding programs compared to biparental populations, as the multiple founders used (typically between 4 and 16) provide the possibility of capturing increased numbers of alleles at any given locus (Wei and Xu, 2016), as well as efficiently combining founder haplotypes via multiple rounds of intercrossing. These properties of MAGIC populations allows resulting QTL to be assessed under a wider range of genetic backgrounds, and increases the chances of detecting disease resistance QTL within the framework of a single genetic mapping population (Cockram and Mackay, 2018). Recently, MAGIC populations have begun to be used for numerous genetic studies of wheat disease resistance and fungal effector sensitivity (Cockram et al., 2015; Downie et al., 2018; Stadlmeier et al., 2019; Lin et al., 2020; Corsi et al., 2020). A recent study by Lin et al. (2020) investigated *P. nodorum* susceptibility at both the seedling and adult plant stages using a UK-relevant eight-founder wheat MAGIC resource, termed the 'NIAB Elite MAGIC' population (Mackay et al., 2014). Numerous QTL were identified,

including *QSnb.niab-2A.3*, which was detected consistently across years and locations. The stability of *QSnb.niab-2A.3* indicated that resistance alleles at this locus could be a useful target for marker assistant selection in SNB resistance breeding.

The 'Bavarian MAGIC winter wheat population' (BMWpop) is an eight-founder wheat MAGIC population of German origin. Evaluating the SNB disease severity of the BMWpop, which has a considerably different genetic background compared to 'NIAB Elite MAGIC', may provide additional SNB resistance resources for improving SNB resistance breeding. In addition, if common QTL could be detected in two MAGIC populations of contrasting origin, marker assisted selection (MAS) for such QTL could be applied with increased confidence in wider European wheat breeding programs. Lin et al. (2020) reported that ToxA-*Tsn1* and Tox3-*Snn3* interactions showed effects on seedling resistance but were not represent in QTL detected by field testing. However, culture filtrate (CF) infiltration of the *P. nodorum* isolate 203649 possessing uncharacterised effectors detected a common QTL *QSnb.niab-2A.3* which was robust for adult plant resistance in the field across years and location (Lin et al., 2020). As all BMWpop founders were insensitive to ToxA, only Tox3 and CF infiltration of isolate 203649 were conducted in this study. Therefore, the objectives of this study were to (1) identify SNB QTL in the German BMWpop by both seedling infiltration and field testing and compare these with QTL identified in the UK 'NIAB Elite MAGIC' BMWpop, and (2) identify haplotypes and determine additive effects at the prioritized QTL that might help future breeding efforts to combine multiple sources of SNB resistance.

2 Materials and Methods

2.1 Germplasm and genotypic data

The BMWpop and associated genotypic data has previously been described by Stadlmeier et al. (2018). Briefly, the population was developed at the Bavarian State Research Center for Agriculture (LfL) using eight founders (the German varieties Event, Format, BAYP4535, Potenzial, Bussard, Firl3565 and Julius, and Danish variety Ambition), selected based on multiple agronomic and disease resistance traits. The population consists of 394 $F_{6:8}$ recombinant inbred lines (RILs). These, together with the eight founders, were genotyped using a 15K + 5K Infinium iSelect single nucleotide polymorphism (SNP) array, which combined markers from the Illumina

90K wheat SNP chip (Wang et al., 2014) and the 820K Axiom array (Winfield et al., 2016). The resulting genotypic datasets were used by Stadlmeier et al. (2018) to make the BMWpop genetic map consisting of 5435 SNPs. These BMWpop resources were used here for QTL analysis of SNB resistance/sensitivity.

2.2 Field trials

Hillplot trials were conducted for SNB leaf blotch over three seasons (2016, 2017, 2018) at Vollebekk research station in Ås, Norway. The 394 RILs and eight founders were arrayed in incomplete alpha lattice designs where founders and controls [Jenga (relatively high resistace), Arina (moderately resistant) and Tarso (susceptible)] were repeated eight times. Field trials were sown in autumn, established over the winter, and phenotyped the following summer as they progressed to maturity. Naturally *P. nodorum* infected straw harvested from the most susceptible lines in the previous field season were used as inoculum, and was applied to the field trials before stem elongation in the spring. Mist irrigation was applied for 5 min every half hour from 10 am to 8 pm to enhance infection. Mist irrigation started at the same time as the inoculum was applied to the field and ended after the final scoring had been done. The selective fungicide Forbel 750 (Bayer Crop Science, a.i.: phenpropimorph) was applied to the field trials every three weeks at the full recommended dose rate to control infections of stripe rust and powdery mildew. Forbel 750 has little to no effect on *P. nodorum* infection.

2.3 Phenotypic evaluation of leaf blotch severity in the field

Leaf blotch severity was scored via visual estimation of the percentage of diseased leaf area in each hillplot canopy. In 2016 and 2017, leaf blotch severity was assessed three times. The first disease scoring was carried out when the diseased area of the canopy reached 70% for the most susceptible lines/controls, followed by approximately weekly assessments. Due to hot and dry weather, plant development was strongly accelerated in 2018, resulting in disease scoring being undertaken only twice. The first scoring followed the same criteria as described above, while the second scoring was done when the most susceptible lines reached 100 % disease severity. Plant height (PH) and days to heading (DH) were also assessed each year. PH (cm) was measured from ground to bottom of the wheat ears, and DH was scored when most plants within a hillplot had ears fully emerged (Zadoks` growth stage 55, GS55).

2.4 Culture filtrate and Tox3 preparation

P. nodorum isolate 203649 used for culture filtrate infiltration of the BMWpop was the same as described by Lin et al. (2020). It is a Norwegian isolate that does not produce none of the three cloned effectors (ToxA, Tox1 and Tox3) (Lin et al., 2020). Following the methods described by Friesen and Faris (2012), the isolate was grown in liquid Fries 3 medium and after three-weeks stationary growth, the culture filtrates were filter-sterilized. For Tox3 effector production, *SnTox3* was expressed in *Pichia pastoris* as described by Tan et al. (2014)**.** The semi-purified Tox3 effector was desalted in 20 mM sodium phosphate (pH 7.0) and freeze-dried for storage. Prior to use, ultra-pure water was used for re-suspension of Tox3.

2.5 Seedling infiltration

Three to four seeds of each of the BMWpop RILs and the eight founders were sown in cones (Stuewe and sons, Tangent, Orlando, USA) filled with peat soil (Gartnerjord, Tjerbo, Norway). Seedlings were grown in a greenhouse with 16 hours light per day, temperature 20/16 °C (day/night) and 65% relative humidity for 14 days. Approximately 50 µL of the culture filtrate or Tox3 effector were infiltrated into the second leaf of two-week-old seedlings using a 1-mL syringe with needle removed. Reactions to culture filtrate or Tox3 effector were scored seven days after infiltration using a 0 to 3 scale (Friesen and Faris, 2012) where 0 represents completely insensitive, 1 represents mottled chlorosis, 2 represents complete chlorosis and 3 represents necrosis. The experiment was conducted with three biological replicates of each RIL and six to nine biological replicates of the eight founders.

2.6 Statistical analysis

The PROC mixed procedure in SAS v.9.4 (SAS Institute Inc.) was used to calculate mean disease severity, PH and DH of each genotype within each year. For the analysis of the field trials within each year multi-linear regression with PH and DH as covariates was carried out in R Studio Version 1.1.442 (RStudio Team, 2015) to determine whether PH and/or DH affected leaf blotch disease severity. The corrected disease severities were obtained by subtracting the residuals from the linear regression model with PH and/or DH as covariate, when PH and/or DH were

significantly ($p < 0.0001$) correlated with leaf blotch disease severity. Shapiro-Wilk tests were carried out in RStudio to test normality of mean/corrected disease severity.

2.7 QTL analysis

A subset of 2804 SNP markers previously assigned to unique map positions in the BMWpop genetic map (Stadlmeier et al., 2019) were used for interval mapping (IM) and composite interval mapping (CIM). Founder probabilities were calculated using the function 'mpprob' in the R/mpMap package V2.0.2 (Huang and George, 2011) at the threshold of 0.7. Interval mapping was carried out using the function 'mpIM' in R/mpMap with the founder haplotype probabilities obtained from the previous step. CIM was undertaken using either 5 (CIM-cov5) or 10 (CIM-cov10) cofactors. 1000 simulations of the phenotypic dataset were conducted and used to obtain an empirical distribution of genome-wide significance p values based on a null QTL hypothesis. The significance threshold was then determined by the genome-wide significance p value at the threshold level $\alpha < 0.05$, on a QTL by QTL basis. All detected QTL were then fitted in a full model using the function 'fit' to obtain additive founder effects (relative to Julius) and the phenotypic variation (R^2) explained by each QTL. The supporting interval of each QTL was defined as markers with $-\log_{10}(p)$ value ± 0.5 of the peak marker`s -log10(p) value. CIM-cov5 and CIM-cov10 were carried out to further confirm and refine the genetic map locations of the QTL detected by IM. In addition, QTL mapping via identical-by-descent (IBD) analysis was undertaken to support the outcome of IM using all 5435 mapped SNP markers, based on a regression model against the founder haplotype probabilities of each marker. The founder haplotype probabilities were calculated as described above and the additive founder effects were estimated relative to the founder Julius. R/qvalue package was used to correct for multiple testing of IBD with a significant threshold $q = 0.05$. Flanking DNA sequences for SNP markers were obtained from websites https://triticeaetoolbox.org and http://www.cerealsdb.uk.net. Physical map positions of SNP markers in the cv. Chinese Spring wheat reference genome assembly, RefSeq v1.0 (International Wheat Genome Sequencing Consortium et al., 2018), were obtained using BLASTn analysis using the website https://urgi.versailles.inra.fr/blast_iwgsc/?dbgroup=wheat_iwgsc_refseq_v1_chromosomes&program=blastn. Genetic linkage groups overlaid with the positions of QTL intervals were graphically displayed using Mapchart 2.32 (Voorrips, 2002).

2.8 Haplotype analysis for QTL *QSnb.nmbu-2A.1* and *QSnb.nmbu-5A.1*

Five markers within the *QSnb.nmbu-2A.1/2018* QTL interval and with the highest -$\log_{10}$(p) values were selected to construct haplotypes. Six most significant markers located at the overlapping supporting interval of *QSnb.nmbu-5A.1* detected in both 2016 and 2018 were selected to construct haplotypes. As the haplotype effect of *QSnb.nmbu-5A.1* was contributed mainly by allelic differences at marker *wsnp_Ex_c898_1738424*, for this QTL the comparison was based on the allele effect of marker *wsnp_Ex_c898_1738424* alone. The mean disease severities from 2016 and corrected disease severities from 2017 and 2018 for each haplotype in the BMWpop RILs were calculated and compared by Kruskalmc test ($p < 0.05$) using the R/pgirmess package (Giraudoux, 2018). An additional haplotype analysis of QTL *QSnb.nmbu-2A.1/2016* was conducted using the peak marker *BobWhite_c3833_815* and the closely linked marker *AX-94825088* for validating the founder effect of Event.

2.9 Analysis of additive effects

Genotypes possessing either only the susceptible haplotype 4 at *QSnb.nmbu-2A.1/2018* or only the susceptible allele of marker *wsnp_Ex_c898_1738424* at *QSnb.nmbu-5A.1*, were grouped together as carrying one resistant allele. Genotypes that carried both susceptible alleles were grouped as carrying none resistant alleles, while the remaining genotypes were grouped as carrying two resistant alleles. Comparison of disease severities between genotype groups were conducted using the same method as described for haplotype analysis.

3 Results

3.1 Phenotypic evaluation of SNB field resistance

The three varieties used as SNB controls performed as expected, with Tarso, Arina and Jenga showing high, medium and low SNB infection in all trials, respectively (Table S1). Among the eight BMWpop founders, Bussard and Event showed the highest mean leaf blotch disease severity (Figure 1A). Although the differences in disease severity between founders were not significant (data not shown), broad and transgressive variation for leaf blotch severity was observed among BMWpop RILs (Figure 1B). PH was not significantly correlated with leaf blotch severity in any of the three years studied, while DH was significantly correlated with disease

severity in both 2017 ($r = -0.31$, $p < 0.0001$) and 2018 ($r = -0.24$, $p < 0.0001$) (Table 1). The mean leaf blotch severities were all significantly ($p < 0.0001$) correlated between years, with phenotypic correlation coefficients ranging from 0.36 (2017-2018) to 0.47 (2016-2017) (Table 1). As both PH and DH were not significantly correlated with disease severity in 2016, the mean disease severities from 2016 were used directly for both QTL and haplotype analysis, while disease severity data from both 2017 and 2018 were corrected for DH effects. Mean disease severity data from 2016 and corrected disease severity data from both 2017 and 2018 were not normally distributed ($p < 0.0001$), being skewed towards lower disease severity (Figure 1B).

3.2 Phenotypic evaluation of seedling infiltration

Founder reactions to infiltration with culture filtrate of *P. nodorum* isolate 203649 are shown in Figure 2A. Ambition, BAYP4535 and Event were completely insensitive (score 0). Two of the nine replicates tested for Julius showed a weak sensitive reaction (score 1), the remaining seven were completely insensitive (score 0), while Bussard, Firl3565, Format and Potenzial showed higher sensitivity (scores between 1 and 2). However, transgressive segregation was observed in the population (Fig. 2B): 8.4% of the RILs showed a culture filtrate sensitivity score >2, which exceeded the sensitivity range of all eight founders (Fig. 2A). 59.4% of the RILs were insensitive (score < 1), while 32% of RILs showed intermediate reactions (1<score<2) (Fig. 2B).

Infiltration with the *P. nodorum* effector Tox3 found three founders (Bussard, Julius and Potenzial) to be highly sensitive (score 3), while Ambition, Event and Firl3565 were completely insensitive (score 0) (Figure 2A). Two founders showed intermediate reactions, with Format being relatively sensitive (score 2) and BAYP4535 being relatively insensitive with a mean score <1 (Figure 2A). Sixty-four percent of the RILs showed high Tox3 sensitivity (score 3) while 18% of the RILs showed complete insensitivity (Figure 2B). The remaining 18% of the RILs showed intermediate sensitivity (Figure 2B).

3.3 Genetic analysis of SNB resistance/sensitivity

Four significant QTL were detected for field leaf blotch resistance/sensitivity on chromosomes 2A, 2B, 2D and 5A, each explaining between 5 and 7% of the phenotypic variation (Table 2). In this study, one QTL was detected for leaf blotch resistance/susceptibility on

chromosome 2A: *QSnb.nmbu-2A.1/2018* and *QSnb.nmbu-2A.1/2016* (Figure 3A). *QSnb.nmbu-2A.1/2018* was the most significant of the two ($-\log_{10}(p) = 3.4$) and explained 5.4% of the phenotypic variation (peak marker *wsnp_CAP8_c2677_1394934*, located at 146.2 cM on the genetic map and 603.5 Mb on the physical map) (Table 2 and Figure 3A). At this QTL, the Event allele increased the corrected disease severity relative to Julius by 5.4%, while alleles from all but one of the remaining founders all decreased the corrected disease severity by >3% relative to Julius - notably Format and Bussard, with disease reductions of 6.2% and 4.7%, respectively (Fig. 3C). *QSnb.nmbu-2A.1/2016* ($-\log_{10}(p) = 2.8$) was detected on chromosome 2A, at 190 cM (692 Mb), observed in the 2016 trial and explaining 5.2% of the phenotypic variation (Table 2 and Fig. 3A). At *QSnb.nmbu-2A.1/2016*, the allele from the founder Event also contributed the most to susceptibility, which increased the mean disease severity relative to Julius by 9.01%. However, in contrast to *QSnb.nmbu-2A.1/2018*, the Format allele had a relatively high increasing effect on mean disease severity (Fig. 3C). *QSnb.nmbu-2A.1/2018* and *QSnb.nmbu-2A.1/2016* were firstly considered as two distinct QTL since their respective QTL peaks were located approximately 40 cM apart on BMWpop genetic map. However, on the wheat physical map, the *QSnb.nmbu-2A.1/2016* interval was located within that of *QSnb.nmbu-2A.1/2018* (Figure 3B). Additionally, the predicted founder effect of these two QTL were similar, where Event contributed the most to disease susceptibility (Figure 3C). As these QTL are close to the highly non-recombining region (Table 3, Figure 3B), the balance of evidence is not sufficient to state these two QTL are different, and are therefore treated as a single QTL subsequently here. However, further validation is required to further confirm this assumption.

Another robust SNB QTL identified in the BMWpop, *QSnb.nmbu-5A.1* on the long arm of chromosome 5A, was detected in both 2016 and 2018 and explained 6.7% and 5.0% of the phenotypic variation, respectively (Table 2, Figure 4). The founder effects of *QSnb.nmbu-5A.1* were not conclusive for two years (data not shown). *QSnb.nmbu-2B.1* (Figure 4) on the long arm of chromosome 2B ($-\log_{10}(p) = 3.5$, $R^2 = 6.9\%$) and *QSnb.nmbu-2D.1* (Figure 4) on short arm of chromosome 2D ($-\log_{10}(p) = 2.6$, $R^2 = 7.0\%$) were also significant, but only detected in single years (Table 2).

3.4 Genetic analysis of seedling infiltration

Six significant QTL were detected for greenhouse infiltration experiments, on chromosomes 5A, 5B, 6A and 7B. Two QTL were identified for Tox3 infiltration and four via infiltration using culture filtrate from *P. nodorum* isolate 203649. For Tox3 infiltration, *QTox3.nmbu-5B.1* co-located with the major *Snn3-B1* Tox3 sensitivity locus on the short arm of chromosome 5B (p = 0, R^2 = 36%, peak marker *wsnp_JD_rep_c48937_33188230*, located at 3.05 cM/ 14.5 Mb) (Table 2, Figure 4). In addition, another Tox3 sensitivity QTL was detected on the long arm of chromosome 6A (*QTox3.nmbu-6A.1*, -$\log_{10}$(p)= 4, R^2= 5.5) (Table 2). However, *QTox3.nmbu-6A.1*was detected using IM and IBD only, and not via CIM-cov5 or -cov10. The most significant QTL for culture filtrate infiltration with isolate 203649 was located on chromosome 7B (*QInf.nmbu-7B.1*: -log10(p)= 14.9, peak marker *wsnp_Ex_c56425_58548596* at 176.9 cM/683.5 Mb) and accounted for 17.1% of the phenotypic variation (Table 2, Figure 4). Three additional QTL less significant than *QInf.nmbu-7B.1* were also detected for culture filtrate infiltration on chromosomes 5A, 5B and 6A (Table 2).

3.5 Haplotype analysis and additive effects of SNB resistance QTL *QSnb.nmbu-2A.1* and *QSnb.nmbu-5A.1*

Markers used for haplotype construction at *QSnb.nmbu-2A.1/2018* are listed in Table 3. In total, the five SNPs used defined five haplotypes. Consistent significant difference ($p < 0.05$) of mean/corrected disease severity was observed between haplotypes 4 and 5 in all tested years (Figure 5). Haplotype 4 was also always the most susceptible haplotype, with approximately 11% higher disease severity compared to haplotype 5 (Table S2). Haplotype 4 originated from the founder Event while haplotype 5 originated from either Bussard and Format. The same haplotype analysis was undertaken using the phenotypic data from culture filtrate infiltration with isolate 203649, however, no significant difference of disease severity between the *QSnb.nmbu-2A.1/2018* haplotypes was observed (data not shown). For QTL *QSnb.nmbu-5A.1*, the allele effect of marker *wsnp_Ex_c898_1738424* (210.95 cM, 574 Mb) on SNB disease severity was significant ($p < 0.05$) in all tested years (Figure 6). The susceptible allele was inherited from Format, while the remaining founders carry the resistance allele (Figure 6). Additional haplotype analysis of *QSnb.nmbu-2A.1/2016* using two significant markers defined three haplotypes, where the haplotype two originated from the founder Event always showed higher susceptibility. Significant differences between haplotype 1 and 2 ($p < 0.05$) were observed in two out of the three-years tested (Figure

S1). Figure 7 shows the decrease in SNB disease severities by stacking resistant alleles. In all tested years, significant differences in mean/corrected SNB disease severity were observed between genotypes carrying no resistant allele and those carrying 1 or 2 resistant alleles (Figure 7). In addition, significant additive effect of stacking resistant alleles was observed in 2016 (Figure 7A).

4 Discussion

Here, SNB field trials using a German MAGIC population ('BMWpop') were carried out over three seasons from 2016 to 2018 at Vollebekk field station in Ås, Norway, side by side with the trials previously reported for the UK MAGIC population ('NIAB Elite MAGIC') (Lin et al. 2020) The two MAGIC populations were subjected to the same *P. nodorum* field population and similar environmental influences. However, due principally to differences in genetic background, QTL identified in the 'NIAB Elite MAGIC' population may not necessarily be detected in the BMWpop, despite the similar field environments the trials were conducted under. Except for cv. Ambition which originated from a Danish breeding program (Nordic Seed), all BMWpop founders originated from German wheat breeding entities (Stadlmeier et al., 2018), while founders of the 'NIAB Elite MAGIC' were commercially released and grown in the UK (Mackay et al., 2014). In addition, the two MAGIC populations were genotyped using different SNP arrays, with 1335 SNP markers in common for direct comparison of genetic maps. The differences in marker density, RIL numbers and crossing designs between the two populations may also result in differences in power and precision with which to detect QTL. Despite all of these factors, two adult plant SNB resistance/sensitivity QTL were detected in common between the two populations: *QSnb.nmbu-2A.1* and *QSnb.nmbu-2D.1*

The BMWpop 2A QTL *QSnb.nmbu-2A.1* was identified as a robust QTL for SNB leaf blotch susceptibility in the UK MAGIC population across multiple years (*QSnb.niab-2A.3*) (Lin et al. 2020). The *QSnb.nmbu-2A.1/2018* interval overlapped with that of *QSnb.niab-2A.3* and the peak marker of *QSnb.nmbu-2A.1/2018* was just ~2 Mb away from that of *QSnb.niab-2A.3* for 2016 in Norway (Table 3). Haplotype analysis of *QSnb.niab-2A.3* has previously confirmed the robustness of this QTL across years and locations in the 'NIAB Elite MAGIC' population (Lin et al. 2020). Interestingly, haplotype analysis also confirmed the consistent effect of BMWpop QTL

QSnb.nmbu-2A.1/2018 for leaf blotch susceptibility in all three tested years and *QSnb.nmbu-2A.1/2016* for two years (Figure 5, Figure S1). When comparing genetic maps of the two MAGIC populations, two common markers *BS00090569_51* and *RAC875_c38018_278* were found within the supporting intervals of both *QSnb.niab-2A.3* and *QSnb.nmbu-2A.1/2018*. Both markers were among the most significant markers detected for *QSnb.nmbu-2A.1/2018* and were used for constructing *QSnb.nmbu-2A.1/2018* haplotypes. *QSnb.nmbu-2A.1/2018* haplotype 4 and *QSnb.nmbu-2A.1/2016* haplotype 2, which were inherited from the founder Event, showed significantly higher disease severity (Figure 5, Figure S1). This observation also fitted the predicted founder effects at this QTL with Event contributing the most to leaf blotch susceptibility (Figure 3C). Therefore, we hypothesize that the susceptible haplotype from founders Xi19 and Rialto in 'NIAB Elite MAGIC' population and the susceptible haplotype from Event in the BMWpop may carry the same susceptibility allele. However, while pedigree analysis shows that Xi-19 was a result of a cross between Rialto and Cadenza, no pedigree information for Event could be identified to confirm possible common allelic origin. Moreover, one flanking marker for the seedling resistance/sensitivity QTL *QSnb.cur-2AS.1* reported by Phan et al. (2016) also aligned to the interval defined by *QSnb.nmbu-2A.1* (Table 3). However, since the QTL on 2A in our study was located within the large physical interval defined by *QSnb.cur-2AS.1* (from 112 to 709 Mb) (Phan et al., 2016), further meaningful comparison is not possible.

In the BMWpop, *QSnb.nmbu-5A.1* on chromosome 5A was the second QTL which was significant in more than one year. On the physical map, previously published QTL for seedling and adult plant resistance co-locate with this QTL (Friesen et al., 2009; Liu et al., 2015) (as detailed in Table S3). In addition, the allele effect using marker *wsnp_Ex_c898_1738424* was significant for all tested years in our study, where only the founder Format carries the susceptibility allele (Figure 6). Given the discriminatory nature of this SNP in our eight founders, these results highlight the potential of this marker for application in marker assisted selection. SNB resistance QTL have previously been reported on chromosome 5A. The best characterized of these is located at 582.6-583.3 Mb on the long arm of chromosome 5A, and is associated with seedling resistance to both tan spot and SNB in two mapping populations (Hu et al. 2019). However, this QTL does not overlap with the supporting interval of our *QSnb.nmbu-5A.1* (558.7-571.7 Mb), indicating these two QTL are different. The BMWpop QTL *QSnb.nmbu-2D.1* (14.6-15.1 Mb) detected in

2016 co-located with the 'NIAB Elite MAGIC' QTL *QSnb.niab-2D.1* (14.8-27.8 Mb), reported by Lin et al. (2020) to be located near the well characterized Tox2 sensitivity locus *Snn2* (6.2-12.4 Mb) (Zhang et al., 2009) and *QSnb.cur-2DS* (14.3-37.0 Mb) (Phan et al., 2016) (Table S4).

QSnb.niab-2A.3 was detected by culture filtrate infiltration with isolate 203649 in the 'NIAB Elite MAGIC' population, with the same haplotype effect for this QTL observed for field resistance and sensitivity to infiltration and inoculation with isolate 203649 (Lin et al. 2020). This is the same isolate as used here for CF infiltration using the BMWpop. However, no CF QTL on chromosome 2A were identified. Rather, culture filtrate infiltration of isolate 203649 in the BMWpop identified QTL on chromosomes 5A, 5B and 7B. Interestingly, the 'weak' 'NIAB Elite MAGIC' QTL *QSnb.niab-7B.2* ($-\log_{10}(p) = 2.91$, $R^2 = 5.83$ %) was detected as a major BMWpop QTL for culture filtrate infiltration (*QInf.nmbu-7B.1*: $-\log_{10}(p) = 14.9$, $R^2 = 17.1$%). The QTL interval of *QInf.nmbu-7B.1* is located within that of *QSnb.niab-7B.2* on the physical map, and their peak markers were located 4 Mb apart (Table S5). Phan et al. (2016) found that *SnTox3* expression levels were increased when the *SnTox1* gene was knocked out in *P. nodorum* isolate SN15, indicating that *SnTox3* expression was suppressed by Tox1. It is possible that the expression of the uncharacterized *P. nodorum* effector which interacted with the *QInf.nmbu-7B.1* locus in this experiment may have suppressed the expression of the uncharacterized effector which has been previously shown via culture filtrate inoculation in the UK MAGIC population to interact with the *QSnb.niab-2A.3* locus (Lin et al. 2020). Recently Peters Haugrud et al. (2019) also reported that effects caused by the NE-host inverse gene for gene interactions varied from epistatic to additive and depended on the genetic backgrounds of both host and pathogen. Therefore, the different genetic background of the host populations might result in the phenomenon where *QSnb.niab-2A.3* was detected in 'NIAB Elite MAGIC' via culture filtrate infiltration but not in the BMWpop, despite infiltration with culture filtrate using the same isolate. In addition, the expression level of the uncharacterized NE which interacted with *QSnb.niab-2A.3* in 'NIAB Elite MAGIC' might be low, thus the detection of this interaction could be masked by the interaction of *QInf.nmbu-7B.1* and the other uncharacterized NE. Similar to CF infiltration results, even though BMWpop segregates for the *Snn3-B1* locus and the *SnTox3* gene is common in the Norwegian *P. nodorum* population (Ruud et al., 2018), the *Snn3-B1* QTL was not detected in our field testing. This observation could be explained by a hypothesis proposed by Peters Haugrud et al. (2019) where *P. nodorum* isolates might not express all of the NE genes they harbor. Alternatively, an epistatic

effect may exist between unknown NE-*Snn* and Tox3-*Snn3-B1* interactions in the field condition. Clearly the situation is relatively complex, and further studies are required to disentangle *P. nodorum* effector-wheat susceptibility interactions as well as *P. nodorum* effector-effector interactions in order to determine which SNB QTL are dependent on host-NE interactions.

Adult plant SNB resistance QTL on chromosomes 2A and 2D, and seedling infiltration QTL on chromosome 7B previously identified in the UK 'NIAB Elite MAGIC' population were validated in the German eight-parent BMWpop winter wheat MAGIC population. In the BMWpop, both haplotype effect at *QSnb.nmbu-2A.1* and allele effect at *QSnb.nmbu-5A.1* were significantly associated with field SNB susceptibility and was significant across years, highlighting the robustness of these QTL. In addition, significant differences in SNB disease severity detected in 2016 between genotype groups showed evidence that the effect of these two field-relevant QTL were additive. As SNB resistance in the field is a complicated quantitative trait, validating field resistance QTL using an independent mapping panel provides robust evidence of the efficacy of target QTL in diverse genetic backgrounds. This knowledge should underpin efficient selection for beneficial SNB resistance alleles across multiple loci in wheat breeding programs, and will assist further research towards the identification of the functional allele(s) underlying these genetic loci.

5 Conflict of Interest

The authors declare that the research was conducted in the absence of any commercial or financial relationships that could be construed as a potential conflict of interest.

6 Author Contributions

MIL carried out glasshouse, field phenotyping and genetic analyses.VM provided the plant material. MS and VM developed the genetic analysis pipeline and helped with genetic analyses. JC and MOL gained project funding. KC supplied Tox3 effector. AF, JC and MOL supervised the research. MIL drafted the manuscript. All authors revised and approved the manuscript.

7 Funding

The research was undertaken within the 'Efectawheat' project supported within the framework of the 2nd call ERA-NET for Coordinating Plant Sciences, with funding to MIL from The Research Council of Norway grant NFR251894, to JC from Biotechnology and Biological Sciences Research Council (BBSRC) grant BB/N00518X/1, to MS from the Deutsche Forschungsgemeinschaft (DFG, HA 5798/2-1) and to KT from Grains Research and Development Corporation grant CUR00023.

8 Acknowledgments

We thank Cecilie Yri and Yalew Tarkegne (NMBU) for help with field phenotyping, Prof. Richard Oliver (CCDM) and Dr. Huyen Phan (CCDM) for supplying the Tox3 effector, and Beatrice Corsi and Keith Gardner (NIAB) for help with QTL mapping training.

Table 1 Pearson correlation coefficients for leaf blotch disease severity, days to heading (DH) and plant height (PH) in the 2016, 2017 and 2018 season trials.

	PH	DH	2016 leaf blotch	2017 leaf blotch
2016 leaf blotch	-0.08	-0.05		
2017 leaf blotch	-0.09	-0.31***	0.47***	
2018 leaf blotch	-0.07	-0.24***	0.37***	0.36***

*** <0.0001

Table 2 *P. nodorum* resistance/sensitivity QTL identified in the BMWpop MAGIC population from field trials at the adult plant stage, as well as from culture filtrate infiltration and Tox3 infiltration at the seedling stage. Reference indicates previously published QTL predicted to co-locate with the BMWpop QTL identified. Chromosome (Chr.), proportion of the variance explained by QTL (R^2). The $-\log_{10}$(p) value for *Snn3-B1* is recorded as 'Inf', as the p-value was 0, resulting in an error when converted to the $\log_{10}$ scale.

QTL	Reference	Trait	Year	Chr	Interval (cM)	Flanking markers	Peak Marker	$-\log_{10}$(p)	IWGSC RefSeq v1.0 start (bp)	IWGSC RefSeq v1.0 end (bp)	R^2 (%)	Methods used to detect QTL
QSnb.nmbu-2A.1		Leaf blotch	2018	2A	130.88-149.29	Kukri_c11327_977 and Tdurum_contig33398_106	wsnp_CAP8_c2677_13949 34	3.4	507691472	718885511	5.4	IM, CIM (cov5, cov10), IBD
QSnb.nmbu-2A.1		Leaf blotch	2016	2A	185.46-190.00	AX-94525393 and BobWhite_c3833_815	BobWhite_c3833_815	2.8	688619335	693294681	5.2	IM, CIM (cov5), IBD
QSnb.nmbu-2B.1		Leaf blotch	2017	2B	191.41-207.19	Excalibur_rep_c66577_159 and AX-94522698	Ra_c71978_532	3.5	572591268	648083739	6.9	IM, IBD
QSnb.nmbu-2D.1	Phan et al., 2016; Lin et al., 2020	Leaf blotch	2016	2D	11.22-14.26	D_F1BEJMU01A0OMY_356 and BS00067698_51	BS00071755_51	2.6	14636197	15115231	7.0	IM, CIM (cov5, cov10), IBD
QInf.nmbu-5A.1		Infil_203649		5A	44.98-59.90	BS00040623_51 and BobWhite_rep_c64913_315	BS00040623_51	3.4	391548987	413418597	6.2	IM, CIM (cov5, cov10), IBD
QSnb.nmbu-5A.1	Friesen et al., 2009; Liu et al., 2015	Leaf blotch	2016	5A	205.90-220.61	Excalibur_c472_914 and Tdurum_contig54785_216	Excalibur_c33923_592	3.0	558692780	568272320	6.7	IM, CIM (cov5, cov10), IBD
QSnb.nmbu-5A.1	Friesen et al., 2009; Liu et al., 2015	Leaf blotch	2018	5A	207.91-220.61	Tdurum_contig44343_1039 and Tdurum_contig54785_216	RAC875_c25339_200	3.1	558692880	571683217	5.0	IM, CIM (cov5, cov10)
QTox3.nmbu-5B.1	Friesen et al., 2009; Downie et al., 2018;	Infil_Tox3		5B	0-4.55	wsnp_Ku_c5308_9450093 and wsnp_Ex_c2459_4591587	wsnp_JD_rep_c48937_33188230	Inf	12324613	16421984	36.0	IM, CIM (cov5), IBD

	Lin et al., 2020										
QInf.nmbu-5B.1		Infil_203649	5B	100.27 - 104.80	BobWhite_c7070_196 and BobWhite_rep_c50822_462	BobWhite_c7070_196	3.8	508795354	516041245	6.0	IM, CIM (cov5, cov10), IBD
QInf.nmbu.6A.1		Infil_203649	6A	6.72-19.59	wsnp_Ex_c21633_30782312 and RAC875_c6135_95	Kukri_c7146_870	3.0	796322	2402510	6.9	IM, CIM (cov5, cov10), IBD
QTox3.nmbu.6A. 1		Infil_Tox3	6A	171.15 - 174.69	wsnp_RFL_Contig1871_1020122 and IAAV151	wsnp_Ku_c3450_6387847	4.0	545832350	574479996	5.5	IM, IBD
QInf.nmbu.7B.1	Lin et al., 2020	Infil_203649	7B	169.77 - 179.91	GENE.4442_121 and BS00057323_51	wsnp_Ex_c56425_58548596	14.9	679800093	700551772	17.1	IM, CIM (cov5, cov10), IBD

Table 3 Overview of published QTL identified for SNB in the *QSnb.nmbu-2A.1* region, based on positions on the wheat reference genome assembly (RefSeq v1.0; IWGSC, 2018). Markers used for constructing *QSnb.nmbu-2A.1/2018* haplotypes are shown bold, while markers used for constructing *QSnb.niab-2A.3* haplotypes are underlined. N: Norway, U: UK, LB: leaf blotch, GB: glume blotch, left: left flanking marker of the QTL, right: right flanking marker of QTL, peak: peak marker of QTL. †Stadlmeier et al. (2018). ‡IWGSC (2018).

Marker ID	Population	Genetic map position (cM) †	Physical map position start (bp)‡	Physical map position end (bp) ‡	P value	Source	QTL name
Kukri_c11327_977	BMWpop	130.88	507691472	507691373	1.42E-03	This study/2018_left	*QSnb.nmbu.2A.1*
BS00055514_51	NIAB Elite MAGIC		543625444	543625544		2014NLB-peak/ (Lin. et al, 2019)	*QSnb.niab-2A.3*
wsnp_CAP8_c2677_1394934	BMWpop	**146.20**	**603524403**	**603524602**	**1.60E-04**	This study/**2018_peak**	*QSnb.nmbu-2A.1*
Ku_c5710_312	NIAB Elite MAGIC		605800158	605800259		2016NLB-peak/ (Lin. et al, 2019)	*QSnb.niab-2A.3*
BS00062679_51	NIAB Elite MAGIC		615287656	615287757		2016NGB-peak/ (Lin. et al, 2019)	*QSnb.niab-2A.3*
RAC875_c9372_94	NIAB Elite MAGIC		635606922	635606992		2017ULB/2018NLB-peak/ (Lin. et al, 2019)	*QSnb.niab-2A.3*
AX-95661975	BMWpop	**134.98**	**639695197**	**639695127**	**3.59E-04**	This study	*QSnb.nmbu-2A.1*
RAC875_c38018_278	BMWpop	**144.67**	**639988422**	**639988522**	**3.47E-04**	This study	*QSnb.nmbu-2A.1*
AX-94508462	BMWpop	**143.15**	**652336037**	**652335967**	**4.27E-04**	This study	*QSnb.nmbu-2A.1*
BS00090569_51	BMWpop	**136.50**	**653680962**	**653680862**	**2.43E-04**	This study	*QSnb.nmbu-2A.1*
BS00010696_51	BMWpop	183.94	688619335	688619436	7.99E-04	This study/2016_left	*QSnb.nmbu-2A.1*
BobWhite_c3833_815	BMWpop	190.00	692850215	692850316	1.80E-04	This study/2016 right_Peak	*QSnb.nmbu-2A.1*
gwm312	Calingiri × Wyalkatchem		709048504	709048682		Phan et al., 2016	*QSnb.cur-2AS1*
Tdurum_contig33398_106	BMWpop	149.29	718885411	718885511	7.52E-04	This study/2018_right	*QSnb.nmbu-2A.1*

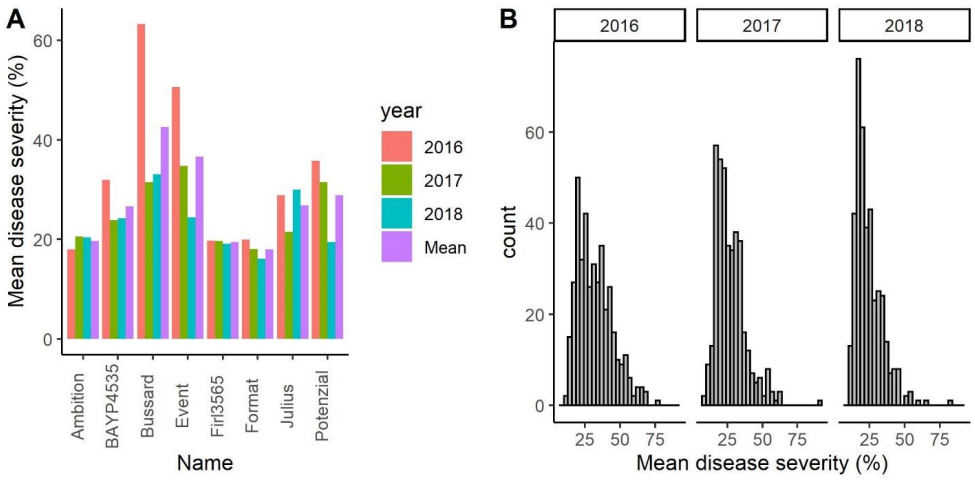

Figure 1. *P. nodorum* leaf blotch phenotypes for BMWpop trials at Ås, Norway, during seasons 2016, 2017 and 2018. (A) Mean leaf blotch disease severity of BMWpop founders, (B) Histograms of disease severity of BMWpop RILs in different years.

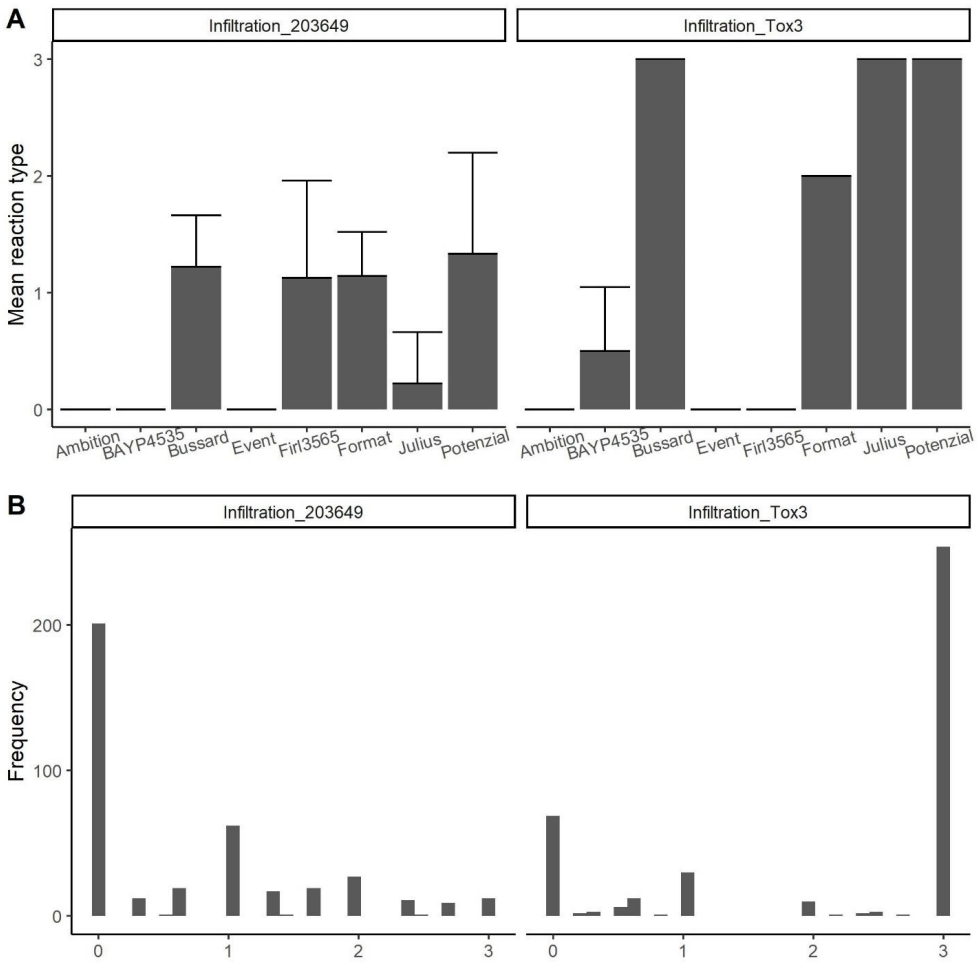

Figure 2 (A) Reactions of BMWpop founders to infiltration with culture filtrates of *P. nodorum* isolate 203649 (left) and Tox3 effector (right). Error bars indicate the standard deviation of mean reaction type for each parent. 9 replicates were used for infiltration with isolate 203649 while 6 replicates were used for infiltration with Tox3. (B) Histogram of the reactions of BMWpop RILs to infiltration with culture filtrates of *P. nodorum* isolate 203649 (left) and Tox3 effector (right).

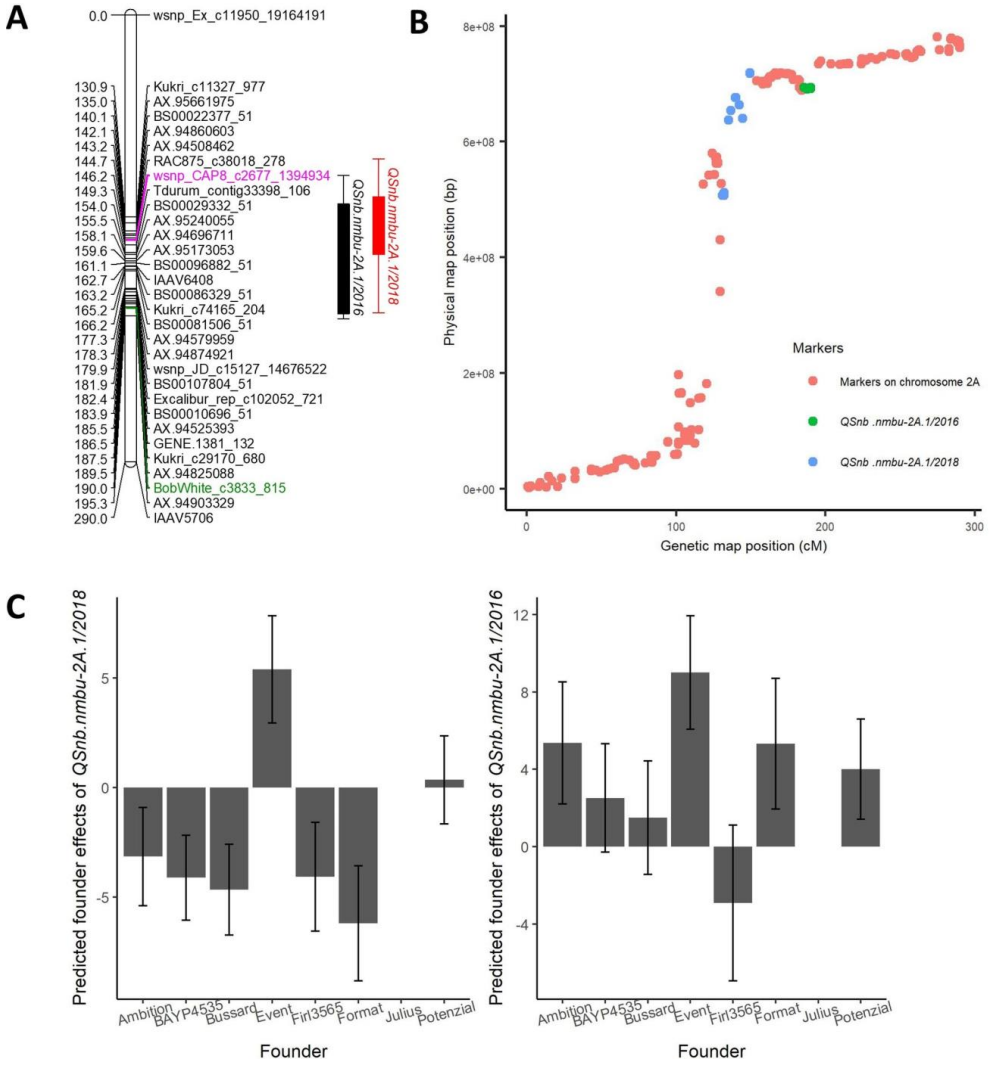

Figure 3 Summary information for leaf blotch QTL identified for leaf blotch on chromosome 2A in the BMWpop population. (A) Results of QTL scan using interval mapping (IM). Peak marker QTL detected in 2018 is indicated in pink, while QTL detected in 2016 is indicated in green. (B) Plot of the genetic (Stadlmeier et al. 2018) versus physical map position (IWGSC RefSeq v1.0) of SNPs mapped to chromosome 2A in the BMWpop. Markers within the support interval of *QSnb.nmbu-2A.1/2016* and *QSnb.nmbu-2A.1/2018* are indicated in green and blue, respectively. (C) Predicted founder effects for *QSnb.nmbu-2A.1/2016* and *QSnb.nmbu-2A.1/2018*, relative to the founder Julius. Error bars indicate the standard error of the estimated founder effects.

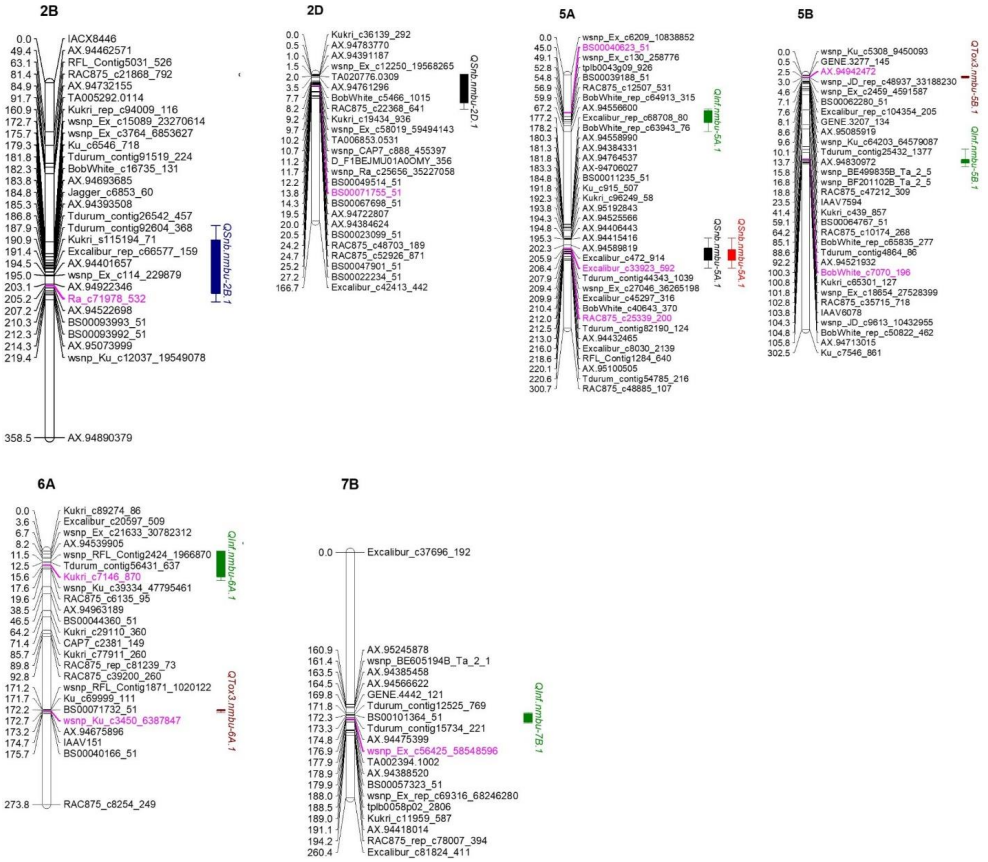

Figure. 4 SNB QTL identified on chromosomes 2B, 2D, 5A, 5B, 6A and 7B. Results of IM are shown. QTL and permutated thresholds ($-\log_{10}(p)$) are colored by trait; field season 2016: black, field season 2017: blue, field season 2018: red, Culture filtrate infiltration of isolate 203649: green, Infiltration of Tox3: brown. Peak markers are indicated in pink.

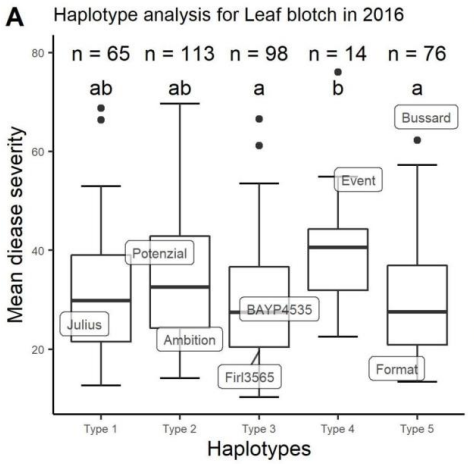

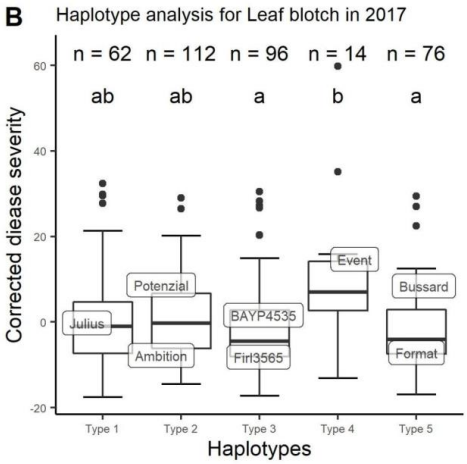

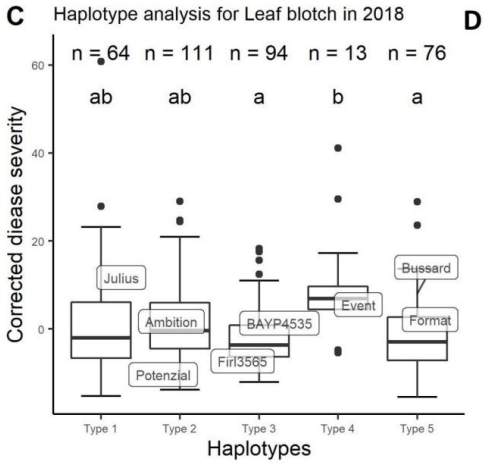

D

Haplotype	Parents	SNP1	SNP2	SNP3	SNP4	SNP5
Type1	Julius	0	0	0	0	2
Type2	Potenzial/ Ambition	0	0	2	2	0
Type3	BAYP4535/ Firl3565	0	2	0	0	0
Type4	Event	2	0	0	0	0
Type5	Bussard/ Format	2	0	0	0	2

Figure 5 Haplotype analysis for BMWpop leaf blotch QTL *QSnb.nmbu-2A.1/2018*. (A) Haplotype analysis of mean disease severity in field season 2016. (B-C) Haplotype analysis of corrected disease severity in field season 2017 and 2018 respectively and the mean disease ratings for the 8 founders are indicated. Haplotypes labeled with same letter represented no significant differences between haplotype disease severities asdetected by Kruskalmc test ($p < 0.05$). (D) Genotype of each haplotype based on five SNP markers. SNP marker names are listed in order as below: *wsnp_CAP8_c2677_1394934, AX-95661975, RAC875_c38018_278, AX-94508462, BS00090569_51*.

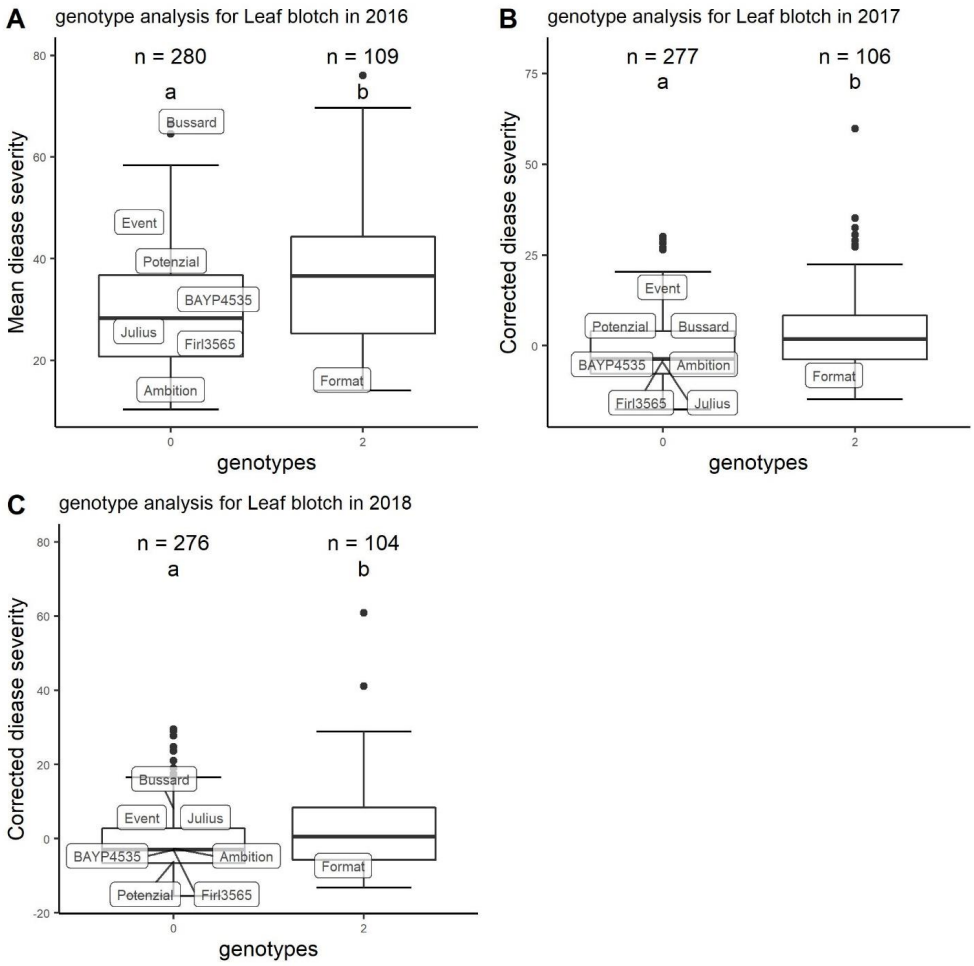

Figure 6 Allele effect analysis of marker *wsnp_Ex_c898_1738424* for BMWpop SNB QTL *QSnb.nmbu-5A.1*. (A) Allele effect of mean disease severity in field season 2016. (B-C) Allele effect of corrected disease severity in field season 2017 and 2018, respectively, and the mean disease ratings for the eight founders are indicated. Genotypes labeled with same letter represented no significant differences between haplotype disease severities as detected by Kruskalmc test ($p < 0.05$).

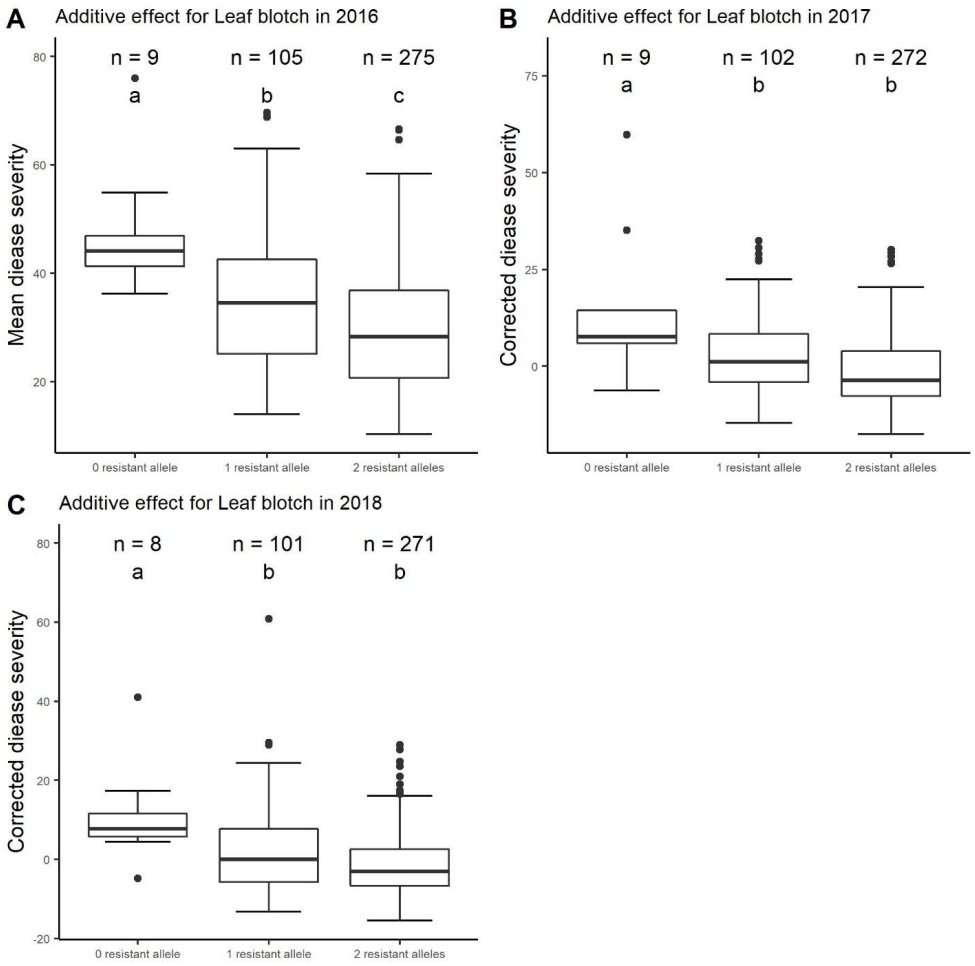

Figure 7 Analysis of additive effects for QTL *QSnb.nmbu-2A.1/2018* and *QSnb.nmbu-5A.1*. (A) Additive effect analysis of mean disease severity in field season 2016. (B-C) Additive effect analysis of corrected disease severity in field season 2017 and 2018 respectively. Genotypes labeled with same letter represented no significant differences between haplotype disease severities as detected by Kruskalmc test ($p < 0.05$).

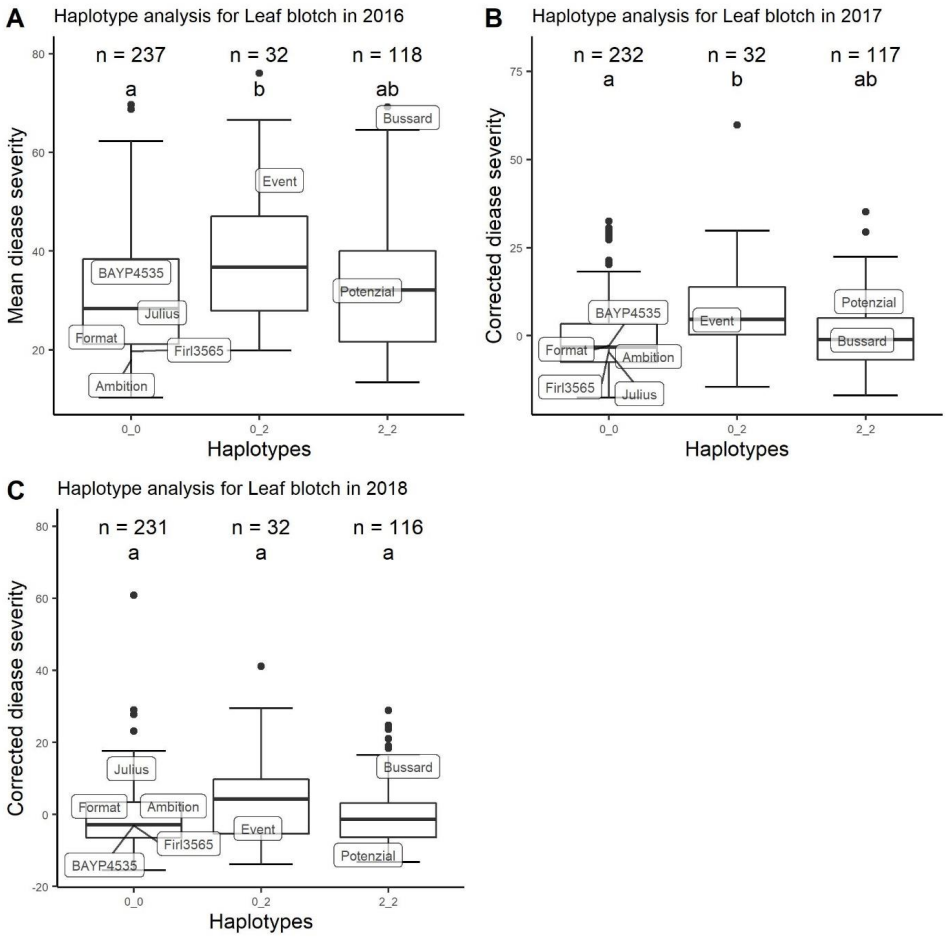

Figure S1 Haplotype analysis for BMWpop leaf blotch QTL *QSnb.nmbu-2A.1/2016*. (A) Haplotype effect of mean disease severity in field season 2016. (B-C) Haplotype effect of corrected disease severity in field season 2017 and 2018, respectively, and the mean disease ratings for the eight founders are indicated. Haplotypes labeled with same letter represented no significant differences between haplotype disease severities as detected by Kruskalmc test ($p < 0.05$).

References

Bhathal, J.S., Loughman, R., and Speijers, J. (2003). Yield reduction in wheat in relation to leaf disease from yellow (tan) spot and septoria nodorum blotch. *Eur J Plant Pathol* 109(5)**,** 435-443. doi: 10.1023/A:1024277420773.

Cockram, J., and Mackay, I. (2018). Genetic Mapping Populations for Conducting High-Resolution Trait Mapping in Plants. *Adv Biochem Eng Biotechnol* 164**,** 109-138. doi: 10.1007/10_2017_48.

Cockram, J., Scuderi, A., Barber, T., Furuki, E., Gardner, K.A., Gosman, N., et al. (2015). Fine-mapping the wheat *Snn1* Locus conferring sensitivity to the *Parastagonospora nodorum* necrotrophic effector SnTox1 using an eight founder Multiparent Advanced Generation Inter-Cross population. *G3 (Bethesda)* 5(11)**,** 2257-2266. doi: 10.1534/g3.115.021584.

Corsi B, Percival-Alwyn L, Downie RC, Venturini L, Iagallo EM, Mantello CC, McCormick-Barnes C, See PT, Oliver RP, Moffat CS, Cockram J (2020). Genetic analysis of wheat sensitivity to the ToxB fungal effector from Pyrenophora tritici-repentis, the causal agent of tan spot. *Theoretical and Applied Genetics,(in press)*

Downie, R.C., Bouvet, L., Furuki, E., Gosman, N., Gardner, K.A., Mackay, I.J., et al. (2018). Assessing european wheat sensitivities to *Parastagonospora nodorum* necrotrophic effectors and fine-mapping the *Snn3-B1* locus conferring sensitivity to the effector SnTox3. *Front Plant Sci* 9**,** 881. doi: 10.3389/fpls.2018.00881.

Duba, A., Goriewa-Duba, K., and Wachowska, U. (2018). A review of the interactions between wheat and wheat pathogens: *Zymoseptoria tritici*, *Fusarium* spp. and *Parastagonospora nodorum*. *Int J Mol Sci* 19(4). doi: https://doi.org/10.3390/ijms19041138.

Faris, J.D., Zhang, Z., Lu, H., Lu, S., Reddy, L., Cloutier, S., et al. (2010). A unique wheat disease resistance-like gene governs effector-triggered susceptibility to necrotrophic pathogens. *Proc Natl Acad Sci U S A* 107(30)**,** 13544-13549. doi: 10.1073/pnas.1004090107.

Ficke, A., Cowger, C., Bergstrom, G., and Brodal, G. (2018). Understanding yield loss and pathogen biology to improve disease management: Septoria nodorum blotch - a case study in wheat. *Plant Dis* 102(4)**,** 696-707. doi: 10.1094/PDIS-09-17-1375-FE.

Food and Agriculture Organization of the United Nations (2016). *FAOSTAT* [Online]. Available: http://www.fao.org/faostat/en/#home [Accessed 03/08 2019].

Francki, M.G. (2013). Improving *Stagonospora nodorum* Resistance in Wheat: A Review. *Crop Science* 53(2)**,** 355-365. doi: 10.2135/cropsci2012.06.0347.

Friesen, T.L., Chu, C.G., Liu, Z.H., Xu, S.S., Halley, S., and Faris, J.D. (2009). Host-selective toxins produced by *Stagonospora nodorum* confer disease susceptibility in adult wheat plants under field conditions. *Theor Appl Genet* 118(8)**,** 1489-1497. doi: 10.1007/s00122-009-0997-2.

Friesen, T.L., and Faris, J.D. (2012). "Characterization of Plant-Fungal Interactions Involving Necrotrophic Effector-Producing Plant Pathogens," in *Plant Fungal Pathogens: Methods and Protocols*, eds. M.D. Bolton & B.P.H.J. Thomma. (Totowa, NJ: Humana Press), 191-207.

Friesen, T.L., Meinhardt, S.W., and Faris, J.D. (2007). The *Stagonospora nodorum*-wheat pathosystem involves multiple proteinaceous host-selective toxins and corresponding host sensitivity genes that interact in an inverse gene-for-gene manner. *Plant J* 51(4)**,** 681-692. doi: 10.1111/j.1365-313X.2007.03166.x.

Giraudoux, P. (2018). "pgirmess: Spatial Analysis and Data Mining for Field Ecologists. R package version 1.6.9. https://CRAN.R-project.org/package=pgirmess".).

Hu, W., He, X., Dreisigacker, S., Sansaloni, C.P., Juliana, P., and Singh, P.K. (2019). A wheat chromosome 5AL region confers seedling resistance to both tan spot and Septoria nodorum blotch in two mapping populations. *The Crop J* doi: 10.1016/j.cj.2019.05.004.

Holloman, D.W. (2015). Fungicide Resistance: 40 Years on and Still a Major Problem, in *Fungicide resistance in plant pathogens*, eds. Ishii, H. and Holloman, DW. . (Springer, Japan), 3-11.Huang, B.E., and George, A.W. (2011). R/mpMap: a computational platform for the genetic analysis of multiparent recombinant inbred lines. *Bioinformatics* 27(5)**,** 727-729. doi: 10.1093/bioinformatics/btq719.

International Wheat Genome Sequencing, C., investigators, I.R.p., Appels, R., Eversole, K., Feuillet, C., Keller, B., et al. (2018). Shifting the limits in wheat research and breeding using a fully annotated reference genome. *Science* 361(6403). doi: 10.1126/science.aar7191.

Lin M, Corsi B, Ficke A, Tan K-C, Cockram J, Lilemo M (2020). Genetic mapping using a wheat multi-founder population reveals a locus on chromosome 2A controlling resistance to both leaf and glume blotch caused by the necrotrophic fungal pathogen *Parastagonospora nodorum*. *Theor Appl Genet* (in press)

Liu, Z., El-Basyoni, I., Kariyawasam, G., Zhang, G., Fritz, A., Hansen, J., et al. (2015). Evaluation and association mapping of resistance to Tan Spot and Stagonospora Nodorum Blotch in adapted winter wheat fermplasm. *Plant Dis* 99(10)**,** 1333-1341. doi: 10.1094/PDIS-11-14-1131-RE.

Liu, Z., Faris, J.D., Oliver, R.P., Tan, K.C., Solomon, P.S., McDonald, M.C., et al. (2009). SnTox3 acts in effector triggered susceptibility to induce disease on wheat carrying the *Snn3* gene. *PLoS Pathog* 5(9)**,** e1000581. doi: 10.1371/journal.ppat.1000581.

Liu, Z., Friesen, T.L., Ling, H., Meinhardt, S.W., Oliver, R.P., Rasmussen, J.B., et al. (2006). The *Tsn1*–ToxA interaction in the wheat–*Stagonospora nodorum* pathosystem parallels that of the wheat–tan spot system. *Genome* 49(10)**,** 1265-1273.

Liu, Z., Zhang, Z., Faris, J.D., Oliver, R.P., Syme, R., McDonald, M.C., et al. (2012). The cysteine rich necrotrophic effector SnTox1 produced by *Stagonospora nodorum* triggers susceptibility of wheat lines harboring *Snn1*. *PLoS Pathog* 8(1)**,** e1002467. doi: 10.1371/journal.ppat.1002467.

Mackay, I.J., Bansept-Basler, P., Barber, T., Bentley, A.R., Cockram, J., Gosman, N., et al. (2014). An eight-parent multiparent advanced generation inter-cross population for winter-sown wheat: creation, properties, and validation. *G3 (Bethesda)* 4(9)**,** 1603-1610. doi: 10.1534/g3.114.012963.

Oliver, R.P., Friesen, T.L., Faris, J.D., and Solomon, P.S. (2012). *Stagonospora nodorum*: from pathology to genomics and host resistance. *Annu Rev Phytopathol* 50**,** 23-43. doi: 10.1146/annurev-phyto-081211-173019.

Peters Haugrud, A.R., Zhang, Z., Richards, J.K., Friesen, T.L., and Faris, J.D. (2019). Genetics of variable disease expression conferred by inverse gene-for-gene interactions in the wheat-*Parastagonospora nodorum* pathosystem. *Plant Physiol* 180(1)**,** 420-434. doi: 10.1104/pp.19.00149.

Phan, H.T., Rybak, K., Furuki, E., Breen, S., Solomon, P.S., Oliver, R.P., et al. (2016). Differential effector gene expression underpins epistasis in a plant fungal disease. *Plant J* 87(4)**,** 343-354. doi: 10.1111/tpj.13203.

RStudio Team (2015). "RStudio: Integrated Development for R. RStudio, Inc., Boston, MA URL http://www.rstudio.com/.").

Ruud, A.K., Dieseth, J.A., and Lillemo, M. (2018). Effects of Three Parastagonospora nodorum Necrotrophic Effectors on Spring Wheat under Norwegian Field Conditions. *Crop Science* 58(1)**,** 159-168. doi: 10.2135/cropsci2017.05.0281.

Ruud, A.K., and Lillemo, M. (2018). "Diseases affecting wheat: Septoria nodorum blotch," in *Integrated disease management of wheat and barley*. (Cambridge, UK: Burleigh Dodds Science Publishing Limited), 109-144.

Ruud, A.K., Windju, S., Belova, T., Friesen, T.L., and Lillemo, M. (2017). Mapping of SnTox3-*Snn3* as a major determinant of field susceptibility to Septoria nodorum leaf blotch in the SHA3/CBRD x Naxos population. *Theor Appl Genet* 130(7)**,** 1361-1374. doi: 10.1007/s00122-017-2893-5.

Shi, G., Zhang, Z., Friesen, T.L., Raats, D., Fahima, T., Brueggeman, R.S., et al. (2016). The hijacking of a receptor kinase-driven pathway by a wheat fungal pathogen leads to disease. *Sci Adv* 2(10)**,** e1600822. doi: 10.1126/sciadv.1600822.

Stadlmeier, M., Hartl, L., and Mohler, V. (2018). Usefulness of a multiparent advanced generation intercross population with a greatly reduced mating design for genetic studies in winter wheat. *Front Plant Sci* 9**,** 1825.

Stadlmeier, M., Jorgensen, L.N., Corsi, B., Cockram, J., Hartl, L., and Mohler, V. (2019). Genetic dissection of resistance to the three fungal plant pathogens *Blumeria graminis*, *Zymoseptoria tritici*, and *Pyrenophora tritici-repentis* using a multiparental winter wheat population. *G3 (Bethesda)* 9(5)**,** 1745-1757. doi: 10.1534/g3.119.400068.

Tan, K.C., Waters, O.D.C., Rybak, K., Antoni, E., Furuki, E., and Oliver, R.P. (2014). Sensitivity to three *Parastagonospora nodorum* necrotrophic effectors in current Australian wheat cultivars and the presence of further fungal effectors. *Crop Pasture Sci* 65(2)**,** 150-158. doi: 10.1071/Cp13443.

Trainor, G., Zaicou-Kunesch, C., Curry, J., Shackley, B. and Nicol, D. (2018). 2019 Wheat variety sowing guide for Western Australia. Department of Primary Industries and Regional Development, Perth, Bulletin 4894. Pages 52.

Vleeshouwers, V.G., and Oliver, R.P. (2014). Effectors as tools in disease resistance breeding against biotrophic, hemibiotrophic, and necrotrophic plant pathogens. *Mol Plant Microbe Interact* 27(3)**,** 196-206. doi: 10.1094/MPMI-10-13-0313-IA.

Voorrips, R.E. (2002). MapChart: software for the graphical presentation of linkage maps and QTLs. *J Hered* 93(1)**,** 77-78. doi: 10.1093/jhered/93.1.77

Wang, S., Wong, D., Forrest, K., Allen, A., Chao, S., Huang, B.E., et al. (2014). Characterization of polyploid wheat genomic diversity using a high-density 90,000 single nucleotide polymorphism array. *Plant Biotechnol J* 12(6)**,** 787-796. doi: 10.1111/pbi.12183.

Wei, J., and Xu, S. (2016). A random-model approach to QTL mapping in multiparent advanced generation intercross (MAGIC) populations. *Genetics* 202(2)**,** 471-486. doi: 10.1534/genetics.115.179945.

Winfield, M.O., Allen, A.M., Burridge, A.J., Barker, G.L., Benbow, H.R., Wilkinson, P.A., et al. (2016). High-density SNP genotyping array for hexaploid wheat and its secondary and tertiary gene pool. *Plant Biotechnol J* 14(5)**,** 1195-1206. doi: 10.1111/pbi.12485.

Zhang, Z.C., Friesen, T.L., Simons, K.J., Xu, S.S., and Faris, J.D. (2009). Development, identification, and validation of markers for marker-assisted selection against the *Stagonospora nodorum* toxin sensitivity genes *Tsn1* and *Snn2* in wheat. *Mol Breed* 23(1)**,** 35-49. doi: 10.1007/s11032-008-9211-5.

Table S1 Average of SNB disease severities (%) of control varieties tested from 2016 to 2018

Name	Control Type	2016	2017	2018
Jenga	Resistant	16	15	15
Arina	Moderate resistant	41	34	31
Tarso	Susceptible	48	51	37

Table S2. Mean of corrected SNB disease severity of each haplotype in different field environments (seasons 216, 2017 and 2018)

Haplotype	Inherited from BMWpop founder	Mean disease severity % (2016)	Corrected disease severity % (2017)	Corrected disease severity % (2018)
1	Julius	31.3	0.776	1.36
2	Ambition, Potenzial	34.9	1.09	1.21
3	BAYP4535, Firl3565	29.7	-2.10	-1.89
4	Event	41.1	10.4	9.47
5	Bussard, Format	30.0	-1.58	-1.50

Table S3 Comparison of marker physical positions for BMWpop and previous published SNB QTL on chromosome 5A. Peak markers are indicated in bold. left: left flanking marker of the QTL, right: right flanking marker of QTL, peak: peak marker of QTL. †Stadlmeier et al. (2018). ‡IWGSC (2018).

Marker ID	Population	Genetic map position†	Physical map position start (bp) ‡	Physical map position end (bp) ‡	Reference	Source
BS00040623_51	BMWpop	44.98	391548987	391548887	This study/ *QInf.nmbu-5A.1*	Infil_203649_left/peak
BobWhite_rep_c64913_315	BMWpop		413418697	413418597	This study/ *QInf.nmbu-5A.1*	Infil_203649_right
BobWhite_rep_c63943_76	BMWpop		547415426	547415526	This study/ *QSnb.nmbu-5A.1*	2016_peak/right
AX-94706027	BMWpop	183.29	548234891	548234821	This study/ *QSnb.nmbu-5A.1*	2016_right
barc151	BR34×Grandin		558340037	558340252	(Friesen et al., 2009)/ *QSnb.fcu-5AL*	Adult/ seedling leaf
Tdurum_contig54785_216	BMWpop	220.61	558692780	558692880	This study/ *QSnb.nmbu-5A.1*	2016_right/2018_right
IWB67424	120 hard red winter wheat (HRWW) cultivars		565753008	565752908	(Liu et al., 2015)	Seedling leaf
Excalibur_c33923_592	BMWpop		568156970	568157070	This study/ *QSnb.nmbu-5A.1*	2016_peak
Excalibur_c472_914	BMWpop	205.9	568272220	568272320	This study/ *QSnb.nmbu-5A.1*	2016_left
RAC875_c25339_200	BMWpop		571683315	571683217	This study/ *QSnb.nmbu-5A.1*	2018_peak
Tdurum_contig44343_1039	BMWpop	207.91	573589801	573589901	This study/ *QSnb.nmbu-5A.1*	2018_left

Table S4 Comparison of marker physical positions for BMWpop SNB QTL *QSnb.nmbu-2D.1* on chromosome 2D. Peak markers are indicated in bold. left: left flanking marker of the QTL, right: right flanking marker of QTL, peak: peak marker of QTL

Marker	Population	Physical position start (bp)	Physical position end (bp)	Source
Xcfd56	BR34×Grandin	6158983	6158963	(Zhang et al., 2009) /*Snn2*
Xcfd51	BR34×Grandin	12360665	12360684	(Zhang et al., 2009) /*Snn2*
BobWhite_c5466_1015	BMWpop	14261151	14261251	2016_left
cfd36	Calingiri × Wyalkatchem	14362782	14362981	(Phan et al., 2016)/ *QSnb.cur-2DS*
BS00029208_51	NIAB Elite MAGIC	14897896	14897996	(Lin et al., 2020) peak
BS00071755_51	BMWpop	15115131	15115231	2016_peak
BS00047901_51	BMWpop	15967348	15967448	2016_right
wsnp_JD_rep_c63957_40798083	NIAB Elite MAGIC	20768482	20768682	(Lin et al., 2020)
BobWhite_c59161_181	NIAB Elite MAGIC	27859904	27859806	(Lin et al., 2020)
wPt-669517	Calingiri × Wyalkatchem	37053347	37053740	(Phan et al., 2016)/ *QSnb.cur-2DS*

Table S5 Comparison of marker physical positions for BMWpop QTL *QSInf.nmbu-7B.1* and *QSnb.niab-7B.2*. Peak markers are indicated in bold. †IWGSC (2018).

Marker ID	Population	Physical map position start (bp) †	Physical map position end (bp) †	QTL name
Kukri_c15912_860	NIAB Elite MAGIC	673961429	673961530	*QSnb.niab--7B.2*
GENE.4442_121	BMWpop	679800093	679799993	*QInf.nmbu-7B.1*
wsnp_Ex_c56425_58548596	**BMWpop**	**683513848**	**683513648**	***QInf.nmbu-7B.1***
BS00077956_51	**NIAB Elite MAGIC**	**687304661**	**687304762**	***QSnb.niab-7B.2***
BS00057323_51	BMWpop	687591650	687591750	*QInf.nmbu-7B.1*
Excalibur_c50612_409	NIAB Elite MAGIC	700551671	700551772	*QSnb.niab-7B.2*

Table S6 Permutated p=0.05 significance threshold in each environment

Trait	Threshold
Leaf blotch in 2016	2.6
Leaf blotch in 2017	2.8
Leaf blotch in 2018	2.2
Infiltration with cultural filtrate of isolate 203649	3.0
Infiltration with Tox3 effector	3.5

Genome-wide association mapping of septoria nodorum blotch resistance in Nordic winter and spring wheat collections

Min Lin[1], Andrea Ficke[2], Jon Arne Dieseth[3], Morten Lillemo[1]

[1] Dep. of Plant Sciences, Norwegian Univ. of Life Sciences, Post Box 5003, NO-1432 ÅS, NORWAY

[2] Division of Biotechnology and Plant Health, Norwegian Inst. of Bioeconomy Research, P.O. Box 115, NO-1431 ÅS, NORWAY

[3] Graminor, AS, Bjørke Gård, Hommelstadvegen 60, NO-2322 Ridabu, NORWAY

*** Correspondence:**
Morten Lillemo
morten.lillemo@nmbu.no

Abstract

Septoria nodorum blotch (SNB), caused by the necrotrophic fungal pathogen *Parastagonospora nodorum*, is the dominant leaf blotch pathogen of wheat in Norway. Resistance/susceptibility to SNB is a quantitatively inherited trait, which can be partly explained by the interactions between wheat sensitivity loci (*Snn*) and corresponding *P. nodorum* necrotrophic effectors (NEs). Two Nordic wheat association mapping panels were assessed for SNB resistance in the field over three to four years: a spring wheat and a winter wheat panel (*n*=296 and 102, respectively). Genome wide association studies (GWAS) found SNB resistance associated quantitative trait loci (QTL) on fourteen wheat chromosomes, although no QTL were found in common between the spring and winter wheat panels. One robust QTL on the short arm of chromosome 2A was detected in the winter wheat panel and explained up to 14 % of the phenotypic variation. Using the four years phenotypic data generated here in combination with five years historical data, the effect of this QTL on SNB severity was confirmed in seven of the nine years for which data was available. However, lines containing the resistant haplotype are rare in both Nordic spring (3.0%) and winter wheat cultivars (13.7%), indicating the potential of integrating this QTL in SNB resistance breeding programs. In addition, clear and significant additive effects were observed by stacking resistant alleles of the detected QTL, suggesting that marker assisted selection can be applied to enhance SNB resistance.

Acknowledgements: This research was undertaken within the 'Efectawheat' project supported within the framework of the 2nd call ERA-NET for Coordinating Plant Sciences, with funding to MIL from The Research Council of Norway, grant NFR251894. The SNP genotyping was paid by Graminor AS. The authors would also like to thank Susanne Windju and Tatiana Belova for their initial analysis on the SNP marker data, Camille Branchereau for the STRUCTURE analysis, Anne Guri Marøy for DNA extraction and SSR genotyping, Danielle Holmes for primer sequences, Yalew Tarkegne and Cecilie Yri for help with the field trials.

Introduction

Wheat (*Triticum aestivum* L.) is the second most cultivated crop worldwide (FAO 2017). Because of the enormous efforts on wheat breeding and optimization of field management, global wheat yield increases continuously and reached 3.5 tons per hectare in 2017 (FAO 2017). However, the grain yield is threatened by various wheat pests and pathogens. Septoria nodorum blotch (SNB), is one of the most devastating fungal diseases of wheat which reduces both grain yield and grain quality and could cause 30% yield loss under warm and humid conditions (Bhathal et al. 2003). The causal agent of SNB is the necrotrophic pathogen *Parastagonospora nodorum*. By secreting necrotrophic effectors (NEs), *P. nodorum* can trigger plant cell death and take up nutrients from dying host tissues to accelerate infection (Friesen and Faris 2012). In contrast to the gene-for-gene model for the interactions between biotrophic pathogens and their hosts (Flor 1956), *P. nodorum* interacts with wheat in an inverse gene-for-gene manner (Friesen and Faris 2012; Friesen et al. 2007). Wheat sensitivity loci (*Snn*) interact with corresponding NEs produced by *P. nodorum*, which leads to susceptibility to SNB. Eight *P. nodorum* NEs have been characterized to interact with nine wheat susceptibility loci, reviewed by Ruud and Lillemo (2018). So far, three *P. nodorum* NEs (ToxA, Tox1 and Tox3) and two wheat susceptibility loci (*Tsn1* and *Snn1*) have been characterized at the sequence level (Faris et al. 2010; Liu et al. 2009; Liu et al. 2012; Shi et al. 2016).

Resistance to SNB is well known as a polygenetic trait involving many genes with minor effects (Fried and Meister 1987; Wicki et al. 1999). The increasing understanding of the NEs-*Snn* interactions indicates that wheat susceptibility to SNB is also a quantitative trait, and the effects of NEs-*Snn* interactions vary from additive to epistatic (Peters Haugrud et al. 2019). Fungicides are widely applied for SNB management (Ficke et al. 2018; Ruud and Lillemo 2018). However, the

potential risk of fungicide resistance and the environmental concerns of chemical application are considerable. Therefore, improving cultivar resistance to SNB is essential as it helps to control this plant disease in a more sustainable manner.

Choosing the QTL for marker assisted selection (MAS) is a challenge when we want to improve SNB resistance. Resistance QTL characterized by seedling experiments are not necessarily relevant for adult plant resistance, and only a few *Snn* loci have shown effects in field studies (Francki 2013; Friesen et al. 2009; Phan et al. 2016; Ruud et al. 2019; Ruud and Lillemo 2018; Ruud et al. 2017; Lin et al., 2020). In addition, *P. nodorum* has both an asexual and a sexual reproduction system, and the rapid co-evolution of the pathogen population makes breeding of cultivars with durable resistance very difficult (McDonald and Linde 2002). Genome wide association studies (GWAS) have been widely used for identifying marker-trait associations (MTAs) of polygenetic traits in plants (Gupta et al. 2014; Gurung et al. 2014; Kidane et al. 2017; Korte and Farlow 2013; Xiao et al. 2017). However, most GWAS studies on SNB resistance were based on seedling resistance (Adhikari et al. 2011; Gurung et al. 2014; Liu et al. 2015; Phan et al. 2018). The first GWAS for SNB adult plant leaf blotch resistance was done by Ruud et al. (2019). Robust QTL for adult plant resistances were identified on eight chromosomes, using a subset of 121 lines of the Nordic spring wheat association mapping panel (MASBASIS) (Ruud et al. 2019). A QTL on the long arm of chromosome 2D turned out to be the most robust QTL for adult plant resistance. It was detected in six out of seven years of testing, and the haplotype analysis confirmed the importance of this QTL (Ruud et al. 2019).

The objectives of this study were (1) to discover robust QTL for adult plant SNB resistance by association analysis using a winter wheat association panel (MASBASIS winter wheat); (2) to compare QTL discovered in a previous GWAS field study by Ruud et al. (2019) using an enlarged spring wheat panel and (3) to compare SNB resistant associated QTL in spring and winter wheat

Methods and Materials

Plant material and genotyping

The Nordic association mapping panel (MASBASIS) contains a collection of 296 spring wheat lines and a collection of 102 winter wheat lines, which includes current and historical Nordic wheat cultivars and a few international lines. The spring wheat and winter wheat panels were tested for adult plant leaf blotch resistance in the field. A subset of 121 spring wheat lines were genotyped

by Illumina 90K wheat SNP chip (Wang et al. 2014) and tested for SNB leaf blotch from 2010 to 2016, as described by Ruud et al. (2019). This study used an expanded panel of 296 spring wheat and 102 winter wheat lines, which were genotyped by the 35K Axiom® array (Allen et al. 2017) and previously used for mapping of agronomic traits (Branchereau et al 2018). In addition, a few KASP markers designed for significant SNB QTL detected in the in previous GWAS by Ruud et al. (2019) and SNB resistance related microsatellite (SSR) markers used in the same study were also included. SSR markers were converted to be biallelic. KASP and SSR markers were first placed on an artificial chromosome. Significant markers from the artificial chromosome were then placed on the consensus map putatively according to physical map positions and LD results. Monomorphic markers and minor alleles with less than 5% allele frequency were filtered out. Heterozygote genotypes were treated as missing data. The final GWAS analysis contained 12353 markers (SNP and SSR) for the winter wheat panel, and 13209 markers (SNP and SSR) for the spring wheat panel.

Field testing

For the spring wheat panel, field testing was conducted for three years from 2016 at Vollebekk research station in Ås, Norway, using alpha lattice designs with three replicates. The winter wheat panel was tested in the field at the same location consistently for four years since 2016, using alpha lattice design with three replicates. Field evaluation and field control methods were previously described by Ruud et al. (2019). Briefly, naturally *P. nodorum* infected straw was used as inoculum, and mist irrigation was carried out to enhance infection (as described by Ruud et al., 2019). Leaf blotch scorings were carried out two to three times, assessing the percentage of diseased leaf area in each hillplot canopy, starting when the most susceptible lines reached 70% disease severity. The following scorings were carried out with approximately one-week time intervals.

Statistical analysis

'Plant height' and 'days to heading' were used as covariates in regression in order to obtain the corrected disease severity of leaf blotch for the MASBASIS spring wheat collection as described by Ruud et al. (2019). No significant association was found between leaf blotch and 'plant height' in most years for the winter wheat collection. Therefore, only 'days to heading' was used as covariate for correcting winter wheat disease severity. The across year means of corrected

disease severity for each genotype were calculated using environments (year) as random effect and genotype as fixed effect by PROC MIXED implemented in SAS 9.4 (SAS Institute, Inc.). Pearson correlation coefficients were calculated by R package `Hmisc` (Harrell 2019). Variance components were calculated by fitting genotype and genotype by environment interaction as random effect using R package lme4 (Bates et al. 2015). Broad sense heritability was calculated using formula $h^2 = \sigma_g^2/(\sigma_g^2 + \sigma_{g\times E}^2/y + \sigma_E^2/ry)$.Where σ_g^2 is the genetic variance, $\sigma_{g\times E}^2$ is the genetic by environment variance, σ_E^2 is the error variance, y is the number of years, and r is the number of replicates.

Linkage disequilibrium and Population structure

The pairwise Linkage disequilibrium (LD) was calculated based on the square frequency correlation (r^2) (Hill and Weir 1988) using functions implemented in TASSEL v.5.2.48 (Bradbury et al. 2007). The whole genome LD analysis used a sliding window with window size 800, while LD analysis for markers on single chromosomes used the full-matrix option in TASSEL (Bradbury et al. 2007). Visualization of the genome wide LD decay was achieved by plotting the pairwise r^2 value from the whole genome LD analysis against the genetic distance (cM). A non-linear model was fitted to summarize the relationship between LD decay and genetic distance (Marroni et al. 2011). Half decay distance was calculated based on the estimated maximum value of LD.

The population structure in the spring and winter wheat panels were investigated previously by (Branchereau 2018) using Bayesian clustering in the software STRUCTURE v2.3.4 (Pritchard et al. 2000). It showed that both panels could be divided in two subpopulations, which largely followed the genetic origin of the lines. For the spring wheat panel, the division was between lines of Nordic origin (subpopulation 1) and exotic lines mainly from CIMMYT and China (subpopulation 2). For the winter wheat panel, the first subpopulation consisted of mainly German and UK wheat lines, while the second was composed of lines from Norway and Sweden.

Association analysis

Association analyses were done separately for the spring and winter wheat. The kinship matrix was calculated by TASSEL v.5.2.48 (Bradbury et al. 2007) using the whole data set of markers according to Pasam et al. (2012). The model used for association analysis was the mixed linear model (MLM) + kinship matrix (K) + population structure (Q) as previously described by Ruud et al. (2019) using TASSEL v.5.2.48 (Bradbury et al. 2007). Since the Bonferroni correction would

be a too strict criterium for declaring significant QTL for a highly quantitative trait like SNB field resistance, we applied the 0.1 percentile of the p-values distribution as an exploratory significance threshold to detect putative QTL (Pasam et al. 2012) as in the previous study by Ruud et al (2019). QTL were considered as robust when associated markers met the more stringent $-\log_{10}(p)$ threshold of 3.5. In addition, the Quantile-Quantile (QQ) plots were inspected to identify the level at which the observed p-values started to deviate from the expected values under the null hypothesis. The databases https://triticeaetoolbox.org and http://www.cerealsdb.uk.net were used for obtaining SNP marker sequences. Physical map positions of markers on the wheat reference genome IWGSC RefSeq v1.0 (International Wheat Genome Sequencing et al. 2018) were obtained from database https://urgi.versailles.inra.fr/blast/?dbgroup=wheat_iwgsc_refseq_v1_chromosomes&program=blastn

Haplotype analysis

One stable field resistance QTL on chromosome 2A identified from the winter wheat panel was selected for haplotype analysis. The peak marker and two significant markers which were in high LD with the peak marker ($r^2 > 0.8$) were selected to construct haplotypes. Pair-wise comparison of corrected disease severity between haplotypes were conducted using Tukey HSD test implemented in R package `multcompView` (Graves et al. 2015). Around 50 lines of the winter wheat panel were tested for leaf blotch resistance in the field from 2010 to 2015 (except 2013). Those historical phenotypic data were also used in the haplotype analysis to confirm the haplotype effects caused by this 2AS QTL.

Stacking resistant alleles

Six SNB QTL were selected for the winter and spring wheat panels, respectively, in order to investigate the effect of stacking resistant alleles. The resistant allele was determined by the predicted allele effect of the corresponding peak marker obtained from the TASSEL output. Wheat lines were grouped by the number of resistant alleles they contained. Tukey`s HSD test implemented in R package `multcompView` (Graves et al. 2015) was used to compare whether there were significant differences of mean disease severities between groups.

Results

Phenotypic evaluation

Variations in SNB resistance were observed in both panels in all tested years (Fig S1). For the spring wheat panel, both 'plant height' and 'days to heading' were significantly correlated with leaf blotch severity (Table 1). For the winter wheat panel, 'days to heading' was significantly correlated with leaf blotch severity while the 'plant height' was only significantly correlated with leaf blotch in 2016 (Table 1). However, the significance level was relatively low ($p < 0.05$) and it was probably due to lodging which was positively correlated with the disease severity that year (data not shown). Corrected disease severities were also highly significantly correlated between environments for both the winter and spring wheat panels ($p < 0.0001$) (Table 2). The heritability of leaf blotch resistance across years was 0.80 for the winter and 0.84 for the spring wheat panel.

Linkage disequilibrium

Rapid LD decays were observed for both panels (Fig S2). The estimated r^2 of half decay (critical threshold of r^2) for the winter wheat panel was 0.23, and the estimated genome-wide half decay distance was 1 cM. Similarly, the estimated r^2 of half decay for the spring wheat panel was 0.22, where the half decay distance was also 1 cM. Therefore, markers located within 1 cM distance on the genetic map were considered as from the same QTL.

Association mapping of the winter wheat panel

For the winter wheat panel, the exploratory $-\log_{10}(p)$ threshold for each environment (year) ranged from 2.55 to 2.78 (Table S1), and yielded a total of 24 putative SNB associated QTL, on chromosomes 1B, 2A, 3A, 3B, 5A, 5B, 6A, 6B and 7A (Fig. 1, Table S2). Out of these, three QTL met the more stringent $-\log_{10}(p)$ threshold of 3.5 in at least one environment in addition to being detected in the mean across years. These were located on the short and long arms of 2A and on 5A (Table S3, Fig. 2). The QTL on 2AL, which was on 83 cM of the consensus map while approximately 79 Mb on the physical map, could explain phenotypic variations up to 17% and was significant in 2017, 2019 and the across-year mean. However, only one marker *AX-94657509* was above threshold and no markers with high LD ($r^2 > 0.8$, $p < 0.001$) could be used for haplotype analysis. The QTL on chromosome 2AS was located at 2 cM of the consensus map and 4-14 Mb on the physical map. This QTL was detected in both 2017 and the across-year mean, and could explain up to 14 % of phenotypic variation (Table S2). Markers of this QTL were used for

constructing haplotypes and analyzing haplotype effects. The QTL on chromosome 5A was above the $-\log_{10}(p)$ threshold of 3.5 in 2016 as well as being detected as a putative QTL in 2019 and the across year mean. All significant markers of this QTL were located on the same genetic map position (72 cM) and mostly within 402-404 Mb on the physical map, and explained from 9.4% to 13.2% of the phenotypic variations (Table S2).

Four additional QTL were considered as important as they were detected above the 0.1 percentile exploratory threshold in two environments (years) or one environment plus the across-year mean. These were all located on chromosome 5B (Table S2, Fig. 1). The QTL identified on chromosome 5BS was identified as the Tox3 sensitivity locus *Snn3-B1*, as the *Snn3* KASP marker *BS00091519_51* (Ruud et al. 2017) was significant and the significant 35K marker *AX-94406039* was also blasted to approximately the same physical location as the KASP marker (6.6 Mb). The second QTL on 5BL was located at 119 cM and was identified in the years 2018 and 2019 (r^2: 9.8-12%) but not detected in the four-year mean. The remaining two QTL on chromosome 5B located on 122 cM and 192 cM respectively, were identified in 2019 and the across-year mean and explained around 11% of the phenotypic variation (Table S2). Marker *fcp618* on chromosome 1B was the Tox1 susceptibility locus *Snn1* linked SSR marker (Zhang et al. 2009). It was not significantly detected in any single year, however, it was above the exploratory 0.1 percentile threshold when analyzing the mean of four years (Table S2, Fig. 1).

Association mapping of the spring wheat panel

The exploratory $-\log_{10}(p)$ threshold for the spring wheat panel varied between 2.57-3.46 (Table S1). In total, 24 putative QTL were detected on chromosomes 1A, 1B, 1D, 2A, 2B, 2D, 3B, 5A, 5B, 6A, 6B, 7A and 7B respectively (Table S3, Fig. 2). Out of these, three QTL on 1A, 2B and 5B met the more stringent $-\log_{10}(p)$ threshold of 3.5 in at least one environment in addition to being detected in the mean data across years. These were considered as robust QTL. All QTL detected in the spring wheat panel showed only minor effects, and none of them could explain more than 10% of the phenotypic variations (Table S3). The R^2 values ranged from 3.1 % to 7.0 % (Table S3). The QTL on chromosome 1AS was the most significant QTL, and it was identified in year 2016 and in the across-year mean. The peak marker *AX-94772289* (r^2 = 7.0%, $-\log_{10}(p)$ = 4.68) was located on 54 cM of the consensus genetic map and 1.23 Mb on the physical map (Table S3). Another QTL on the short arm of chromosome 2B was significantly detected in 2016 and in the across-year mean,

and the peak marker *AX-94390683* explained up to 5.3% of the phenotypic variation. The QTL identified in 2018 and the across-year mean was located on 105 cM of chromosome 2B and 742 to 749 Mb on the physical map, explaining up to 4.5 % of the phenotypic variation. The QTL on chromosome 5B, which was significantly detected in 2017 and in the across year mean (Fig. 2), co-located with the ToxA sensitivity locus *Tsn1* (Friesen et al. 2009), as the *Tsn1* linked SSR marker *fcp620* (Zhang et al. 2009) was significant and in high LD (r^2 = 0.99) with another significant SNP marker *AX-94598077*. In addition, both markers mapped to similar physical positions (approx. 547 Mb). A SNP marker *AX-94771499* on chromosome 5B (142 cM) was significant in year 2018 and was mapped to 542 Mb on the physical map. Since the physical map position of marker *AX-94771499* was close to the *Tsn1* linked markers, it was first considered as a *Tsn1* related marker. However, it was in low LD (r^2 = 0.03) with both *Tsn1* linked markers and, therefore, probably represented a different QTL. In addition to these consistent QTL, the SSR marker *TC253803*, previously known to be linked to the Tox2 sensitivity locus *Snn2* (Zhang et al. 2009), was detected above the exploratory 0.01 percentile threshold both in 2017 and the across-year mean. Another putative, but consistent QTL was detected at 72 cM on chromosome 5A. Three markers were detected for this QTL in year 2017, and two markers were in full LD (r^2 = 1). However, the third marker *AX-94749386*, which was the marker that was also identified in the across-year mean, was in relatively low LD (r^2 = 0.5) with the other two markers. The large distance between marker *AX-94749386* and the remaining two makers *AX-94525900* and *AX-95165003* on the physical map also confirmed this result (Table S3). Therefore, these markers were considered to indicate two closely located QTL.

Haplotype analysis

Four haplotypes were constructed based on the combination of alleles from three markers of the 2AS QTL (Table S4, Fig. 3). In total, 9 years of leaf blotch data of the winter wheat panel were used for haplotype analysis of the 2AS QTL. Significant differences of corrected leaf blotch severities were detected between resistant and susceptible haplotypes in seven out of nine years of testing and also the across year mean from 2016 to 2019 (Fig. 3). The susceptible haplotype 2 always had higher disease severity compared to the resistant haplotype 4. The same haplotype analysis was also carried out for the spring wheat panel. However, only 9 lines (3%) in the spring wheat panel carry the resistant haplotype 4, while the majority of the panel (73.6%) carried the

susceptible haplotype 2. No significant haplotype effect was detected probably due to the extremely uneven sample size between haplotypes (Fig S3).

Stacking resistant alleles

Markers used for stacking resistant alleles are listed in Table S5. Fig. 4a shows the result of stacking resistant alleles in the winter wheat panel. There was only one line, Xi19, which had no resistant allele, and it was also the most susceptible line to SNB in this association mapping panel. The remaining lines were grouped to have from 2 to 6 resistant alleles. A decreasing trend of disease severity could be observed when the number of resistant alleles was increasing. From Fig. 4a, at least two more resistant alleles were required to obtain significant differences in mean of disease severities between groups. Similar results could also be seen for the spring wheat panel (Fig. 4b). There was only one line containing none of the resistant alleles, which was a Norwegian breeding line GN12658. Lines with 3 to 4 resistant alleles were significantly more resistant than lines with 1 or 2 resistant alleles (Fig. 4b). The more resistant alleles the lines carried, the lower disease severities they had. Lines with 5 resistant alleles had the lowest disease severity which was significantly lower than all previous groups.

Discussion

Important QTL for adult plant resistance/susceptibility

Ruud and Lillemo (2018) reviewed that only a few of the know NE-sensitivity loci had been proven to show effects in adult plant susceptibility in the field. In this study we found that some NE-sensitivity loci were among the most important susceptibility QTL in adult plants, which were significantly identified in at least one environment, and explained up to 12% phenotypic variation (Table S2 and S3). Ruud et al. (2018) showed that sensitivity to ToxA was common in the Norwegian spring wheat panel, and that it was associated with high disease severity in the field. However, markers linked to the susceptibility locus *Tsn1* were not significantly detected above threshold in the GWAS study using the subset of the MASBASIS spring wheat panel (Ruud et al. 2019). In this study, a larger panel of spring wheat lines were assessed for field SNB resistance from 2016 to 2018, and *Tsn1* linked markers were detected above thresholds in 2017 and in the mean across years. Another well-documented SNB sensitivity locus, *Snn2* which showed an effect on adult plant susceptibility (Friesen et al. 2009), was also identified in one year and in the mean across years in the winter wheat panel. Moreover, both *Snn1* and *Snn3-B1* linked markers were

detected in the across-year mean using our winter wheat panel. In addition, the QTL on the short arm of chromosome 1A in the spring wheat panel could be the Tox4 sensitivity locus *Snn4* (Abeysekara et al. 2012; Abeysekara et al. 2009). Flanking markers of *Snn4* were blasted to 3.84-4.20 Mb of the physical map, while our 1AS QTL was blasted to 1.14-3.38 Mb (Table S6). Ruud et al. (2019) also found a QTL on 1AS by seedling inoculation with isolate 201618, however, culture filtrate infiltration of the same isolate could not induce sensitivity reaction on the *Snn4* differential line (AF89). The significant marker *RAC875_c30657_82* of that 1AS QTL from Ruud et al. (2019) was blasted to 7.18 Mb on the physical map which was further away from our 1AS QTL compared to the *Snn4* locus (Table S6). Moreover, the significant marker *AX-95211290* of the 6A QTL in the winter wheat panel detected in 2019 was blasted to 606.99 Mb on the physical map, which was close to the *Snn6* interval (603.13-606.98 Mb) (Gao et al. 2015). According to LD analysis, no markers were found to have high LD ($r^2 > 0.8$) with this marker *AX-95211290* on chromosome 6A. Culture filtrate infiltration of Tox4 and Tox6 on this mapping panel is needed to confirm the co-location of these NE-sensitivity QTL.

Beside the NE sensitivity loci, we also compared other identified QTL with those published in the previous GWAS by Ruud et al. (2019). The significant spring wheat QTL detected on 72 cM of chromosome 5A could co-locate with the robust QTL detected by Ruud et al. (2019). We found out that our 5A QTL could be split into two QTL as only two of the three significant markers were in high LD. The marker which was not in high LD with the other two significant markers was blasted to a physical map position 50 Mb away from the other two markers. Interestingly, the other two markers were located close to the significant marker *wsnp_Ex_c10231_16783750* which was detected in 2012 by Ruud et al. (2019) and blasted to 49 Mb on the physical map (Table S7). Another significant marker *gwm293* from Ruud et al. (2019), which was significantly detected in 2010, was blasted to the region close to our third marker (Table S7). In addition, another QTL on chromosome 7A detected by the across-year mean using the spring wheat panel might co-locate with the significant QTL by Ruud et al. (2019). According to Table S8, three markers which were significantly detected in 2013 by Ruud et al. (2019) were blasted within the physical interval defined by our 7A QTL.

Haplotype analysis

Significant markers of the 2AS QTL were blasted to the reference genome, and the physical map positions were compared with other published SNB resistance QTL (Table S9). Four QTL were blasted to the short arm of chromosome 2A and two of them were identified by seedling inoculation (Lin et al. 2020; Rybak et al. 2017), two for flag leaf resistance (Francki et al. 2018). The physical interval of *Qsnb.cur-2AS2* was between 2.32 to 3.78 Mb (Rybak et al. 2017), while the interval of *QSnb.niab-2A.1* was between 0.82-2.37 Mb (Lin et al., 2020). Our QTL on 2AS, however, had a relatively larger interval between 4.17 to 14.48 Mb, and the peak marker was blasted to approximately 11 Mb on the physical map (Table S9). Therefore, our QTL would be more likely the same QTL as the adult plant resistant QTL published by Francki et al. (2018), which located at 14-19 Mb on the physical map (Table S9). Strong haplotype effects of our 2AS QTL were detected not only in the years when this QTL was significant, but also in years when the QTL was below the threshold. In addition, the historical data from previous years provided evidence of the strong haplotype effects (Fig. 3). Most of the lines which had the resistant haplotype 4 are of German origin. This group includes Jenga and Kuban which are used as resistant checks for SNB field trials in Norway. Most of the Norwegian and Swedish cultivars and breeding lines belong to the big group with the susceptible haplotype 2. The resistant haplotype seems to be rare in the Norwegian breeding material, and only found in the breeding line GN13023. Haplotype effects of this QTL were not significant in the spring wheat panel, which was probably due to the low allele frequency of marker *AX-94398906* (< 5%). All 9 spring wheat lines with haplotype 4 came from CIMMYT and the majority of lines in our spring wheat panel carry the susceptible haplotype. Interestingly, haplotype 4 did always show lower average corrected disease severity compared to other haplotypes (Table S10) although it was not significant due to the low allele frequency. Integrating this resistance QTL into Nordic breeding programs would be a useful strategy to improve SNB resistance.

Comparing QTL detected from spring wheat panel and winter wheat panel

The SNB QTL that we identified varied from year to year, and only few QTL were detected in more than two environments (years). In addition, we were not able to identify QTL which were significant in both the spring and winter wheat panels. However, these results were not unexpected. Interactions between *P. nodorum* and wheat depend on both NEs expressed in the pathogen and the hosts` genetic background (Peters Haugrud et al. 2019). In our study, naturally infected straw

was used as inoculum and the pathogen population might vary from year to year due to *P. nodorum*`s mixed reproduction system. In addition, our winter and spring wheat panels were quite diverged with different genetic backgrounds and allele frequencies. Owing to the limitation of association studies, potentially associated markers might be excluded from the analysis due to rare allele frequencies (Gupta et al. 2014).

Conclusion

Our results illustrated the challenge of selecting reliable QTL for improving SNB resistance in wheat breeding. Only a few QTL were detected across years and no QTL were common between spring and winter wheat panels. However, the haplotype analysis confirmed the robustness of the QTL on chromosome 2AS. As the resistant haplotype was rare in both Norwegian winter wheat and spring wheat lines, integrating this resistance allele in the local wheat germplasm would help to improve the SNB resistance. In addition, by stacking resistance alleles, the SNB disease severity was significantly reduced, indicating that marker-assisted allele pyramiding can be a promising strategy for reducing SNB susceptibility. However, QTL validations in the field using different plant materials and testing in different environments are needed to reduce the unnecessary cost of integrating inconsistent QTL.

References

Abeysekara NS, Faris JD, Chao S, McClean PE, Friesen TL (2012) Whole-genome QTL analysis of Stagonospora nodorum blotch resistance and validation of the SnTox4-Snn4 interaction in hexaploid wheat. Phytopathology 102:94-104 doi:10.1094/PHYTO-02-11-0040

Abeysekara NS, Friesen TL, Keller B, Faris JD (2009) Identification and characterization of a novel host-toxin interaction in the wheat-Stagonospora nodorum pathosystem. Theor Appl Genet 120:117-126 doi:10.1007/s00122-009-1163-6

Adhikari TB, Jackson EW, Gurung S, Hansen JM, Bonman JM (2011) Association mapping of quantitative resistance to Phaeosphaeria nodorum in spring wheat landraces from the USDA National Small Grains Collection. Phytopathology 101:1301-1310 doi:10.1094/PHYTO-03-11-0076

Allen AM et al. (2017) Characterization of a Wheat Breeders' Array suitable for high-throughput SNP genotyping of global accessions of hexaploid bread wheat (Triticum aestivum). Plant Biotechnol J 15:390-401 doi:10.1111/pbi.12635

Bates D, Machler M, Bolker BM, Walker SC (2015) Fitting Linear Mixed-Effects Models Using lme4. Journal of Statistical Software 67:1-48 doi:10.18637/jss.v067.i01

Bhathal JS, Loughman R, Speijers J (2003) Yield reduction in wheat in relation to leaf disease from yellow (tan) spot and septoria nodorum blotch. Eur J Plant Pathol 109:435-443 doi:10.1023/A:1024277420773

Bradbury PJ, Zhang Z, Kroon DE, Casstevens TM, Ramdoss Y, Buckler ES (2007) TASSEL: software for association mapping of complex traits in diverse samples. Bioinformatics 23:2633-2635 doi:10.1093/bioinformatics/btm308

Branchereau C (2018) Genome-wide association mapping of three agronomic traits and resistance to Parastagonospora nodorum in spring and winter wheat. Master thesis, Université de Rennes

FAO (2017) Production/Yield quantities of Wheat in World. http://www.fao.org/faostat.

Faris JD et al. (2010) A unique wheat disease resistance-like gene governs effector-triggered susceptibility to necrotrophic pathogens. Proc Natl Acad Sci U S A 107:13544-13549 doi:10.1073/pnas.1004090107

Ficke A, Cowger C, Bergstrom G, Brodal G (2018) Understanding Yield Loss and Pathogen Biology to Improve Disease Management: Septoria Nodorum Blotch - A Case Study in Wheat. Plant Dis 102:696-707 doi:10.1094/PDIS-09-17-1375-FE

Flor H (1956) The complementary genic systems in flax and flax rust. In: Advances in genetics, vol 8. Elsevier, pp 29-54. doi:10.1016/S0065-2660(08)60498-8

Francki MG (2013) Improving Stagonospora nodorum Resistance in Wheat: A Review. Crop Sci 53:355-365 doi:10.2135/cropsci2012.06.0347

Francki MG, Walker E, Li DA, Forrest K (2018) High-density SNP mapping reveals closely linked QTL for resistance to Stagonospora nodorum blotch (SNB) in flag leaf and glume of hexaploid wheat. Genome 61:145-149 doi:10.1139/gen-2017-0203

Fried PM, Meister E (1987) Inheritance of Leaf and Head Resistance of Winter Wheat toSeptoria nodorumin a Diallel Cross. Phytopathology 77:1371-1375 doi:10.1094/Phyto-77-1371

Friesen TL, Chu CG, Liu ZH, Xu SS, Halley S, Faris JD (2009) Host-selective toxins produced by Stagonospora nodorum confer disease susceptibility in adult wheat plants under field conditions. Theor Appl Genet 118:1489-1497 doi:10.1007/s00122-009-0997-2

Friesen TL, Faris JD (2012) Characterization of Plant-Fungal Interactions Involving Necrotrophic Effector-Producing Plant Pathogens. In: Bolton MD, Thomma BPHJ (eds) Plant Fungal Pathogens: Methods and Protocols. Humana Press, Totowa, NJ, pp 191-207

Friesen TL, Meinhardt SW, Faris JD (2007) The Stagonospora nodorum-wheat pathosystem involves multiple proteinaceous host-selective toxins and corresponding host sensitivity genes that interact in an inverse gene-for-gene manner. Plant J 51:681-692 doi:10.1111/j.1365-313X.2007.03166.x

Gao Y et al. (2015) Identification and Characterization of the SnTox6-Snn6 Interaction in the Parastagonospora nodorum-Wheat Pathosystem. Mol Plant Microbe Interact 28:615-625 doi:10.1094/MPMI-12-14-0396-R

Graves S, Piepho H, Selzer L (2015) Dorai-Raj, S. multcompView: Visualizations of Paired Comparisons Version 01-7 Available online: https://cran r-project org/web/packages/multcompView/index html (accessed on 5 July 2018)

Gupta PK, Kulwal PL, Jaiswal V (2014) Association mapping in crop plants: opportunities and challenges. Adv Genet 85:109-147 doi:10.1016/B978-0-12-800271-1.00002-0

Gurung S, Mamidi S, Bonman JM, Xiong M, Brown-Guedira G, Adhikari TB (2014) Genome-wide association study reveals novel quantitative trait Loci associated with resistance to multiple leaf spot diseases of spring wheat. PLoS One 9:e108179 doi:10.1371/journal.pone.0108179

Harrell F (2019) Hmisc: Harrell Miscellaneous. R package version 4.2-0.

Hill WG, Weir BS (1988) Variances and covariances of squared linkage disequilibria in finite populations. Theor Popul Biol 33:54-78

Kidane YG, Hailemariam BN, Mengistu DK, Fadda C, Pe ME, Dell'Acqua M (2017) Genome-Wide Association Study of Septoria tritici Blotch Resistance in Ethiopian Durum Wheat Landraces. Front Plant Sci 8:1586 doi:10.3389/fpls.2017.01586

Korte A, Farlow A (2013) The advantages and limitations of trait analysis with GWAS: a review Plant Methods 9:29 doi:10.1186/1746-4811-9-29

Lin M, Corsi B, Ficke A, Tan K-C, Cockram J, Lilemo M (2020) Genetic mapping using a wheat multi-founder population reveals a locus on chromosome 2A controlling resistance to both leaf and glume blotch caused by the necrotrophic fungal pathogen Parastagonospora nodorum (accepted)

Liu Z et al. (2015) Evaluation and Association Mapping of Resistance to Tan Spot and Stagonospora Nodorum Blotch in Adapted Winter Wheat Germplasm. Plant Dis 99:1333-1341 doi:10.1094/PDIS-11-14-1131-RE

Liu Z et al. (2009) SnTox3 acts in effector triggered susceptibility to induce disease on wheat carrying the Snn3 gene. PLoS Pathog 5:e1000581 doi:10.1371/journal.ppat.1000581

Liu Z et al. (2012) The cysteine rich necrotrophic effector SnTox1 produced by Stagonospora nodorum triggers susceptibility of wheat lines harboring Snn1. PLoS Pathog 8:e1002467 doi:10.1371/journal.ppat.1002467

Marroni F, Pinosio S, Zaina G, Fogolari F, Felice N, Cattonaro F, Morgante M (2011) Nucleotide diversity and linkage disequilibrium in Populus nigra cinnamyl alcohol dehydrogenase (CAD4) gene Tree Genet Genomes 7:1011-1023 doi:10.1007/s11295-011-0391-5

McDonald BA, Linde C (2002) Pathogen population genetics, evolutionary potential, and durable resistance. Annu Rev Phytopathol 40:349-379 doi:10.1146/annurev.phyto.40.120501.101443

Pasam RK, Sharma R, Malosetti M, van Eeuwijk FA, Haseneyer G, Kilian B, Graner A (2012) Genome-wide association studies for agronomical traits in a world wide spring barley collection. BMC Plant Biol 12:16 doi:10.1186/1471-2229-12-16

Peters Haugrud AR, Zhang Z, Richards JK, Friesen TL, Faris JD (2019) Genetics of Variable Disease Expression Conferred by Inverse Gene-For-Gene Interactions in the Wheat-Parastagonospora nodorum Pathosystem. Plant Physiol 180:420-434 doi:10.1104/pp.19.00149

Phan HT, Rybak K, Furuki E, Breen S, Solomon PS, Oliver RP, Tan KC (2016) Differential effector gene expression underpins epistasis in a plant fungal disease. Plant J 87:343-354 doi:10.1111/tpj.13203

Phan HTT et al. (2018) Novel sources of resistance to Septoria nodorum blotch in the Vavilov wheat collection identified by genome-wide association studies. Theor Appl Genet doi:10.1007/s00122-018-3073-y

Pritchard JK, Stephens M, Donnelly P (2000) Inference of population structure using multilocus genotype data. Genetics 155:945-959

Ruud AK et al. (2019) Genome-Wide Association Mapping of Resistance to Septoria Nodorum Leaf Blotch in a Nordic Spring Wheat Collection. The Plant Genome 12:1-15 doi:10.3835/plantgenome2018.12.0105

Ruud AK, Dieseth JA, Lillemo M (2018) Effects of Three Parastagonospora nodorum Necrotrophic Effectors on Spring Wheat under Norwegian Field Conditions. Crop Sci 58:159-168 doi:10.2135/cropsci2017.05.0281

Ruud AK, Lillemo M (2018) Diseases affecting wheat: Septoria nodorum blotch. In: Integrated disease management of wheat and barley. Burleigh Dodds Series in Agricultural Science. Burleigh Dodds Science Publishing Limited, Cambridge, UK, pp 109-144. doi:10.19103/as.2018.0039.06

Ruud AK, Windju S, Belova T, Friesen TL, Lillemo M (2017) Mapping of SnTox3-Snn3 as a major determinant of field susceptibility to Septoria nodorum leaf blotch in the SHA3/CBRD x Naxos population. Theor Appl Genet 130:1361-1374 doi:10.1007/s00122-017-2893-5

Rybak K, See PT, Phan HT, Syme RA, Moffat CS, Oliver RP, Tan KC (2017) A functionally conserved Zn2 Cys6 binuclear cluster transcription factor class regulates necrotrophic effector gene expression and host-specific virulence of two major Pleosporales fungal pathogens of wheat. Mol Plant Pathol 18:420-434 doi:10.1111/mpp.12511

Shi G et al. (2016) The hijacking of a receptor kinase-driven pathway by a wheat fungal pathogen leads to disease. Sci Adv 2:e1600822 doi:10.1126/sciadv.1600822

Wicki W, Winzeler M, Schmid JE, Stamp P, Messmer M (1999) Inheritance of resistance to leaf and glume blotch caused by Septoria nodorum Berk. in winter wheat. Theoretical and Applied Genetics 99:1265-1272 doi:10.1007/s001220051332

Xiao Y, Liu H, Wu L, Warburton M, Yan J (2017) Genome-wide Association Studies in Maize: Praise and Stargaze. Mol Plant 10:359-374 doi:10.1016/j.molp.2016.12.008

Zhang ZC, Friesen TL, Simons KJ, Xu SS, Faris JD (2009) Development, identification, and validation of markers for marker-assisted selection against the Stagonospora nodorum toxin sensitivity genes Tsn1 and Snn2 in wheat. Molecular Breeding 23:35-49 doi:10.1007/s11032-008-9211-5

Author contributions: M. Lin and M. Lillemo carried out field work. M. Lin carried out genetic analyses. M. Lillemo gained project funding. AF and M. Lillemo supervised the research. JAD developed and contributed plant material. M. Lin drafted the manuscript. All authors revised and approved the manuscript.

Funding: Research was undertaken within the framework of the 2nd call ERA-NET for Coordinating Plant Sciences, within the 'EfectaWheat' project, with funding from The Research Council of Norway, grant NFR251894.

Conflict of Interest: The authors declare that they have no conflict of interest.

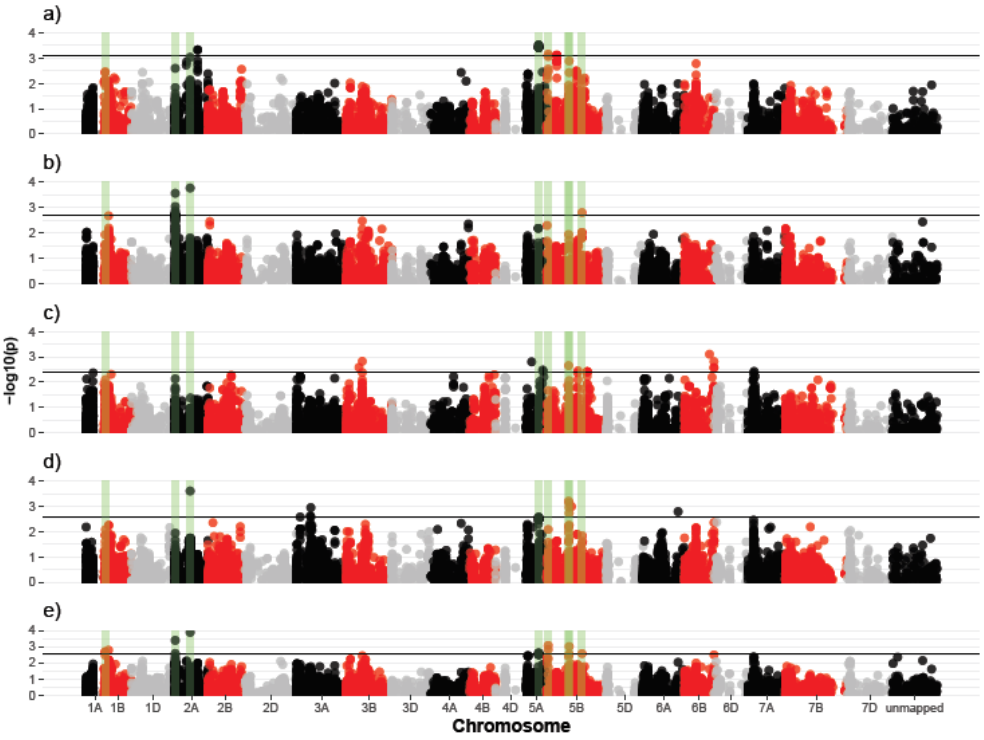

Fig. 1 Manhattan plots of marker-trait association for corrected SNB disease severity in the winter wheat panel. a) year 2016, b) year 2017, c) year 2018, d) year 2019 e) mean of four years. The 0.1 percentile threshold is indicated as horizontal line in each subplot. Dots above threshold indicate significant markers. Important QTL (significant in at least two environments or one year and mean across years) are labeled with green rectangles.

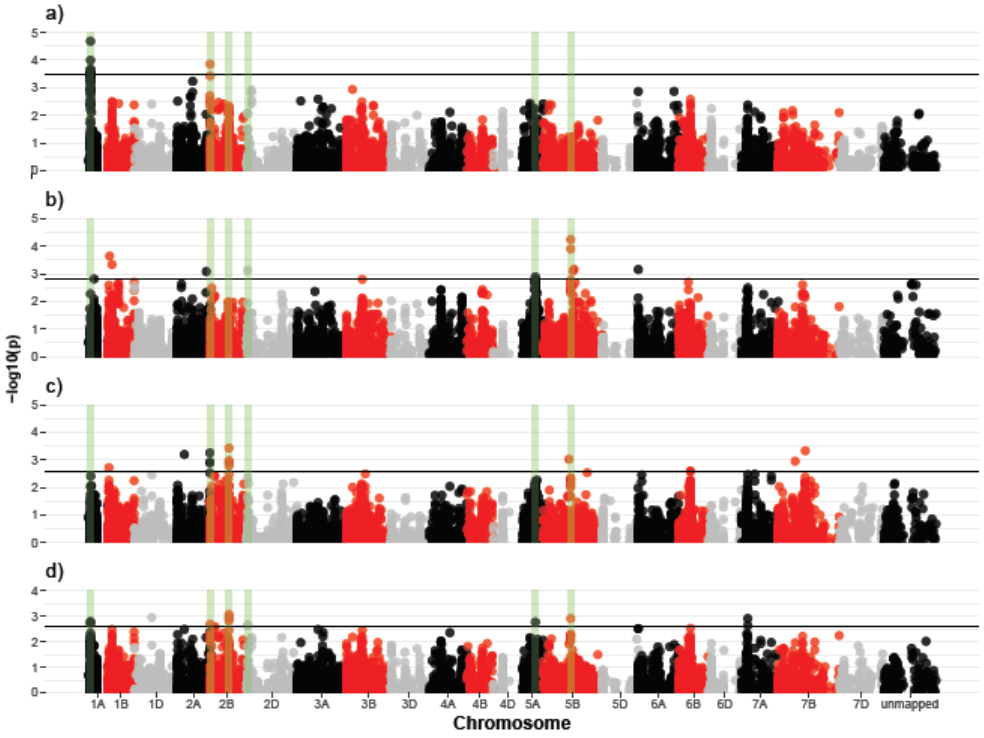

Fig.2 Manhattan plots of marker-trait association for corrected SNB disease severity in the spring wheat panel. a) year 2016, b) year 2017, c) year 2018, d) mean of three years. The 0.1 percentile threshold is indicated as horizontal line in each subplot. Dots above the threshold indicate significant markers. Important QTL (significant in at least two environments or one year and mean across years) are labeled with green rectangles.

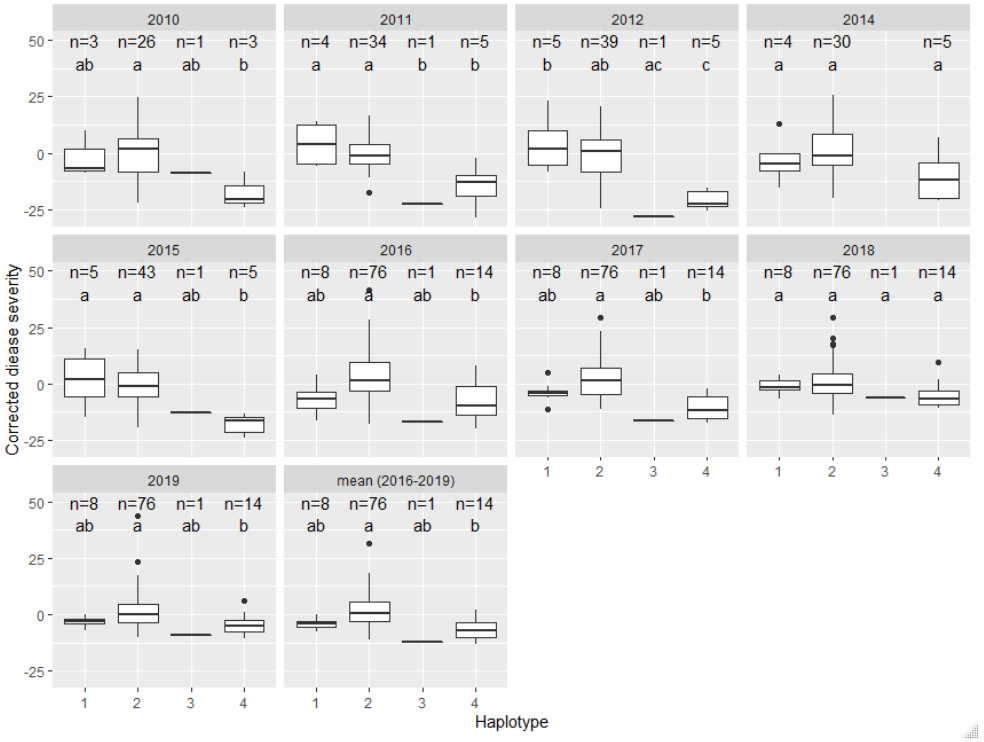

Fig.3 Haplotype analysis of the 2AS QTL in the winter wheat panel of nine years field trial and mean of four years from 2016 to 2019 (Bottom right). Same letter on boxplots indicate no significant difference between haplotypes determined by Tukey`s HSD test ($p < 0.05$)

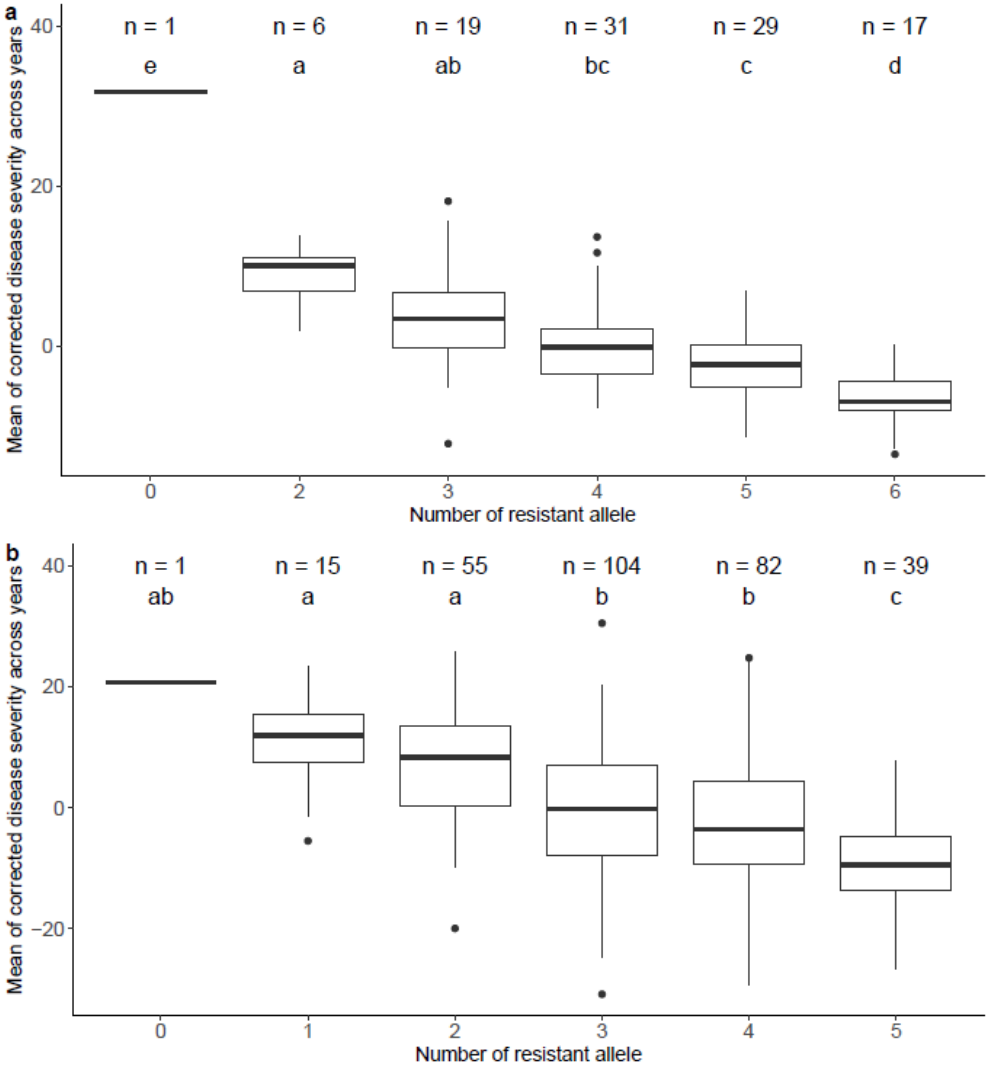

Fig. 4 Boxplots showing effects of stacking resistant alleles. (a) Stacking resistant alleles of six selected QTL associated with SNB in the winter what panel. (b) Stacking resistant alleles of six selected QTL associated with SNB in the spring what panel. Same letter on boxplots indicate no significant difference in mean of disease severities between groups by Tukey`s HSD test ($p < 0.05$).

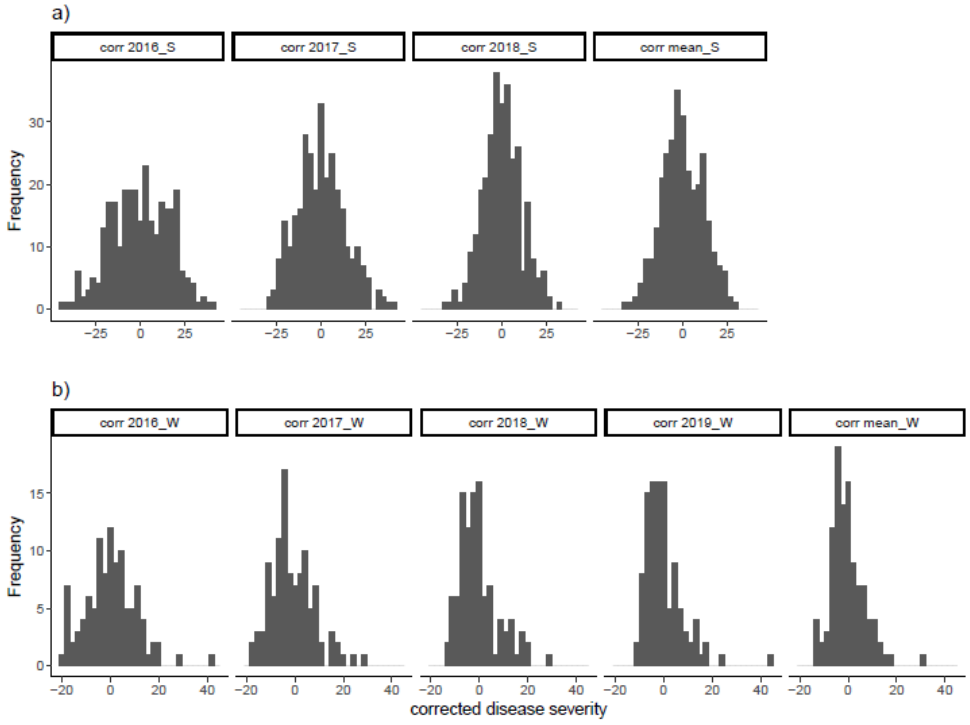

Fig. S1 Histograms of distributions of corrected SNB disease severities for (a) the spring wheat panel from year 2016 to 2018 and mean for three years. (b) the winter wheat panel from year 2016 to 2019 and mean for four years

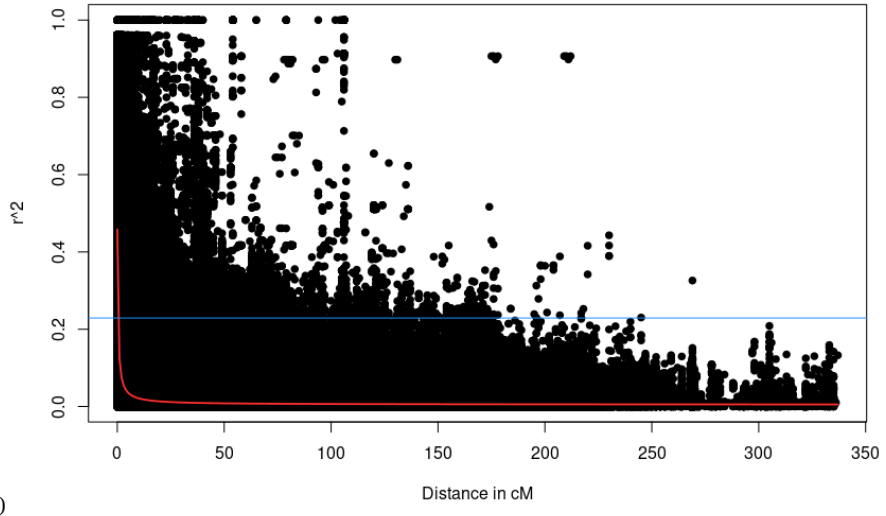

(a)

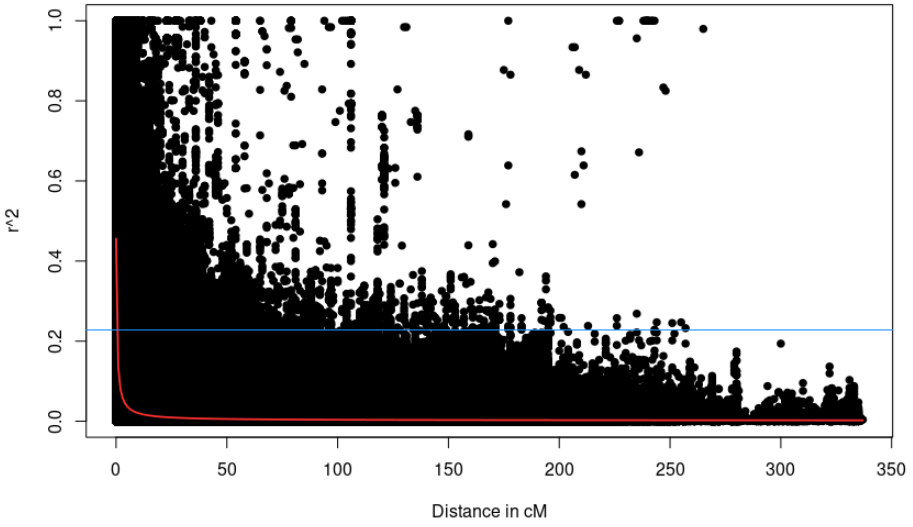

(b)

Fig. S2 Genome wide LD decay plot of (a) winter wheat panel (b) spring wheat panel. The red curve indicates the estimated LD points while the horizontal line indicates the critical r^2 value of the estimated LD value for half decay.

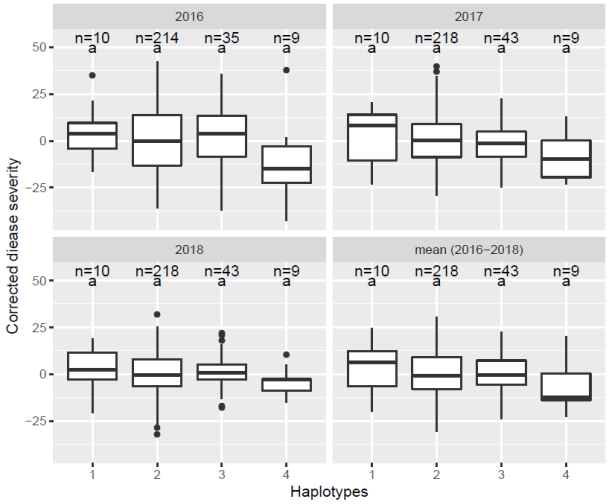

Fig. S3 Haplotype analysis of the 2AS QTL in the spring wheat panel of three years field trial and mean of four years from 2016 to 2018 (Bottom right). Same letter on boxplots indicate no significant difference between haplotypes determined by Tukey`s HSD test ($p < 0.05$)

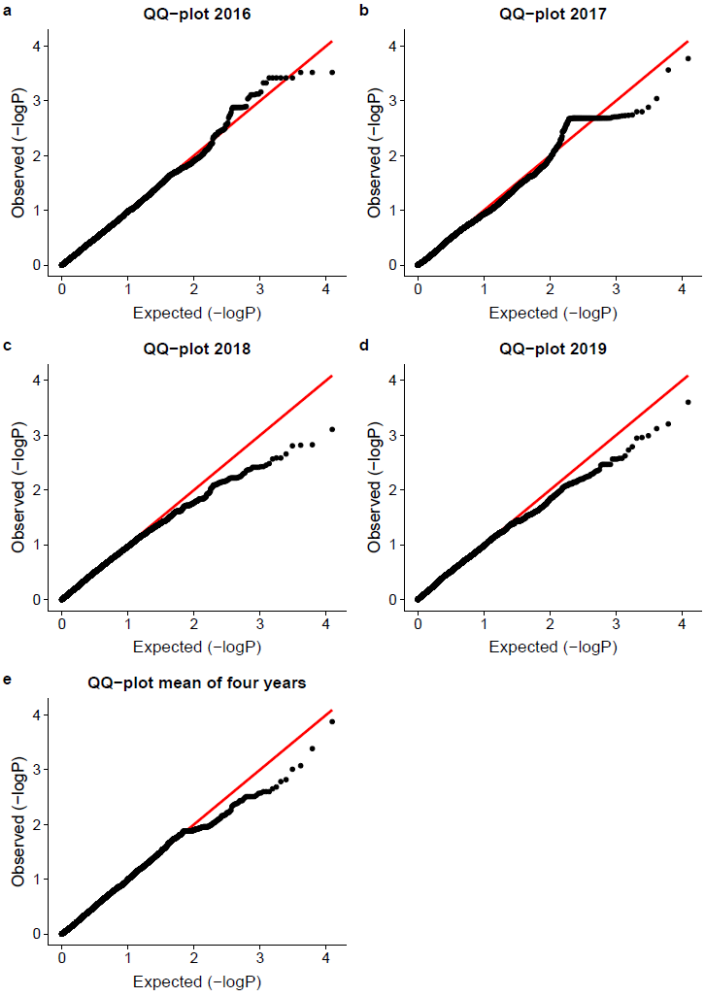

Fig. S4 QQ plots of marker-trait association for corrected SNB disease severity in the winter wheat panel. a) year 2016, b) year 2017, c) year 2018, d) year 2019 e) mean of four years.

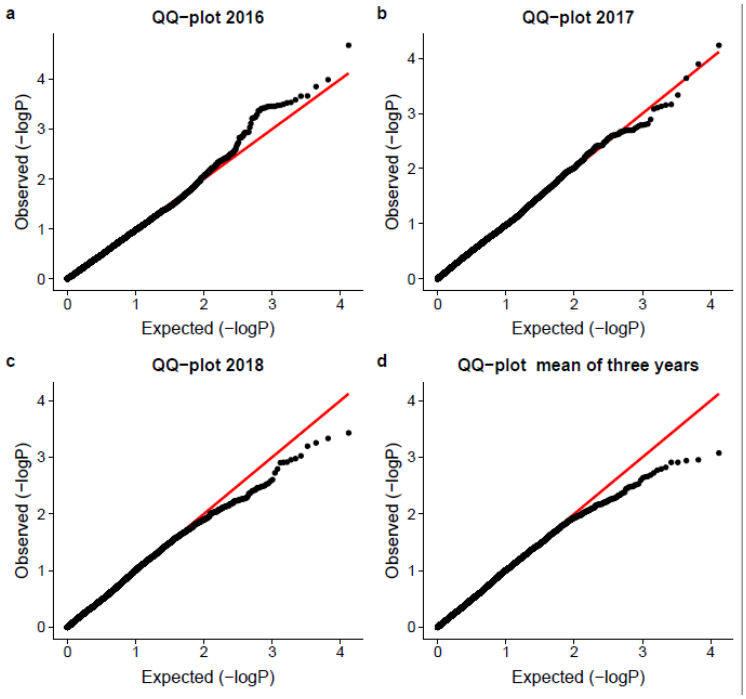

Fig. S5 QQ plots of marker-trait association for corrected SNB disease severity in the spring wheat panel. a) year 2016, b) year 2017, c) year 2018, d) mean of three years.

Table 1 Pearson`s correlation coefficient between leaf blotch and plant height (PH) and days to heading (DH) for each year of the winter and spring wheat panels

Year	PH	DH
2016_winter	0.21*	-0.47***
2017_winter	-0.03	-0.71***
2018_winter	-0.04	-0.46***
2019_winter	0.02	-0.36***
2016_spring	-0.26***	-0.55***
2017_spring	-0.12*	-0.63***
2018_spring	-0.51***	-0.67***

***P < 0.0001, *P < 0.05,

Table 2 Pearson`s correlation coefficients of corrected leaf blotch severities between years

	Winter_2016	Winter_2017	Winter_2018
Winter_2017	0.57***		
Winter_2018	0.44***	0.42***	
Winter_2019	0.73***	0.57***	0.49***

***P < 0.0001

	Spring 2016	Spring_2017
Spring_2017	0.60***	
Spring_2018	0.61***	0.58***

Table S1 The -log10(p) value of the 0.1 percentile threshold in each environment

Trait	Threshold (-log10(p))
Winter wheat 2016	3.12
Winter wheat 2017	2.71
Winter wheat 2018	2.42
Winter wheat 2019	2.56
Winter wheat mean	2.55
Spring wheat 2016	3.46
Spring wheat 2017	2.79
Spring wheat 2018	2.57
Spring wheat mean	2.58

Table S2 Significant markers associated with SNB field resistance of winter wheat panel in year 2016 to 2019 and the mean of four years. Physical positions were based on blastn result against reference genome IWGSC RefSeq v1.0 (International Wheat Genome Sequencing et al. 2018)

Trait	chr	SNP	Position (cM)	R^2	-log10(p)	Physical position start (bp)	Physical position end (bp)
2016	2A	AX-94881363	124	0.12	3.33	700955023	700955093
	2A	AX-95166109	124	0.12	3.33	NA	NA
	5A	AX-94895395	72	0.13	3.42	357103294	357103364
	5A	AX-94874389	72	0.13	3.52	402541541	402541611
	5A	AX-95175890	72	0.13	3.42	402965575	402965645
	5A	AX-94453179	72	0.13	3.42	403351698	403351768
	5A	AX-94563516	72	0.13	3.52	403703600	403703670
	5A	AX-94798019	72	0.13	3.42	403900092	403900162
	5A	AX-95196820	72	0.13	3.42	404177200	404177270
	5A	AX-94998787	72	0.13	3.42	404311211	404311281
	5A	AX-94641644	72	0.13	3.52	404535326	404535396
	5B	AX-94406039	8	0.12	3.16	6651421	6651491
	5B	AX-95187081	55	0.11	3.12	356183887	356183957
	5B	AX-95249855	55	0.11	3.12	366008948	366009018
2017	2A	AX-94479993	0	0.10	2.73	24364941	24365009
	2A	AX-94914308	2	0.10	2.72	4168471	4168541
	2A	AX-94668319	2	0.10	2.74	7550238	7550308
	2A	AX-94671978	2	0.10	2.80	8935904	8935973
	2A	AX-94485036	2	0.11	3.04	10587435	10587504
	2A	AX-95633606	2	0.14	3.56	10993073	10993143
	2A	AX-94398906	2	0.10	2.88	11870754	11870824
	2A	AX-94528064	2	0.10	2.73	14484793	14484863
	2A	AX-94381554	2	0.10	2.73	646858327	646858397
	2A	AX-94657509	83	0.16	3.77	78844042	78844112
	5B	AX-95180386	192	0.12	2.80	NA	NA
2018	3B	AX-95082930	67	0.09	2.58	43313638	43313708
	3B	AX-94838752	85	0.10	2.83	562731079	562731149
	5A	AX-94416605	34	0.10	2.81	673720244	673720314
	5A	AX-94418483	94	0.09	2.48	552525080	552525150
	5A	AX-94848284	97	0.09	2.43	NA	NA

	5B	AX-94727885	119	0.10	2.66	488107941	488108011
	5B	AX-94450951	170	0.09	2.45	573143297	573143367
	6B	AX-94933012	136	0.12	3.11	708623254	708623324
	6B	AX-95152423	160	0.09	2.59	719676748	719676818
	6B	AX-94878340	160	0.10	2.82	719676892	719676962
	6B	AX-94554671	160	0.09	2.57	719734180	719734250
	7A	AX-94412117	33	0.09	2.43	32626959	32627029
2019	2A	AX-94657509	83	0.15	3.60	78844042	78844112
	3A	AX-94398071	20	0.09	2.58	NA	NA
	3A	AX-94638235	75	0.09	2.62	470097253	470097323
	3A	AX-94509316	78	0.09	2.58	477593061	477593131
	3A	AX-94435188	78	0.11	2.95	477708703	477708773
	5A	AX-94874389	72	0.09	2.56	402541541	402541611
	5A	AX-94563516	72	0.09	2.56	403703600	403703670
	5A	AX-94641644	72	0.09	2.56	404535326	404535396
	5B	AX-95227398	119	0.12	3.21	478756057	478756123
	5B	AX-94539614	122	0.11	2.96	505154307	505154377
	5B	AX-94736181	122	0.10	2.73	512582144	512582214
	5B	AX-95629871	122	0.11	3.12	NA	NA
	5B	AX-94388286	135	0.11	2.99	536046967	536047037
	6A	AX-95211290	190	0.10	2.79	606985497	606985567
mean	1B	fcp618	6	0.10	2.68	720472	720504
	1B	AX-95154820	7	0.10	2.65	4222929	4222999
	1B	AX-94823205	25	0.10	2.78	106765081	106765151
	2A	AX-94485036	2	0.09	2.58	10587435	10587504
	2A	AX-95633606	2	0.13	3.38	10993073	10993143
	2A	AX-94657509	83	0.17	3.88	78844042	78844112
	5A	AX-94874389	72	0.09	2.60	402541541	402541611
	5A	AX-94563516	72	0.09	2.60	403703600	403703670
	5A	AX-94641644	72	0.09	2.60	404535326	404535396
	5B	BS00091519_51	8	0.12	3.07	6648517	6648617
	5B	AX-94406039	8	0.10	2.82	6651421	6651491
	5B	AX-95629871	122	0.11	3.01	NA	NA
	5B	AX-95180386	192	0.10	2.57	NA	NA

Table S3 Significant markers associated with SNB field resistance of spring wheat panel in year 2016 to 2018 and the mean of three years. Physical positions were based on blastn result against reference genome IWGSC RefSeq v1.0 (International Wheat Genome Sequencing et al. 2018)

Trait	Chr	SNP	Position (cM)	R^2	-log10(p)	Physical position start (bp)	Physical position end (bp)
2016	1A	AX-94422082	54	0.05	3.59	1145850	1145919
	1A	AX-94669331	54	0.05	3.47	1159654	1159724
	1A	AX-95183288	54	0.05	3.67	1159678	1159748
	1A	AX-94966051	54	0.06	3.99	1209952	1210021
	1A	AX-94889872	54	0.05	3.50	1211671	1211741
	1A	AX-94772289	54	0.07	4.68	1236413	1236483
	1A	AX-94492529	54	0.05	3.53	3118337	3118407
	1A	AX-95004364	54	0.05	3.48	3387729	3387799
	1A	AX-94479695	54	0.05	3.66	NA	NA
	1A	AX-94763828	54	0.05	3.54	NA	NA
	2B	AX-94390683	1	0.05	3.86	10618289	10618359
2017	1A	AX-94456055	74	0.04	2.81	47806029	47806099
	1B	AX-95258492	12	0.05	3.64	26186107	26186177
	1B	AX-94537311	25	0.05	3.34	84413175	84413245
	2A	AX-94740180	160	0.04	3.08	746821494	746821564
	2D	TC253803	22	0.04	3.13	8567394	8567413
	3B	AX-95629357	87	0.04	2.80	617683213	617683283
	5A	AX-94525900	72	0.03	2.79	49587684	49587751
	5A	AX-95165003	72	0.03	2.79	51221640	51221709
	5A	AX-94749386	72	0.04	2.89	102631191	102631261
	5B	fcp620	152	0.05	3.90	546567834	546568058
	5B	AX-94598077	152	0.06	4.24	546705760	546705830
	5B	AX-95133096	164	0.04	3.10	558622122	558622192
	6A	AX-94966145	0	0.04	3.15	5221691	5221761
2018	1B	AX-95245523	8	0.03	2.72	15745695	15745765
	2A	AX-94682021	39	0.04	3.20	NA	NA
	2A	AX-94447690	180	0.04	2.91	769759846	769759916
	2A	AX-94702227	180	0.04	2.90	769761664	769761734
	2A	AX-95254393	180	0.04	3.25	769761786	769761856
	2B	AX-94546397	105	0.04	2.97	742817944	742818014

	2B	AX-94842524	105	0.04	3.43	743746421	743746491
	2B	AX-95652625	105	0.03	2.79	747821490	747821560
	2B	AX-94453359	105	0.04	2.91	748984982	748985052
	5B	AX-94771499	142	0.04	3.02	542952919	542952989
	6B	AX-95630458	63	0.03	2.60	492193491	492193561
	6B	AX-95652828	63	0.03	2.58	515184896	515184966
	7B	AX-94726653	94	0.04	2.95	648608832	648608902
	7B	AX-94912900	150	0.04	3.33	157689450	157689520
mean	1A	AX-94772289	54	0.04	2.72	1236413	1236483
	1A	AX-94409545	54	0.04	2.79	NA	NA
	1D	AX-94425541	96	0.04	2.95	168486153	168486223
	2B	AX-94390683	1	0.03	2.69	10618289	10618359
	2B	AX-94508024	27	0.03	2.59	28452629	28452699
	2B	AX-94546397	105	0.04	2.94	742817944	742818014
	2B	AX-94842524	105	0.04	3.07	743746421	743746491
	2B	AX-94453359	105	0.04	2.82	748984982	748985052
	2D	TC253803	22	0.03	2.66	8567394	8567413
	2D	cfd51	22	0.04	2.65	12360665	12360684
	5A	AX-94749386	72	0.04	2.77	102631191	102631261
	5B	AX-94598077	152	0.04	2.91	546705760	546705830
	7A	AX-94763718	34	0.03	2.64	612990623	612990693
	7A	AX-95653125	34	0.04	2.91	617690340	617690410

Table S4 Four haplotypes identified for 2AS QTL in the winter wheat panel.

Haplotype	AX-94398906	AX-94485036	AX-95633606
Haplotype1	1	1	0
Haplotype2	1	0	1
Haplotype3	1	0	0
Haplotype4	0	1	0

Table S5 Markers used for stacking resistant alleles

Marker	chromosome	Consensus map position	Association panel
AX-94485036	2A	2	Winter wheat
AX-94657509	2A	83	Winter wheat
AX-94563516	5A	72	Winter wheat
BS00091519_51	5B	8	Winter wheat
AX-95629871	5B	122	Winter wheat
AX-95180386	5B	192	Winter wheat
AX-94772289	1A	54	Spring wheat
AX-94390683	2B	1	Spring wheat
AX-94842524	2B	105	Spring wheat
TC253803	2D	22	Spring wheat
AX-94749386	5A	72	Spring wheat
fcp620	5B	152	Spring wheat

Table S6 Comparison of QTL on chromosome 1A with other published QTL

QTL	marker	Start Mb	End Mb	source	Mapping population	R^2	Reference
	AX-94422082	1145850	1145919	Adult plant resistance in 2016	MASBASIS Spring wheat	0.05	This study
	AX-94669331	1159654	1159724	Adult plant resistance in 2016	MASBASIS Spring wheat	0.05	This study
	AX-95183288	1159678	1159748	Adult plant resistance in 2016	MASBASIS Spring wheat	0.05	This study
	AX-94966051	1209952	1210021	Adult plant resistance in 2016	MASBASIS Spring wheat	0.06	This study
	AX-94889872	1211671	1211741	Adult plant resistance in 2016	MASBASIS Spring wheat	0.05	This study
	AX-94772289	1236413	1236483	Adult plant resistance in 2016	MASBASIS Spring wheat	0.07	This study
	AX-94492529	3118337	3118407	Adult plant resistance in 2016	MASBASIS Spring wheat	0.05	This study
	AX-95004364	3387729	3387799	Adult plant resistance in 2016	MASBASIS Spring wheat	0.05	This study
QSnb.fcu1A	BG262267-Ksum182.1	3846832	4202646	*Snn4*	Salamouni× Katepwa	0.24	(Abeysekara et al. 2012)
	RAC875_c30657_82	7185981	7186081	Seedling infection	MASBASIS Spring wheat (subset of 121 lines)	0.14	(Ruud et al. 2019)

Table S7 Comparison of QTL on chromosome 5A with QTL published by Ruud et al. (2019)

marker	Start Mb	End Mb	source	Mapping population	R^2	Reference
wsnp_Ex_c10231_16783750	48969097	48969296	Adult plant resistance in 2012	MASBASIS Spring wheat (subset of 121 lines)	0.09	(Ruud et al. 2019)
AX-94525900	49587684	49587751	Adult plant resistance in 2017	MASBASIS Spring wheat	0.03	This study
AX-95165003	51221640	51221709	Adult plant resistance in 2017	MASBASIS Spring wheat	0.03	This study
AX-94749386	102631191	102631261	Adult plant resistance in 2017/across-year mean	MASBASIS Spring wheat	0.04/0.04	This study
gwm293	104158583	104225387	Adult plant resistance in 2010	MASBASIS Spring wheat (subset of 121 lines)	0.16	(Ruud et al. 2019)

Table S8 Comparison of QTL on chromosome 7A with QTL published by Ruud et al. (2019)

marker	Start bp	End bp	source	Mapping population	R^2	Refence
	612990623	612990693	Adult plant resistance for mean across years	MASBASIS Spring wheat	0.03	This study
AX-94763718						
	612990634	612990573	Adult plant resistance in 2013	MASBASIS Spring wheat (subset of 121 lines)	0.11	(Ruud et al. 2019)
BobWhite_c47283_127						
	617578333	617578433	Adult plant resistance in 2013	MASBASIS Spring wheat (subset of 121 lines)	0.11	(Ruud et al. 2019)
BS00070857_51						
	617690280	617690377	Adult plant resistance in 2013	MASBASIS Spring wheat (subset of 121 lines)	0.11	(Ruud et al. 2019)
Excalibur_c12996_775						
	617690340	617690410	Adult plant resistance for mean across years	MASBASIS Spring wheat	0.04	This study
AX-95653125						

Table S9 Comparison of QTL on chromosome 2A with other published QTL

QTL	marker	Start Mb	End Mb	source	Mapping population	R^2	Reference
Qsnb.cur-2AS2	wmc382a-Barc124a	2320465	3784367	Seedling infection	Calingiri × Wyalkatchem	0.15	(Rybak et al. 2017)
Qsnb.niab-2A.1	RAC875_c44680_90-BS00111318_51	820443	2378574	Seedling infection	NIAB Elite MAGIC	0.05	(Lin et al. 2020)
	AX-94914308	4168471	4168541	Adult plant resistance in 2017	MASBASIS winter wheat	0.10	This study
	AX-94668319	7550238	7550308	Adult plant resistance in 2017	MASBASIS winter wheat	0.10	This study
	AX-94671978	8935904	8935973	Adult plant resistance in 2017	MASBASIS winter wheat	0.10	This study
	AX-94485036	10587435	10587504	Adult plant resistance in 2017/ across-year mean	MASBASIS winter wheat	0.11/0.09	This study
	AX-95633606	10993073	10993143	Adult plant resistance in 2017/across-year mean	MASBASIS winter wheat	0.14/0.13	This study
	AX-94398906	11870754	11870824	Adult plant resistance in 2017	MASBASIS winter wheat	0.11	This study
	AX-94528064	14484793	14484863	Adult plant resistance in 2017	MASBASIS winter wheat	0.10	This study
QSnl05.daw-2A	IWB22268-IWB29103	14815405	19649817	Flag leaf resistance	P92201D5× P91193D1	0.21	(Francki et al. 2018)

QSnl04.daw-2A	IWB32474-IWB9206	15608826	16321745	Flag leaf resistance	P92201D5× P91193D1	0.13	(Francki et al. 2018)

Table S10 Average of corrected disease severity (%) of each haplotype in in each environment of the spring and winter wheat panels

Wheat type	Year	Haplotype 1	Haplotype 2	Haplotype 3	Haplotype 4
spring	2016	5[a]	0[a]	2[a]	-10[a]
spring	2017	2[a]	1[a]	-1[a]	-8[a]
spring	2018	2[a]	0[a]	1[a]	-4[a]
spring	Mean (2016-2018)	3[a]	0[a]	0[a]	-7[a]
Winter	2010	-2[ab]	0[a]	-9[ab]	-18[b]
Winter	2011	4[a]	-1[a]	-22[b]	-15[b]
Winter	2012	4[b]	-1[ab]	-28[ac]	-21[c]
Winter	2014	-3[a]	1[a]	NA	-10[a]
Winter	2015	2[a]	0[a]	-13[ab]	-18[b]
Winter	2016	-7[ab]	3[a]	-17[ab]	-7[b]
Winter	2017	-4 [ab]	2 [a]	-16 [ab]	-10[b]
Winter	2018	-1[a]	1[a]	-6[a]	-5[a]
Winter	2019	-3[ab]	2[a]	-9[ab]	-5[b]
Winter	Mean (2016-2019)	-4[ab]	2[a]	-12[ab]	-7[b]

Same letter indicate no significant difference between haplotypes determined by Tukey`s HSD test ($p < 0.05$)

ISBN: 978-82-575-1684-0
ISSN: 1894-6402

Norwegian University
of Life Sciences

Postboks 5003
NO-1432 Ås, Norway
+47 67 23 00 00
www.nmbu.no